THERMAL AND MAGNETIC PROPERTIES OF NEUTRON STARS

Thesis by

Lars Hernquist

In Partial Fulfillment of the Requirements

for the Degree of

Doctor of Philosophy

California Institute of Technology

Pasadena, California

1985

(Submitted August 2, 1984)

"Beware if you expect truth from astronomy lest you leave this field a greater fool than when you entered."

--A. Osiander, in Foreword to *On the Revolutions of the Heavenly Spheres*, N. Copernicus (1543). (From O. Gingerich, *Scientific American* **247**, 132 (1982).)

"...there is no such thing as relativistic degeneracy! ... If one takes the mathematical derivation of the relativistic degeneracy formula as given in astronomical papers, no fault is to be found. One has to look deeper into its physical foundations, and these are not above suspicion. The formula is based on a combination of relativity mechanics and non-relativity quantum theory, and I do not regard the offspring of such a union as born in lawful wedlock."

--A.S. Eddington, *The Observatory*, **58**, 38 (1935).

ACKNOWLEDGEMENTS

I owe thanks to a great number of people who have given me encouragement and support through the years.

Foremost, I owe my advisor, Roger Blandford, a debt of gratitude that I undoubtedly will never be able to repay. From the beginning, when he agreed to take me on as a student, Roger has never failed to give me just the right amount of inspiration to get me through the difficult moments. He has always been willing to discuss new ideas and patiently answer my (many!) questions, even at the busiest of times, and from him I have learned much about physics and the nature of good research. I am continually amazed by both his breadth and depth of knowledge. Without his help this thesis would never have come to fruition. I also thank Roger for sharing his overall sense of personal integrity and decency-- qualities which I hope have been transmitted to me, even if only in small measure. Having Roger as my advisor has been, by far, the highlight of my academic career.

I thank Kip Thorne and all the members of his group for providing a friendly and exciting atmosphere to work in. I am especially grateful to Yekta Gürsel, Doug Macdonald, and Peter Quinn for explaining the intricacies of our computing facilities to me, to Pat Lyon for administrative support, and to Cynthia Eller for many hours of typing. Most of all I thank Jim Applegate for being almost a second advisor to me. Our collaborative efforts and countless number of stimulating discussions about physics have been a memorable part of my stay at Caltech. His valuable suggestions helped to get me out of more jams than I care to remember during the course of my research.

I also profited, at various times, from discussions with Peter Goldreich, David Stevenson, Chris Pethick, Einar Gudmundsson, David Pines, and Sachiko Tsuruta about many aspects of neutron star physics.

Special thanks are due to those who have helped to develop and maintain my interest in physics and astronomy– in particular to Vic Mansfield (my first undergraduate advisor), to Karl Berkelman (my second undergraduate advisor), and to Steve Channon (a good friend and mentor since our first days at F.E.C. together).

While at Caltech, I was supported at various times by an Earl C. Anthony Fellowship, a National Science Foundation Fellowship, teaching assistantships, and graduate research assistantships. To both Caltech and the National Science Foundation I give my thanks.

Finally, I thank my family-- my parents, Tom, and Ingrid-- and most of all my wife, Dale, for their love and support during my graduate years. Without their generous and patient understanding none of this would have been possible. And so, it is to them that I dedicate this thesis.

ABSTRACT

The interaction of the magnetic field with the heat flux in neutron stars is investigated.

It is proposed that the magnetic field develops as a result of thermal processes in the liquid and solid phases of neutron star envelopes. Necessary conditions for the growth to occur are derived and it is shown that surface fields comparable to those observed would result. The magnetization of neutron stars in binary systems (which have magnetic properties differing substantially from those of isolated pulsars) can be explained by thermal processes associated with accretion flows.

In order to study magnetic effects on neutron star cooling a number of subsidiary issues are considered.

The thermal structure of unmagnetized neutron star envelopes is examined using approximate analytical models. From the results it is possible to justify a number of simplifying assumptions and extend them to the magnetized case. For example, it is shown that an accurate treatment of photon transport is not required in order to determine the relation between the heat flux and the core temperature of neutron stars.

The effect of the field on the magnetic properties of the electron gas in neutron star crusts is considered. It is shown that the gas is unstable to the formation of domains of alternating magnetization. It is further argued that the domain structure will have a negligible influence on the heat flux because of the small free energy associated with the domains.

The influence of the field on the electron transport properties of neutron star envelopes is examined in detail. Accurate expressions are derived for all

components of the relevant transport tensors, taking into account quantum mechanical and relativistic effects. In addition, allowance is made for arbitrary degree of degeneracy and scattering mechanism.

Finally, these results are used to study the thermal structure of magnetized neutron star envelopes. It is shown that the enhancement in the heat flux due to quantum effects is almost completely canceled by the suppression of the heat flux due to geometrical effects. Thus the magnetic field is expected to play only a minor role in neutron star cooling, contrary to earlier claims.

TABLE OF CONTENTS

CHAPTER 1

Introduction.

Introduction

Fifty years have passed since Baade and Zwicky (1934) first proposed that dense stars comprised primarily of neutrons could be created as by-products of supernova explosions. Initial skepticism to this hypothesis has long-since faded and the importance of neutron stars to astrophysical phenomena is now well-established. A variety of galactic objects (e.g., radio pulsars, binary pulsars, pulsating x-ray sources, γ-ray bursters, x-ray bursters, and SS433) are most easily understood in terms of models which incorporate neutron stars. In addition, the study of neutron stars contributes significantly to our understanding of stellar evolution, stellar structure, and physical processes under extreme conditions. Inasmuch as the current investigation is concerned with the thermal and magnetic properties of neutron stars, it is appropriate to review the prior effort to unravel the mysteries of these fascinating stellar fossils.

Structural Properties and Evidence for the Existence of Neutron Stars

The possible existence of neutron stars was first proposed informally by Landau on the day of the discovery of the neutron in 1932 (Rosenfeld 1974) and independently by Baade and Zwicky in 1934. Initial calculations of neutron star structure were performed by Oppenheimer and Volkoff (1939) for a dense, free neutron gas (for an excellent review, see the book by Shapiro and Teukolsky 1983; henceforth ST). Theoretical interest in the neutron star hypothesis remained at a relatively low level until 1967 because of the apparent impossibility of directly observing neutron stars at optical wavelengths (ST). However, refinements to the equation of state at high densities led to more detailed stellar models (e.g., Harrison, *et al.* 1958; Cameron 1959; Ambartsumyan and Saakyan 1960; Hamada and Salpeter 1961; Harrison, *et al.* 1965). In addition, preliminary examinations of rotational (Hoyle, *et al.* 1964; Tsuruta and Cameron 1966a), magnetic (Woltjer 1964; Hoyle, *et al.* 1964), and energetic (Wheeler 1966; Pacini 1967) properties of neutron stars were undertaken. Finally, a number of observations (e.g., Duyvendak 1942; Mayall and Oort 1942; Baade 1942; Minkowski 1942) suggested the presence of a neutron star in the Crab nebula, but a definitive conclusion was not yet possible (ST).

The situation was dramatically altered by the discovery of the first radio pulsar in 1967 (Hewish, *et al.* 1968). The interpretation of pulsars as rapidly rotating, magnetized neutron stars was initially made by Gold (1968, 1969). Detailed models of the conversion of rotational energy into radiation soon followed (e.g., Pacini 1968; Gunn and Ostriker 1969, 1970; Goldreich and Julian 1969; Ostriker and Gunn 1969), as did the discovery of many more radio pulsars. Approximately 350 are currently known, including three that are associated with supernova remnants--the Crab (Staelin and Reifenstein 1968; Richards and Comella 1969; Cocke, Disney, and Taylor 1969), Vela (Large, Vaughan, and Mills

1968), and MSH 15-52 (Seward and Harnden 1982; Manchester, *et al.* 1982). (For a review of the status of the observational link between supernovae and compact stellar remnants see Helfand and Backer 1984.)

The rotating neutron star model of radio pulsars is generally accepted because it is the only one which can account for the range of pulsar periods, the stability of pulsar periods, and the rate of increase of pulsar periods (for a detailed argument see Ruderman 1972; Manchester and Taylor 1977; ST). The detection of four radio pulsars in binary systems (Hulse and Taylor 1975; Manchester, *et al.* 1980; Damashek, *et al.* 1982; Boriakoff, Buccheri, and Fauci 1983) has made it possible to directly measure the masses of neutron stars (Blandford and Teukolsky 1975, 1976; Brumberg, *et al.* 1975; Smarr and Blandford 1976; Epstein 1977; Kelley and Rappaport 1981; Blandford and DeCampli 1981; Taylor and Weisberg 1982). The implied limits are consistent with current theories. In addition, the observed glitches in the timing data of the Crab and Vela pulsars (e.g., Boynton, *et al.* 1972; Löhsen 1975; Manchester, *et al.* 1978; Downs 1981) and the timing noise associated with most pulsars (Boynton, *et al.* 1972; Cordes and Helfand 1980) can be understood in terms of the properties of neutron stars (e.g., Baym, *et al.* 1969; Ruderman 1969; Baym and Pines 1971; Pines, Shaham, and Ruderman 1972, 1974; Pines and Shaham 1974; Groth 1975; Pandharipande, Pines, and Smith 1976; Pines 1980; Alpar, *et al.* 1981; Cordes and Greenstein 1981; Boynton 1981; Alpar, *et al.* 1984a,b). Finally, the discovery of the millisecond pulsar (Backer, *et al.* 1982) has provided further theoretical constraints, but has not contradicted the neutron star model of pulsars (e.g., Shapiro, Teukolsky, and Wasserman 1983).

The existence of neutron stars has been corroborated by x-ray and γ-ray observations. The first pulsating x-ray sources (Cen X-3 and Her X-1) were discovered by the UHURU satellite in 1971 (Schreier, *et al.* 1972; Tananbaum,

et al. 1972). Approximately 350 discrete x-ray sources have been identified, including 19 which are periodic (Forman, *et al.* 1978; ST). The standard interpretation of the periodic sources invokes the accretion of matter from a normal star onto a compact companion in order to account for the short time variability of the emission and the confirmed presence of many of these sources in binary systems (ST). In addition, such a scheme provides an efficient mechanism for the conversion of gravitational energy into radiation. The periodicity results from a misalignment of the rotational and magnetic axes of the neutron star (for a detailed discussion see ST). Theories of x-ray emission from a binary system containing a neutron star had actually been proposed prior to the discovery of the pulsating x-ray sources (e.g., Shklovskii 1967a,b; Prendergast and Burbidge 1968). The current neutron star accretion models can, in principle, account for the observed properties of x-ray pulsars (e.g., Pringle and Rees 1972; Davidson and Ostriker 1973; Lamb, Pethick, and Pines 1973; Lamb, *et al.* 1975; Arons and Lea 1976, 1980; Elsner and Lamb 1976, 1977; Ghosh and Lamb 1978, 1979ab; Rappaport and Joss 1981; Burnard, Lea, and Arons 1983). Finally, the implied limits on the masses of the neutron stars are in agreement with stellar models (e.g., Bahcall 1978).

A more recent discovery has been the detection of aperiodic bursts of x-ray (Grindlay, *et al.* 1976; Grindlay 1981) and γ-ray (Klebesadel, *et al.* 1973; Klebesadel, *et al.* 1982) radiation from discrete galactic sources. (A γ-ray burst source may also have been discovered in the Large Magellanic Cloud. See Cline 1982 and the relevant references therein.) Models of bursters assume accretion onto a compact object in order to account for the short timescales associated with the bursts and to provide an efficient mechanism for the conversion of gravitational energy into radiation. Direct evidence for the binary nature of bursters has been provided by recent observations which indicate a long-period

modulation of the signal from several x-ray bursters (e.g., Walter, White, and Swank 1981; White and Swank 1982; Walter, *et al.* 1982; McClintock and Petro 1981; Pedersen, *et al.* 1981). The identification of the compact objects as neutron stars is somewhat tenuous because of the lack of pulsations which would result from the interaction of the accreted matter with the magnetic field. However, it is possible in these sources that the magnetic field is either too weak to influence the accretion flow (as a result of ohmic decay) or is aligned with the rotation axis. The current accreting neutron star models of x-ray bursters (e.g., Joss 1977, 1980; Lamb and Lamb 1978; Lewin and Joss 1981; Taam 1982) and γ-ray bursters (e.g., Ruderman 1975; Lamb 1982) can, in principle, account for the observed properties of these sources.

The accumulation of observational evidence to support the existence of neutron stars has been accompanied by an intense theoretical effort to understand the structural properties of these objects (see Baym and Pethick 1975, 1979). This has included investigations of the equation of state at low (e.g., Baym, Pethick, and Sutherland 1971) and high (e.g., Pandharipande 1971; Baym, Bethe, and Pethick 1971; Walecka 1974; Bethe and Johnson 1974; Friedman and Pandharipande 1971; Pandharipande and Smith 1975ab) densities; phase transitions at high densities (e.g., superfluidity, pion condensation, free quarks or hyperons, and neutron crystals); and detailed stellar models (ST). (Studies of the thermal and magnetic properties of neutron stars will be discussed below.)

Although many uncertainties remain (primarily in the equation of state at high densities), a consensus on the structural properties of neutron stars has been achieved. Stellar models predict masses $\sim 1\,M_{\odot}$, radii $\sim 10\,\mathrm{km}$, central densities $\sim 10^{15}\,\mathrm{gm\ cm^{-3}}$ and a density distribution which can be summarized as follows (ST):

1. The surface (depth $\lesssim$ a few meters, $\rho < 10^6 \mathrm{gm\ cm^{-3}}$); in which magnetic effects may dominate the equation of state and the composition may deviate from nuclear statistical equilibrium.

2. The envelope (depth $\lesssim 1$ km, $\rho < 4.3\times10^{11} \mathrm{gm\ cm^{-3}}$); in which exotic nuclei are stable and the electrons are degenerate and relativistic. A phase transition from a liquid to a solid Coulomb lattice occurs within this zone.

3. The neutron drip regime (depth $\lesssim$ several km, $\rho \lesssim 2\times10^{14} \mathrm{gm\ cm^{-3}}$); in which free (possibly superfluid) neutrons appear, along with neutron rich nuclei, free electrons, and free (possibly superfluid) protons.

4. The core region ($\rho \gtrsim 2\times10^{14} \mathrm{gm\ cm^{-3}}$); in which the nuclei dissolve into a uniform sea of superfluid neutrons, normal electrons, and superfluid, superconducting (type II) protons. The state of the matter at the highest densities is uncertain. Among the possibilities are the appearance of pions, hyperons, quarks, and neutron crystals.

Thermal Properties and Evidence for the Thermal Radiation of Neutron Stars

Neutron stars are expected to be intense sources of thermal x-ray radiation, releasing gravitational energy generated during the core collapse of the progenitor. Because of the anticipated low level of optical emission, little interest was shown in neutron star cooling calculations until the first non-solar x-ray sources were observed in 1962 (Giacconi, *et al.* 1962, 1963; Bowyer, *et al.* 1964a). It was immediately suggested that the radiation could be from cooling

neutron stars, initiating investigations of neutron star thermal structure (Chiu 1964; Chiu and Salpeter 1964; Tsuruta 1964; Bahcall and Wolf 1965abc; Tsuruta and Cameron 1965, 1966b). However, it was soon shown that the sources were either extended (e.g., Bowyer, *et al.* 1964b) or did not have blackbody spectra (Clark 1965; Giacconi, Gursky, and Waters 1965; Chodil, *et al.* 1965) and, hence, could not be isolated neutron stars. Nevertheless, prior to the discovery of the first radio pulsar, it was assumed that neutron stars would first be detected through their thermal x-ray radiation.

Recent cooling calculations have included studies of the physical properties of the core (e.g., Tsuruta 1974, 1975; Malone 1974; Maxwell 1979; Glen and Sutherland 1980; Nomoto and Tsuruta 1981; Van Riper and Lamb 1981; Yakovlev and Urpin 1981; Richardson, *et al.* 1982) and of the envelope (Gudmundsson 1981; Gudmundsson, Pethick, and Epstein 1982, 1983; Epstein, Gudmundsson, and Pethick 1983). A consensus on the thermal evolution of neutron stars has yet to be reached because of the uncertainties in the equation of state at high densities. Neutrino cooling rates are sensitive to assumptions about superfluidity, pion condensation, and the appearance of free hyperons or quarks (e.g., Iwamoto 1980; Burrows 1980). In addition, calculations of the opacity in the envelope do not agree in detail and magnetic effects have been included only superficially.

In spite of the uncertainties a general picture of neutron star cooling has emerged. Immediately after forming, neutron stars have internal temperatures $\sim 10^{11}\,K$. Neutrino cooling is extremely efficient and the temperature drops to $\sim 10^{9}\,K$ within a few days. The thermal structure is then determined by neutrino losses from the core until the internal temperature has fallen to $\sim 10^{8}\,K$ (after $\sim 10^{4}$ years). Thereafter, photon surface emission becomes the dominant energy drain and the cooling curves drop rapidly (e.g., Tsuruta 1979).

In principle, the sensitivity of the predicted x-ray flux to the input physics allows the internal structure of neutron stars to be probed. The recent success of the Einstein X-Ray Observatory (HEAO-2) has made this possible. Because of the presumed association of supernovae and the formation of neutron stars, a survey was made of young galactic supernova remnants (e.g., Harnden, *et al.* 1979ab; Helfand, Chanan, and Novick 1980; Helfand 1981; Murray, *et al.* 1979; Pye, *et al.* 1981; Tuohy and Garmire 1980; Helfand and Becker 1984). Evidence for an unpulsed x-ray point source was found in only five remnants (Crab, Vela, RCW103, 3C58, and CTB80). The neutron star x-ray fluxes could not be determined unambiguously because of the lack of spectral data and the difficulty of subtracting magnetospheric emission. The implied upper limits for the surface temperatures of the neutron stars are marginally consistent with standard cooling calculations. However, it may be necessary to invoke rapid cooling due to uncertain phenomena in the core (e.g., pion condensation) if future observations lower the derived surface temperatures. Furthermore, the possible discrepancy between the supernova rate and the neutron star birth rate may widen unless point sources are detected in a larger fraction of supernova remnants.

Magnetic Properties and Evidence for the Magnetization of Neutron Stars

The evidence to support the hypothesis that most neutron stars are strongly magnetized ($B \sim 10^{12}$ *G*) is as compelling as the evidence in favor of the existence of neutron stars. Prior to the discovery of the first radio pulsar it had been suggested that neutron stars might be strongly magnetized (e.g., Woltjer 1964; Hoyle, *et al.* 1964; Pacini 1967). The first models of pulsars (e.g., Gold 1968; Pacini 1968) assumed the existence of strong magnetic fields for the

conversion of rotational energy into radiation, as have all subsequent theories (e.g., Goldreich and Julian 1969; Gunn and Ostriker 1969, 1970; Ostriker and Gunn 1969; Ruderman 1972; Ruderman and Sutherland 1975; Ruderman 1980). The arguments in favor of the neutron star interpretation of pulsars, therefore, support the existence of associated magnetic fields. Furthermore, timing observations of radio pulsars are well fit by a narrow distribution of field strengths ($\propto (P\dot{P})^{1/2}$) in the range $1-5\times10^{12}$ *G* (e.g., Manchester 1981).

Models of pulsating x-ray sources rely on a misalignment of the spin and magnetic axes in order to account for the periodicity of the emission. In addition, fields $\sim 10^{12}$ *G* are required to provide the necessary coupling between the accreted matter and the neutron star to explain the secular decrease in the periods of pulsating x-ray sources. Finally, cyclotron lines have been observed in the x-ray spectra of the Crab pulsar (Manchanda, *et al.* 1982) and the pulsating x-ray sources Her X-1 (Trümper, *et al.* 1978), 4U0115+63 (Wheaton, *et al.* 1979), GX1+4 (Maurer, *et al.* 1982), and 4U1626-67 (Pravdo, *et al.* 1979). Field strengths $\sim 1-5\times10^{12}$ *G* are implied if the lines originate from electron transitions between the two lowest Landau levels (uncertainties $\sim 50\%$ result from assumptions about the gravitational redshift of the radiation and the identification of the features as absorption vs. emission lines, e.g., Basko and Sunyaev 1975).

Cyclotron lines and possible red-shifted positron annihilation lines which have been observed in the x-ray spectra of γ-ray bursters (Mazets, *et al.* 1981) are consistent with fields $\sim 10^{12}$ *G*. Furthermore, it has been suggested that x-ray and γ-ray bursters are differentiated by the absence or presence of a strong magnetic field (Woosley and Wallace 1982).

A consensus on the importance of the magnetic field to the internal physical processes of neutron stars has not been achieved. The origin of neutron star

magnetic fields is uncertain, although it has generally been assumed that fields $\sim 10^{12}$ *G* would result from flux freezing during the core collapse of the progenitor. In addition, previous attempts to include magnetic fields in thermal structure calculations (e.g., Tsuruta, *et al.* 1972; Tsuruta 1974, 1975, 1979; Glen and Sutherland 1980; Van Riper and Lamb 1981; Yakovlev and Urpin 1981), in models of burst sources (e.g., Joss and Li 1980), and in subsurface flows of accreted matter (e.g., Blandford, *et al.* 1979) have been rather idealized and must be regarded as preliminary.

The effect of the magnetic field on structural properties of neutron stars has been considered in detail. Unless the field in the core is $\sim 10^{16}$ *G* the equation of state will be modified only in the surface layers ($\rho < 10^6$ gm cm^{-3}). It has been suggested (e.g., Ruderman 1974; Chen, *et al.* 1974; Flowers, *et al.* 1977) that in the presence of a magnetic field $\sim 10^{12}$ *G* the matter at low densities would be arranged in long, linear chains of atoms, resulting in an abrupt termination of the density distribution at $\rho \sim 10^4$ gm cm^{-3}. However, the most recent calculations (Müller 1984) indicate that magnetic crystallization will not occur for iron, which is the equilibrium nucleus at these densities.

The magnetic structure of the core has also been investigated (e.g., Easson 1976, 1979ab; Arons and Spencer 1978; Easson and Pethick 1979) and may be relevant to models of glitching and to frictional heating of neutron stars (e.g., Greenstein 1979ab).

Finally, a considerable amount of work has been done on the properties of the magnetic field above the neutron star surface. Applications have included pulsar emission mechanisms (e.g., Arons and Scharlemann 1979; Ruderman 1980; Arons 1981; Ruderman 1981), the structure of the magnetosphere (e.g., Arons 1979; Mestel 1981; Michel 1982; Arons 1983), models of plerionic supernova remnants (e.g., Ruderman 1972; Cheng 1983), and accretion onto magnetized

neutron stars (e.g., Pringle and Rees 1972; Davidson and Ostriker 1973; Lamb, Pethick, and Pines 1973; Lamb 1979; Arons and Lea 1976, 1980; Elsner and Lamb 1976, 1977, 1984; Ghosh and Lamb 1978, 1979ab).

Synopsis of Thesis

This thesis is composed of five distinct, self-contained papers, each of which examines a topic relevant to the thermal and magnetic properties of neutron stars. A brief summary of each paper now follows.

Paper I (Blandford and Hernquist 1982) examines the magnetization of the electron gas in neutron star crusts in the presence of a strong, external magnetic field. The magnetic susceptibility is calculated for an appropriate range of densities ($\rho \sim 10^5 - 10^{11}$ gm cm^{-3}) and field strengths ($B \sim 10^{12} - 10^{14}$ G). (At lower densities the susceptibility is essentially zero.) Under these conditions the electrons are relativistic, degenerate, and effectively free (electron-electron interactions and lattice corrections have a negligible effect on the electron distribution function). In general the magnetization is much smaller than the magnetic field. However, due to the quantization of electron orbits, the susceptibility undergoes large de Haas- van Alphen oscillations when the temperature is sufficiently low. (The requirement is that the thermal energy be smaller than the spacing of the Landau levels, or $T \lesssim 10^7$ K for $\rho \sim 10^7$ gm cm^{-3} and $B \sim 10^{12}$ G.) As a result, it is energetically favorable for the electron gas to sustain a phase transition in which domains of alternating magnetization are formed. It is argued that the domain structure will have a negligible influence on the heat transport and surface properties of neutron stars, but could be coupled indirectly to observable effects. In addition, the associated anisotropic

magnetostrictive stresses provide constraints on the strength of the magnetic field that can be supported by the crust in equilibrium.

In paper II (Blandford, Applegate, and Hernquist 1983) a novel mechanism for the origin of magnetic field in neutron stars is proposed. Substantial observational evidence exists (e.g., the narrow range of field strengths $B \sim 1-5\times10^{12}$ G derived from pulsar timing data, cyclotron lines in the spectra of pulsating x-ray sources, and redshifted positron annihilation lines in the spectra of γ-ray bursters) to suggest that neutron star magnetic fields have a common physical origin. Additional observations indicate that the magnetization is not permanent (e.g., the finite lifetime of radio pulsars) and furthermore may have been generated long after the neutron star was formed (e.g., the presence of a pulsar with timing age $\sim$ 1550 years embedded in supernova remnant MSH 15-52 estimated to be $\sim 10^4$ years old). Conventionally, it has been assumed that the magnetic field results from flux freezing during the core collapse of the progenitor. However, if ohmic dissipation is to be effective on the timescale of pulsar lifetimes then the magnetic field must be confined to densities $\rho \lesssim 10^{11}$ gm cm^{-3}. In this paper it is suggested that the magnetic field arises as a result of thermal effects in the liquid and solid phases of neutron star envelopes. If the instabilities develop, the subsurface field will grow to a saturation value $\sim 10^{14}$ G, implying a field $\sim 10^{12}$ G at the surface. The field is maintained for as long as heat flows through the crust. Thereafter, the dipole moment will decay on a timescale comparable to pulsar lifetimes. This model is capable of accounting for the observed properties of neutron star magnetization in all contexts. For example, x-ray bursters are thought to be much older ($\sim 10^8$ years) than isolated radio pulsars. The magnetization of these objects could be explained by thermal processes associated with accretion rather than with the initial cooling of the neutron star. Furthermore, binary radio pulsars are

observed to have unusually weak but long-lived magnetic fields. It is possible that these neutron stars became magnetized during a long x-ray binary phase and that the magnetic field penetrated to a greater depth than in an isolated pulsar, increasing the ohmic decay time.

The influence of a strong magnetic field on the thermodynamic and transport properties of the electron gas in neutron star envelopes is considered in paper III (Hernquist 1984a). At the relevant densities and field strengths the classical description of electron orbits is not valid and quantum effects must be taken into account. The physical conditions will be influenced by the discrete nature of the density of states factor. For example, the transition from the non-degenerate to degenerate regimes will be shifted to higher densities by a sufficiently strong magnetic field. Transport properties will additionally be affected by the dependence of the collision time on the magnetic field. Previous calculations of quantum transport have generally been either unreliable or incomplete. In particular, large errors can be introduced if the completely degenerate limit ($T = 0$) is assumed. Thermal effects smooth and damp the oscillations of the transport coefficients. Furthermore, the Wiedemann-Franz law no longer holds and it is not possible to compute the thermal conductivity from the electrical conductivity. Finally, at the densities and field strengths of interest a relativistic treatment is essential. In the present work, relativistic effects are included by calculating transition rates from the exact solutions to the Dirac equation, assuming elastic scattering. Expressions for all of the independent components of the transport tensors (electrical conductivity, thermoelectric coefficient, and thermal conductivity) are derived for arbitrary degree of degeneracy and scattering mechanism. The resulting formulae, though compact in form, are difficult to evaluate. Computations of intermediate functions containing most of the numerical complexity are performed and fits

are provided which allow the transport coefficients to be more easily calculated. Results are given for the scattering potentials of most importance to neutron star envelopes (e-ion and e-phonon collisions). Finally, the necessary conditions for the quantization to be important thermodynamically and the relevance of the results to thermal structure calculations are discussed.

Paper IV (Hernquist and Applegate 1984) investigates the thermal structure of unmagnetized neutron star envelopes using approximate analytical formulae. In the degenerate regime the thermal structure equation is solved exactly for electron-dominated heat transport. In the non-degenerate layers it is shown that if the opacity is a power law function of density and temperature then the $T(\rho)$ profiles lie along curves of constant thermal conductivity. The two solutions are matched at intermediate densities to give an approximate relation between the heat flux and core temperature of the neutron star. The dependence on various uncertain factors is found explicitly, allowing a detailed understanding of the physical processes that control the heat flux. In particular, it is shown that for a given core temperature the heat flux is virtually independent of effects at low densities, in the non-degenerate regime. Included are corrections to the free-free photon opacity and to the free electron equation of state. In addition, partial ionization is not important. At high densities, in the degenerate layers, the results are insensitive to the slow variation in ionic composition and uncertainties in the melting curve and the electron conductivity in the solid phase. The flux- core temperature relation depends strongly only on the electron conductivity in the liquid phase. The significance of these results to magnetized cooling calculations is discussed. For example, it is argued that reliable expressions for bound-bound and bound-free absorption in the presence of a strong magnetic field are not necessary in order to compute the heat flow along the field. Furthermore, the dominance of the electron thermal conductivity

implies that meaningful cooling calculations are possible, using the results of paper III.

The influence of a strong magnetic field ($B \sim 10^{10} - 10^{14} G$) on the thermal structure of neutron star envelopes is studied in paper V (Hernquist 1984b) using the method of Gudmundsson, *et al.* (Gudmundsson 1981; Gudmundsson, Pethick, and Epstein 1982,1983; Epstein, Gudmundsson, and Pethick 1983) and the most recent calculations of radiative (Silant'ev and Yakovlev 1980) and electronic (paper III) thermal conductivities. It is shown that the temperature of the core, T_c, scales with flux and surface gravity in the ratio F/g_s, in agreement with the unmagnetized case (e.g., paper IV; Gudmundsson, Pethick, and Epstein 1983). The effect of the magnetic field on the relation between the core temperature and F/g_s is considered for effective surface temperatures in the range $T_s = 10^{5.5} - 10^{6.5} K$. For a purely vertical field geometry it is found that quantum effects will enhance (relative to the zero field case) the heat flux, for a given core temperature, by a factor $\lesssim 3$. It is further argued that the anisotropic nature of the electron transport in a magnetic field will suppress the heat flux for a more realistic field geometry by a factor $\lesssim 3$. Thus the magnetic field is expected to have only a minor effect on neutron star cooling. This conclusion differs substantially from those of earlier magnetized cooling calculations and a detailed comparison is performed to isolate sources of discrepancy. (It is argued that the disagreement results primarily from inaccurate approximations to the electronic thermal conductivity used in past calculations.) The sensitivity of the flux- core temperature relation to variations in the input physics is studied in a manner analogous to Gudmundsson (1981). As in the zero field case it is found that the flux- core temperature relation is highly sensitive to the thermal conductivity only in a narrow strip in which e-ion scattering dominates, in agreement with the expectations stated in paper IV. The results of the

sensitivity analysis are further used to argue that disagreements among the existing calculations of the conductivity will not alter the basic conclusion that magnetic effects on the flux- core temperature relation are relatively unimportant.

References

Alpar, M., Anderson, P., Pines, D., and Shaham, J. 1981, *Astrophys. J. Lett.* **249**, L29.

Alpar, M., Anderson, P., Pines, D., and Shaham, J. 1984a, *Astrophys. J.* **276**, 325.

Alpar, M., Anderson, P., Pines, D., and Shaham, J. 1984b, *Astrophys. J.* **278**, 791.

Ambartsumyan, V. and Saakyan, G. 1960, *Soviet Astronomy* **4**, 187.

Arons, J. 1979, *Sp. Sci. Rev.* **24**, 437.

Arons, J. 1981, in *IAU Symposium* 95: *Pulsars* , ed. Sieber, W. and Wielebinski, R., Reidel, Dordrecht.

Arons, J. 1983, *Astrophys. J.* **266**, 215.

Arons, J. and Lea, S. 1976, *Astrophys. J.* **207**, 914.

Arons, J. and Lea, S. 1980, *Astrophys. J.* **235**, 1016.

Arons, J. and Scharlemann, E. 1979, *Astrophys. J.* **231**, 854.

Arons, J. and Spencer, R. 1978, *Astrophys. J.* **220**, 640.

Baade, W. and Zwicky, F. 1934, *Phys. Rev.* **45**, 138.

Baade, W. 1942, *Astrophys. J.* **96**, 188.

Backer, D., Kulkarni, S., Heiles, C., Davis, M., and Goss, W. 1982, *Nature* **300**, 615.

Bahcall, J. and Wolf, R. 1965a, *Phys. Rev. Lett.* **14**, 343.

Bahcall, J. and Wolf, R. 1965b, *Phys. Rev. B* **140**, 1445.

Bahcall, J. and Wolf, R. 1965c, *Phys. Rev. B* **140**, 1452.

Bahcall, J. 1978, *Ann. Rev. Astron. Astrophys.* **16**, 241.

Basko, M. and Sunyaev, R. 1975, *Astron.* and *Astrophys.* **42**, 311.

Baym, G., Pethick, C., Pines, D., and Ruderman, M. 1969, *Nature* **224**, 872.

Baym, G. and Pines, D. 1971, *Ann. Phys.* **66**, 816.

Baym, G., Bethe, H., and Pethick, C. 1971, *Nucl. Phys. A* **175**, 225.

Baym, G., Pethick, C., and Sutherland, P. 1971, *Astrophys. J.* **170**, 299.

Baym, G. and Pethick, C. 1975, *Ann. Rev. Nucl. Sci.* **25**, 27.

Baym, G. and Pethick, C. 1979, *Ann. Rev. Astron. Astrophys.* **17**, 415.

Bethe, H. and Johnson, M. 1974, *Nucl. Phys. A* **230**, 1.

Blandford, R. and Teukolsky, S. 1975, *Astrophys. J. Lett.* **198**, L27.

Blandford, R. and Teukolsky, S. 1976, *Astrophys. J.* **205**, 580.

Blandford, R., DeCampli, W., and Königl, A. 1979, *Bull. Am. Astr. Soc.* **11**, 703.

Blandford, R. and DeCampli, W. 1981, in *IAU Symposium* 95: *Pulsars* , ed. Sieber, W. and Wielebinski, R., Reidel, Dordrecht.

Blandford, R. and Hernquist, L. 1982, *J. Phys. C: Solid State Physics* **15**, 6233.

Blandford, R., Applegate, J., and Hernquist, L. 1983, *Mon. Not. R. astr. Soc.* **204**, 1025.

Boriakoff, V., Buccheri, R., and Fauci, F. 1983, *Nature* **304**, 417.

Bowyer, S., Byram, E., Chubb, T., and Friedman, H. 1964a, *Nature* **201**, 1307.

Bowyer, S., Byram, E., Chubb, T., and Friedman, H. 1964b, *Science* **146**, 912.

Boynton, P., Groth, E., Hutchinson, D., Nanos, G., Partridge, R., and Wilkinson, D. 1972, *Astrophys. J.* **175**, 217.

Boynton, P. 1981, in *IAU Symposium* 95: *Pulsars* , ed. Sieber, W. and Wielebinski, R., Reidel, Dordrecht.

Brumberg, V., Zel'dovich, Ya., Novikov, I., and Shakura, N. 1975, *Sov. Astron. Lett.* **1**, 2.

Burnard, D., Lea, S., and Arons, J. 1983, *Astrophys. J.* **266**, 175.

Burrows, A. 1980, *Phys. Rev. Lett.* **44**, 1640.

Cameron, A. 1959, *Astrophys. J.* **130**, 884.

Chen, H.-H., Ruderman, M., and Sutherland, P. 1974, *Astrophys. J.* **191**, 473.

Cheng, A. 1983, *Astrophys. J.* **275**, 790.

Chiu, H.-Y. 1964, *Ann. Phys.* **26**, 364.

Chiu, H.-Y. and Salpeter, E. 1964, *Phys. Rev. Lett.* **12**, 413.

Chodil, G., Jopson, R., Mark, H., Seward, F., and Swift, C. 1965, *Phys. Rev. Lett.* **15**, 605.

Clark, G. 1965, *Phys. Rev. Lett.* **14**, 91.

Cline, T. 1982, in *Gamma Ray Transients and Related Astrophysical Phenomena*, ed. Lingenfelter, R., Hudson, H., and Worrall, D., American Institute of Physics, New York.

Cocke, W., Disney, H., and Taylor, D. 1969, *Nature* **221**, 525.

Cordes, J. and Helfand, D. 1980, *Astrophys. J.* **239**, 640.

Cordes, J. and Greenstein, G. 1981, *Astrophys. J.* **245**, 1060.

Damashek, M., Backus, P., Taylor, J., and Burkhardt, R. 1982, *Astrophys. J. Lett.* **253**, L57.

Davidson, K. and Ostriker, J. 1973, *Astrophys. J.* **179**, 585.

Downs, G. 1981, *Astrophys. J.* **249**, 687.

Duyvendak, J. 1942, *Proc. Astron. Soc. Pacific* **54**, 91.

Easson, I. 1976, *Nature* **263**, 486.

Easson, I. 1979a, *Astrophys. J.* **228**, 257.

Easson, I. 1979b, *Astrophys. J.* **233**, 711.

Easson, I. and Pethick, C. 1979, *Astrophys. J.* **227**, 995.

Elsner, R. and Lamb, F. 1976, *Nature* **262**, 356.

Elsner, R. and Lamb, F. 1977, *Astrophys. J.* **215**, 897.

Elsner, R. and Lamb, F. 1984, *Astrophys. J.* **278**, 326.

Epstein, R. 1977, *Astrophys. J.* **216**, 92. Errata: **231**, 644.

Epstein, R., Gudmundsson, E., and Pethick, C. 1983, *Mon. Not. R. astr. Soc.* **204**, 471.

Flowers, E., Lee, J.-F., Ruderman, M., Sutherland, P., Hillebrandt, W., and Müller, E. 1977, *Astrophys. J.* **215**, 291.

Forman, W., Jones, C., Cominsky, L., Julien, P., Murray, S., Peters, G., Tananbaum, H., and Giacconi, R. 1978, *Astrophys. J. Suppl.* **38**, 357.

Friedman, B. and Pandharipande, V. 1981, *Nucl. Phys. A* **361**, 502.

Ghosh, P. and Lamb, F. 1978, *Astrophys. J. Lett.* **223**, L83.

Ghosh, P. and Lamb, F. 1979a, *Astrophys. J.* **232**, 259.

Ghosh, P. and Lamb, F. 1979b, *Astrophys. J.* **234**, 296.

Giacconi, R., Gursky, H., Paolini, F., and Rossi, B. 1962, *Phys. Rev. Lett.* **9**, 439.

Giacconi, R., Gursky, H., Paolini, F., and Rossi, B. 1963, *Phys. Rev. Lett.* **11**, 530.

Giacconi, R., Gursky, H., and Waters, J. 1965, *Nature* **207**, 572.

Glen, G. and Sutherland, P. 1980, *Astrophys. J.* **239**, 671.

Gold, T. 1968, *Nature* **218**, 731.

Gold, T. 1969, *Nature* **221**, 25.

Goldreich, P. and Julian, W. 1969, *Astrophys. J.* **157**, 869.

Greenstein, G. 1979a, *Nature* **277**, 521.

Greenstein, G. 1979b, *Astrophys. J.* **231**, 880.

Grindlay, J., Gursky, H., Schnopper, H., Parsignault, D., Heise, J., Brinkman, A., and Schrijver, J. 1976, *Astrophys. J. Lett.* **205**, L127.

Grindlay, J. 1981, in *X-Ray Astronomy with the Einstein Satellite* , ed. Giacconi, R., Reidel, Dordrecht.

Groth, E. 1975, *Astrophys. J. Suppl.* **29**, 453.

Gudmundsson, E. 1981, licentiate thesis, University of Copenhagen.

Gudmundsson, E., Pethick, C., and Epstein, R. 1982, *Astrophys. J. Lett.* **259**, L19.

Gudmundsson, E., Pethick, C., and Epstein, R. 1983, *Astrophys. J.* **272**, 286.

Gunn, J. and Ostriker, J. 1969, *Nature* **221**, 454.

Gunn, J. and Ostriker, J. 1970, *Astrophys. J.* **160**, 979.

Hamada, T. and Salpeter, E. 1961, *Astrophys. J.* **134**, 683.

Harnden, F., Buehler, B., Giacconi, R., Grindlay, J., Hertz, P., Schreier, E., Seward, F., Tananbaum, H., and Van Speybroeck, L. 1979a, *Bull. Am. Astr. Soc.* **11**, 789.

Harnden, F., Hertz, P., Gorenstein, P., Grindlay, J., Schreier, E., and Seward, F. 1979b, *Bull. Am. Astr. Soc.* **11**, 424.

Harrison, B., Wakano, M., and Wheeler, J. 1958, in *La Structure et l'évolution de l'univers* , Onzième Conseil de Physique Solvay, Stoops, Brussels.

Harrison, B., Thorne, K., Wakano, M., and Wheeler, J. 1965, *Gravitation Theory and Gravitational Collapse* , University of Chicago Press, Chicago.

Helfand, D., Chanan, G., and Novick, R. 1980, *Nature* **283**, 337.

Helfand, D. 1981, in *IAU Symposium* 95: *Pulsars* , ed. Sieber, W. and Wielebinski, R., Reidel, Dordrecht.

Helfand, D. and Becker, R. 1984, *Nature* **307**, 215.

Hernquist, L. 1984a, submitted to *Astrophys. J. Suppl.*

Hernquist, L. 1984b, submitted to *Mon. Not. R. astr. Soc.*

Hernquist, L. and Applegate, J. 1984, submitted to *Astrophys. J.*

Hewish, A., Bell, S., Pilkington, J., Scott, P., and Collins, R. 1968, *Nature* **217**, 709.

Hoyle, F., Narlikar, J., and Wheeler, J. 1964, *Nature* **203**, 914.

Hulse, R. and Taylor, J. 1975, *Astrophys. J. Lett.* **195**, L51.

Iwamoto, N. 1980, *Phys. Rev. Lett.* **44**, 1637.

Joss, P. 1977, *Nature* **270**, 310.

Joss, P. and Li, F. 1980, *Astrophys. J.* **238**, 287.

Joss, P. 1980, *Ann. Rev. New York Acad. Sci.* **336**, 479.

Kelley, R. and Rappaport, S. 1981, in *IAU Symposium* 95: *Pulsars* , ed. Sieber, W. and Wielebinski, R., Reidel, Dordrecht.

Klebesadel, R., Strong, I., and Olson, R. 1973, *Astrophys. J. Lett.* **182**, L85.

Klebesadel, R., Fenimore, E., Laros, J., and Terrell, J. 1982, in *Gamma Ray Transients and Related Astrophysical Phenomena*, ed. Lingenfelter, R., Hudson, H., and Worrall, D., American Institute of Physics, New York.

Lamb, D., Lamb, F., Pines, D., and Shaham, J. 1975, *Astrophys. J. Lett.* **198**, L21.

Lamb, D. and Lamb, F. 1978, *Astrophys. J.* **220**, 291.

Lamb, D. 1982, in *Gamma Ray Transients and Related Astrophysical Phenomena*, ed. Lingenfelter, R., Hudson, H., and Worrall, D., American Institute of Physics, New York.

Lamb, F. 1979, in *Proceedings of the Sydney Chapman Conference on Magnetospheric Boundary Layers*, ed. Battrick, B., ESA SP Series.

Lamb, F., Pethick, C., and Pines, D. 1973, *Astrophys. J.* **184**, 271.

Large, M., Vaughan, A., and Mills, B. 1968, *Nature* **220**, 340.

Lewin, W. and Joss, P. 1981, *Space Sci. Rev.* **28**, 3.

Löhsen, E. 1975, *Nature* **258**, 688.

Malone, R. 1974, Ph.D. Thesis, Cornell University.

Manchanda, R., Bazzano, A., La Padula, C., Polcaro, V., and Ubertini, P. 1982, *Astrophys. J.* **252**, 172.

Manchester, R. and Taylor, J. 1977, *Pulsars* , Freeman, San Francisco.

Manchester, R., Newton, L., Goss, W., and Hamilton, P. 1978, *Mon. Not. R. astr. Soc.* **184**, 35*P*.

Manchester, R., Newton, L., Cooke, D., and Lyne, A. 1980, *Astrophys. J. Lett.* **236**, L25.

Manchester, R. 1981, in *IAU Symposium* 95: *Pulsars* , ed. Sieber, W. and Wielebinski, R., Reidel, Dordrecht.

Manchester, R., Tuohy, I., and D'Amico, N. 1982, *Astrophys. J. Lett.* **262**, L31.

Maurer, G., Johnson, W., Kurfess, J., and Strickman, M. 1982, *Astrophys. J.* **254**, 271.

Maxwell, O. 1979, *Astrophys. J.* **231**, 201.

Mayall, N. and Oort, J. 1942, *Proc. Astron. Soc. Pacific* **54**, 95.

Mazets, E., Golenetskii, S., Aptekar', R., Gur'yan, Yu., and Il'inskii, V. 1981, *Nature* **290**, 378.

McClintock, J. and Petro, L. 1981, IAU Circular 3615.

Mestel, L. 1981, in *IAU Symposium* 95: *Pulsars*, ed. Sieber, W. and Wielebinski, R., Reidel, Dordrecht.

Michel, F. 1982, *Rev. Mod. Phys.* **54**, 1.

Minkowski, R. 1942, *Astrophys.J.* **96**, 199.

Müller, E. 1984, *Astron. Astrophys.* **130**, 415.

Murray, S., Fabbiano, G., Fabian, A., Epstein, A., and Giacconi, R. 1979, *Astrophys. J. Lett.* **234**, L69.

Nomoto, K. and Tsuruta, S. 1981, *Astrophys. J. Lett.* **250**, L19.

Oppenheimer, J. and Volkoff, G. 1939, *Phys. Rev.* **55**, 374.

Ostriker, J. and Gunn, J. 1969, *Astrophys. J.* **157**, 1395.

Pacini, F. 1967, *Nature* **216**, 567.

Pacini, F. 1968, *Nature* **219**, 145.

Pandharipande, V. 1971, *Nucl. Phys. A* **178**, 123.

Pandharipande, V. and Smith, R. 1975a, *Nucl. Phys. A* **237**, 507.

Pandharipande, V. and Smith, R. 1975b, *Phys. Lett. B* **59**, 15.

Pandharipande, V., Pines, D., and Smith, R. 1976, *Astrophys. J.* **208**, 550.

Pedersen, H., van Paradijs, J., and Lewin, W. 1981, *Nature* **294**, 725.

Pines, D., Shaham, J., and Ruderman, M. 1972, *Nature Phys. Sci.* **237**, 83.

Pines, D. and Shaham, J. 1974, *Comments Astrophys. Sp. Phys.* **6**, 37.

Pines, D., Shaham, J., and Ruderman, M. 1974, in *IAU Symposium* 53: *Physics of Dense Matter* , ed. Hansen, C., Reidel, Dordrecht.

Pines, D. 1980, *J. Phys. Colloq.* **41**, *C2/* 111.

Pravdo, S., White, N., Boldt, E., Holt, S., Serlemitsos, P., Swank, J., Szymkowiak, A., Tuohy, I., and Garmire, G. 1979, *Astrophys. J.* **231**, 912.

Prendergast, K. and Burbidge, G. 1968, *Astrophys. J. Lett.* **151**, L83.

Pringle, J. and Rees, M. 1972, *Astron. Astrophys.* **21**, 1.

Pye, J., Pounds, K., Rolf, D., Seward, F., Smith, A., and Willingale, R. 1981, *Mon. Not. R. astr. Soc.* **194**, 569.

Rappaport, S. and Joss, P. 1981, in *X−Ray Astronomy with the Einstein Satellite* , ed. Giacconi, R., Reidel, Dordrecht.

Richards, D. and Comella, J. 1969, *Nature* **222**, 551.

Richardson, M., Van Horn, H., Ratcliff, K., and Malone, R. 1982, *Astrophys. J.* **255**, 624.

Rosenfeld, L. 1974, in *Astrophysics and Gravitation* , Proc. 16th Solvay Conference on Physics, Editions de l'Université de Bruxelles, Brussels.

Ruderman, M. 1969, *Nature* **223**, 597.

Ruderman, M. 1972, *Ann. Rev. Astron. Astrophys.* **10**, 427.

Ruderman, M. 1974, in *IAU Symposium* 53: *Physics of Dense Matter* , ed. Hansen, C., Reidel, Dordrecht.

Ruderman, M. 1975, *Ann. New York Acad. Sci.* **262**, 164.

Ruderman, M. and Sutherland, P. 1975, *Astrophys. J.* **196**, 51.

Ruderman, M. 1980, *Ann. New York Acad. Sci.* **336**, 409.

Ruderman, M. 1981, in *IAU Symposium* 95: *Pulsars*, ed. Sieber, W. and Wielebinski, R., Reidel, Dordrecht.

Schreier, E., Levinson, R., Gursky, H., Kellogg, E., Tananbaum, H., and Giacconi, R. 1972, *Astrophys. J. Lett.* **172**, L79. Errata: **173**, L51.

Seward, F. and Harnden, F. 1982, *Astrophys. J. Lett.* **256**, L45.

Shapiro, S. and Teukolsky, S. (ST) 1983, *Black Holes, White Dwarfs, and Neutron Stars*, Wiley, New York.

Shapiro, S., Teukolsky, S., and Wasserman, I. 1983, *Astrophys. J.* **272**, 702.

Shklovskii, I. 1967a, *Soviet Astronomy* **11**, 749.

Shklovskii, I. 1967b, *Astrophys. J. Lett.* **148**, L1.

Silant'ev, N. and Yakovlev, D. 1980, *Ap. Sp. Sci.* **71**, 45.

Smarr, L. and Blandford, R. 1976, *Astrophys. J.* **207**, 574.

Staelin, D. and Reifenstein, E. 1968, *Science* **162**, 1481.

Taam, R. 1982, *Astrophys. J.* **258**, 761.

Tananbaum, H., Gursky, H., Kellogg, E., Levinson, R., Schreier, E., and Giacconi, R. 1972, *Astrophys. J. Lett.* **174**, L143.

Taylor, J. and Weisberg, J. 1982, *Astrophys. J.* **253**, 908.

Trümper, J., Pietsch, W., Reppin, C., Voges, W., Staubert, R., and Kendziorra, E. 1978, *Astrophys. J. Lett.* **219**, L105.

Tsuruta, S. 1964, Ph.D. Thesis, Columbia University.

Tsuruta, S. and Cameron, A. 1965, *Nature* **207**, 364.

Tsuruta, S. and Cameron, A. 1966a, *Nature* **211**, 356.

Tsuruta, S. and Cameron, A. 1966b, *Can. J. Physics* **44**, 1863.

Tsuruta, S., Canuto, V., Lodenquai, J., and Ruderman, M. 1972, *Astrophys. J.*, **176**, 739.

Tsuruta, S. 1974, in *IAU Symposium* 53: *Physics of Dense Matter* , ed. Hansen, C., Reidel, Dordrecht.

Tsuruta, S. 1975, *Astrophys.* and *Sp. Sci.* **34**, 199.

Tsuruta, S. 1979, *Phys. Rept.* **56**, 237.

Tuohy, I. and Garmire, G. 1980, *Astrophys. J. Lett.* **239**, L107.

Van Riper, K. and Lamb, D. 1981, *Astrophys. J. Lett.* **244**, L13.

Walecka, J. 1974, *Ann. Phys.* **83**, 491.

Walter, F., White, N., and Swank, J. 1981, IAU Circular 3611.

Walter, F., Bowyer, S., Mason, K., Clarke, J., Henry, J., Halpern, J., and Grindlay, J. 1982, *Astrophys. J. Lett.* **253**, L67.

Wheaton, W., Doty, J., Primini, F., Cooke, B., Dobson, C., Goldman, A., Hecht, M., Hoffman, J., Howe, S., Scheepmaker, A., Tsiang, E., Lewin, W., Matteson, J., Gruber, D., Baity, W., Rothschild, R., Knight, F., Nolan, P., and Peterson, L. 1979, *Nature* **282**, 240.

Wheeler, J. 1966, *Ann. Rev. Astron. Astrophys.* **4**, 393.

White, N. and Swank, J. 1982, *Astrophys. J. Lett.* **253**, L61.

Woltjer, L. 1964, *Astrophys. J.* **140**, 1309.

Woosley, S. and Wallace, R. 1982, *Astrophys. J.* **258**, 716.

Yakovlev, D. and Urpin, V. 1981, *Soviet Astronomy Letters* **7**, 88.

CHAPTER 2

Magnetic Susceptibility of a Neutron Star Crust.

Roger Blandford and Lars Hernquist

Published in the

Journal of Physics C: Solid State Physics

(1982, **15**, 6233).

Magnetic Susceptibility of a Neutron Star Crust

R.D. Blandford and L. Hernquist

California Institute of Technology

Pasadena, CA 91125

ABSTRACT

The magnetic susceptibility of the degenerate free electrons in the crust of a neutron star is computed for a range of densities, temperatures, and field strengths. It is shown that when the temperature is low enough (typically less than 10^7K for densities $\sim 10^7 \mathrm{g\,cm^{-3}}$ and 10^{12} Gauss fields), the susceptibility undergoes large de Haas-van Alphen oscillations. The crust is then unstable to the formation of layers of domains of alternating magnetization. Associated with these domains are magnetic field fluctuations of a few percent amplitude and anisotropic magnetostrictive stresses which may be large enough to crumble the crust. It is argued that these domains are unlikely to directly influence the surface properties of the neutron star but may possibly be coupled indirectly to observable effects.

1. Introduction

Observation of radio pulsars and pulsating X-ray sources indicate that many neutron stars have surface flux densities $B \sim 10^{12}$ G. The outer crusts of neutron stars are believed to be in the form of a BCC ionic lattice supported against gravitational collapse by the pressure of effectively free degenerate electrons (e.g., Baym and Pethick 1975). At densities $\rho \gtrsim 10^5 \, \mathrm{g\,cm^{-3}}$, electron-electron interactions and lattice corrections will have a negligible effect on the electron distribution function. The electron Fermi temperature T_F increases with depth z below the surface and becomes relativistic at a density $\rho \sim 10^6 \, \mathrm{g\,cm^{-3}}$ and $z \sim 10 \, \mathrm{m}$ for a standard $1.4 M_\odot$, 10 km neutron star. The equilibrium ions range from ^{56}Fe to ^{76}Fe as the density increases from $10^5 \, \mathrm{g\,cm^{-3}}$ to $10^{11} \, \mathrm{g\,cm^{-3}}$. We limit the discussion to densities $\rho \gtrsim 10^5$ g cm^{-3} since the susceptibility at field strengths $\gtrsim 10^{12}$ G is effectively zero at lower densities. Possible observational consequences will be associated with effects at greater densities.

The magnetization of the crust is generally very small compared with the magnetic field H. Nevertheless, when the electrons are sufficiently cool that their thermal energy is smaller than the spacing of the Landau levels, the magnetization can undergo large de Haas-van Alphen oscillations with either changing field or changing Fermi energy. Under these conditions it sometimes becomes energetically favorable for the electron gas to separate into two phases containing different flux densities.

Earlier discussions of the magnetic susceptibility of neutron star crusts (e.g., Lee *et al.* 1969; O'Connell and Roussel 1972; Schmid-Burgk 1973) have concentrated upon the discussion of whether or not the observed field may result from spontaneous magnetization. This almost certainly cannot occur because the crust is insufficiently cool and, in any case, the magnetized state is at best metastable. In this paper it is assumed that the field is supported by conduction

currents frozen into the interior of the star. The possibility that the field is produced by currents in the surface layers is currently under investigation (Blandford, Applegate, and Hernquist 1983).

In § 2 the calculation of free electron magnetic susceptibility is reviewed and generalized. Domain structure and formation is discussed in § 3 and the results are applied to neutron stars in § 4. In § 5 possible observational consequences are considered.

2. Magnetic Susceptibility of a Free Electron Gas

2.1 Magnetization

Consider a gas of free electrons in a quantizing, homogeneous magnetic field of flux density B. Unless explicitly stated, we set $m_e = c = k = 1$ and measure B in units of the critical field $B_c = m_e^2 c^3 e^{-1} \hbar^{-1} = 4.41 \times 10^{13}$ G and volume V in units of $e^2 \hbar^2 m_e^{-3} c^{-4}$. For the simple geometry under consideration, the Dirac equation can be solved exactly (e.g., Berestetskii, *et al.* 1982) to give the energy spectrum

$$\varepsilon_r = (1 + p_\parallel^2 + 2rB)^{1/2}, \quad r = 0,1,2,\cdots \tag{1}$$

The energy levels, which are known as Landau levels, are doubly degenerate for $r \neq 0$ and non-degenerate for $r = 0$. The quantity ε_r, and hence the magnetization, should be regarded as functions of B, and not H, because it is B that is derived from the vector potential appearing in the Hamiltonian (e.g., Pippard 1980). This view has experimental support (e.g., Shoenberg 1962).

The magnetization M is conveniently calculated from the grand potential Ω which for small susceptibility is given by

$$\Omega = -\alpha \frac{BVT}{4\pi^2} \sum_{r=0}^{\infty} g_r \int_{-\infty}^{\infty} dp_{\parallel} \ln\{1 + \exp[(\mu - \varepsilon_r)/T]\} \tag{2}$$

where α is the fine structure constant, V is the volume, $g_r = 2 - \delta_{r0}$ is the degeneracy, and μ is the chemical potential including rest mass (e.g., Lifshitz and Pitaevskii 1980). The Fermi temperature T_F is defined to be the temperature corresponding to the Fermi kinetic energy of the same density of electrons in the absence of a magnetic field, i.e.,

$$T_F = \mu - 1 + \frac{\pi^2}{6} \frac{T^2}{\mu} \frac{2\mu^2 - 1}{\mu^2 - 1} + O(T^4) . \tag{3}$$

Now, the magnetization M is given by

$$M = -\frac{1}{V} \left(\frac{\partial \Omega}{\partial B} \right)_{\mu, V, T} \tag{4}$$

and the susceptibility $\chi = M/H \simeq M/B$ for the small values of concern to us. In addition, we will also be interested in the differential susceptibility, η, which is defined by

$$\eta = (\partial M / \partial B)_{T, V, \mu} . \tag{5}$$

Although, in general, $4\pi|\chi| \ll 1$ for a relativistic electron gas, in certain regimes $4\pi|\eta|$ can exceed unity, indicative of the possibility of the existence of magnetic domains.

The magnetization is easily computed under three separate approximations which we now consider.

2.1.1. Weak field ($B \ll \mu T \ll \mu T_F$)

When the thermal energy ($\sim T$) is large compared with the spacing of the Landau levels ($\sim B/\mu$) but small compared with the Fermi temperature, we can

replace the sum in equation (2) by using the Euler-MacLaurin sum formula (e.g., Lifshitz and Pitaevskii 1980),

$$\tfrac{1}{2}\sum_{r=0}^{\infty} g_r f(r) = \int_0^{\infty} f(s)ds - \sum_{k=1}^{\infty} \frac{B_{2k}}{(2k)!} f^{(2k-1)}(0) \tag{6}$$

where B_{2k} are the Bernoulli numbers. The integral is independent of B and does not contribute to the magnetization. Ignoring a constant,

$$\Omega = -\frac{\alpha V}{12\pi^2} B^2 \int_0^{\infty} \frac{dp_{\parallel}}{(1+p_{\parallel}^2)^{1/2}[\exp\{(\varepsilon_0-\mu)/T\}+1]} + O(B^4) . \tag{7}$$

Using equation (4) to compute M we obtain, after some manipulation,

$$\chi = \frac{\alpha}{6\pi^2}\ln[\mu + (\mu^2-1)^{1/2}] - \frac{\alpha\mu(\mu-1)^{1/2}}{36(\mu+1)^{3/2}}\left[\frac{T}{T_F}\right]^2 + O\left[\frac{T}{T_F}\right]^4 + O(B^2) . \tag{8}$$

This is the relativistic generalization of the standard non-relativistic susceptibility (e.g., Lifshitz and Pitaevskii 1980). The first term has been given previously by Rukhadze and Silin (1960). Note that non-relativistically only 1/3 of the Pauli paramagnetic spin susceptibility is canceled by the diamagnetic contribution from the orbital motion, whereas in the extreme relativistic limit, the purely paramagnetic part, $\chi_p = (\alpha/4\pi^2)\mu(\mu^2-1)^{1/2}$, is almost completely canceled. The magnetic susceptibility is always less than 10^{-3} in the weak field limit.

2.1.2. Intermediate field ($\mu T < B \ll \mu T_F$)

When the thermal energy is small compared with the Landau level spacing, Ω develops an oscillatory part $\tilde{\Omega}$. As a result, the differential susceptibility can become large in magnitude. The computation of $\tilde{\Omega}$ is a straightforward relativistic generalization of the calculation in Lifshitz and Pitaevskii (1980). We obtain

$$\tilde{\Omega} = \frac{\alpha B^{3/2} VT}{2\pi^2}\sum_{k=1}^{\infty} \frac{\cos[2\pi(kr_{\max}-1/8)]}{k^{3/2}\sinh(kT/T_c)} \tag{9}$$

where $r_{max} = (\mu^2-1)/2B$ is the Landau level of highest energy occupied and $T_c = B/2\pi^2\mu$ is the critical temperature for the appearance of oscillations. The oscillatory part of the susceptibility is given by

$$\tilde{\chi} = -\frac{\alpha T(\mu^2-1)}{2\pi B^{3/2}} \sum_{k=1}^{\infty} \frac{\sin[2\pi(kr_{max}-1/8)]}{k^{1/2}\sinh(kT/T_c)}. \tag{10}$$

The non-oscillatory part is smaller than $\tilde{\chi}$ by $\sim O(r_{max}^{-1/2})$ and may be ignored. The quantity $\tilde{\chi}$ is still always less than $1/4\pi$. In the low temperature limit $T \ll T_c$, $\tilde{\chi}$ becomes

$$\tilde{\chi} = -\frac{\alpha}{4\pi^3} \frac{(\mu^2-1)}{\mu B^{1/2}} \sum_{k=1}^{\infty} \frac{\sin[2\pi(kr_{max}-1/8)]}{k^{3/2}}. \tag{11}$$

The sum is bounded above by $\zeta(3/2) = 2.61$.

The oscillatory part of the differential susceptibility is

$$\tilde{\eta} = \frac{\alpha T(\mu^2-1)^2}{2B^{5/2}} \sum_{k=1}^{\infty} \frac{k^{1/2}\cos[2\pi(kr_{max}-1/8)]}{\sinh(kT/T_c)}. \tag{12}$$

This quantity, which is $\sim r_{max}\tilde{\chi}$, can exceed $1/4\pi$.

2.1.3 Strong field ($\mu T \ll \mu T_F \lesssim B$)

When r_{max}, the number of Landau levels occupied, becomes small, the sum in equation (2) must be evaluated numerically. In the limit $B \to \infty$ all electrons occupy the ground level and the differential susceptibility vanishes.

In Figure 1, we display the regions of validity of these three approximations.

2.2 Numerical evaluation

We have computed the free electron differential susceptibility for different combinations of the temperature and Fermi temperature. Four cases are

plotted in Figure 2. As the flux density is increased into the intermediate field regime, de Haas-van Alphen oscillations set in and $|\tilde{\eta}|$ soon reaches its maximum value before declining $\propto B^{-3/2}$ at greater flux density. In the strong field region the period in $1/B$ becomes comparable with $1/B$.

3. Domain Formation

For a bounded sample in a uniform field the magnetic field H is related to the flux density B by the relation

$$H = B - 4\pi(1-n)M(B) \tag{13}$$

where n is the demagnetization coefficient which is fixed by the shape of the sample. For our application to a thin neutron star crust, permeated by an approximately vertical field, $n \sim 0$ and will henceforth be ignored. When the differential susceptibility $\tilde{\eta}$ exceeds $1/4\pi$, $(\partial H/\partial B)_{\mu,T}$ becomes negative, and the thermodynamic equilibrium becomes unstable (e.g., Lifshitz and Pitaevskii 1980). In fact, for the case $n = 0$, as discussed at length by Pippard (1963), Condon (1966), Azbel' (1970), and Pippard (1980), the material will separate into two phases corresponding to different (usually anti-parallel) magnetizations.

In Figure 3 we show the region of the $T-T_F$ plane in which the electrons are unstable to phase separation for different values of the flux density. We see that for low enough temperatures domain formation occurs over a density range limited at the low end by thermal effects and at the high end by the explicit dependence of $\tilde{\eta}$ upon the Fermi energy.

We may evaluate the change in magnetization across a domain interface using the boundary conditions for $\vec{B}$ and $\vec{H}$. If the fractional change in B is small and the field makes an angle θ with the interface, then

$$\frac{H_2-H_1}{B_2-B_1} \approx -\tan^2\theta \tag{14}$$

where the subscripts 1 and 2 refer to the two domains. The field is deflected through an angle

$$\delta\theta \simeq \frac{B_2-B_1}{B_1}\tan\theta \tag{15}$$

at the interface. Equation (14) shows that the field H must decrease as the flux density B increase across the interface separating two domains.

A second relation between the flux density and the field strength is furnished by the "equal area" rule

$$\int_{B_1}^{B_2} H(B)dB = \frac{1}{2}(B_2-B_1)(H_1+H_2) \tag{16}$$

where the integral is over the unstable portion of the $H(B)$ curve. Thus, given the angle θ, both B_1 and B_2 are fixed by equations (14) and (16) and the shape of the magnetization curve. Note that there is a maximum allowed angle θ.

If the electron gas is to be regarded as a fluid in thermodynamic equilibrium, i.e., there are no strains in the ionic lattice communicated to the electron gas by electric fields, then there is a third condition which must be satisfied. The pressure, which is hydrostatic and is given by $-\Omega/V$, must be the same on either side of the domain interface. This implies that

$$\int_{B_1}^{B_2} M\,dB = 0 \tag{17}$$

or

$$B_1 + B_2 = H_1 + H_2 \tag{18}$$

using equations (4) and (16). In this case equation (18) should apply and the angle θ will be fixed at some non-zero value.

In Figure 4 we show the $H(B)$ relation for an electron gas at a temperature $T = 0.1$ keV for two different Fermi temperatures.

4. Neutron Star Crusts

4.1 Structure

As can be seen from Figure 3, domain formation should occur in the crust of magnetized ($B \sim 10^{12}$ G) neutron stars at densities $\rho \sim 10^6\,\mathrm{g\,cm^{-3}}$ below temperatures $T \sim 10^7$ K. According to cooling calculations (e.g., Tsuruta 1981), the crust should become sufficiently cool after $\sim 10^4$ yr, a time much shorter than a typical radio pulsar age ($\sim 3\times10^6$ yr).

The variation of the magnetic susceptibility is, however, crucially different from the usual situation encountered in solid state physics in which oscillatory magnetization appears as H is varied. In a neutron star crust, we expect that H will be determined by currents which flow within a region ~ 10 km in size and that the field is locally constant. However, as the depth z below the surface increases, the Fermi temperature T_F increases and it is this variation which is responsible for the oscillatory magnetization.

The thickness of the crust is determined by the surface gravity $g = 10^{14} g_{14}\,\mathrm{cm\,s^{-2}}$. It can be shown that for degenerate electron pressure support,

$$z = \frac{1}{m_p g}\int \frac{dT_F}{\mu_e} \simeq 50\left[\frac{T_F}{1\,\mathrm{MeV}}\right] g_{14}^{-1}\left[\frac{\mu_e}{2}\right]^{-1}\mathrm{m} \qquad (19)$$

where μ_e is the mean molecular weight per electron which varies between $\sim 2-3$

in the crust (e.g., Baym and Pethick 1975).

At the surface density $\rho \sim 10^4\,\mathrm{g\,cm^{-3}}$ for a field $B = 10^{12}B_{12}G$ all the electrons will be in the ground state Landau orbital. However, as the density increases, the number of Landau orbitals $r_{max} \simeq 20(\mu^2-1)B_{12}^{-1}$ will also increase. The spacing between layers associated with successive integral values of r_{max} is

$$\Delta z = \frac{B}{\mu}\frac{dz}{d\mu} = \frac{B}{\mu\mu_e m_p g} \approx 55 g_{14}^{-1}\left(\frac{\mu_e}{2}\right)^{-1}\mu^{-1}B_{12}\,\mathrm{cm}\,. \tag{20}$$

At non-relativistic Fermi temperatures, the spacing is constant. If the temperature is low enough for domains to form, then Δz is the average vertical spacing between domain interfaces. In this case, the horizontal variation in the field will be

$$\frac{\delta B}{B} = \frac{2B\beta}{(\mu^2-1)} \simeq 0.48 B_{12}(\mu^2-1)^{-1}\beta \tag{21}$$

where $\beta \lesssim 1$ is the strength of the oscillation relative to the maximum allowed oscillation. For $T \ll T_c$, $\beta \sim 1$.

The actual size and shape of the domains is problematical. There seem to be two possibilities. The first is that the domains have a horizontal scale $\sim\Delta z$ which is in general required if there is to be a balance in the electron pressures. The second possibility is that the domains form a two-dimensional lattice of vertical needles of thickness given roughly by the geometrical mean of the Larmor radius and $\Delta z \sim 10^{-4}\,\mathrm{cm}$. This second configuration minimizes the sum of magnetic and surface energy (e.g., Pippard 1980). The choice between these two possibilities is probably governed by the magnetization history and the ability of the lattice to withstand stresses (see § 4.4 below).

In either case, unless there is some magnetization structure on a length scale comparable with the depth z, there should not be any influence on the

surface field as the amplitude of the field perturbation will be smaller than that given by equation (21) by a factor $\sim\exp(-\pi z/\Delta z)$.

4.2 Collisional broadening

Electron scattering will broaden the Landau levels and may damp the de Haas-van Alphen oscillations (Dingle and Schoenberg 1950; Springford 1980). Collisional broadening is negligible when the collision frequency ν_c is much smaller than the gyrofrequency eB/μ. An approximate non-relativistic calculation gives the result that the terms in the sum in equation (9) must each be multiplied by a factor $\exp[-k\pi\nu_c/eB]$ (Higgins and Lowndes 1980). The collision frequency has been computed by Urpin and Yakovlev (1980a,b) and Yakovlev and Urpin (1980). For solid iron, neglecting impuring scattering, $\nu_c \sim 3\times10^{16}(T/10^6\,\mathrm{K})\rho_6^{-1/3}\,\mathrm{Hz}$. By inspection of Figure 1, we see that electron collisions should not affect the de Haas-van Alphen oscillations.

4.3 Eddy Currents

As the neutron star crust cools and regions of previously uniform magnetization become unstable, internal conduction currents will grow and lead to the creation of domains on the ohmic dissipation time, t_d. Using the Yakovlev and Urpin (1980) conductivity for a solid crust, we obtain

$$t_d \sim 3\times10^5(w/1\mathrm{m})^2\rho_6^{4/3}T_6^{-1}\,\mathrm{s} \qquad (22)$$

where w is the horizontal length-scale for field variation. We have assumed that the geometry is such as to allow the creation of a Hall field. Again, we have ignored possible impurities and lattice defects. We can also use equation (22) to verify that small scale conduction currents in the outer crust ($\rho \lesssim 10^8\,\mathrm{g\,cm^{-3}}$) will probably have decayed. (See Blandford, Applegate, and Hernquist 1983, for

an alternative viewpoint.)

4.4 Magnetostriction

As can be seen from Figures 1 and 3 the crust will be solid whenever domain formation is possible. In general the formation or adjustment of domain structure involves anisotropic magnetostrictive stresses $\sim 2\pi M^2$ (see Appendix). These will be balanced by elastic stresses in the lattice provided that they do not exceed the yield stress for shear flow Y. From Ruderman (1972), we estimate

$$Y \sim Z^2 e^2 (\rho / A m_p)^{4/3} \varepsilon \sim 4 \times 10^{18} \rho_6^{4/3} \varepsilon_{-3} \text{ dyne cm}^{-2} \tag{23}$$

where $\varepsilon = 10^{-3} \varepsilon_{-3}$ is the maximum allowed strain angle. Unless the crystal is unusually pure, we expect that $\varepsilon_{-3} \sim 1$. Using equation (11) we find that the maximum flux density which the crystal lattice can withstand satisfies

$$B_{\max 12} \sim (1 + 0.6 \rho_6^{2/3}) \varepsilon_{-3} \, . \tag{24}$$

If $B > B_{\max}$, the crust will crumble and the domains will adjust to a lower energy state on the eddy current decay time given by equation (22). The domain structure will be constrained by electron pressure balance.

5. Discussion

Most old radio pulsars appear to have surface flux densities in the range $1-5 \times 10^{12}$ G (e.g., Manchester 1981) and surface gravities $\sim 2 \times 10^{14} \text{ cm s}^{-2}$ (e.g., Bahcall 1978). We expect the outer crust to be isothermal with a temperature $T \leq 10^6$ K (e.g., Arons 1981). Therefore domains will form below a depth $z \sim 5-10$ m with a vertical spacing $\Delta z \sim 20-50$ cm.

Old pulsars often show complex and stable pulse profiles. There is no well-accepted theory of pulsar radio emission, but it is widely believed that the pulse structure has its origin in quasi-permanent magnetic or topographic features on the neutron star surface. These features indicate the places where current is preferentially drawn from the stellar surface (e.g., Ruderman 1981). It is intriguing to enquire if they could be connected in any way with sub-surface domain structure.

This connection is unlikely to be direct unless the domains have horizontal structure on a length-scale $\sim z$, since structure on smaller scales will lead to exponentially small surface effects. Further, the maximum free energy associated with the domains ($\sim 10^{20}$ ergs per domain) is very small by neutron star standards.

However, there are some possibilities for an indirect connection. The current believed to be flowing through the polar cap of a pulsar with period $\sim$0.3–3 s is roughly $I \sim 10^{11}$–$10^{12} A$. If this current crosses the field at a depth d then the associated magnetic perturbation is $\delta B \sim 10^{10}(I/10^{12}\mathrm{A})(d/1\mathrm{m})^{-1}\,\mathrm{G}$. The depth to which the currents flow is determined by the surface potential variation and the time that has elapsed since the potential was established. Presumably the currents flow over a region as large as the polar cap $\sim$100 m in size. However, for the currents to penetrate to a depth $\sim$100 m requires $\sim 10^6 T_6^{-1}$ yr, using equation (22). If these currents flow at depths in the range 10–100 m then they may be responsible for establishing large-scale patterns of magnetization.

Secondly, the fact that the maximum field given by equation (24) is close to the observed surface field suggests that the crustal regions are seismically active. Any sudden readjustment of the domain structure will cause a local departure from isostasy which will be relieved on the ohmic dissipation

timescale. At the surface this time is of the order a few seconds, which is a characteristic timescale for marching subpulses.

Finally, there will be small-scale fluctuations in the transport properties of the crust because of the domains. If the domains are arranged regularly, then it is possible that they cause thermal or potential patterns on the surface.

However, we have no more specific proposals for the possible observational consequences of domain formation. It is most likely that their effects are negligible.

Acknowledgements

We thank Nordita and the Institute of Astronomy for hospitality and financial support. We acknowledge helpful discussions with E. Gudmundsson, C. Pethick, and S. Tsuruta. The support of the National Science foundation [AST80-17752] and the Alfred P. Sloan Foundation is gratefully acknowledged.

Appendix

Some confusion has arisen in the literature concerning the pressure of a degenerate electron gas in a magnetic field (e.g., Canuto and Chiu 1971; Schmid-Burgk 1973). From a thermodynamic point of view, the pressure can be derived from the grand potential as

$$P = -\left(\frac{\partial \Omega}{\partial V}\right)_{\mu,T,B} = -\frac{\Omega}{V}. \tag{A1}$$

This pressure is isotropic. However, the *kinetic* pressure of the electrons is anisotropic. The components resolved parallel and perpendicular to the field direction can be expressed as follows

$$P_{\parallel}^{k} = \int_{-\infty}^{\infty} dp_{\parallel} \sum_{r=0}^{\infty} \frac{\alpha B}{4\pi^2} g_r \frac{p_{\parallel}^2}{\varepsilon_r} [\exp(\varepsilon_r - \mu)/T + 1]^{-1}$$

$$= -\Omega/V \tag{A2}$$

$$P_{\perp}^{k} = \int_{-\infty}^{\infty} dp_{\parallel} \sum_{r=1}^{\infty} \frac{\alpha B}{4\pi^2} g_r \frac{\langle p_{\perp}^2 \rangle}{\varepsilon_r} [\exp(\varepsilon_r - \mu)/T + 1]^{-1}. \tag{A3}$$

Now $\langle p_{\perp}^2 \rangle = rB$, averaging over the two spin states. Equation (A3) can be related to equation (2) after an integration by parts by

$$P_{\perp}^{k} = \frac{B^2}{V}\left(\frac{\partial}{\partial B}(\Omega/B)\right)_{\mu,V,T} = -\frac{\Omega}{V} - MB. \tag{A4}$$

However, if we compress the electron gas perpendicular to B then must also do work against the Lorentz force density involving the magnetization current density, $(\nabla \times \vec{M}) \times \vec{B}$. There is therefore an additional magnetic contribution to the perpendicular pressure of magnitude MB which cancels the second term in (A4). The composite pressure tensor is therefore isotropic, in agreement with the

thermodynamic result, equation (A1).

In a body of arbitrary shape, there will be additional anisotropic stresses $\sim 2\pi M^2$ associated with the demagnetization field. In a solid these will be balanced by elastic stresses.

References

Arons, J. 1981, *Astrophys. J.* **248**, 1009.

Azbel' M. Ya. 1970, *Soviet Phys. Uspekhi* **12**, 507.

Bahcall, J. N. 1978, *Ann. Rev. Astron. Astrophys.* **16**, 241.

Baym, G. and Pethick, C. 1975, *Ann. Rev. Nucl. Sci.* **25**, 27.

Berestetskii, V. B., Lifshitz, E. M., and Pitaevskii, L. P. 1982, *Quantum Electrodynamics* , Pergamon Press, Oxford.

Blandford, R. B., Applegate, J., and Hernquist, L. 1983, *Mon. Not. R. astr. Soc.* **204**, 1025.

Canuto, V. and Chiu, H. Y. 1971, *Sp. Sci. Rev.* **12**, 3.

Condon, J. H. 1966, *Phys. Rev.* **145**, 526.

Dingle, R. B. and Shoenberg, D. 1950, *Nature* **166**, 652.

Flowers, E. and Itoh, N. 1981, *Astrophys. J.* **250**, 750.

Higgins, R. J. and Lowndes, D. H. 1980, in *Electrons at the Fermi Surface*, ed. Springford, M., Cambridge University Press, Cambridge.

Lee, H. J., Canuto, V., Chiu, H. Y., and Chiuderi, C. 1969, *Phys. Rev. Lett.* **23**, 390.

Lifshitz, E. M. and Pitaevskii, L. P. 1980, *Statistical Physics* , Pergamon Press, Oxford.

Manchester, R. N. 1981, in *Pulsars*, ed. Sieber, W. and Wielebinski, R., Reidel, Dordrecht, Holland.

O'Connell, R. F. and Roussel, K. M. 1972, *Astron. Astrophys.* **18**, 198.

Pippard, A. B. 1963, *Proc. Roy. Soc. A* **272**, 192.

Pippard, A. B. 1980, in *Electrons at the Fermi Surface*, ed. Springford, M., Cambridge University Press, Cambridge.

Ruderman, M. A. 1972, *Ann. Rev. Astron. Astrophys.* **10**, 427.

Ruderman, M. A. 1981, in *Pulsars*, ed. Sieber, W. and Wielebinski, R., Reidel, Dordrecht, Holland.

Rukhadze, A. A. and Silin, V. P. 1960, *Sov. Phys. JETP* **11**, 463.

Schmid-Burgk, J. 1973, *Astron. Astrophys.* **26**, 335.

Schoenberg, D. 1962, *Phil. Trans. R. Soc. A* **255**, 85.

Slattery, W. L., Doolen, G. D. and De Witt, H. E. 1980, *Phys. Rev. A* **21**, 2087.

Springford, M. 1980, in *Electrons at the Fermi Surface*, ed. Springford, M., Cambridge University Press, Cambridge.

Tsuruta, S. 1981, in *Pulsars*, ed. Sieber, W. and Wielebinski, R., Reidel, Dordrecht, Holland.

Urpin, V. A. and Yakovlev, D. G. 1980a, *Soviet Astronomy* **24**, 126.

Urpin, V. A. and Yakovlev, D. G. 1980b, *Soviet Astronomy* **24**, 425.

Yakovlev, D. G. and Urpin, V. A. 1980, *Soviet Astronomy* **24**, 303.

Figure Captions

Figure 1.

Weak, intermediate, and strong field regions in the $T-T_F$ plane. For each value of the flux density B the curved line separates the intermediate field region where de Haas-van Alphen oscillations can occur from the weak field region at higher temperature. Each line is terminated on the left by a vertical line denoting the boundary of the strong field region. Also shown are the limit of the degenerate region (dashed line) and the melting curve for neutron star matter (e.g., Flowers and Itoh 1981; Slattery, Doolen, and De Witt 1980). The densities correspond to the lowest energy ionic lattice.

Figure 2.

Differential susceptibility $\tilde{\eta}$ as a function of B for two values of both the Fermi temperature T_F and the temperature T. At low flux densities, where the de Haas-van Alphen oscillation frequency becomes large, only the envelope of the susceptibility is shown.

Figure 3.

Region of $T-T_F$ plane in which $4\pi\tilde{\eta}$ can exceed unity. When T is less than the value indicated the electron gas is unstable to the formation of two phases of different magnetization.

Figure 4.

$H(B)$ curve for T = 0.1 keV and flux density B near 10^{12} G for electron gases of Fermi temperatures 0.3 and 1 MeV. The corresponding densities are

$\rho = 3.9\times10^{6}$, $4.5\times10^{7}\,\mathrm{g\,cm^{-3}}$, respectively. Also shown is the line (dashed) representing $B = H$. Both curves are unstable and the phase diagram for $T = 0.3\,\mathrm{MeV}$ is drawn, assuming an angle of 30° between the domain interface and the field.

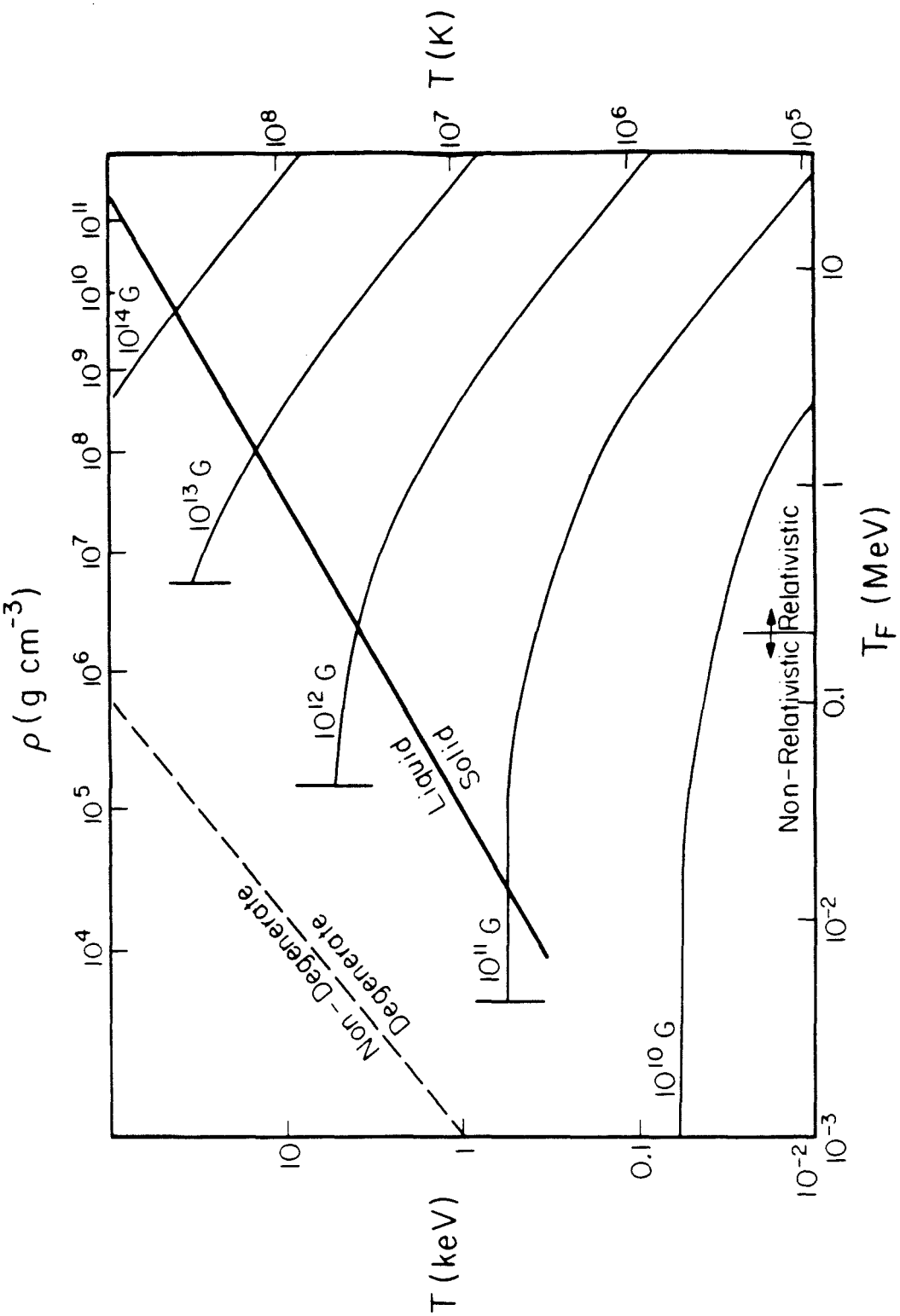
ρ (g cm⁻³)
T (K)
T (keV)
T_F (MeV)
Non-Degenerate
Degenerate
Liquid
Solid
Non-Relativistic
Relativistic
10¹⁴ G
10¹³ G
10¹² G
10¹¹ G
10¹⁰ G

Figure 1

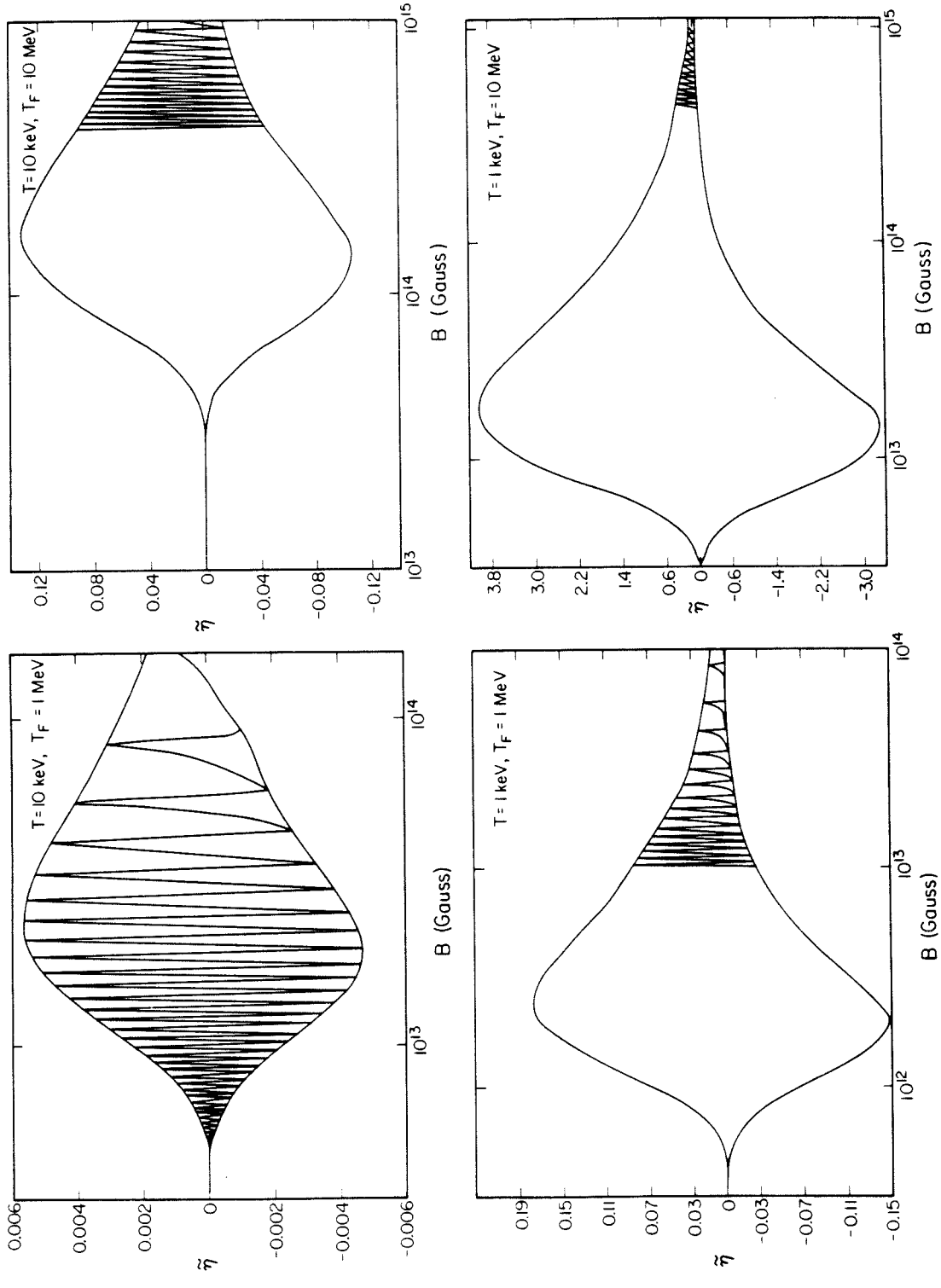
T = 10 keV, T_F = 10 MeV
T = 1 keV, T_F = 10 MeV
T = 10 keV, T_F = 1 MeV
T = 1 keV, T_F = 1 MeV
$\tilde{\eta}$
B (Gauss)

Figure 2

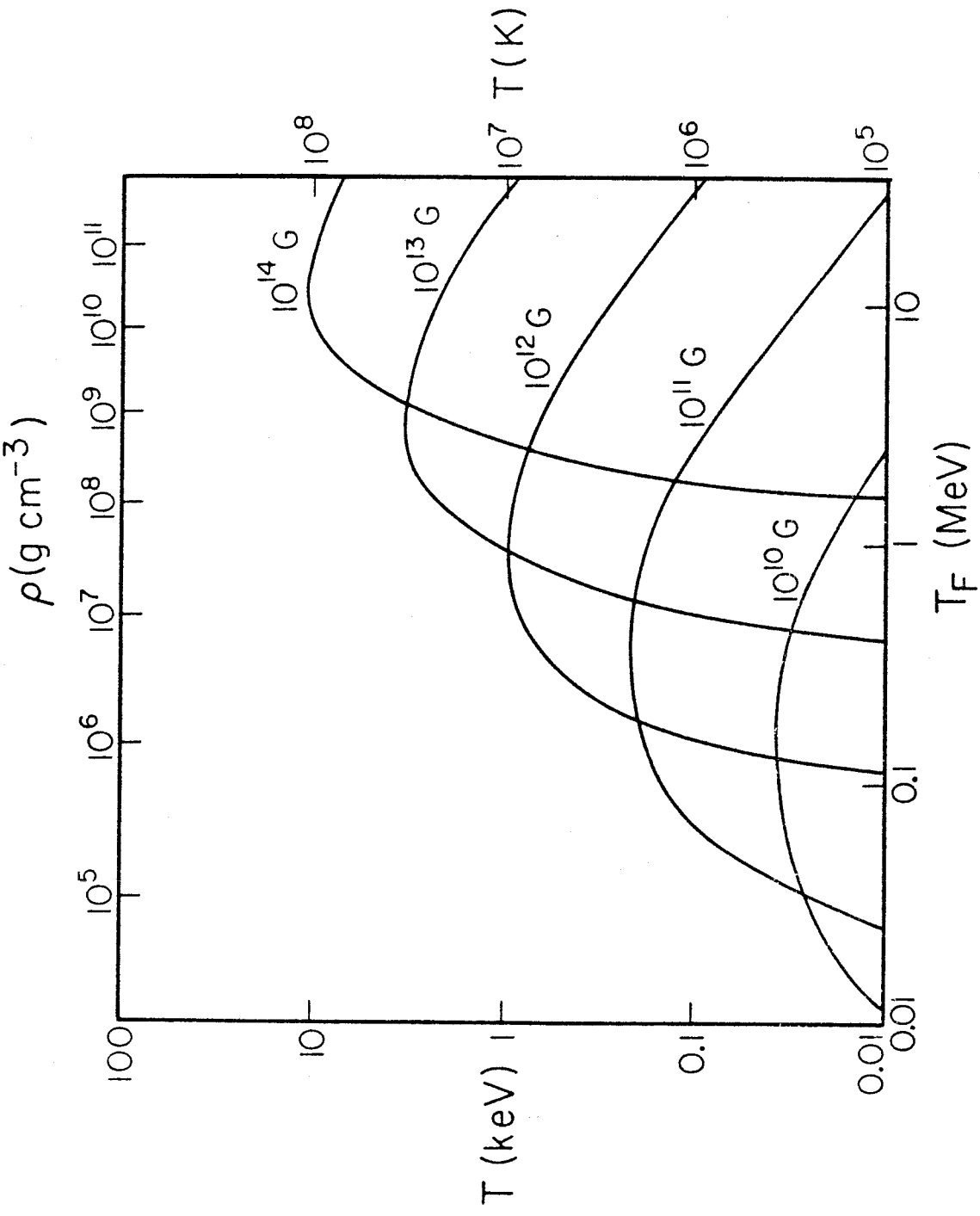
ρ(g cm^{-3})
10^{5}
10^{6}
10^{7}
10^{8}
10^{9}
10^{10}
10^{11}
100
10
1
0.1
0.01
T (keV)
10^{8}
10^{7}
10^{6}
10^{5}
T (K)
10^{14} G
10^{13} G
10^{12} G
10^{11} G
10^{10} G
10
1
0.1
0.01
T_F (MeV)

Figure 3

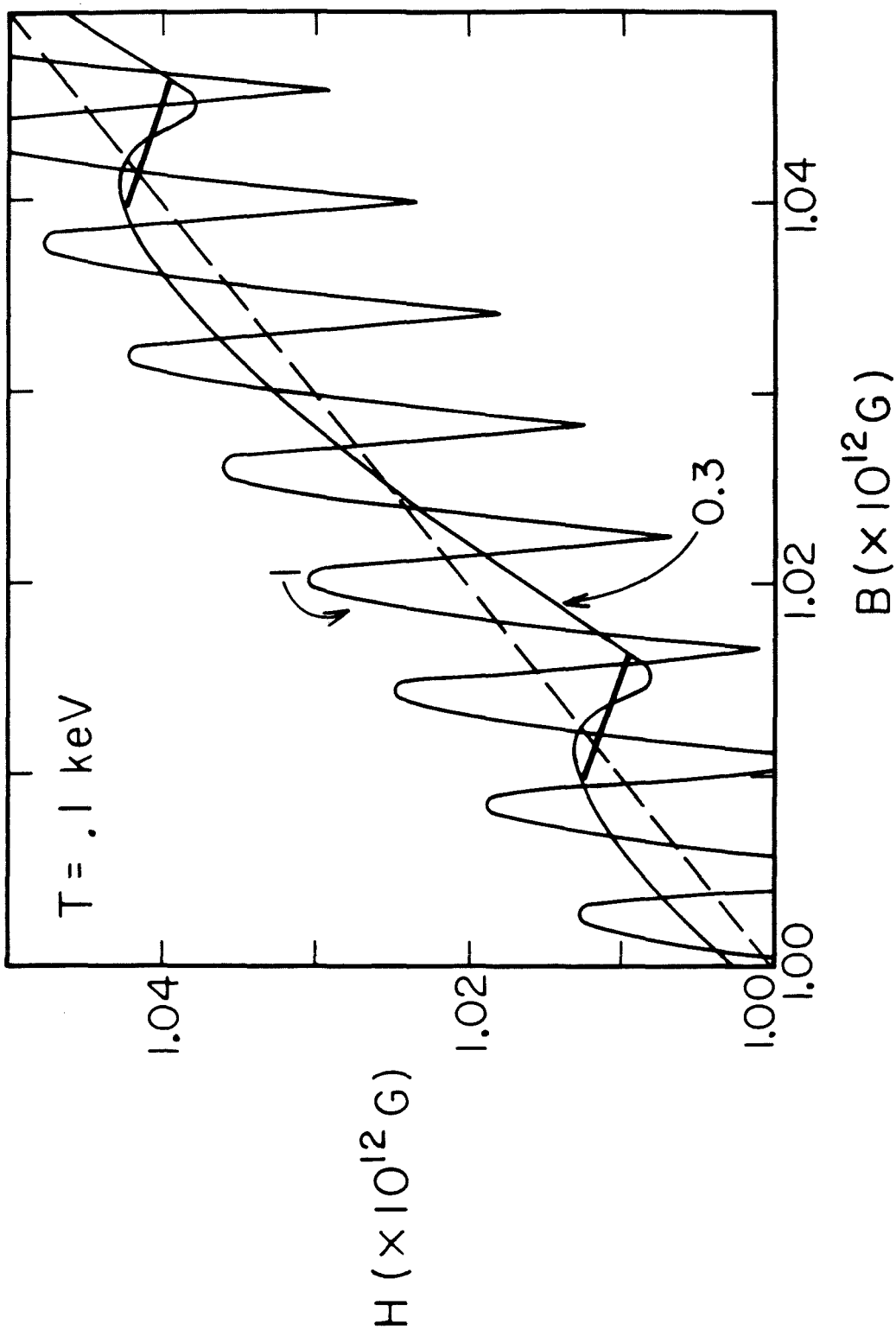

Figure 4

CHAPTER 3

Thermal Origin of Neutron Star Magnetic Fields.

Roger Blandford, James Applegate, and Lars Hernquist

Published in

Monthly Notices of the Royal Astronomical Society

(1983, **204**, 1025).

Thermal Origin of Neutron Star Magnetic Fields

R.D. Blandford, J.H. Applegate, and L. Hernquist

Theoretical Astrophysics, California Institute of Technology

ABSTRACT

It is proposed that magnetic field arises naturally in neutron stars as a consequence of thermal effects occurring in their outer crusts. The heat flux through the crust, which is carried mainly by degenerate electrons, can give rise to a possible thermoelectric instability in the solid crust which causes horizontal magnetic field components to grow exponentially with time. However, in order for the thermally driven growth to exceed ohmic decay, either the electron collision time must exceed existing estimates by a factor ~3 or the surface layers comprise helium. A second instability is possible if the liquid phase that lies above the solid crust also contains a horizontal magnetic field. The heat flux will drive circulation which should amplify the field strength provided that there is a seed field in excess of $\sim 10^6$ G.

If either of these two instabilities develops the field will quickly grow to a strength of $\sim 10^{12}$ G, where the instabilities become non-linear. Further growth will saturate when either the magnetic stress exceeds the lattice yield stress or the temperature perturbations become non-linear, both of which occur at a subsurface field strength of $\sim 10^{14}$ G; the corresponding surface field strength

is $\sim 10^{12}$ G. Further evolution of the magnetic field should lead to long range order and yield neutron star magnetic dipole moments $\sim 10^{30}$ G cm^3, comparable with those observed.

Newly-formed neutron stars should be able to develop their dipole moments in a hundred thousand years, and maintain them for as long as heat flows through the crust. Thereafter, the dipole moment should decay in several million years, as observed in the case of most radio pulsars. Neutron stars that are formed spinning rapidly, like that in the Crab Nebula, should be able to grow magnetic fields far more rapidly since their rotational energy can also be tapped to drive thermoelectric currents. The interiors of neutron stars in binary systems may be heated by the energy released by accreting matter. The resulting heat flux may cause the production of magnetic fields in these objects. Binary pulsars, with their unusually low and persistent fields, have probably passed through this phase.

1. Introduction

Timing observations indicate that surface magnetic fields of radio pulsars ($\propto(P\dot{P})^{1/2}$, where $\dot{P}$ is the period derivative) have values in the range $1-5\times10^{12}$ G, with surprisingly little scatter (e.g., Manchester 1981). This range of neutron star surface field strengths has been corroborated by the direct observation of cyclotron lines in Her X-1 (Trümper *et al.* 1978), 4U0115+63 (Wheaton *et al.* 1979), GX1+4 (Maurer *et al.* 1982), 4U1626-67 (Pravdo *et al.* 1979), and the Crab Pulsar (Manchanada *et al.* 1982). Analyses of period changes in pulsating X-ray sources (e.g., Rappaport and Joss 1977; Ghosh and Lamb 1979) caused by magnetic coupling between the neutron star and the accreting plasma yield values of neutron star magnetic moments consistent with surface fields $\sim10^{12}$ G. The spectra of gamma ray bursts show features interpretable as cyclotron absorption lines, as well as possible positron annihilation features, indicating that the burst sources are magnetized neutron stars with surface fields $\sim10^{12}$ G (Mazets *et al.* 1981; but see Fenimore *et al.* 1982).

There are indications that the magnetization of neutron stars is not permanent. Radio pulsars have a scale height ~500 pc above the galactic plane and one-dimensional velocities ~100 km/s away from the galactic plane, strongly suggesting that they are active for no more than a few million years (e.g., Lyne 1981). Comparison of the kinetic ages (distance above the galactic plane/velocity normal to the galactic plane) of pulsars with the timing ages, $P/2\dot{P}$, shows serious disagreement. The kinetic age, believed to be the true age, is shorter than the timing age for pulsars older than a few million years (e.g., Lyne 1981), a fact that may be concluded independently from the joint distribution of pulsars in P and $\dot{P}$ (e.g., Lyne 1981). One long-standing explanation for these difficulties (e.g., Gunn and Ostriker 1970) is that the magnetic field decays in a few million years, suppressing coherent radio emission and

increasing the timing age (alternative explanations may be found in Goldreich 1970; Flowers and Ruderman 1977; Vivekanand and Radhakrishnan 1981). Further evidence for a changing magnetization is supplied by galactic X-ray sources, the majority of which show no evidence of pulsation and presumably involve emission from an entire neutron star surface, rather than just a polar cap (e.g., Joss 1980; but see Inoue *et al.* 1981).

The simplest mechanism for field decay is ohmic diffusion; however, apart from the outermost crust, neutron stars cannot ohmically disspate a magnetic field in a million years. The protons in the core of a neutron star are believed to form a type II superconductor; any flux threading the core when the star cools below the transition temperature will be trapped there, essentially forever. At densities below nuclear, where there are no superconducting protons, the electrical conductivity is far too high to allow ohmic dissipation in a million years. Thus, if field decay is to occur, it appears essential that the surface flux penetrate only to a depth $\lesssim 1$ km, where the electrical conductivity is low enough to allow ohmic dissipation to operate on the requisite timescale. The subsurface field would then be $\gtrsim 10^{13}$ G, assuming 10^{12} G fields at the polar caps. A field of this size will cause a substantial modification of the surface structure and transport properties.

There is an additional reason for believing that neutron stars possess subsurface horizontal fields. In the pulsating X-ray sources, matter is believed to be accreted at the magnetic poles of the neutron star. However, there must be a continuous flow of matter from the poles to the equatorial regions in order for the star to re-establish hydrostatic equilibrium. If the stellar field were just a simple dipole, the matter would sink to a depth at which its pressure could overcome the magnetic stresses. At this point the matter would spread sideways, dragging the magnetic field lines with it, as ohmic dissipation is quite ineffective

on a flow timescale (Blandford *et al.* 1979).

There is evidence that neutron stars become magnetized after they are formed. Observations of the supernova remnant MSH 15-52 and its embedded pulsar (Seward and Harnden 1982; Seward *et al.* 1983; Weisskopf, *et al.* 1983) show a pulsar with a timing age of $P/2\dot{P} = 1550\,\mathrm{yr}$ in a supernova remnant estimated to be $\sim 10^4\,\mathrm{yr}$ old. The apparent ages, discrepant if the pulsar field is a stellar fossil, are reconciled if the neutron star is as old as the SNR, but became a pulsar $\sim 10^3\,\mathrm{yr}$ ago when its magnetic field grew to sufficient strength. Vivekanand and Narayan (1981) have suggested on the basis of the distribution of pulsars in P , $\dot{P}$ that the majority of neutron stars do not become pulsars until long after being formed. Observations of the supernova remnant RCW103 (Tuohy and Garmire 1980) show a hot neutron star but no radio pulsar or plerionic nebula, suggesting that the neutron star does not possess a magnetic field. The X-ray source Her X-1 is estimated to be $\sim 10^8\,\mathrm{yr}$ old (van den Heuvel 1977), and yet possesses a magnetic field of $\sim 5\times 10^{12}\,\mathrm{G}$ (Trümper *et al.* 1978). The unusual longevity of the field, difficult to understand if the field is a fossil, is explained if the field is a product of the accretion process that powers the X-ray source.

Detailed cooling calculations (e.g., Tsuruta 1979; Glen and Sutherland 1980; Nomoto and Tsuruta 1981; Van Riper and Lamb 1981; Richardson *et al.* 1982) have shown that the interior temperature of a neutron star falls from $>10^9\,\mathrm{K}$ to $\sim 10^8\,\mathrm{K}$ in the first 10^5 years of its life. At these early times the neutron star cools predominantly by neutrino emission; however, there is still a heat flux through the crust, decreasing from $\sim 10^{22}\,\mathrm{erg/cm^2 s}$ to $\sim 10^{19}\,\mathrm{erg/cm^2 s}$, as the star cools. This heat flux, insignificant in the total energetics, is quite important observationally; it is the source of the thermal X-rays observed from neutron stars (e.g., Helfand *et al.* 1980). At densities above $10^5\,\mathrm{g/cm^3}$ the heat

transport is by electron conduction; at lower densities photon transport dominates. The magnitude of the heat flux is largely determined by the electron conduction opacity in the liquid ($10^6\,\mathrm{g/cm^3} \le \rho \le 10^8\,\mathrm{g/cm^3}$ for $T \sim 10^8\,\mathrm{K}$) (Gudmundsson *et al.* 1982).

The principal effect leading to field generation can be understood as follows. Suppose that there is a small horizontal component of magnetic field of strength B. Hot electrons from below will be deflected horizontally by the field; cooler electrons from above will be deflected slightly less in the opposite direction. The net effect is to produce a horizontal heat flux, $F_\perp \sim (e\tau/\mu)\vec{B}\times\vec{F}$, where $e = |e|$ is the magnitude of the electronic charge, τ is the electron collision time, μ is the electron chemical potential, and $\vec{F}$ is the vertical heat flux. (We use units in which $c = k_B = \hbar = 1$.) Fourier components of the magnetic field with horizontal wavelength comparable with the depth z create horizontal temperature gradients $\sim F_\perp/\kappa$, where κ is the thermal conductivity. The pressure of a degenerate, relativistic free electron gas is $P(n_e,T) = P(n_e,T=0) + (\pi^2/6)n_e T^2/\mu$. Hence there is an additional pressure gradient $\sim n_e T\nabla T/\mu$, which must be balanced by a thermoelectric field $E \sim T\nabla T/\mu e \sim BF/\mu n_e$. This field has a non-vanishing curl and so $-\vec{\nabla}\times\vec{E} = \partial\vec{B}/\partial t = \Gamma_+\vec{B}$, where $\Gamma_+ \sim F/\mu n_e z$. The growth rate Γ_+ is positive when the heat flows down the density gradient. If we substitute characteristic values $F = 10^{20}\,\mathrm{erg/cm^2 s}$, $\mu = 4\,\mathrm{MeV}$, $n_e = 3\times10^{31}\,\mathrm{cm^{-3}}$, $z = 50\,\mathrm{m}$, then $\Gamma_+ \sim 300\,\mathrm{yr^{-1}}$. It is clear from this estimate, which does not depend directly upon the local transport coefficients, that there may be time for the field to grow as the star cools. Note that the potential difference across the crust associated with this electric field is only $\sim(B/10^8\,\mathrm{G})\mathrm{mV}$, far smaller than the potential differences induced by gravity and rotation. The important point is that this field alone has a non-vanishing curl.

It is necessary for the growth rate Γ_+ to exceed the ohmic decay rate Γ_- if the field is to grow. This may be estimated by $\Gamma_- \sim 1/4\pi\sigma z^2$. Substituting $\sigma \sim 10^{21}\,s^{-1}$ appropriate to these conditions yields a decay rate comparable to the growth rate. A more detailed calculation is necessary to determine if neutron star magnetic fields can have a thermal origin.

The idea of using thermoelectric currents to generate astrophysical fields is not new. Biermann (1950) (*cf.* Mestel 1961; Roxburgh 1966) showed that differential rotation in fluid stars can produce a misalignment of the isobars and the equipotentials, resulting in a battery effect. This idea, and its terrestrial counterpart (e.g., Hibberd 1979), have generally not found favor because the effect is quantitatively quite small and dynamo action induced by helical motion in the fluid is thought to be far more effective (e.g., Parker 1979; and in the neutron star case see Ruderman and Sutherland 1973). Thermoelectric effects can be far more important in a neutron star because standard dynamo action is inoperative in the solid crust.

This mechanism does have a laboratory counterpart. Megagauss magnetic fields are routinely produced in the coronal plasma surrounding laser fusion targets; however, the details of the mechanism are rather different because inertial effects allow a departure from hydrostatic equilibrium in this case (e.g., Stamper *et al.* 1971).

Linear growth of the field is impossible in the liquid phase. However, when the field exceeds $\sim 10^8$ G, magnetic perturbations to the heat flow will drive circulatory motion in the fluid with turnover times that are short compared with the ohmic decay time. These motions will probably induce dynamo-like action and can further enhance the field strength at the solid surface.

In the following section we summarize and extend the analysis of thermoelectric phenomena in degenerate stars due to Urpin and Yakovlev (1980b)

and calculate necessary conditions for field generation. In §3, a linearized calculation of the growth of the field in the solid crust is given, which demonstrates that small seed fields can grow exponentially for sufficiently large heat fluxes. Non-linear growth of the field in the liquid is described in §4. If the field strength can grow to $\sim 10^{11}$G, the electron gyrofrequency will exceed the collision frequency and the field growth in the solid will enter the non-linear phase. The Hall effect will lead to rapid convection of magnetic flux and the creation of progressively larger scale structure, perhaps resulting in the establishment of an axisymmetric field geometry. In the absence of external heat sources, the interior of the star will cool and the field will decay. These issues are discussed in §5. In §6 we outline some of the observational consequences of this theory for pulsars, binary X-ray sources, X- and γ-ray bursters, and white dwarfs.

2. Thermoelectric effects

We are concerned with the properties of the outer crust in the density range $10^7 \mathrm{g/cm^3} \leq \rho \leq 10^{11} \mathrm{g/cm^3}$, and for temperatures $T \sim 10^8$K. Under these conditions the electron gas is degenerate, and may be treated as ultrarelativistic and free to an accuracy of better than a few percent. In the presence of electric fields and gradients of chemical potential and temperature the laws of charge and heat transport are

$$\vec{j} = \overleftrightarrow{\sigma} \cdot \vec{\varepsilon} - \overleftrightarrow{\lambda} \cdot \vec{\nabla} T \tag{2.1a}$$

and,

$$\vec{F} = T \overleftrightarrow{\lambda} \cdot \vec{\varepsilon} - \overleftrightarrow{\gamma} \cdot \vec{\nabla} T \tag{2.1b}$$

where the electrochemical field $\vec{\varepsilon}$ is the sum of the electric field and the

chemical potential gradient $\vec{\varepsilon} = \vec{E} + \vec{\nabla}\mu/e$ (*cf.* Landau and Lifshitz 1960; Ashcroft and Mermin 1976; Ziman 1972). In these expressions $\vec{j}$ is the electrical current, $\vec{F}$ is the heat current, and $\vec{\sigma}$ is the electrical conductivity. The thermal conductivity $\vec{\kappa}$ and thermopower $\vec{Q}$ are related to the coefficients $\vec{\lambda}$ and $\vec{\gamma}$ by

$$\vec{Q} = (\vec{\sigma})^{-1}\cdot\vec{\lambda} \tag{2.2a}$$

$$\vec{\kappa} = \vec{\gamma} - T\vec{\lambda}\cdot\vec{Q}\,. \tag{2.2b}$$

The difference between $\vec{\kappa}$ and $\vec{\gamma}$ is of order $(T/\mu)^2$ for a free electron gas, and will be neglected in this paper. Various thermogalvanomagnetic effects (Hall, Nernst, Leduc-Righi, and Ettingshausen; *cf.* Landau and Lifshitz 1960) result from electric currents driven by temperature gradients, heat currents driven by electric fields, and the magnetic field dependence of the coefficients in (2.1a,b). The magnetization of the crust is much smaller than the magnetic field (Blandford and Hernquist 1982) and will be neglected.

Expressions for the transport coefficients $\vec{\sigma}$, $\vec{\kappa}$, and $\vec{\lambda}$ are derived from the relativistic Boltzmann transport equation

$$\vec{v}\cdot\vec{\nabla}_r f - e[\vec{E} + \vec{v}\times\vec{B}]\cdot\vec{\nabla}_k f = \int \frac{d^3k'}{(2\pi)^3} W(\vec{k},\vec{k}')[f(\vec{r},\vec{k}) - f(\vec{r},\vec{k}')] \tag{2.3}$$

where $f(\vec{r},\vec{k})$ is the electron distribution function and $W(\vec{k},\vec{k}')$ is the scattering rate. The scattering of electrons is by individual ions in the case of a liquid, and by phonons in the case of a solid. The scattering in the liquid is always elastic (ion mass $\gg$ electron mass); the scattering by phonons is elastic if the temperature exceeds the Debye temperature. As these are the important scattering mechanisms for the case of interest, elastic scattering is assumed, and the energy-dependent relaxation time approximation used (*cf.* Yakovlev and Urpin 1980).

The Boltzmann equation, (2.3), is solved by linearization in the standard manner (*cf.* Ashcroft and Mermin 1976). The distribution function is split into a Fermi-Dirac distribution, $f^{(0)}$, evaluated at the local values of T and μ, and a perturbation δf responsible for transporting heat, charge, etc. The scattering term in (2.3) is replaced by $-\delta f / \tau$, where the relaxation time τ is given by

$$\tau(\varepsilon_k)^{-1} = \int \frac{d^3k'}{(2\pi)^3} W(\varepsilon_k, \hat{k}\cdot\hat{k}')[1 - \hat{k}\cdot\hat{k}'] \tag{2.4}$$

where $\varepsilon_k = (k^2 + m^2)^{1/2}$ is the single particle energy. The resulting momentum space differential equation is integrated along unperturbed orbits to give

$$\delta f = \left[-\frac{\partial f^{(0)}}{\partial \varepsilon_k}\right] \tau \vec{v}\cdot\overleftrightarrow{\chi}\cdot\left[e\vec{E} + \vec{\nabla}\mu + \left[\frac{\varepsilon_k - \mu}{T}\right]\vec{\nabla}T\right] \tag{2.5}$$

where the inverse of the tensor $\overleftrightarrow{\chi}$ is

$$(\chi^{-1})_{ij} = \delta_{ij} + \varepsilon_{ijk} X_k \ , \tag{2.6}$$

with $\vec{X} = (e\tau/\mu)\vec{B}$.

Expressions for the transport coefficients $\overleftrightarrow{\sigma}$, $\overleftrightarrow{\kappa}$, and $\overleftrightarrow{\lambda}$ are obtained by substitution of (2.5) into expressions for the currents

$$\vec{j} = -2e \int \frac{d^3k}{(2\pi)^3} \vec{v}\,\delta f \tag{2.7a}$$

$$\vec{F} = 2 \int \frac{d^3k}{(2\pi)^3} \vec{v}(\varepsilon_k - \mu)\delta f \ . \tag{2.7b}$$

The electrical current, (2.7a), is the current of electrons times the charge per electron. The thermal current, (2.7b), is obtained by applying the first law of thermodynamics to a fixed volume. The change in energy is $-\vec{\nabla}\cdot\int(\varepsilon_k + \varphi)\vec{v}\,\delta f$ where φ is the single particle potential. However, adding particles with energy equal to the chemical potential adds no heat. To obtain the heat added

$-\vec{\nabla}\cdot(\mu+\varphi)\int\vec{v}\,\delta f$ must be subtracted from the energy added, where μ is the chemical potential of the system in the absence of the single particle potential. Writing the heat added as the negative of a divergence gives (2.7b) for the heat current. The transport coefficients obtained by substitution of (2.5) into (2.7a,b) are

$$\vec{\sigma} = \sigma_0\vec{\chi} = \frac{n_e e^2\tau}{\mu}\vec{\chi}, \tag{2.8}$$

$$\vec{\kappa} = \kappa_0\vec{\chi} = \frac{\pi^2 n_e T\tau}{3\mu}\vec{\chi}, \tag{2.9}$$

and

$$\vec{\chi} = -\frac{\pi^2 T}{3e}\frac{d\vec{\sigma}}{d\mu} \tag{2.10}$$

where n_e is the density of electrons.

Equation (2.1a) can be written in the form of a fluid equation as follows. Use the thermodynamic identity $d\mu = dP/n_e - S_e dT$, where $S_e = \pi^2 T/p_F v_F$ is the entropy per electron of the electrons, and multiply equation (2.1a) by the inverse of the electrical conductivity tensor, (2.8), to obtain

$$-en_e\vec{E} + \vec{j}\times\vec{B} - \vec{\nabla}P_e + \frac{\mu\vec{j}}{e\tau} - \vec{F}\,\frac{d(\mu/\tau)}{d\mu} = 0 \tag{2.11}$$

where $-\vec{\kappa}\cdot\vec{\nabla}T$ has been replaced by the heat flux $\vec{F}$, which is accurate to order $(T/\mu)^2$. The direct influence of gravity upon the electrons has been neglected, which is acceptable for $\mu \ll m_p$.

The first two terms in (2.11) constitute the Lorentz force per unit volume acting upon the electron gas. The third term is the electron pressure gradient. The fourth and fifth terms are derived from the force density exerted by the lattice upon the electrons, which may be written as

$$-2\int \frac{d^3k}{(2\pi)^3}\frac{\vec{p}}{\tau}\delta f = \frac{\mu\vec{j}}{e\tau} - \vec{F}\,\frac{d(\mu/\tau)}{d\mu} \tag{2.12}$$

expanding in a Taylor series about $\varepsilon_k = \mu$. In a nonrelativistic system with an energy independent relaxation time the vanishing of the electrical current implies the vanishing of the force density (2.12). This is not the case in a relativistic system because the ratio of momentum to velocity, $k/v = \varepsilon_k$, is variable; thus, the second term in (2.12) can contribute even if the first term vanishes and τ is constant.

The equation of hydrostatic equilibrium for the crust as a whole is

$$-\vec{\nabla}P_e - \rho\vec{\nabla}\varphi + \vec{j}\times\vec{B} + \vec{Y} = 0 \tag{2.13}$$

where φ is the gravitational potential, including centrifugal terms, and $\vec{Y}$ is the force density given by the divergence of the lattice stress tensor. The total charge density is negligible on length scales much larger than the Debye length. In writing the centrifugal terms as the gradient of a potential we have assumed that the crust is not differentially rotating. The equation of hydrostatic balance for the ionic lattice is the difference of (2.13) and (2.11)

$$en_e\vec{E} - \rho\vec{\nabla}\varphi - \frac{\mu\vec{j}}{e\tau} + \vec{Y} + \vec{F}\,\frac{d(\mu/\tau)}{d\mu} = 0\,. \tag{2.14}$$

To calculate the growth rate of the field write (2.1a) as $\vec{\varepsilon} = \vec{\sigma}^{-1}\cdot\vec{j} + \vec{Q}\cdot\vec{\nabla}T$, and take the curl, using Faraday's law to obtain

$$\frac{\partial\vec{B}}{\partial t} = -\vec{\nabla}\times\vec{\varepsilon} = \vec{\nabla}\times(\vec{V}\times\vec{B}) - \vec{\nabla}Q_0\times\vec{\nabla}T - \vec{\nabla}\times\left[\frac{\vec{\nabla}\times\vec{B}}{4\pi\sigma_0}\right] \tag{2.15}$$

with

$$\vec{V} = \frac{\vec{k}\cdot\vec{\nabla}T}{n_e\mu}\,\frac{d\ln(\mu/\tau)}{d\ln\mu} - \frac{\vec{j}}{en_e} \tag{2.16}$$

and where

$$Q_0 = -\frac{\pi^2 T}{3e\mu}\frac{d\ln\kappa_0}{d\ln\mu} \tag{2.17}$$

is the thermopower of the unmagnetized electron gas (*cf.* Urpin and Yakovlev 1980b). The three terms in (2.15) are interpretable as:

i) A convection of the field at a velocity given by the sum of the thermal diffusion velocity and the electron mobility. Note that at low field strength ($X \ll 1$) the thermal drift is in the direction of the temperature gradient.

ii) A battery term $\propto\vec{\nabla}n_e\times\vec{\nabla}T$, which describes the creation of field by thermoelectric currents. If, as is usually the case, $\vec{\nabla}T\cdot\vec{B}\times\vec{F} > 0$, this term will contain a part $\propto(-\vec{\nabla}n_e\cdot\vec{F})\vec{B}$ leading to exponential field growth when the heat flows down the density gradient. In a fluid the isotherms and equipotentials will coincide with the constant density surfaces and this term will vanish* (*cf.* eq. (2.13)).

iii) An ohmic decay term (third term in (2.15)).

*A rather different view has been expressed by Dolginov and Urpin (1980b; cf. also Dolginov and Urpin 1980a). They consider the possibility of thermomagnetic instability within fluid white dwarfs. They perform a linearized perturbation analysis based on the induction and energy equations (2.15) and (2.1b). However, they do not include hydrostatic equilibrium, which should be achieved on timescales far shorter than those associated with thermoelectric effects. In particular, in a fluid $\vec{\nabla}\rho\times\vec{\nabla}T = 0$, which implies that the r.h.s. of their equation (7b) vanishes, along with their growth rate.

3. Growth of Magnetic Field in the Solid Crust

3.1 STRUCTURE OF CRUST

We are interested in the crust at densities high enough to solidify at temperatures $T \sim 10^8$ K, and low enough to be a poor enough electrical conductor to allow ohmic decay in a million years. These requirements confine our attention to the density range $10^7 \text{g/cm}^3 \leq \rho \leq 10^{11} \text{g/cm}^3$. Here the crust is supported by degenerate relativistic electron pressure. The mean molecular weight per electron, μ_e, and the nuclear charge, Z, vary as a function of density through the crust (e.g., Baym and Pethick 1975); we adopt the average values $\mu_e = 2.5$ and $Z = 32$ and use these throughout the crust. For a thin crust the depth below the surface is given as a function of density as

$$z_4 = 1.5 \rho_9^{1/3} g_{14}^{-1} \tag{3.1}$$

where $10^4 z_4$ cm is the depth, $10^9 \rho_9 \text{g/cm}^3$ is the density, and $10^{14} g_{14} \text{cm/s}^2$ is the effective surface gravity. For a non-rotating star of gravitational mass M and surface area $4\pi R^2$ the surface gravity is

$$g = \frac{GM}{R^2}\left(1 - \frac{2GM}{R}\right)^{-1/2} = \frac{1}{\rho}\frac{dP}{dz}. \tag{3.2}$$

Most models of $1.4 M_\odot$ neutron stars have radii in the range 8–16 km and surface gravities $.85 \leq g_{14} \leq 4.2$.

The ions will form a Coulomb crystal when the plasma parameter Γ ($\Gamma \equiv (Ze)^2/ak_B T$, where a is the interionic spacing) exceeds $\approx$150 (Pollack and Hansen 1973; Slattery, Doolen, and DeWitt 1980). Using the average values for Z and μ_e given above, the melting curve is

$$T_8 = 3.6 \rho_9^{1/3}. \tag{3.3a}$$

Combining this with (3.1), we find that the ions will be crystalline below a depth

$$z_{M,4} = .4 T_8 g_{14}^{-1} \tag{3.3b}$$

where $10^8 T_8$ K is the temperature. At depths less than the melting depth, z_M, the ions form a liquid metal.

3.2 TRANSPORT COEFFICIENTS

We require transport coefficients for both the solid and liquid metal regimes and consider two calculations: those of Flowers and Itoh (1976) and Yakovlev and Urpin (1980). We include electron-phonon scattering above the Debye temperature in the solid and electron-ion scattering in the liquid. Impurity scattering and the electron-electron contribution to the thermal conductivity, which is small for the large nuclear charges found in the crust, are neglected (*cf.* Urpin and Yakovlev 1980a). Quantizing effects of the magnetic field (Yakovlev 1980a,b; Kaminker and Yakovlev 1980; Blandford and Hernquist 1982) are neglected. Consider first the solid metal regime.

Electron-phonon scattering is elastic for temperatures well above the Debye temperature; the electron-phonon relaxation time is calculated explicitly by Yakovlev and Urpin (1980). They obtain

$$\tau_{YU} = 8.1 \times 10^{-19} T_8^{-1} \text{ s} \tag{3.4}$$

independent of density. The relaxation time may be extracted from Table 3 of Flowers and Itoh (1976) with the result that

$$\tau_{FI} = 2.2 \times 10^{-18} T_8^{-1} \text{ s} \tag{3.5}$$

a factor of 2.7 larger than τ_{YU}. Note that (3.4) and (3.5) scale the same way with temperature and density. Yakovlev and Urpin (1980) argue that the discrepancy

between the calculations is due to their use of the Monte-Carlo results of Pollack and Hansen (1973) for the phonon spectrum of a Coulomb crystal, as opposed to Flowers and Itoh's use of an approximate spectrum. In particular, Yakovlev and Urpin (1980) use the Pollack and Hansen (1973) value of the moment of the phonon spectrum $u_{-2} \equiv \langle \omega^{-2}(k)/\omega_p^{-2} \rangle = 13$, where ω_p is the ion plasma frequency. The approximation used by Flowers and Itoh (1976) corresponds to $u_{-2} = 4.4$. Flowers and Itoh (Itoh 1982, private communication) argue that their calculation is more accurate due to their inclusion of electron screening ($k_{TF} \simeq 1/4q_D$ where k_{TF} is the Thomas-Fermi wavevector, and q_D is the Debye wavevector), and its neglect (Pollack and Hansen assume a static neutralizing background of electrons) by Yakovlev and Urpin (1980).

We shall, without prejudice, use the Flowers and Itoh (1976) value in our numerical estimates, and consider the relaxation time for electron-phonon scattering to be uncertain to a factor ~3. Using the relaxation time (3.5), the coefficients σ_0 and κ_0 are

$$\sigma_0 = 1.8\times10^{22}\rho_8^{2/3}T_8^{-1}\ \mathrm{s}^{-1} \tag{3.6}$$

$$\kappa_0 = 4.9\times10^{17}\rho_8^{2/3}\ \mathrm{erg\,cm^{-1}s^{-1}K^{-1}}\,. \tag{3.7}$$

Evaluating these at the melt surface, using (3.3a), gives

$$\sigma_M = 1.4\times10^{21}T_8\,\mathrm{s}^{-1} \tag{3.8}$$

$$\kappa_M = 3.8\times10^{16}T_8^2\ \mathrm{erg\,cm^{-1}s^{-1}K^{-1}}\,. \tag{3.9}$$

These coefficients must be reduced by a factor of 2.7 if the relaxation time (3.4) is used

Transport coefficients in the liquid metal are, if anything, less certain than those in the solid. Comparison of the formulae for the thermal conductivity

given by Yakovlev and Urpin (1980) and Flowers and Itoh (1981) yield a factor ~2 disagreement, with Flowers and Itoh giving the larger value. The disagreement is due to different models for the ionic correlations and screening. Flowers and Itoh (1976) screen the interaction using the Thomas-Fermi theory, and take the ionic correlations into account explicitly by modeling the results of Brush, Sahlin, and Teller (1966) to obtain a liquid structure function (see Flowers and Itoh 1976 for details). Yakovlev and Urpin (1980) ignore electron screening, which is a good approximation in the regime of interest ($k_{FT}/p_F \sim .1$), and cut the interaction off at roughly the interionic distance. We shall again use the Flowers and Itoh (1981) formula for the thermal conductivity due to electron-ion collisions, which is a fit to the results of Flowers and Itoh (1976) for the thermal conductivity of Baym, Pethick, and Sutherland (1971) matter. We omit the electron-electron scattering contribution to the thermal conductivity. This gives

$$\kappa = 10^{17}\rho_9^{1/3}T_8 \,\mathrm{erg\,cm^{-1}\,s^{-1}\,K^{-1}}\,. \tag{3.10}$$

The electron-ion relaxation time implied by (3.10) is

$$\tau = 4.5\times10^{-19}\rho_9^{-1/3}\,\mathrm{s}\,. \tag{3.11}$$

3.3 STATIONARY TEMPERATURE DISTRIBUTION WITH HORIZONTAL FIELD

An important physical quantity in the problem is the ratio of the thermal diffusion time to the ohmic diffusion time. Numerically, this quantity is

$$\frac{C_v}{4\pi\kappa_0\sigma_0} = 5\times10^{-4} \tag{3.12}$$

evaluated at the solid surface. The smallness of the ratio (3.12) means that the heat flow equilibrates rapidly, reaching a steady flow pattern in the presence of

a slowly changing magnetic field. This behavior is in contrast to that of laboratory metals; the ratio (3.12) for copper is $\sim 10^3$. Thermally driven growth of magnetic fields will not occur in laboratory solids since any magnetic field present will dissipate before significant temperature perturbations can be set up.

Due to the smallness of the ratio (3.12), which may be thought of as a magnetic Prandtl number, the temperature distribution may be calculated from the steady state heat flow equation assuming a slowly changing magnetic field. In particular, consider a constant, vertical heat flux, $\vec{F}_0 = -\kappa_0 \vec{\nabla} T_0$, flowing through a plane-parallel, unmagnetized, crust. (The scale height of the crust is much less than the stellar radius so curvature effects may be ignored.) Impose a small ($X \ll 1$) magnetic field

$$\vec{B}(x,z) = B(z)\sin(kx)\hat{y} \tag{3.13}$$

and calculate the resulting temperature perturbation

$$\delta T(x,z) = \delta T(z)\cos(kx)\,. \tag{3.14}$$

Only the horizontal component of the magnetic field affects the heat flow for small fields, hence we have specialized to the case of a horizontal field.

The temperature distribution is given by the solution of the steady state heat flow equation, which may be written (*cf.* Landau and Lifshitz 1960)

$$\dot{E} = \vec{\nabla}\cdot(\vec{\kappa}\cdot\vec{\nabla}T) + \vec{j}\cdot(\vec{\sigma})^{-1}\cdot\vec{j} - T\vec{j}\cdot(\vec{\nabla}\cdot\vec{Q}) = 0 \tag{3.15a}$$

where E is the internal energy density, and a dot denotes a time derivative. If the temperature perturbation and the magnetic field are treated as small perturbations to the heat flow, (3.15a) may be simplified to

$$\dot{E} = \vec{\nabla}\cdot(\vec{\kappa}\cdot\vec{\nabla}T) = 0 \tag{3.15b}$$

where the Joule heat term has been dropped because it is of second order in the magnetic field, and the Thomson effect term has been dropped because it is of order $(T/\mu)^2$ times the terms kept. The divergence of the electrical current has been set to zero. The divergence of the zeroth order heat flux is zero, so we are left with

$$\vec{\nabla}\cdot\delta\vec{F} = 0 \tag{3.16}$$

where the perturbation in the heat flux is given by

$$\delta\vec{F} = -\kappa_0\vec{\nabla}T - \frac{d\kappa_0}{dT}\delta T\vec{\nabla}T_0 + \kappa_0\vec{X}\times\vec{\nabla}T_0 \,. \tag{3.17}$$

The derivative $d\kappa_0/dT$ includes both the explicit temperature dependence of the thermal conductivity, which vanishes in our case, and the implicit temperature dependence due to the thermal expansion of the lattice. The thermal expansion effect may be shown to be negligibly small, thus we set the derivative $d\kappa_0/dT = 0$. Setting to zero the divergence of (3.17), we obtain an equation for the temperature perturbation

$$\frac{d}{dz}\left(\kappa_0\frac{d\delta T}{dz}\right) - \kappa_0 k^2\delta T - kX|F_0| = 0 \,. \tag{3.18}$$

We now scale the depth in units of the melting depth, $z = z_M\xi$, define $\beta = kz_M$, use (3.1) and (3.7) to write $\kappa_0 = \kappa_M\xi^2$, and write $A = 4\pi e^2\kappa_M\delta T/\mu_M$ to obtain

$$\frac{d}{d\xi}\left(\xi^2\frac{dA}{d\xi}\right) - \beta^2\xi^2 A - \frac{\alpha\beta B}{\xi} = 0 \tag{3.19}$$

where

$$\alpha = \frac{4\pi e^2\tau_M z_M|F_0|}{\mu^2} = \frac{|F_0|t_M}{n_M\mu_M z_M} \tag{3.20}$$

is the diffusion velocity associated with the heat flux measured in units of the melting depth and the ohmic diffusion timescale at the melt surface $t_M = 4\pi\sigma_0 z^2|_M$. In (3.20) n_M is the electron density at the melt surface. As is clear from (3.19), α describes the strength of the coupling between the magnetic field and the temperature perturbation.

Suitable boundary conditions for (3.19) are $\delta T = 0$ at z_M and ∞. The former seems reasonable because the thermal time greatly exceeds the dynamical time in the liquid. The latter embodies our hypothesis that the field is confined to the surface layers. Equation (3.19) may be solved by a Green's function if the small variations of T_0 through the crust are neglected. We find

$$A(\xi) = \frac{4\pi e^2 \kappa_M}{\mu_M}\delta T = \frac{\alpha\beta}{\xi}\int_1^\infty \frac{d\xi'}{\xi'^2} G(\xi,\xi')B(\xi') \tag{3.21}$$

where $G(\xi,\xi')$ is given by

$$\begin{aligned} G(\xi,\xi') &= \sinh\beta(\xi-1)e^{-\beta(\xi'-1)} \quad 1 \le \xi \le \xi' \\ G(\xi,\xi') &= \sinh\beta(\xi'-1)e^{-\beta(\xi-1)} \quad \xi' \le \xi\ . \end{aligned} \tag{3.22}$$

3.4 LINEAR GROWTH OF THE MAGNETIC FIELD

The evolution of the magnetic field is governed by the induction equation (2.15), with the temperature gradient computed from the heat flow equation, (3.15a). For small fields the heat flow equation becomes (3.19). To linearize the induction equation write the field convection velocity, (2.16), as $\vec{V} = -\vec{F}_0/n_e\mu$, where the relaxation time has been taken independent of density. The linearized induction equation is $\partial\vec{B}/\partial t = -\vec{\nabla}\times\delta\vec{\varepsilon}$ where the perturbation in the electrochemical field is

$$\delta\vec{\varepsilon} = \vec{j}/\sigma_0 + Q_0\vec{\nabla}\delta T + \vec{V}\times\vec{B}\ . \tag{3.23}$$

The convection velocity is due to the perturbation of the thermopower caused by the magnetic field, $\delta\vec{Q}\cdot\vec{\nabla}T_0 = \vec{V}\times\vec{B}$. If the perturbations (3.13) and (3.14) are used, along with the scalings leading to (3.19), the induction equation may be written in the form

$$\frac{d}{d\xi}\left[\frac{1}{\xi^2}\frac{dB}{d\xi}\right] - \alpha\frac{d}{d\xi}\left[\frac{B}{\xi^4}\right] - \frac{\beta^2 B}{\xi^2} + \frac{2A}{\xi^2} = \lambda B \,. \tag{3.24}$$

In deriving (3.24) the time dependence of the magnetic field has been assumed to have the form

$$B(\xi,t) = B(\xi)e^{\lambda t/t_M} \,. \tag{3.25}$$

Equations (3.19) and (3.24) may be combined into a single fourth-order eigenvalue equation for the growth rate λ. Eliminating $A(\xi,t) \propto \delta T$ we find

$$\frac{d^4B}{d\xi^4} - \frac{\alpha}{\xi^2}\frac{d^3B}{d\xi^3} + \left[\frac{6\alpha}{\xi^3} - 2\beta^2\right]\frac{d^2B}{d\xi^2} + \left[\frac{\alpha\beta^2}{\xi^2} - \frac{18\alpha}{\xi^4}\right]\frac{dB}{d\xi} + \left[\frac{24\alpha}{\xi^5} + \beta^4 - \frac{6\alpha\beta^2}{\xi^3}\right]B$$

$$= \lambda\left[\xi^2\frac{d^2B}{d\xi^2} + 6\xi\frac{dB}{d\xi} + (6 - \beta^2\xi^2)B\right] . \tag{3.26}$$

The fourth order equation, (3.26), requires four boundary conditions. Two are provided by the requirement that the temperature perturbation vanish at the melt surface and at infinity. A third boundary condition is provided by the requirement that the magnetic field vanish at infinity. The fourth boundary condition is less certain. The rate of production of magnetic flux in the solid and the rate at which flux is convected in from the liquid may be calculated using Faraday's law and (3.23) for the perturbation of the electrochemical field. The magnetic field, (3.13), varies horizontally as $\sin(kx)$; to calculate the flux production and convection integrate Faraday's law over the surface $z \in [z_M,\infty), x \in [0,\pi/k]$ and use Stokes' theorem to obtain, using (3.23) for $\delta\vec{\mathcal{E}}$

$$\frac{d\Phi}{dt} = \int d\vec{l} \cdot \left[\vec{V} \times \vec{B} - Q_0 \vec{\nabla} \delta T - \frac{\vec{\nabla} \times \vec{B}}{4\pi\sigma_0} \right]. \tag{3.27}$$

where $\Phi = \int \vec{B} \cdot d\vec{\Sigma}$ is the magnetic flux. Specializing to the case $\vec{B} = B(\xi)\sin(kx)\hat{y}$, $\vec{V} = V(\xi)\hat{z}$, and $\delta T = \delta T(\xi)\cos(kx)$ we see that the thermopower term $Q_0 \vec{\nabla} \delta T$ is the only term which represents the production of flux. The convection and diffusion of flux through the melt surface is given by the integral of the $\vec{V} \times \vec{B}$ and the $(\vec{\nabla} \times \vec{B})/4\pi\sigma_0$ terms along the melt. Evaluating these terms and transforming to the dimensionless variables used above, the rate of flux flow through the melt is found to be

$$\left[\frac{d\Phi}{dt} \right]_{conv} = \frac{2z_M^2}{\beta t_M} \left[\alpha B - \frac{dB}{d\xi} \right] \tag{3.28}$$

evaluated at the melt surface. Thus the condition $dB/d\xi = \alpha B$ represents all of the flux production taking place in the solid. In §4 the possibility of flux production in the liquid will be discussed, thus we shall discuss the eigenvalues λ of (3.26) corresponding to various values of the logarithmic derivative $d\ln B/d\xi$.

3.5 NUMERICAL SOLUTIONS

We have obtained numerical solutions to the fourth order eigenvalue equation (3.26) for a variety of boundary conditions. The solutions were obtained by writing (3.26) in finite difference form using the variable $s = e^{\xi}$. A grid of 75 equally spaced points on the interval $s \in [0,2.5]$ was employed. The boundary conditions at infinity were applied at the rightmost point of the grid. We consider two cases:

a) The production of magnetic flux is confined to the solid. In this case the proper boundary condition is $d\ln B/d\xi = \alpha$ at the solid surface $\xi = 1$. We find that a growing mode exists for $\alpha \geq 5$. In order for the growth rate to be large enough to be of interest in neutron star crusts ($\lambda \geq 0.1$, see §6) we require $\alpha \geq 22$ (Fig. 1). If we examine the eigenfunctions (Fig. 2) we find that the flux is concentrated well below the surface, near $\xi = 3$–4. The explanation for this form of the eigenfunction can be seen from (3.24). For $1 \leq \xi \leq 5$ the convection term, (2.17), dominates ohmic loss and produces the steep vertical gradient of horizontal field, as $V \sim \xi^{-4}$. For $\xi \gtrsim 5$ ohmic loss dominates, and the field strength decreases exponentially with depth. We find that the growth rates are maximized for $\beta \sim 1$ (Fig. 3). The horizontal and vertical field gradients are comparable, as expected.

b) There is significant production of flux in the liquid. In this case flux will be convected into the solid crust from the liquid; the proper boundary condition at the melt surface is $d\ln B/d\xi < \alpha$. The amount by which the logarithmic derivative is lowered from the case in which all of the flux production takes place in the solid depends on the rate of flux production in the liquid. Efficient flux production in the liquid allows growing modes for values of α much lower than those needed in case (a). In particular, if we have $d\ln B/d\xi = 0.75\alpha$ we obtain a growing mode with $\lambda \simeq 0.1$ for $1 \leq \alpha \leq 5$ (see Fig. 1). The fraction of the flux convected in from the liquid can be calculated using the eigenfunctions and the boundary condition $d\ln B/d\xi = 0.75\alpha$. If we consider the mode with $\alpha = 5$, then we find that 90% of the flux production takes place in the liquid. For the case $B' = 0$ a growing mode with $\lambda = 0.1$ is obtained with $\alpha = 0.2$ (see Figs. 1 and 2).

3.6 COMPARISON WITH COOLING CALCULATIONS

A calculation of direct relevance to the subject of this paper has been performed by Gudmundsson, Pethick, and Epstein (1982) (see also Gudmundsson 1981). These authors have studied the variation of the heat flux through the outer crust assuming a fixed interior temperature, evaluated at $\rho \sim 10^{11}\,\mathrm{g/cm^3}$. They used electron conductive opacities from Yakovlev and Urpin (1980) at high density, and the radiative and conductive opacities of the Los Alamos group (e.g., Hübner *et al.* 1977) at lower densities. They find an empirical relation, good to a few percent, that relates the heat flux to the interior temperature and the surface gravity. Furthermore, they showed that the flux was almost completely controlled by the electron conduction opacity in the liquid at densities $10^6\,\mathrm{g/cm^3} \leq \rho \leq 10^8\,\mathrm{g/cm^3}$ for a central temperature $T = 10^{8.5}\,\mathrm{K}$. The controlling density range moves to lower density for lower central temperatures.

In common with earlier authors, Gudmundsson *et al.* confined their attention to a crust in local nuclear statistical equilibrium (i.e., composed of ^{56}Fe for densities $\rho < 8\times10^6\,\mathrm{g/cm^3}$, Baym, Pethick, and Sutherland 1971). If we consider the response of the flux to changes in the composition of the crust in the controlling density range we find that the opacities scale as the nuclear charge, Z, and, for a given internal temperature, the flux scales as $1/Z$, since the neutron star envelope tends strongly to the radiative zero solution (e.g., Schwarzschild 1958). The surface composition of neutron stars has been discussed by Michel (1975), and Rosen and Cameron (1972) with the conclusion that $\sim10^{21}\,\mathrm{g}$ of helium could survive on the surface of the star. The helium will compress to a density given by $\Delta M = 4\pi R^2 \int \rho dz = 4\times10^{21}\rho_6^{5/3} g_{14}^{-1}\,\mathrm{g}$. Thus a small amount of helium can reach a high enough density to be the controlling factor in determining the heat flux, lowering the effective Z in (3.29) and (3.30) to $Z = 2$ and substantially increasing the heat flux for a given internal temperature.

We have confirmed and generalized the Gudmundsson *et al.* relation, using the opacities given by Flowers and Itoh (1981), and find, to adequate accuracy

$$F \simeq 7\times10^{19} g_{14}\left(\frac{26}{Z}\right) T_8^{2.3}\ \mathrm{erg\,cm^{-2}s^{-1}} \quad 0.3 \lesssim T_8 \lesssim 3\,. \tag{3.29}$$

This flux is a factor ~2 larger than is obtained using the Yakovlev and Urpin (1980) opacity. If we adopt this relation, then we find

$$\alpha = 0.5 T_8^{0.3}\left(\frac{26}{Z}\right) \tag{3.30}$$

independent of the surface gravity, and only weakly dependent on the interior temperature.

The numerical value of α is sensitive to the collision time τ. As can be seen from (3.20), α is proportional to the collision time at the melt surface. In addition, the heat flux F_0 is proportional to the collision time in the liquid (Gudmundsson *et al.* 1982). Thus, the factor of 2.7 discrepancy between the collision times of Flowers and Itoh (1976) and Yakovlev and Urpin (1980) leads to an overall factor ~6 uncertainty in the value of α. This is in addition to the uncertainty in α due to ignorance of the surface composition.

4. Growth of the Field in the Liquid Phase

As we showed in §2, the battery term which derives the linear growth of the field in the solid is absent in the liquid phase because hydrostatic equilibrium requires a vertical temperature gradient. However, this implies that a horizontal component of magnetic field will produce a horizontal component to the heat flux, given in the linear approximation by

$$\delta\vec{F} = \vec{X}\times\vec{F}_0 + O(X^2) \tag{4.1}$$

where $\vec{F}_0 = -\kappa_0\vec{\nabla}T_0$ is the vertical heat flux. For a general field geometry, this perturbation will not be solenoidal and as a result temperature perturbations will start to grow, thereby generating pressure perturbations and driving a circulation of the fluid in a manner akin to the Eddington-Sweet process (e.g., Schwarzschild 1958). The circulation velocity adjusts itself to convect away the local entropy production,

$$T\rho(\vec{v}\cdot\vec{\nabla})S + \vec{\nabla}\cdot\delta\vec{F} = 0 \tag{4.2}$$

where S is the entropy per unit mass and $\vec{v}$ is the circulation velocity. We rewrite equation (4.2) as

$$\rho v_z = -\frac{\vec{F}\cdot\vec{\nabla}\times\vec{X}}{T(dS/dz)} = \left[\vec{\nabla}\times\left[\frac{F_0\vec{X}}{T(dS/dz)}\right]\right]_z \tag{4.3}$$

where $F_0 = |\vec{F}_0|$. Continuity of mass implies that $\vec{\nabla}\cdot\rho\vec{v} = 0$; thus, a solution for the velocity field is

$$\vec{v} = \frac{1}{\rho}\vec{\nabla}\times\left[\frac{F_0\vec{X}}{T(dS/dz)}\right]. \tag{4.4}$$

This is the only solution that vanishes in the absence of a field. Equation (4.4) is valid for $X \ll 1$.

We are most interested in the circulation in the liquid close to the solidification point. Under these conditions the entropy is dominated by the ionic contribution, and the entropy gradient is dominated by the density gradient ($dT/dz \ll T/z$ near the melting depth). We may use the results of Pollack and Hansen (1973) to obtain

$$\left[\frac{\partial S}{\partial n_i}\right]_T = -\frac{1.24}{\rho} \tag{4.5}$$

where n_i is the density of ions. Equation (4.4) can then be re-written

$$\vec{v} = -\frac{eF_0\tau_M A m_p}{3.7\rho_M \mu_M T}\frac{z_M}{\xi^4}\vec{\nabla}\times(\vec{B}/\xi) \tag{4.6}$$

where we have used the approximation

$$\tau(\xi) = \tau_M \xi^{-1} \tag{4.7}$$

which is valid in the liquid ($\xi < 1$) (Yakovlev and Urpin 1980).

There is a competing effect that dominates in normal stars (e.g., Parker 1979). Magnetic pressure contributes to the total pressure in the fluid and so, if there is to be static equilibrium, there must be associated temperature gradients. Individual magnetic filaments will rise or fall until they are at the same density as their surroundings and stable to buoyancy forces. The main difference in pressure between the inside and outside of a filament will be contributed by the ions, and so the temperature difference will satisfy $(\delta T/T) \sim (B^2/8\pi P_i)$ where P_i is the ion pressure. This will induce perturbations to the heat flux of magnitude $\delta F \sim (B^2/8\pi P_i)(kz)F_0$, which are generally small compared to the perturbations caused by the anisotropy, (4.1). Henceforth, we ignore this effect.

If the magnetic field is strong enough, it will be modified by the fluid motion faster than ohmic decay and the thermoelectric effects described in §2 can act. This requires that the circulation velocity be larger than the ohmic diffusion velocity and the field convection velocity. Fluid motion dominates if

$$B \gtrsim (T/e\tau)[\min(1,\alpha)]^{-1} \tag{4.8}$$

or

$$B \gtrsim 10^8 T_8^2 [\min(1,\alpha)]^{-1}\,. \tag{4.9}$$

When this inequality is strongly satisfied, the electric field will be given by

$$\vec{E} = -\vec{v}\times\vec{B} = \frac{4\pi K z_M}{\xi^4}\vec{j}\times\vec{B} - \frac{K}{\xi^6}(\vec{B}\times\vec{\xi})\times\vec{B} \qquad (4.10)$$

where

$$K = \frac{eF_0\tau_M Am_p}{3.7\rho_M\mu_M T} = 5.5\times10^{-25}F_{19}T_8^{-6}G^{-1} \qquad (4.11)$$

where F_{19} is the heat flux in units of $10^{19}\,\mathrm{erg\,cm^{-2}\,s^{-1}}$. The magnetic field will then evolve according to $\partial\vec{B}/\partial t = -\vec{\nabla}\times\vec{E}$.

These thermal effects may drive a non-linear dynamo mechanism. The first term on the right hand side of equation (4.10) dominates in the short wavelength limit, and describes the creation of horizontal field out of vertical fluid and vice versa — a crucial ingredient of a dynamo process. However, this term alone does not lead to enhancement of the magnetic energy density, as can be seen by noting that it does not contribute to the rate of performance of mechanical work, $-\vec{j}\cdot\vec{E}$. The second term on the right hand side of (4.10) also represents the creation of perpendicular components of magnetic field, and can contribute to an increase in the magnetic energy density.

If thermally driven circulation in the liquid does drive a non-linear dynamo process the magnetic field in the liquid will grow to non-linear ($X \gg 1$) strength in a time $t_+ \sim z_M/KB = 80T_8/B_8 g_{14}\,\mathrm{yr}$ shorter than the timescale for field growth or decay in the solid. In this case most of the flux is made in the liquid and convected into the solid. The surface boundary condition in §3 will be determined by the rate of flux production in the liquid and the rate at which flux can be convected into the solid. This allows growing modes in the solid for values of α much smaller than those required if all of the flux production is to take place in the solid.

5. Growth and Decay of the Magnetic Field

In the preceding two sections, we have described magnetic field generation in both the solid and the liquid under the assumption that the field is weak. Both calculations can break down for strong fields.

The magnetic stress in the liquid may become large enough to influence the circulation. The circulation velocity, given by equation (4.4), is sub-Alfvénic; hence, magnetic flux tubes will quickly adjust to hydromagnetic equilibrium. This implies that there will be small temperature perturbations on the equipotential surfaces of magnitude $\delta T/T \sim B^2/8\pi P_i$ where P_i is the ion pressure, which is larger than the thermal component of the electron pressure. The circulation velocity (4.4) should be a reasonable approximation for magnetic field variations with $kz \sim 1$ as long as the perturbations to the heat flux $\sim\kappa_0\delta T/z$ associated with the temperature fluctuations are small compared to the perturbations due to the magnetic field $\sim XF_0$. The condition for this to be true is that

$$B \lesssim 1.5\times10^{11}F_{19}g_{14}^{-1}\ \mathrm{G} \tag{5.1}$$

or

$$B \lesssim 10^{12}T_8^{2.3}\ \mathrm{G} \tag{5.2}$$

assuming the relation (3.29), as we shall henceforth. An equivalent condition arises from the requirement that the magnetic stresses be smaller than the thermally induced pressure fluctuations and should therefore be unable to influence the circulation.

Secondly, the non-linear terms in equations (2.15) and (4.10) describing the evolution of the field in the solid and liquid respectively must be included when $X \gtrsim 1$ or

$$B \gtrsim 2\times10^{11}T_8^2\ \mathrm{G}\,. \tag{5.3}$$

Note that conditions (5.2) and (5.3) are similar for $T_8 \sim 1$.

We expect that the end result of the evolution of the linear instability will be to produce a disorganized array of horizontal magnetic loops of size $\sim z$. However, when $X \gtrsim 1$, the horizontal temperature gradient should exceed the vertical temperature gradient. The dominant contributions to the convective velocity (2.16) are now

$$\vec{V} \simeq -\frac{\vec{F}}{n_e \mu} - \frac{\vec{j}}{n_e e} . \tag{5.4}$$

The battery term in (2.15) is unchanged. There is an additional field convection with the drift velocity of the conduction electrons. This term alone, like its counterpart in the fluid circulation analysis, causes no change in the total magnetic energy. However, when $X \gtrsim 1$, it dominates the ohmic decay term and leads to the production of vertical magnetic field out of horizontal field. The vertical field will penetrate the lower density regions where the thermal resistance is largest, and where X, and therefore the inhibition of the cross-field thermal conductivity, is much larger. The vertical heat flux will therefore increase locally in those parts of the solid where the field is vertical, increasing the production rate of horizontal field.

Horizontal electrical current and heat flux can also transport the field horizontally. Hence, magnetic field can be generated within one part of the stellar surface where the heat flux is large and then transported to another region where the field production is lower.

As a consequence of these effects, we believe that the rate of field growth in the solid is enhanced in the non-linear phase. What probably happens under conditions when field growth can occur is that magnetic flux is freely created in the vicinity of the solid surface and is then convected downwards into the crust with a speed $V \sim F/\mu n_e \propto z^{-4}$. For $\xi \gg 1$ the ohmic diffusion term should

dominate and in a time $10^5 t_5$ yr, the flux should be able to diffuse down to a depth

$$z_{max} \sim 5\times10^4 g_{14}^{-1/2} t_5^{1/4} T_8^{3/4} \text{ cm} \quad . \tag{5.5}$$

As long as heat continues to flow through the crust, magnetic flux will be created and drawn downwards subject to two saturation effects. When the magnetic stress becomes comparable to the yield stress of the solid, the lattice will become visco-elastic and magnetic buoyancy will oppose field amplification. The shear modulus of the lattice is $4\times10^{25}\rho_9^{4/3}$ dyne cm^{-2} (Ruderman 1972). If the lattice flows when the strain angle is $\sim10^{-2}$, then the saturation field strength will be

$$B_{max} \sim 3\times10^{13} g_{14} t_5^{1/2} T_8^{1/2} \text{ G} \tag{5.6}$$

(Blandford and Hernquist 1982).

Secondly, the temperature fluctuations induced by the magnetic field can no longer be regarded as perturbations when $XF/\kappa_0 \gtrsim T/z$. This condition yields

$$B_{max} \gtrsim 10^{14} g_{14} T_8^{0.3} t_5^{0.5} \text{ G} \tag{5.7}$$

independent of depth. The field can probably not grow to values much larger than this. This condition is similar to, but marginally weaker than, that given by the yield stress. (Note that the heat flux used in equation (5.7) may be reduced from the value appropriate to an unmagnetized crust. Note also that the field strength is not limited to the critical value $m_e^2/e = 4.4\times10^{13}$ G; Adler *et al.* 1970.)

After the magnetic field has reached its saturation value, it can still be moved around by the Hall currents. Adjacent loops of field will approach one

another, establishing steep magnetic gradients which allow reconnection to proceed through X-type neutral points located near the surface where the resistivity is larger. We believe that there will be a steady progression towards larger scale magnetic structure until the horizontal scale length approaches the stellar radius. Thereafter, it seems that the only quasi-steady field geometry is one in which the field is axisymmetric and poloidal. In this case, the electrical current will be totally toroidal and the heat flux predominantly toroidal. If we estimate the integral $\int_0^\infty B dz$ by $B_{max} z_{max}$ and assume that this is constant over the surface, then we can calculate the associated dipole moment. Flux conservation implies that the radial component of the field is $\propto \cot\theta$ where θ is the spherical polar angle. (This prescription clearly needs modification at the poles.) We can then expand in spherical harmonics to compute the magnetic dipole moment, M

$$M = \frac{3\pi R^2}{8} \int B dz \ . \tag{5.8}$$

At this point we should comment upon the efficiency of the mechanisms that we have described. In the linear regime, a fraction $\sim B^2 / 8\pi\mu n_e \sim B^2 / 8\pi\rho g z$ of the vertical heat flux is converted into magnetic energy density provided that ohmic losses are not dominant. As we have argued, this is probably a conservative estimate in the non-linear phase. However, this is always far below the maximum efficiency dictated by thermodynamics $\sim z\nabla T / T$ for a heat engine to do work against the magnetic stresses.

An axisymmetric magnetic structure can be maintained against ohmic loss as long as heat continues to flow through the crust. After the interior cools, the electrical conductivity will increase and the magnetic flux will diffuse away in a time dictated by its new value.

6. Astrophysical Applications

Up to this point we have tried to determine general conditions under which magnetic field can grow in the outer crust of a neutron star. We now specialize by considering in turn slow pulsars, fast pulsars, pulsating X-ray sources, X-ray and γ-ray bursters, binary pulsars, and white dwarfs.

6.1 SLOW PULSARS

The majority of radio pulsars appear to have been formed spinning slowly and to have dipole moments $\sim 10^{30}\,\mathrm{G\,cm^3}$ which last $\sim 3\times 10^6\,\mathrm{yr}$. Under the assumptions described in §III, we found that $\alpha \simeq 0.7$, independent of the surface gravity and weakly dependent on the temperature. Unless either the transport coefficients in both the liquid and the solid have been underestimated by factors ~ 3 or the surface layers are of helium composition, the linear instability described in §III will not develop. However, if the neutron star retains a seed field $\gtrsim 10^8\,\mathrm{G}$, then, as discussed in §IV, magnetic flux can be created in the liquid and supplied to the solid.

The cooling of neutron stars has been a topic of considerable theoretical discussion since the Einstein X-ray satellite failed to discover hot neutron stars in most young supernova remnants. Cooling calculations have not agreed in detail with each other in part because of uncertainties in the transport properties of the matter in the crust. At early times the cooling is dominated by neutrino processes and the interior temperature is independent of the surface properties. For an unmagnetized $1.4M_\odot$ neutron star with a superconducting interior and no pion condensate (e.g., Richardson *et al.* 1982; Nomoto and Tsuruta 1981), the interior temperature is roughly

$$T_8 \sim 1.3 t_5^{-0.2} \tag{6.1}$$

where $t_5 10^5$ yr is the age of the neutron star. This cooling law is valid until the photon flux from the surface $\sim 2\times10^{33} T_8^{2.2}$ erg s^{-1} for $M \sim 1.4 M_\odot$, is able to remove the internal energy $9\times10^{45} T_8^2$ erg. The cooling time is therefore

$$t_{cool} \sim 2\times10^5 \text{ yr} . \tag{6.2}$$

This estimate of the cooling time will be increased if the magnetic inhibition of the heat flux in the liquid is taken into account.

If the growth rate, $\lambda \sim 0.1$ then a seed field of 10^8 G will grow to a strength $\sim 10^{12}$ G in a time $t \sim 10 t_M / \lambda \sim 10^4$ yr. This estimate is uncertain due to the dependence on the details of the non-linear evolution and the strength of the seed field; however, it does admit the possibility that most supernova remnants contain neutron stars in which the surface fields are sufficiently strong to reduce the surface X-ray luminosity but still sufficiently weak and disordered to have comparatively small dipole moments. (An investigation of the effects of magnetic fields on neutron star cooling is currently in progress.) In this way the theoretical expectation that type II supernova explosions generally produce neutron stars can be reconciled with the failure to observe them as either X-ray sources or radio pulsars. Recent searchs for pulsars associated with supernova remnants in the Galaxy and in the Magellanic Clouds, which avoid selection effects, have confirmed this discrepancy (Manchester, Tuohy, and D'Amico 1982).

The field will grow to the limiting value, (5.6) or (5.7), in $\sim 10^5$ yr, and penetrate the crust to a depth $\sim$500 m. If long range order has been established, the dipole moment will be 2×10^{30} G cm^3, using (5.8), in agreement with pulsar observations. Roughly 10^{-3} of the heat flux is converted into magnetic energy. No correlation between the magnetic and spin axes is expected, so most stars should be able to pulse.

After $\sim 2\times10^5$ yr, the interior of a pulsar should cool very rapidly. (The luminosity is usually larger than the rate of loss of spin energy.) A simple estimate gives $T_8 \propto t_5^{-5}$. At a depth ~500 m, the Debye temperature is $\sim 4\times10^8$ K. Well below the Debye temperature, the electron collision time and therefore the ohmic decay time increases unless limited by the presence of impurities (Urpin and Yakovlev 1980b). In order for the decay time to be lengthened to the observed value of $\sim 3\times10^6$ yr, the conductivity must be decreased by a factor ~20, which is certainly allowed but is by now means dictated by our theory.

6.2 FAST PULSARS

A subset of young pulsars, including those in the Crab, Vela and MSH 15-52 remnants are spinning comparatively rapidly and have inflated plerionic nebulae around themselves. A large magnetic dipole moment seems to have formed very quickly in these objects. It is possible that the spin energy $\sim 10^{46} P^{-2}$ erg, is powering the production of sub-surface field, perhaps through the dissipation of currents flowing through the magnetosphere. Another possibility is that additional heat flux is generated by friction between the core and the crust (Greenstein 1979a,b).

The deceleration parameter, $n = -P\ddot{P}/\dot{P}^2 + 2$, has been measured for the Crab pulsar only, with the result $n = 2.5$, inconsistent with the simple electromagnetic pulsar theory (e.g., Manchester and Taylor 1977) which predicts $n = 3$. The measured deceleration parameter can be reconciled with the simple theory if the field is still growing, as expected on the basis of our theory. Specifically, $B \propto t^{1/6}$ gives $n = 2.5$.

The recent discovery of a 1.56 ms radio pulsar (Backer, *et al.* 1982) for which $\dot{P} < 10^{-15}$ s^{-1} (Backer 1982, private communication) is apparently inconsistent with this idea as the surface field strength is almost certainly $< 10^{10}$ *G*. A

possible explanation for this discrepancy is that the star is sufficiently massive to allow the formation of a central pion condensate (e.g., Baym and Pethick 1975). The core and inner crust would then cool very quickly by neutrino emission. This would also be consistent with the absence of a detectable radio source surrounding the pulsar.

6.3 PULSATING X-RAY SOURCES

it is thought that the pulsating X-ray sources in massive binary systems are older than $\sim 10^6$ yr, and those systems with less massive primaries are even older, $\sim 10^8$ yr in the case of Her X-1, since the binary does not become an X-ray source until the primary evolves off the main sequence (e.g., van den Heuvel 1977). Therefore, it is natural to postulate that the magnetic field in these stars is produced thermally as a result of accretion processes rather than the initial cooling of the neutron star. As the X-ray luminosity of pulsating binary X-ray sources is much greater than that of isolated, cooling neutron stars, the power to generate magnetic fields is readily available.

If the accreted gas were deposited at a uniform rate over the entire surface and the heat flow were radially inward, then the battery term in (2.15) would lead to field destruction, and the field convection velocity, (2.16), would lead to the expulsion of field from the star (see the discussion following (2.15)). However, it is far more probable that matter will be accreted over a small fraction of the surface and that heat will flow from the hot regions to the remainder of the surface via the interior since the thermal conductivity of the interior is much greater than that of the surface layers. We may idealize the problem as follows.

Consider a highly thermally conducting sphere of temperature T_2 and radius R covered with a thin insulating layer. Let a fraction f of the surface be maintained at a temperature T_1. Further assume that there exists a

relationship $F(T)$ between the heat flux and the maximum temperature on either side of the layer. The central temperature will satisfy the relation $fF(T_1) = (1-f)F(T_2)$, as the heat conducted inward must balance the heat conducted outward for a steady state to exist. If we substitute equation (3.29) for $F(T)$, then we obtain

$$T_2 \sim \left[\frac{f}{(1-f)}\right]^{0.45} T_1 . \tag{6.3}$$

The time required to achieve equilibrium is roughly

$$t_{eq} \sim \frac{U}{4\pi R^2 f F(t_1)} \tag{6.4}$$

where U is the internal energy of the star.

For $L \sim 10^{38}\,\mathrm{erg\,s^{-1}}$ and $f \sim 0.1$ the interior temperature is $\sim 10^7\,\mathrm{K}$ and thermal equilibrium will be established after $\sim 3\times10^5\,\mathrm{yr}$. Using equation (5.8), the magnetic moment is $M \sim 4\times10^{29} t_5^{3/4}$. After $\sim 3\times10^6\,\mathrm{yr}$ the magnetic moment will be equal to the typically observed value $3\times10^{30}\,\mathrm{G\,cm^3}$. Therefore, if a neutron star accretes at roughly the Eddington rate for a typical mass transfer timescale (e.g., van den Heuvel 1976) it can generate its own magnetic field. Accretion at a much slower rate is probably not able to power magnetic field generation. This may have occurred in the majority of cases, in particular in the bulge sources with their low mass stellar companions (e.g., van den Heuvel 1977).

6.4 X-RAY AND γ-RAY BURSTERS

It has been proposed that X-ray and γ-ray bursters are differentiated by the absence or presence of a strong magnetic field (Woosley and Wallace 1982). A neutron star in a binary system that has in the past experienced a large enough and long enough accretion rate will have generated a strong surface field and be

susceptible to γ-ray bursting. A star that has accreted less gas will be essentially unmagnetized and observable as an X-ray burster.

6.5 BINARY PULSARS

Two of the three known binary pulsars (PSRs 1913+16 and 0655+64) have anomalously small values of $\dot{P}$ (Damashek *et al.* 1982). Recently $\dot{P}$ was measured for the third binary pulsar PSR 0820+02 (Manchester, *et al.* 1983). Although the value obtained ($\dot{P} = 0.125\times10^{-15}\,s^{-1}$) is not as small as for the other two binary pulsars, it is nevertheless significantly less than the $\dot{P}$ for most isolated radio pulsars. The inferred dipole moments are, therefore, small, $\sim10^{29}\,G\,cm^{-3}$ (somewhat larger for PSR 0820+02, though still significantly smaller than values derived for isolated radio pulsars). It is also thought that these objects are older than the typical radio pulsars. In both cases it has been suggested that the observed pulsar was formed in a supernova explosion before the companion completed its evolution (Smarr and Blandford 1976; Blandford and DeCampli 1981; van den Heuvel 1981). It is possible that these neutron stars became magnetized during a very long X-ray binary phase and that the magnetic field penetrated to a greater depth than in an isolated pulsar, increasing the ohmic dissipation time.

6.6 WHITE DWARFS

Some white dwarfs are magnetized with surface fields $\lesssim10^{8}$ G. However, none of the processes discussed in this paper are likely to be relevant for white dwarfs. Crystallization does not occur until white dwarfs are very old and little thermal energy remains. Thus, the processes described in §2 and §3 cannot lead to efficient field production. In addition, the circulation velocity in the interior of a white dwarf (*cf.* §4) is only $V \sim FX/P_i \sim 3\times10^{-9}B_8\,cm/s$. The turnover time

therefore exceeds the cooling time for all reasonable field strengths.

7. Conclusions

In this paper we have endeavored to present a complete and self-consistent description of neutron star magnetization that is an alternative to the usual view that the magnetic flux has been frozen into the collapsing core during the supernova explosion. We have argued on observational grounds that neutron star magnetic fields are ephemeral, and on theoretical grounds that the field must therefore be confined to the surface layers of the star.

We have extended the work of Urpin and Yakovlev (1980b) and suggested two possible mechanisms for the generation of magnetic flux. We have shown how small seed fields can grow exponentially within the solid crust, and specified necessary conditions for this to occur. Our understanding of heat transport in neutron stars is still sufficiently uncertain, as evidenced by the difficulties posed by the X-ray observations of supernova remnants, that we do not know whether or not this instability can be responsible for the production of neutron star magnetic fields. Secondly, we have demonstrated that the coexistence of heat flux and magnetic field in the liquid will cause the fluid to circulate, which may lead to effective dynamo action. If so, seed fields in excess of $\sim 10^8$ G will grow rapidly and supply flux to the solid below.

Our treatment of the subsequent evolution of the field is far more conjectural. We have sketched plausible mechanisms that may occur in the non-linear phase of field growth and lead to saturation, explaining the striking clustering of neutron star field strengths around 10^{12} G. Finally, we have considered the consequences of the theory in the context of various types of neutron stars. The theory seems to account for the principal observed properties of neutron star

magnetic fields.

The first priority for an improved understanding of these processes is a better description of the transport properties of the outer crust and the liquid above it. This should be possible in the near future. However, it appears that it will be far more difficult to solve for the non-linear and necessarily three-dimensional growth of the field in any satisfactory quantitative manner.

Acknowledgements

We thank the staff of NORDITA, where this work was initiated, for hospitality and especially Drs. Gudmundsson and Pethick for guidance and encouragement. We thank Tom Hagstrom for assistance with the numerical computations. RB thanks the Director of the Institute for Theoretical Physics for hospitality during the completion of this paper and participants in the Space and Astrophysics Program for valuable comments. This research was supported by the National Science Foundation under grants AST80-17752 and PHY77-27084 and the Alfred P. Sloan Foundation. JHA acknowledges the support of a Bantrell Fellowship at Caltech.

References

Adler, S. L., Bahcall, J. N., Callan, C. G., and Rosenbluth, M. N. 1970, *Phys. Rev. Lett.* **25,** 1061.

Ashcroft, N. W., and Mermin, N. D. 1976, *Solid State Physics*, (New York: Holt, Rinehart and Winston).

Backer, D., Kulkarni, S., Heiles, C., Davies, M., and Goss, W. 1982, *Nature* **300**, 615.

Baym, G., and Pethick, C. 1975, *Ann. Rev. Nucl. Sci.* **25,** 27.

Baym, G., Pethick, C., and Sutherland, P. G. 1971, *Astrophys. J.* **170,** 299.

Biermann, L. 1950, *Z. Naturf. A.* **5,** 65.

Blandford, R. D. and DeCampli, W. M. 1981, in *Pulsars*, ed. Sieber, W. and Wielebinski, R. (Dordrecht, Holland: Reidel).

Blandford, R. D., DeCampli, W. M., and Königl, A. 1979, *Bull. Am. Astr. Soc.* **11,** 703.

Blandford, R. D., and Hernquist, L. E. 1982, *Journ. Phys. C.* **15,** 6233.

Brush, S. G., Sahlin, H. L., and Teller, E. 1966, *J. Chem. Phys.* **45,** 2102.

Damashek, M., Backus, P. R., Taylor, J. H., and Burkhardt, R. K. 1982, *Astrophys. J. Lett.* **253,** L57.

Dolginov, A. Z., and Urpin, V. A. 1980a, *Sov. Astron.* **24,** 177.

Dolginov, A. Z. and Urpin, V. A. 1980b, *Astrophys. and Space Sci.* **69,** 259.

Fenimore, E. E., Laros, J. G., Klebesadel, R. W., Stockdale, R. E., and Kane, S. 1982, in *Gamma Ray Transients and Related Astrophysical Phenomena*, ed. Lingenfelter, R. E., Hudson, H. S., and Worrall, D. M. (New York: American Institute of Physics).

Flowers, E., and Ruderman, M. A. 1977, *Astrophys. J.* **215,** 302.

Flowers, E., and Itoh, N. 1976, *Astrophys. J.* **206,** 218.

Flowers, E., and Itoh, N. 1981, *Astrophys. J.* **250,** 750.

Ghosh, P., and Lamb, F. K. 1979, *Astrophys. J.* **234,** 296.

Glen, G., and Sutherland, P. G. 1980, *Astrophys. J.* **239,** 671.

Goldreich, P. 1970, *Astrophys. J. Lett.* **160,** L11.

Greenstein, G. 1979a, *Nature* **277,** 521.

Greenstein, G. 1979b, *Astrophys. J.* **231,** 880.

Gudmundsson, E. H. 1981, Unpublished Thesis, University of Copenhagen.

Gudmundsson, E. H., Pethick, C., and Epstein, R. I. 1982, *Astrophys. J. Lett.* **259,** L19.

Gunn. J. E., and Ostriker, J. P. 1970, *Astrophys. J.* **160,** 979.

Helfand, D. J., Chanan, G. A., and Novick, R. 1980, *Nature* **283,** 337.

Hibberd, F. H. 1979, *Proc. R. Soc. Lond.* **A369,** 31.

Hübner, W. F., Merts, A. L., Magee, N. H., Jr., and Argo, M. F. 1977, *Astrophysical Opacity Table* (Report No. LA6760M, Los Alamos).

Inoue, H., Koyama, K., Makishima, K., Matsuoka, M., Murakomi, T., Oda, M., Ogarawa, Y., Ohashi, T., Shibazaki, N., Tanaka, Y., Kondo, I., Hayakawa, S., Kunieda, H., Makino, F., Masai, K., Nagase, F., Tawara, I., Miyamoto, S., Tsunemi, H., and Yamashita, K. 1981. *Astrophys. J. Lett.* **250,** L71.

Joss, P. C. 1980, *Ann. Rev. New York Acad. Sci.* **336,** 479.

Kaminker, A. D., and Yakovlev, D. G. 1980, Preprint No. 681 A. F. Ioffe Institute of Physics and Technology, Leningrad.

Landau, L. D. and Lifshitz, E. M. 1960, *Electrodynamics of Continuous Media* (Oxford: Pergamon Press).

Lyne, A. G. 1981, in *Pulsars*, ed. Sieber, W., and Wielebinski, R. (Dordrecht, Holland: Reidel).

Manchanada, R. K., Bazzano, A., La Padula, C. D., Polcaro, V. F., and Ubertini, P. 1982, *Astrophys. J.* **252,** 172.

Manchester, R. N. 1981, in *Pulsars*, ed. Sieber, W., and Wielebinski, R. (Dordrecht, Holland: Reidel).

Manchester, R. N., and Taylor, J. H. 1977, *Pulsars* (San Francisco: Freeman and Co.).

Manchester, R. N., Newton, L. M., Cooke, D. J., Backus, P. R., Damashek, M., Taylor, J. H., and Condon, J. J. 1983, *Astrophys. J.* **268**, 832.

Manchester, R. N., Tuohy, J. R., and D'Amico, N. 1982, preprint.

Maurer, G. S., Johnson, W. N., Kurfess, J. D., and Strickman, M. S. 1982, *Astrophys. J.* **254,** 271.

Mazets, E. P., Golenetskii, S. V., Aptekar', R. L., Gur'yan, Yu. A., and Il'inskii, V. N. 1981, *Nature* **290,** 378.

Mestel, L. 1961, *Mon. Not. R. astr. Soc.* **122,** 473.

Michel, F. C. 1975, *Astrophys. J.* **198,** 683.

Nomoto, K., and Tsuruta, S. 1981, *Astrophys. J. Lett.* **250,** L19.

Parker, E. N. 1979, *Cosmical Magnetic Fields* (Oxford: Clarendon Press).

Pollock, E. L., and Hansen, J. P. 1973, *Phys. Rev. A* **8,** 3110.

Pravdo, S. H., White, N. E., Boldt, E. A., Holt, S. S., Serlemitsos, P. J., Swank, J. H., Szymkowiak, A. E., Tuohy, I., and Garmire, G. 1979, *Astrophys. J.* **231,** 912.

Rappaport, S., and Joss, P. C. 1977, *Nature* **266,** 683.

Richardson, M. B., Van Horn, H. M., Ratcliff, K. F., and Malone, R. C. 1982, *Astrophys. J.* **255**, 624.

Rosen, L. C., and Cameron, A. G. W. 1972, *Astrophys. and Sp. Sci.* **15,** 137.

Roxburgh, I. W. 1966, *Mon. Not. R. astr. Soc.* **132,** 201.

Ruderman, M. A. 1972, *Ann. Rev. Astron. and Astrophys.* **10,** 427.

Ruderman, M. A., and Sutherland, P. G. 1973, *Nature Phys. Sci.* **246,** 93.

Schwarzschild, M. 1958, *Structure and Evolution of the Stars* (New York: Dover).

Seward, F. D., and Harnden, F. R., Jr. 1982, *Astrophys. J. Lett.* **256,** L45.

Seward, F. D., Harnden, F. R., Jr., Murdin, P., and Clark, D. H. 1983, *Astrophys. J.* **267,** 698.

Slattery, W. L., Doolen, G. D., and DeWitt, H. E. 1980, *Phys. Rev. A* **21,** 2087.

Smarr, L. L., and Blandford, R. D. 1976, *Astrophys. J.* **207,** 574.

Stamper, J. A., Papadopoulos, K., Sudan, R. N., Dean, S. O., McLean, E. A., and Dawson, J. M. 1971, *Phys. Rev. Lett.* **26,** 1012.

Trümper, J., Pietsch, W., Reppin, C., Voges, W., Staubest, R., and Kendziorra, E. 1978, *Astrophys. J. Lett.* **219,** L105.

Tsuruta, S. 1979, *Phys. Rept.* **56,** 237.

Tuohy, I., and Garmire, G. 1980, *Astrophys. J. Lett.* **239,** L107.

Urpin, V. A., and Yakovlev, D. G. 1980a, *Soviet Astronomy* **24,** 126.

Urpin, V. A., and Yakovlev, D. G. 1980b, *Soviet Astronomy* **24,** 425.

van den Heuvel, E. P. J. 1976, in *Structure and Evolution of Close Binary Systems*, ed. Eggleton, P., *et al.*, (Dordrecht, Holland: Reidel).

van den Heuvel, E. P. J. 1977, *Ann. New York Acad. Sci.* **302,** 14.

van den Heuvel, E. P. J. 1981, in *Pulsars*, ed. Sieber, W., and Wielebinski, R. (Dordrecht, Holland: Reidel).

Van Riper, K. A. and Lamb, D. Q. 1981, *Astrophys. J. Letters* **244,** L13.

Vivekanand, M. and Narayan, R. 1981, *Astrophys. Astr.* **2,** 315.

Vivekanand, M. and Radhakrishnan, V. 1981, in *Pulsars*, ed. Sieber, W. and Wielebinski, R., (Dordrecht, Holland: Reidel).

Weisskopf, M. C., Elsner, R. F., Darbro, W., Leahy, D., Naranan, S., Sutherland, P. G., Grindlay, J. E., Harnden, F. R. Jr., and Seward, F. D. 1983, *Astrophys. J.* **267**, 711.

Wheaton, Wm. A., Doty, J. P., Primini, F. A., Cooke, B. A., Dobson, C. A., Goldman, A., Hecht, M., Hoffman, J. A., Howe, S. K., Scheepmaker, A., Tsiang, E. Y., Lewin, W. H. G., Matteson, J. L., Gruber, D. E., Baity, W. A., Rothschild, R., Knight, F. K., Nolan, P., and Peterson, L. E. 1979, *Nature* **282**, 240.

Woosley, S. E. and Wallace, R. K. 1982, *Astrophys. J.* **258**, 716.

Yakovlev, D. G. 1980a, Preprint No. 678, A. F. Ioffe Institute of Physics and Technology, Leningrad.

Yakovlev, D. G. 1980b, Preprint No. 679, A. F. Ioffe Institute of Physics and Technology, Leningrad.

Yakovlev, D. G., and Urpin, V. A. 1980, *Soviet Astronomy* **24**, 303.

Ziman, J. M. 1972, *Principles of the Theory of Solids* (Cambridge: Cambridge University Press).

Figure Captions

Figure 1.

Maximum growth rate, λ_{max}, with respect to β as a function of α for various boundary conditions at $\xi = 1$: (a) $B' = \alpha B$, (b) $B' = 0.75\alpha B$, (c) $B' = 0.5\alpha B$, and (d) $B' = 0$. For the boundary condition $B' = 0$ two different growing modes are present. Mode 1 resembles the growing mode for $B' = \alpha B$ with all of the flux being produced in the solid. In mode 2, all of the flux originates in the liquid and is convected across the solid surface into the solid crust.

Figure 2.

Eigenfunctions of growing modes with $\lambda_{max} = 0.1$ for three boundary conditions at $\xi = 1$: (a) $B' = \alpha B$, (b) $B' = 0.75\alpha B$, and (c) $B' = 0$. For $B' = \alpha B$, all the flux is produced in the solid and $\alpha = 22.5$. For $B' = 0.75\alpha B$ 90 percent of the flux is produced in the liquid and $\alpha = 5$. For $B' = 0$, (mode 2 in Figure 1), all the flux originates in the liquid and $\alpha = 0.2$.

Figure 3.

Growth rate as a function of β for fixed α with $\lambda_{max} = 0.1$ for the boundary conditions (a)-(c) of Figure 2.

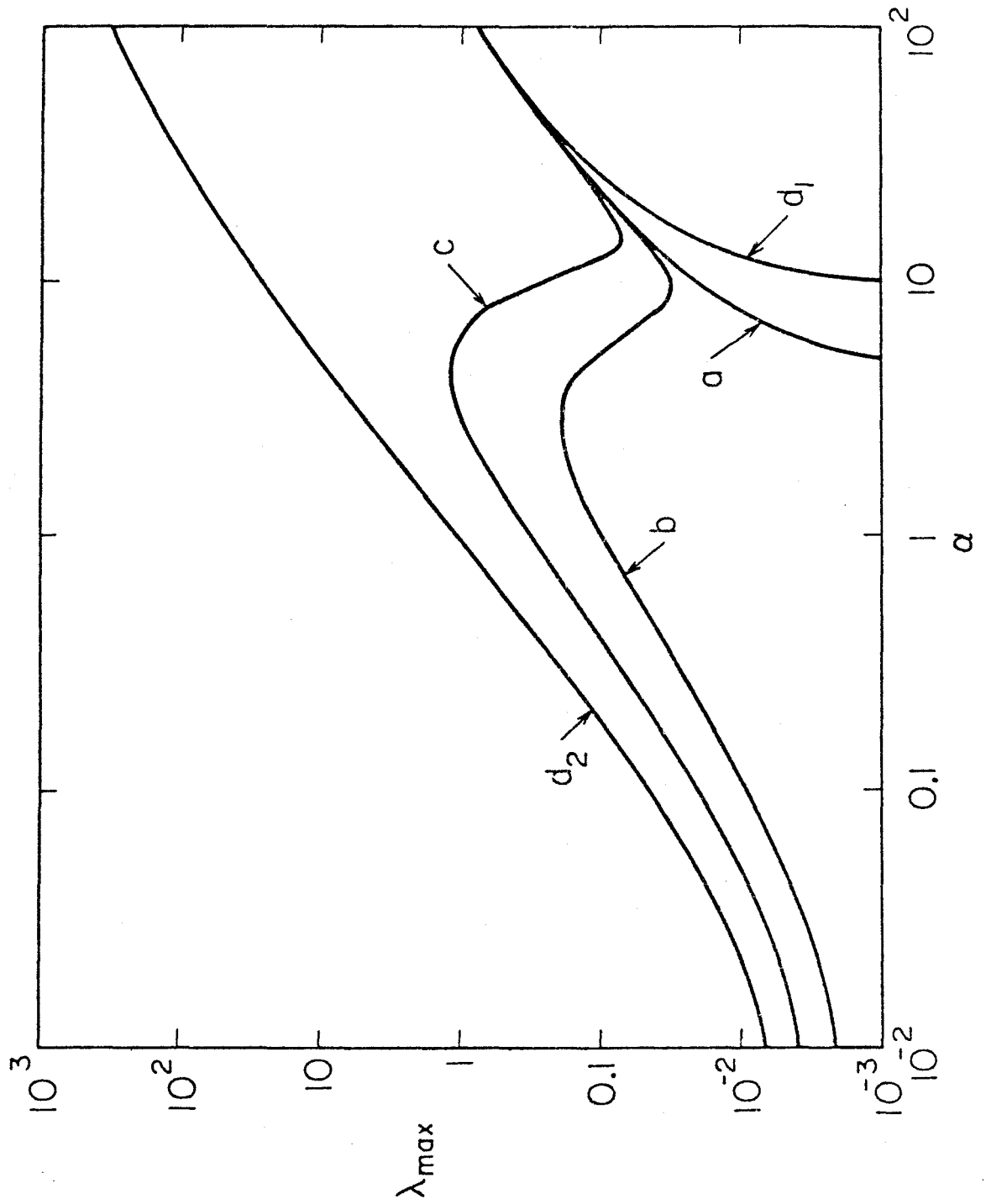

Figure 1

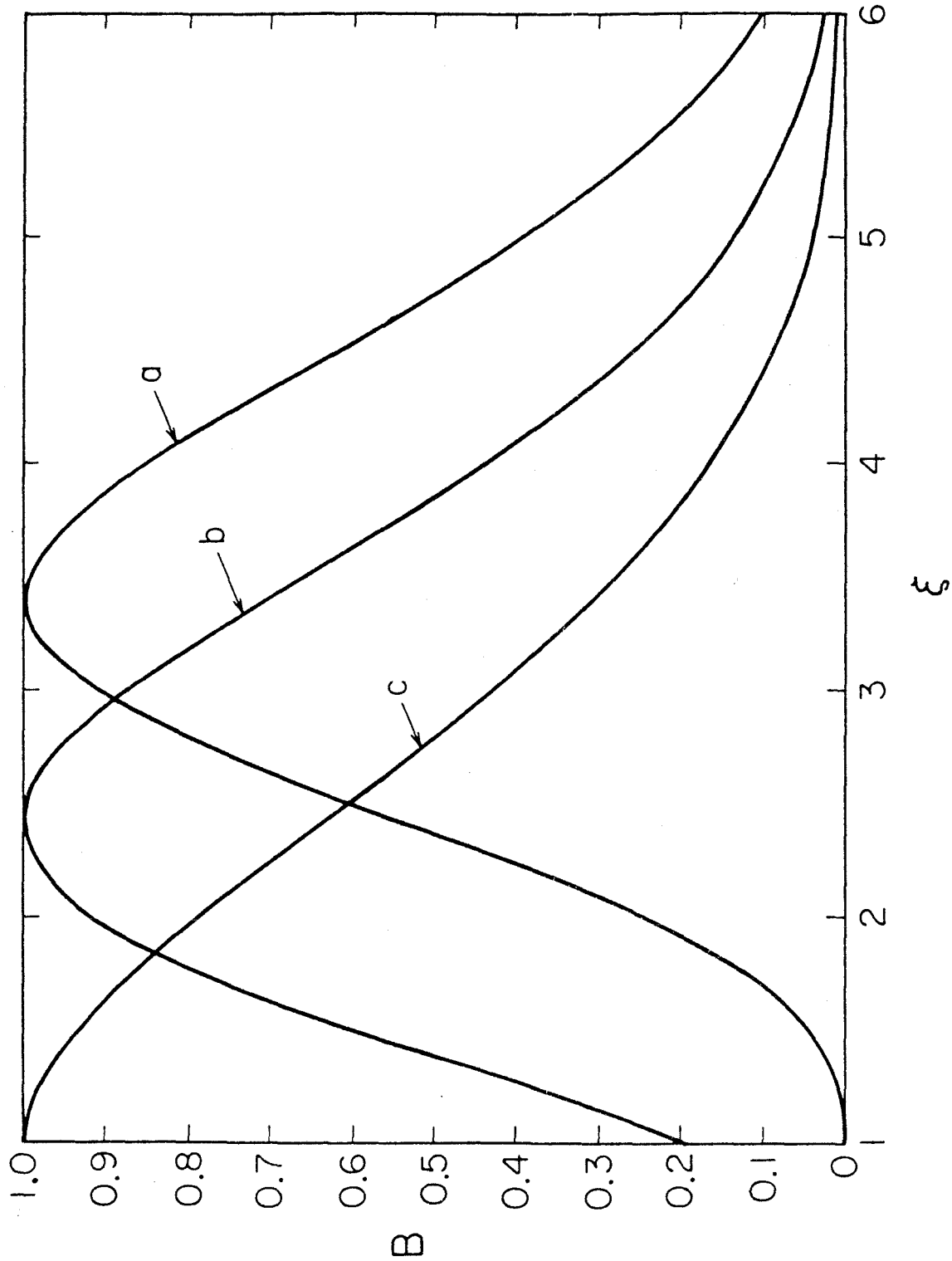

Figure 2

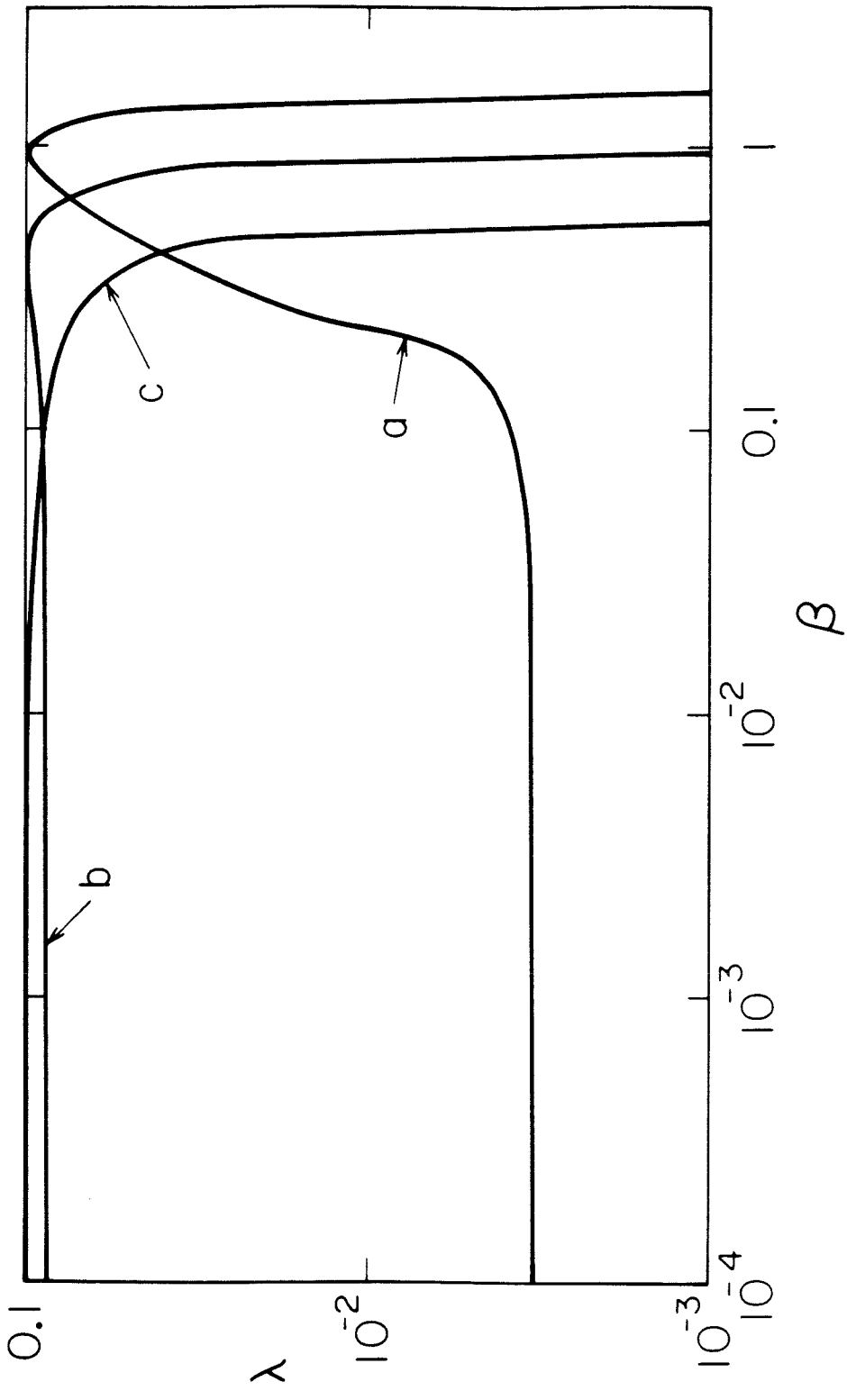

Figure 3

CHAPTER 4

Relativistic Electron Transport in a Quantizing Magnetic Field

Lars Hernquist

To be published in

The Astrophysical Journal Supplement Series,

1984 Nov 15.

Relativistic Electron Transport in a Quantizing Magnetic Field

Lars Hernquist

130-33 Caltech, Pasadena, California 91125, U.S.A.

ABSTRACT

For sufficiently strong magnetic fields the classical description of electron orbits is no longer valid and quantum effects must be taken into account. Transport properties will be affected through the influence of the discrete energy spectrum on the density of states and collision time. The physical conditions under which quantization can have significant thermodynamic consequences are analyzed, in connection with neutron star crusts. At the relevant densities and field strengths a relativistic treatment is essential. The transition rates between quantum states are derived using the exact solutions to the Dirac equation, assuming elastic scattering. Expressions for all of the independent components of the transport tensors (electrical conductivity, thermoelectric coefficient, and thermal conductivity) are derived for arbitrary degree of degeneracy and scattering mechanism. The resulting formulae, although compact in form, are difficult to evaluate. Computations of intermediate functions containing most of the numerical complexity are performed and fits are provided which allow the transport coefficients to be more easily calculated.

Results are given for the scattering potentials of most importance to neutron star applications (e-ion and e-phonon collisions). The fitting formulae are used to compute examples of transport coefficients for selected field strengths to demonstrate the value of this approach.

I. Introduction

The accurate determination of transport coefficients in a strong magnetic field is of importance to several astrophysical processes associated with neutron stars. Included are problems involving accretion flows (e.g., Blandford, DeCampli, and Königl 1979), stellar cooling (e.g., Tsuruta 1979; Glen and Sutherland 1980; Nomoto and Tsuruta 1981; Van Riper and Lamb 1981; Richardson *et al.* 1982), and the possible link between thermal processes and magnetic field evolution (Blandford, Applegate, and Hernquist 1983). Magnetic effects on electron transport are straightforward to take into account if the quantization of electron orbits is neglected. In general, however, this is not strictly valid under conditions of interest (field strengths range from $\sim 10^9 G$ for the millisecond pulsar to $\sim 10^{14} G$ for models which allow strong subsurface fields [Blandford, Applegate, and Hernquist 1983]).

Full quantum treatments have been made by Canuto and Chiu (1969), Canuto and Chiuderi (1970), Ventura (1973), Canuto and Ventura (1977), Yakovlev (1980a,b, 1982), and Kaminker and Yakovlev (1981). Difficulties with the earlier calculations have been noted by Yakovlev (1980a,b, 1982). In particular, large errors can be introduced if the completely degenerate limit ($T = 0$) is assumed. Thermal effects smooth and damp the quantum oscillations of the transport coefficients. Furthermore, the Wiedemann-Franz law no longer holds and it is not possible to compute the thermal conductivity from the electrical conductivity, as had been done earlier. The work of Yakovlev (1980a,b, 1982) corrects these omissions but is valid only in the non-relativistic limit. Relativistic transport perpendicular to the field has been considered by Kaminker and Yakovlev (1981), but final numerical calculations have not been performed. Because of the field strengths and densities relevant to neutron stars a relativistic treatment is essential.

The aim of this paper is to extend the work of Yakovlev (1980a,b, 1982) to relativistic matter and to present results which can more easily be used in applications. Detailed derivations of all elements of the transport tensors are presented in order to resolve the discrepancies between the existing calculations.

In § II the thermodynamic relations defining the transport coefficients are summarized. The quantum description of a relativistic electron in a magnetic field is given in § III . The necessary conditions for quantum effects to be important thermodynamically are also discussed, in connection with neutron star parameters. In § IV the possible effects of the magnetic field on the physical conditions in a neutron star crust are considered. The scattering rates required to determine the conductivities are derived in § V . Interaction potentials relevant to astrophysical processes are introduced in § VI . General expressions for the transport coefficients are derived in §§ VII, VIII, and IX . In § X computations of intermediate functions are given and technical issues are discussed. Accurate fits to these functions are presented and tabulated in the appendices. These results are used to calculate examples of transport coefficients in § XI . Finally, § XII states conclusions and considers remaining questions.

II. Thermodynamic Relations

In the presence of a magnetic field the relativistic laws of charge and heat transport are (e.g., Landau and Lifshitz 1960)

$$\vec{j} = \overleftrightarrow{\sigma} \cdot \vec{\varepsilon} - \overleftrightarrow{\lambda} \cdot \nabla T \tag{1}$$

$$\vec{F} = T\overleftrightarrow{\lambda} \cdot \vec{\varepsilon} - \overleftrightarrow{\gamma} \cdot \nabla T \tag{2}$$

The electrochemical field $\vec{\varepsilon} = \vec{E} + \nabla\mu / |e|$ accounts for electric fields as well as chemical potential gradients (Einstein's relation). The appearance of $\overleftrightarrow{\lambda}$ in both

equations (1) and (2) is the result of an Onsager relation. Note that μ includes the electron rest mass mc^2. In the absence of an electric current ($\vec{j} = 0$), equations (1) and (2) can be combined to give $\vec{F} = -\vec{\kappa} \cdot \nabla T$ where the thermal conductivity $\vec{\kappa}$ is related to the tensor $\vec{\gamma}$ by

$$\vec{\kappa} = \vec{\gamma} - T\vec{\lambda} \cdot (\vec{\sigma})^{-1} \cdot \vec{\lambda} \tag{3}$$

The thermoelectric coefficient $\vec{\lambda}$ is related to the thermopower $\vec{Q}$ by

$$\vec{Q} = (\vec{\sigma})^{-1} \cdot \vec{\lambda} \tag{4}$$

For a degenerate gas the difference between $\vec{\kappa}$ and $\vec{\gamma}$ is $\sim O(T/T_F)^2$ where the Fermi temperature is

$$kT_F = \mu - mc^2 + O(T^2) \tag{5}$$

(e.g., Blandford and Hernquist 1982). Relations (1)-(5) remain valid in a quantizing field.

If the quantizing nature of the magnetic field is neglected the Boltzmann equation can be solved in the relaxation time approximation to give (Urpin and Yakovlev 1980b)

$$\begin{bmatrix} \sigma_{0ij} \\ \lambda_{0ij} \\ \gamma_{0ij} \end{bmatrix} = -\frac{1}{12\pi^3\hbar^3} \int d^3p_0 \begin{bmatrix} -|e|(\varepsilon_0 - \mu_0)/T \\ (\varepsilon_0 - \mu_0)^2/T \end{bmatrix} v_0^2 \chi_{0ij}(\varepsilon_0) \frac{\partial f_0}{\partial \varepsilon_0} \tag{6}$$

where $\varepsilon_0^2 = p_0^2c^2 + m^2c^4$, $v_0 = p_0c^2/\varepsilon_0$ is the electron velocity, $f_0 = (1 + e^{(\varepsilon_0 - \mu_0)/kT})^{-1}$ is the Fermi-Dirac distribution, and the tensor χ_{0ij} is

$$\vec{\chi}_0(\varepsilon_0) = \frac{\tau_0(\varepsilon_0)}{1 + \Omega_0^2(\varepsilon_0)\tau_0^2(\varepsilon_0)} \begin{bmatrix} 1 & -\tau_0(\varepsilon_0)\Omega_0(\varepsilon_0) & 0 \\ \tau_0(\varepsilon_0)\Omega_0(\varepsilon_0) & 1 & 0 \\ 0 & 0 & 1 + \Omega_0^2(\varepsilon_0)\tau_0^2(\varepsilon_0) \end{bmatrix} \tag{7}$$

where τ_0 is the relaxation time and $\Omega_0 = |e|Bc/\varepsilon_0$ is the relativistic

gyrofrequency. (The subscript zero will be used throughout to denote a quantity in the absence of a quantizing magnetic field.) For a strongly degenerate gas ($T \ll T_{F_0}$) the lowest order terms in the Sommerfeld expansions give

$$\vec{\sigma}_0 = \frac{n_e e^2 c^2}{\mu_0} \vec{\chi}_0(\mu_0) \tag{8}$$

$$\vec{\lambda}_0 = -\frac{\pi^2 k^2 T}{3|e|} \frac{\partial \vec{\sigma}_0}{\partial \mu_0} \tag{9}$$

$$\vec{\gamma}_0 = \vec{\kappa}_0 = \frac{\pi^2 k^2 T}{3e^2} \vec{\sigma}_0 \tag{10}$$

The relation between $\vec{\kappa}_0$ and $\vec{\sigma}_0$ is the Wiedemann-Franz law, which is valid only to lowest order in T / T_{F_0}.

If the effects of a quantizing magnetic field are included much of the above description needs to be modified. However, several of the symmetries between elements of the transport tensors will still hold. In particular, the conductivities will obey the off-diagonal anti-symmetry of tensor (7) and have only three independent components. These can be taken to be, for example, Γ_{yy}, Γ_{yx}, and Γ_{zz}, where Γ denotes any of the transport coefficients and Γ_{yx} is the positive component ($\Gamma_{xy} = -\Gamma_{yx}$). In the limit of interest ($\Omega\tau \gg 1$) it will also be true that $\chi_{yy} \sim 1/\tau$, χ_{yx} will be independent of τ, and $\chi_{zz} \sim \tau$. At this point the similarity ends. In general the collision times will be different for each conductivity, will not be the same for χ_{yy} and χ_{zz}, and will furthermore depend on the magnetic field as well as the energy.

III. Quantization of Electron Orbits

For sufficiently strong magnetic fields the classical description of the trajectories of free electrons is no longer valid and quantum effects must be included. Consider a uniform magnetic field $\vec{B}$ along the z-axis in the Landau gauge: $\vec{A} = (-By,0,0)$. The Dirac equation can be solved exactly (e.g., Berestetskii, Lifshitz, and Pitaevskii 1982; Kaminker and Yakovlev 1981). The positive energy states are labeled by the quantum numbers ε, p_z, p_x, n, s where ε is the electron energy, $p_x = m\omega_B y_B$ characterizes the y-coordinate of the guiding center, p_z is the electron momentum along the field, $s = \pm 1$ is the helicity, and $n = 0,1,2\cdots$ enumerates the Landau levels. Note that the quantity ω_B, as used in this paper, is not the relativistic gyrofrequency $\Omega = |e|Bc/\varepsilon$, but is

$$\omega_B = |e|B/mc \tag{11}$$

The positive energy levels are

$$\varepsilon = (p_z^2c^2 + m^2c^4 + 2n\hbar\omega_B mc^2)^{1/2} \tag{12}$$

and the spinors are

$$\Psi(\vec{r}) = \frac{e^{i(p_x x + p_z z)/\hbar}}{\sqrt{L_x L_z}} \begin{pmatrix} \tilde{\alpha}\tilde{A}\tilde{H}_{n-1}(\xi) \\ -s\tilde{\alpha}\tilde{B}\tilde{H}_n(\xi) \\ s\tilde{\beta}\tilde{A}\tilde{H}_{n-1}(\xi) \\ -\tilde{\beta}\tilde{B}\tilde{H}_n(\xi) \end{pmatrix} \tag{13}$$

$$\begin{pmatrix} \tilde{\alpha} \\ \tilde{\beta} \end{pmatrix} = \sqrt{\tfrac{1}{2}(1 \pm mc^2/\varepsilon)}\,, \quad \begin{pmatrix} \tilde{A} \\ \tilde{B} \end{pmatrix} = \left[\tfrac{1}{2}\left(1 \pm \frac{sp_z c}{\sqrt{\varepsilon^2 - m^2c^4}}\right)\right]^{1/2} \tag{14}$$

$$\xi = \sqrt{m\omega_B/\hbar}\,(y - y_B)\,, \quad \tilde{H}_n(\xi) = \left[\frac{m\omega_B}{\pi\hbar}\right]^{1/4} (2^n n!)^{-1/2} \exp(-\xi^2/2) H_n(\xi) \tag{15}$$

The $H_n(\xi)$ are Hermite polynomials and the $\tilde{H}_n(\xi)$ are normalized harmonic

oscillator wave functions. The states $\Psi(\vec{r})$ are normalized to unity in the volume $L_x L_y L_z$. The states $n \neq 0$ are doubly degenerate in s ($s = \pm 1$). For the ground state ($n = 0$), however, the only allowed value of s is the one opposite in sign to p_z ($s = -\text{sign}\, p_z$). (See Kaminker and Yakovlev 1981 for a detailed discussion.)

As is apparent from equation (12) the electron is free parallel to $\vec{B}$, but the motion perpendicular to $\vec{B}$ is quantized. Because the statistical properties of an electron gas are determined, in part, by the available energy states, it is clear that the transport coefficients can be altered significantly. Several conditions must be met for the quantization to be important thermodynamically. In a real physical system the Landau levels will be thermally broadened. Quantum effects will be non-negligible only if the levels are narrow in comparison to the spacings between the levels. For a relativistic, degenerate gas this condition gives (e.g., Blandford and Hernquist 1982)

$$kT \ll \hbar\Omega \tag{16}$$

where $\Omega = |e|Bc/\mu$.

Similarly, collisions between the electrons and various scatterers will give rise to an uncertainty in the energies of the states and introduce a broadening of the levels $\Delta\varepsilon \sim \hbar/\tau$, where τ is the collision time. The condition analogous to relation (16) is

$$\Omega\tau \gg 1 \tag{17}$$

Finally, quantum effects will generally be negligible unless the system as a whole occupies only a small number of Landau levels. (The conductivities will approach the classical limit as $n \to \infty$ when thermal effects are included. If the completely degenerate forms ($T = 0$) are assumed the classical limit is never strictly achieved; however the deviations from the conductivities in the absence

of a quantizing field are practically negligible.) If n_{max} is the highest level populated this condition is, very roughly, for a degenerate gas (Blandford and Hernquist 1982)

$$n_{max} = (\mu^2 - m^2c^4)/2mc^2\hbar\omega_B < 10 \tag{18}$$

The relevance of these conditions to neutron star crusts ($10^4 \lesssim \rho \lesssim 10^{11}$) can be investigated by using the expressions for μ and τ in the absence of a quantizing field. In general, μ_0 is related to ρ through

$$\mu_0^2 = p_{F_0}^2c^2 + m^2c^4 \tag{19}$$

$$p_{F_0} = \hbar(3\pi^2)^{1/3}n_e^{1/3} \tag{20}$$

$$n_e = \frac{Z}{A}\frac{\rho}{m_p} \tag{21}$$

Equation (21) is valid only if a single ion species is present. Taking $Z = 26$, $A = 56$ relations (16) and (18) give

$$T_8 \ll B_{12}(1 + .6\rho_6^{2/3})^{-1/2} \tag{22}$$

$$\rho_6 < .6B_{12}^{3/2} \tag{23}$$

where $T = 10^8T_8$, $B = 10^{12}B_{12}$, and $\rho = 10^6\rho_6$.

The relaxation time τ_0 for a relativistic, degenerate gas has been calculated by Yakovlev and Urpin (1980). In the liquid phase electron-ion scattering dominates while in the solid phase electron-phonon scattering is most important. Electron-electron scattering will generally be negligible in neutron star crusts unless low Z ions ($Z \lesssim 10$) are present (e.g., Lampe 1968; Urpin and Yakovlev 1980a). The collision times are

$$\tau_0 = \frac{p_{F_0}^2 v_{F_0}}{4\pi Z^2 e^4 n_i \Lambda_{ei}} \qquad (e-\text{ion}) \tag{24}$$

$$\tau_0 = \frac{\hbar^2 v_{F_0}}{e^2 kT(2 - v_{F_0}^2/c^2)u_{-2}} \qquad (e-\text{phonon}) \tag{25}$$

where $v_{F_0} = p_{F_0}c^2/\mu_0$ is the electron velocity, Λ_{ei} is the Coulomb logarithm, and the parameter u_{-2} is related to the mean square thermal displacement of the ions, $\overline{\xi^2}$, by

$$\overline{\xi^2} = \frac{3kT}{m_i \omega_{p_i}^2} u_{-2} \tag{26}$$

$$\omega_{p_i}^2 = \frac{4\pi Z^2 e^2 n_i}{m_i} \tag{27}$$

where $n_i = n_e/Z$ is the ion number density.

For $\Lambda_{ei} = 1$ and iron, relation (17) gives in the liquid

$$1 + .6\rho_6^{2/3} \ll 40B_{12} \tag{28}$$

and for $u_{-2} = 13$ (Yakovlev and Urpin 1980) in the solid

$$\frac{1 + .3\rho_6^{2/3}}{\rho_6^{1/3}} \ll 5.5\,\frac{B_{12}}{T_8} \tag{29}$$

The ions are non-relativistic and nondegenerate and the state of the matter is determined by the parameter

$$\Gamma = Z^2 e^2/kTa \; ; \quad a = (3/4\pi n_i)^{1/3} \tag{30}$$

The liquid-solid phase transition occurs at $\Gamma = \Gamma_m$, with the matter being liquid for $\Gamma < \Gamma_m$ and solid for $\Gamma > \Gamma_m$. Estimates for Γ_m are in the range ~150–170 (e.g., Pollock and Hansen 1973; Slattery, Doolen, and DeWitt 1980). Using the average value $\Gamma_m = 160$ gives, for iron

$$T_7 = 2.5\rho_6^{1/3} \tag{31}$$

In Figure 1 $kT = \hbar\Omega_0$, $n_{max} = 10$, $\Omega_0\tau_0 = 1$, and the melting curve are given for a field strength $B = 10^{13}G$. Also shown is the sensitivity region from the work of Gudmundsson, Pethick, and Epstein (1983). It is within this zone that the unmagnetized cooling rates for a given central temperature depend most strongly on the values of the thermal conductivity.

Several tentative conclusions can be drawn from Figure 1, assuming that the location of the sensitivity region will not be greatly shifted when all magnetic effects are accounted for. The approximation $\Omega_0\tau_0 \gg 1$ is valid at all temperatures and densities of interest. This is significant because the derivations of the transport coefficients are valid only in this limit. Secondly, the restrictions $\hbar\Omega_0 \gg kT$ and $n_{max} < 10$ are stronger than $\Omega_0\tau_0 \gg 1$. Finally quantum effects can be important throughout much of the sensitivity strip, and a detailed calculation is necessary to determine the transport properties and the self-consistency of the above assumptions.

IV. Magnetic Effects on Physical Conditions

In addition to influencing the electron transport properties the magnetic field can affect the physical conditions in a neutron star crust (Yakovlev 1980a, 1982). For example, the boundary between the non-relativistic and relativistic limits will be shifted if the magnetic field is sufficiently strong. This arises because the simple unmagnetized relation between the chemical potential, μ, and density, ρ, is no longer valid.

Following Yakovlev (1980a, 1982), it is useful to define the following dimensionless parameters

$$\zeta = \frac{\mu}{\hbar\omega_B}, \quad \zeta_0 = \frac{\mu_0}{\hbar\omega_B}, \quad t = \frac{kT}{\mu - mc^2}, \quad \beta = \frac{\hbar\omega_B}{mc^2} \tag{32}$$

Thus t is a measure of the degree of degeneracy and β is the magnetic field in

units of $4.414\times10^{13}G$. As always μ and μ_0 include the electron rest mass. The chemical potential and density are related by

$$n_e = \frac{m\omega_B}{(2\pi\hbar)^2}\sum_{n=0}^{\infty} g_n \int_{-\infty}^{\infty} \frac{dp_z}{1+e^{(\varepsilon_n-\mu)/kT}} \tag{33}$$

where the ε_n are given by equation (12) and the factor g_n includes the spin degeneracy

$$g_n = 2 - \delta_{n0} \tag{34}$$

Equation (33) determines the chemical potential for given values of density, temperature, and field strength and is responsible for quantum oscillations in μ. It is instructive to view equation (33) as a relation between the four parameters in definition (32). I.e., in the $t \to 0$ limit, using equations (19)-(21)

$$\zeta_0 = \frac{1}{\beta}\left[\left(\frac{3}{2}\beta\sum_{n=0}^{n_{max}} g_n\sqrt{\beta^2\zeta^2 - 1 - 2n\beta}\right)^{2/3} + 1\right]^{1/2} \tag{35}$$

The upper limit in the sum is $n_{max} = (\beta^2\zeta^2 - 1)/2\beta$. In contrast to the non-relativistic limit (Yakovlev 1980a, 1982) this expression explicitly involves the magnetic field strength through β.

An example of the relation of ζ to ζ_0 is shown in Figure 2 for $B = 10^{13}G$ ($\beta = .2266$). The $t = 0$ limit was found from equation (35) and the $t = .05$ case required a numerical integration of equation (33). The kinks in the $t = 0$ curve reflect the appearance of a new Landau level in the sum in relation (35). As is obvious, even a small amount of thermal smoothing quickly damps out the deviation between ζ and ζ_0. Only in the limit $\zeta \to 1/\beta$ is there a pronounced difference.

Nevertheless, this effect can alter the physical conditions at low densities in a degenerate neutron star crust. Consider the $t = 0$ limit with only the ground

state (n = 0) populated. From equation (35), for iron

$$T_{F_9} \approx 6(\sqrt{1 + 2\rho_5^2 / B_{12}^2} - 1) \tag{36}$$

which is valid for $n_{max} = 0$ or, roughly, $B_{13} > 2\rho_6^{2/3}$. In the absence of a quantizing field

$$T_{F_{0_9}} \approx 6(\sqrt{1 + .6\rho_6^{2/3}} - 1) \tag{37}$$

Thus, at a given density, the following physical properties will be changed (Yakovlev 1980a, 1982): degree of degeneracy, level of ionization, the ideality of the gas, and the degree to which the matter is relativistic. From relations (36) and (37), for iron, including quantum effects (Q) and neglecting quantum effects (NQ)

Non-relativistic limit: $B_{12} = 1.4\rho_5$ (Q), $\rho_6 = 2$ (NQ) (38)

Degenerate limit: $T = T_F$ (Q), $T = T_{F_0}$ (NQ)

Ideal gas ($Ze^2 = kT_F a$): $B_{12} = 9\rho_5^{5/6}$ (Q), $\rho_6 = 6.5\times10^{-4}$ (NQ) (39)

where a is defined in equation (30). The limit of complete ionization is roughly $\varepsilon_I \approx kT_F$. Neglecting quantum effects $\varepsilon_I \approx 13.6Z^2$eV. For strong fields the value of ε_I is uncertain. A non-relativistic calculation (see Yakovlev 1980a, 1982) gives $\varepsilon_I \sim 13.6\ Z^2\ln^2(B/1.6\times10^{12})$eV for $B \gg 1.6\times10^{12}G$. Using these values

Complete ionization: $\rho_4 \sim B_{12}\ln(.6B_{12})$ (Q), $\rho_4 = 1.5$ (NQ) (40)

The limits (38)-(40) are indicated in the $B-\rho$ plane in Figure 3. The degeneracy limit ($T = T_F$) is shown for the values $T_F = 10^8, 10^7$. It has been assumed that the field has no influence on these properties if more than one Landau level is populated. For weaker fields ($n_{max} > 0$) the NQ limits are shown.

Finally it will be assumed throughout that the magnetic field does not affect the ions. This requires that $\omega_{B_i} = Z|e|B/m_i c \ll \omega_{p_i}$ or $B_{14} \ll \rho_6^{1/2}$ (Yakovlev 1980a, 1982). In this case the melting curve (31) still applies. For stronger fields possible effects include changes in the phonon spectrum and a shift in the melting curve (Yakovlev 1980a, 1982).

V. Scattering Rates

In order to derive expressions for the transport coefficients it is necessary to determine the rates at which electrons are scattered through various interactions. Electron-electron collisions are significant only for low Z ($Z \lesssim 10$) metals (Urpin and Yakovlev 1980a) and will be neglected. It is unlikely that these elements will be present at the densities where electron transport is dominant. Electron-impurity scattering will also not be considered because of the uncertainty in the detailed structure of the crystals. It is expected, however, that the solid phase of a neutron star crust will have fewer imperfections than terrestrial metals. (In any case it is relatively easy to extend the analysis to include impurities -- see Yakovlev 1980a, 1982 for details.)

Elastic scattering will be assumed throughout (for a discussion of recoil effects see Pavlov and Yakovlev 1976; Langer 1981). In the liquid (e-ion) this requires $\Delta\varepsilon \sim (kT/m_i)^{1/2} 2p_F \ll kT$. Neglecting quantum effects ($p_F = p_{F_0}$) this implies (for iron) $\rho \ll .02\, T^{3/2}$, which evaluated at the melt surface (31) gives $\rho \ll 6\times10^{12}$. Quantization will change p_F significantly only in the limit $n_{\max} = 0$. In the $t = 0$ limit, from relation (35)

$$p_F(n = 0) = \frac{2\pi^2\hbar^2 n_e}{m\omega_B} \tag{41}$$

Then the above condition is $\rho_6 \ll .5 T_7^{1/2} B_{12}$. Evaluating at the melt surface (31)

and for the minimum value of B for which equation (41) is valid ($B_{13} = 2\rho_6^{2/3}$) gives $\rho \ll 10^{13}$. Both limits are obviously true throughout the liquid crust.

In the solid (e-phonon) the scattering is elastic as long as $T > \Theta$ where Θ is the Debye temperature

$$\Theta = .45 \frac{\hbar}{k} \omega_{p_i} \tag{42}$$

with ω_{p_i} defined by relation (27). The condition $T > \Theta$ gives, for iron, $T_6 > 1.6\rho_6^{1/2}$. This can be violated at high densities. A quantizing magnetic field is unlikely to play a role in inelastic electron-phonon scattering. Quantum effects will be small unless $n_{max} \lesssim 10$ which requires $\rho_6 < .6B_{12}^{3/2}$. The field strength will probably be limited to $\sim 10^{14}G$, otherwise the magnetic stress will exceed the lattice yield stress (Blandford, Applegate, and Hernquist 1983), giving $\rho_6 < 6\times 10^2$. At this density the collisions will be elastic if $T_6 > 40$. The cooling calculations of Gudmundsson, Pethick, and Epstein (1983) indicate that this will always be true for temperature distributions of neutron stars with ages $\lesssim 10^6$ years. Only if magnetic effects radically alter the thermal structure will the electron-phonon collisions become inelastic at densities where quantum effects are non-negligible.

The scattering rate from initial state Ψ_i to final state Ψ_f is given by (e.g., Berestetskii, Lifshitz, and Pitaevskii 1982)

$$dw_{fi} = \frac{2\pi}{\hbar} |U_{fi}|^2 \delta(\varepsilon_f - \varepsilon_i) d\nu_f \tag{43}$$

The factor $d\nu_f$ is the density of final states, the δ-function accounts for energy conservation, and U_{fi} is the matrix element of the scattering potential. The matrix element is to be regarded as an ensemble average over the positions of uncorrelated scattering centers (correlation effects are discussed in § VI). I.e.,

(Canuto and Ventura 1977)

$$|\langle f \mid U \mid i\rangle|^2 = \sum_j \sum_{j'} \langle \psi_f(\vec{r}) \mid U(\vec{r} - \vec{R}_j) \mid \psi_i(\vec{r})\rangle \langle \psi_f(\vec{r}) \mid U(\vec{r} - \vec{R}_{j'}) \mid \psi_i(\vec{r})\rangle^* \quad (44)$$

where $\vec{r}$ are the electron coordinates and $\vec{R}_j$, $\vec{R}_{j'}$ are the scattering center coordinates. Expanding $U(\vec{r} - \vec{R}_j)$ in a Fourier series (e.g., Pavlov and Yakovlev 1976)

$$U(\vec{r} - \vec{R}_j) = \sum_{\vec{q}} U_q \, e^{i\vec{q} \cdot (\vec{r} - \vec{R}_j)} \quad (45)$$

(It is assumed that the wave functions are normalized in the volume $V = L_x L_y L_z$ where L_x, L_y, and L_z are much greater than any physical length-scales in the problem. Thus it will be possible to pass to the continuum limit with negligible error in sums such as that in eq. (45), when convenient.) Then

$$|\langle f \mid U \mid i\rangle|^2 = \sum_{\vec{q}} \sum_{\vec{q}'} U_q U_{q'}^* \left(\sum_j \sum_{j'} e^{-i\vec{q} \cdot \vec{R}_j} e^{i\vec{q}' \cdot \vec{R}_{j'}}\right) \langle f \mid e^{i\vec{q} \cdot \vec{r}} \mid i\rangle \langle f \mid e^{i\vec{q}' \cdot \vec{r}} \mid i\rangle^* \quad (46)$$

The ensemble average over scattering centers gives (e.g., Canuto and Ventura 1977)

$$\underset{\text{avg.}}{\text{ens.}} \left\{\sum_j \sum_{j'} e^{-i\vec{q} \cdot \vec{R}_j} e^{i\vec{q}' \cdot \vec{R}_{j'}}\right\} = V n_i \delta_{\vec{q}\vec{q}'} \quad (47)$$

where n_i is the number density of scattering centers. Thus the matrix element is

$$|U_{fi}|^2 = V n_i \sum_{\vec{q}} |U_q|^2 \, |\langle f \mid e^{i\vec{q} \cdot \vec{r}} \mid i\rangle|^2 \quad (47a)$$

Next, consider $\langle f \mid e^{i\vec{q} \cdot \vec{r}} \mid i\rangle$ using the wave functions defined by relations (13)-(15). The sums over x and z contribute the factors $\delta_{p_x', -p_x, \hbar q_x} \delta_{p_z', -p_z, \hbar q_z}$. For the y-sum, pass to the continuum limit and assume elastic scattering ($\varepsilon = \varepsilon'$,

$\tilde{\alpha} = \tilde{\alpha}'$, $\tilde{\beta} = \tilde{\beta}'$). This gives

$$\langle f \mid e^{i\vec{q}\cdot\vec{r}} \mid i \rangle = \delta_{p_x'-p_x,\hbar q_x}\delta_{p_z'-p_z,\hbar q_z}\,(ss'\tilde{\alpha}^2+\tilde{\beta}^2)[ss'\tilde{A}\tilde{A}'I_{n'-1n-1} + \tilde{B}\tilde{B}'I_{n'n}] \tag{48}$$

$$I_{n'n} = \int_{-\infty}^{\infty} e^{iq_y y}\tilde{H}_{n'}(\xi')\tilde{H}_n(\xi)dy \tag{49}$$

where primes are now used to denote quantities after the collision. The integrals (49) can be done (e.g., Kaminker and Yakovlev 1981) with the result

$$I_{n'n} = e^{i(n-n')\theta + iq_y(y_B + y_B')/2}F_{n'n}(u) \tag{50}$$

where $\theta = \tan^{-1}(q_y/q_x)$ and

$$u = \frac{\hbar}{2m\omega_B}(q_x^2 + q_y^2) \tag{51}$$

$$F_{n'n}(u) = (-1)^{n'-n}F_{nn'}(u) = \sqrt{n'!/n!}\;u^{(n-n')/2}e^{-u/2}L_{n'}^{n-n'}(u) \tag{52}$$

The functions $L_{n'}^{n-n'}(u)$ are Laguerre polynomials and the $F_{n'n}(u)$ are normalized so that $\int_0^{\infty} F_{n'n}^2 du = 1$. Note that the $F_{n'n}(u)$ defined in Kaminker and Yakovlev (1981) are not the same as those defined in Yakovlev (1980a,b, 1982). The matrix element becomes

$$|\langle f \mid U \mid i \rangle|^2 = V n_i \sum_{q_y} |U_q|^2\,|(ss'\tilde{\alpha}^2 + \tilde{\beta}^2)[ss'\tilde{A}\tilde{A}'I_{n'-1n-1}(u) + \tilde{B}\tilde{B}'I_{n'n}(u)]|^2 \tag{53}$$

Passing to the continuum limit, $U_q \to U_q/V$, where U_q now denotes a Fourier transform, and $\sum_{q_y} \to \frac{L_y}{2\pi}\int_{-\infty}^{\infty} dq_y$. The density of states factor is

$$d\nu_f = L_x L_z\,\frac{m\omega_B}{(2\pi\hbar)^2}\,dy_B'\,dp_z' \tag{54}$$

Combining, and using the definitions (14) of $\tilde{\alpha}$, $\tilde{\beta}$, $\tilde{A}$, and $\tilde{B}$ the scattering rate is

$$dw_{fi} = \frac{n_i m \omega_B}{32\pi^2\hbar^3}\left[1 + ss' + \frac{m^2c^4}{\varepsilon^2}(1-ss')\right]\int_{-\infty}^{\infty} |U_q|^2 \cdot$$

$$\left\{\left[1 - \frac{sp_z c + s'p_z'c}{\sqrt{\varepsilon^2 - m^2c^4}} + \frac{ss'p_z p_z'c^2}{\varepsilon^2 - m^2c^4}\right]F^2_{n'n}(u)\right.$$

$$+ \left[1 + \frac{sp_z c + s'p_z'c}{\sqrt{\varepsilon^2 - m^2c^4}} + \frac{ss'p_z p_z'c^2}{\varepsilon^2 - m^2c^4}\right]F^2_{n'-1n-1}(u)$$

$$\left. + 2ss'\left[1 - \frac{p_z^2c^2 + p_z'^2c^2}{\varepsilon^2 - m^2c^4} + \frac{p_z^2 p_z'^2 c^4}{(\varepsilon^2 - m^2c^4)^2}\right]^{1/2} F_{n'n}(u)\,F_{n'-1n-1}(u)\right\} \cdot$$

$$\cdot\, \delta(\varepsilon_f - \varepsilon_i)dq_y dy_B' dp_z' \qquad (55)$$

Simplifying, using the following recursion relation (Kaminker and Yakovlev 1981)

$$4\sqrt{nn'}F_{n'-1n-1}F_{n'n} = (n + n')(F^2_{n'-1n-1} + F^2_{n'n}) - u(F^2_{n'-1n} + F^2_{n'n-1}) \qquad (56)$$

gives

$$dw_{fi} = \frac{n_i m \omega_B}{32\pi^2\hbar^3}\left[1 + ss' + \frac{m^2c^4}{\varepsilon^2}(1 - ss')\right]\int_{-\infty}^{\infty} |U_q|^2 \cdot$$

$$\left\{\left[1 + ss' - \frac{1}{2}\frac{ss'c^2}{\varepsilon^2 - m^2c^4}(p_z' - p_z)^2\right](F^2_{n'n}(u) + F^2_{n'-1n-1}(u))\right.$$

$$- \frac{ss'u\hbar\omega_B mc^2}{\varepsilon^2 - m^2c^4}(F^2_{n'-1n}(u) + F^2_{n'n-1}(u))$$

$$\left. - \frac{sp_z c + s'p_z'c}{\sqrt{\varepsilon^2 - m^2c^4}}(F^2_{n'n}(u) - F^2_{n'-1n-1}(u))\right\}\delta(\varepsilon_f - \varepsilon_i)dq_y dy_B' dp_z' \qquad (57)$$

In some applications (e.g., cross-field conductivity) it is necessary to have the scattering rate summed over initial and final spins. Assuming spin-independent interaction potentials

$$\sum_{ss'} dw_{fi} = \frac{n_i m \omega_B}{4\pi^2\hbar^3} \frac{m^2c^4}{\varepsilon^2} \int_{-\infty}^{\infty} |U_q|^2 \left\{ \left[\frac{\varepsilon^2}{m^2c^4} - \frac{(p_z' - p_z)^2}{4m^2c^2} \right] (F^2_{n'n}(u) + F^2_{n'-1n-1}(u)) \right.$$

$$\left. - \frac{u}{2} \frac{\hbar\omega_B}{mc^2} (F^2_{n'-1n} + F^2_{n'n-1}) \right\} \delta(\varepsilon_f - \varepsilon_i) dq_y dy_B' dp_z' \qquad (58)$$

In the non-relativistic limit this becomes

$$\sum_{ss'} dw_{fi} \to \frac{n_i m \omega_B}{4\pi^2\hbar^3} \int_{-\infty}^{\infty} |U_q|^2 (F^2_{n'n}(u) + F^2_{n'-1n-1}(u)) \, \delta(\varepsilon_f - \varepsilon_i) dq_y dy_B' dp_z' \qquad (59)$$

which agrees with results given earlier (Pavlov and Yakovlev 1976).

As a result of energy conservation p_z and p_z' are determined up to a sign for given ε, n, n'. It is useful to define the factors $\eta(=\pm 1)$ and $\eta'(=\pm 1)$ by

$$p_z = \eta p_n \qquad (60)$$

$$p_n = \frac{1}{c} \sqrt{\varepsilon^2 - m^2c^4 - 2n\hbar\omega_B mc^2} \qquad (61)$$

and similarly for η'. Then the δ-function in the scattering rate can be written

$$\delta(\varepsilon_f - \varepsilon_i) dp_z' = \frac{\varepsilon}{p_{n'}c^2} (\delta(p_z' - p_{n'}) + \delta(p_z' + p_{n'})) \, dp_z' \qquad (62)$$

Finally, it should be noted that by adopting the Born approximation for the scattering rate (43) it has been implicitly assumed that $\Omega\tau \gg 1$ (condition [17]). That is, the Born approximation does not account for multiple scatterings. Thus the dynamics of the electron must be dominated by the field and not the collisions. For purposes of calculating quantum effects on electron transport this is

not a serious limitation, in view of the discussion in § III. However, it should not be surprising that this assumption can lead to difficulties in certain derivations (see § VIII) which must be corrected by non-rigorous methods.

VI. Interaction Potentials

In the liquid phase electron-ion collisions represent the dominant scattering mechanism. The standard procedure (e.g., Yakovlev and Urpin 1980) is to use a screened Coulomb potential. The term $|U_q|^2$ is then (Yakovlev 1980a, 1982)

$$|U_q|^2 = \left(\frac{4\pi Ze^2}{q^2 + r_d^{-2}}\right)^2 \tag{63}$$

where r_d is the screening length. It is useful for the applications to follow to write this in terms of dimensionless quantities. Defining

$$\nu = \varepsilon/\hbar\omega_B \tag{64}$$

$$a_d = \hbar/2m\omega_B r_d^2 \tag{65}$$

and using relation (51) gives

$$|U_q|^2 = \frac{4\pi\hbar^4\sigma_0}{m^2}\,\frac{1}{(u + \xi_n^{n'}(\nu,\beta)/2\beta + a_d)^2} \tag{66}$$

where

$$\xi_n^{n'}(\nu,\beta) = (\eta'\sqrt{\nu^2\beta^2 - 2n'\beta - 1} - \eta\sqrt{\nu^2\beta^2 - 2n\beta - 1})^2 \tag{67}$$

$$\sigma_0 = \frac{\pi Z^2 e^4}{\hbar^2\omega_B^2} \tag{68}$$

The exact choice for r_d is somewhat problematical. Fortunately the transport

coefficients do not depend sensitively on this factor and the most convenient choice will be discussed in § X .

In the solid phase of the neutron star crust the electron kinetic energy is much greater than the Coulomb interaction energy. The result of this is that, unlike terrestrial metals, the scattering will be dominated by *Umklapp* processes. The electrons will then interact with individual ions participating in the collective motion. This will be true if the momentum transfer is sufficiently large that the major contribution to the scattering comes from Brillouin zones distant from the first one. This condition can be expressed as (Yakovlev and Urpin 1980) $8p_F^3/6\pi^2 n_i \hbar^3 \gg 1$. Neglecting quantum effects, this gives $4Z \gg 1$, which is always valid in neutron star crusts. If only the lowest Landau level is occupied, p_F is given by relation (41) and the requirement is roughly (for iron) $\rho_6 \gg .04 B_{13}^{3/2}$. Equation (41) is valid only if $n_{max} = 0$ or $\rho_6 < .35 B_{13}^{3/2}$. Thus it is possible that this condition could be violated over a narrow range of densities. However, the cooling calculations of Gudmundsson, Pethick, and Epstein (1983) show that crystallization will not occur at these low densities during time-scales of interest. Again, as with the condition for elastic scattering, this will not be a problem unless the thermal structure is radically altered by magnetic effects.

If, in addition, $T > \Theta$ the scattering will be elastic and the electrons may be thought of as interacting with the single particle potential $U(\vec{r}) = -Ze^2(|\vec{r} - \vec{\xi}|^{-1} - r^{-1}) \approx -Ze^2(\vec{r} \cdot \vec{\xi})/r^3$ (Yakovlev and Urpin 1980). The quantity $\vec{\xi}$ measures the deviation of an ion from equilibrium. Averaging over all displacements and performing the Fourier transform gives (Yakovlev 1980a, 1982)

$$|U_q|^2 = \frac{(4\pi Ze^2)^2}{3q^2}\overline{\xi^2} \tag{69}$$

where $\overline{\xi^2}$ is related to u_{-2} through equation (26). In terms of dimensionless

quantities

$$|U_q|^2 = \frac{4\pi\hbar^4\sigma_0}{m^2}\frac{1}{u + \xi_n^{\eta'\eta}/2\beta} \tag{70}$$

$$\sigma_0 = \frac{2\pi}{3}\frac{Z^2e^4m}{\hbar^3\omega_B}\bar{\xi}^2 \tag{71}$$

There is a great deal of uncertainty in the value of the quantity u_{-2}. Estimates range from ~4.4 (Flowers and Itoh 1976) to 13 (Yakovlev and Urpin 1980). In the determination of transport coefficients u_{-2} will appear only as an overall multiplicative factor. The tabulated results presented will not depend on u_{-2}. The examples in § XI will be calculated in such a form (transport coefficients in terms of the zero field values) that they do not depend on u_{-2}. In order to actually compute numerical values for the transport coefficients, however, a value for u_{-2} must be assumed and the uncertainty in this factor should be kept in mind.

Equations (66) and (70) can be conveniently summarized as

$$|U_q|^2 = \frac{4\pi\hbar^4\sigma_0}{m^2}h_n^{\eta'\eta}(u;\nu,\beta) \tag{72}$$

$$h_n^{\eta'\eta}(u;\nu,\beta) = \begin{cases} \dfrac{1}{(u + \xi_n^{\eta'\eta}/2\beta + a_d)^2} & \text{(ions)} \\ \dfrac{1}{u + \xi_n^{\eta'\eta}/2\beta} & \text{(phonons)} \end{cases} \tag{73}$$

where σ_0 is given by equation (68) for e-ion scattering and by equation (71) for e-phonon scattering.

VII. Transport Parallel to $\vec{B}$

The quantum theory of transport phenomena has been discussed by many authors (e.g., Kohn and Luttinger 1957; Kubo, Yokota, and Nakajima 1957; Luttinger 1964; Kubo, Miyake, and Hashitsume 1965; Stinchcombe 1974). In this paper the method developed by Zyryanov (e.g., Zyryanov and Guseva 1969; Zyryanov and Klinger 1976) will be used for compatibility with Yakovlev (1980a,b, 1982). As is well known, the quantum theory of electron conduction is formulated in terms of the density matrix. It is often convenient to use the density matrix to define the Wigner function, which is analogous to the distribution function of classical statistical physics (e.g., ter Haar 1961). It can be shown (e.g., Kahn and Frederikse 1959; Stinchcombe 1961; Zyryanov and Guseva 1969) that if one considers small $\vec{E}$, $\nabla\mu$, and ∇T parallel to $\vec{B}$, then the Wigner function evolves according to the Boltzmann equation. Physically the justification for this method lies in the fact that the electrons are free parallel to $\vec{B}$. For transport perpendicular to $\vec{B}$ this is not the case, and other methods must be used.

The relativistic Boltzmann equation is

$$\frac{\partial f_{np_zs}}{\partial t} + v_z \frac{\partial f_{np_zs}}{\partial z} - |e| E \frac{\partial f_{np_zs}}{\partial p_z} = \left.\frac{\partial f_{np_zs}}{\partial t}\right]_{\text{coll}} \tag{74}$$

The function f_{np_zs} describes the population of electrons in the quantum state labeled by n,s. Taking into account the exclusion principle the collision term can be written

$$\left.\frac{\partial f_{np_zs}}{\partial t}\right]_{\text{coll}} = \sum_f W_{if} \left(f_{n'p_z's'} - f_{np_zs}\right) \tag{75}$$

where the sum is over the quantum numbers n',s',p_z',y_B'. Since the inhomogeneities in the system $(\nabla\mu,\nabla T)$ are parallel to $\vec{B}$, f_{np_zs} is independent of y_B (Zyryanov and Guseva 1969) and the scattering rate can be integrated over y_B'

immediately. Also, the sum over p_z' in equation (75) can be performed, absorbing the δ-function in the scattering rate. Then

$$\left.\frac{\partial f_{np_zs}}{\partial t}\right]_{\text{coll}} = \sum_{n's'\eta'} W(np_zs \to n'\eta's')(f_{n'\eta's'} - f_{np_zs}) \tag{76}$$

Where, from equation (57), the scattering rate $W(np_zs \to n'\eta's')$ is

$$W(np_zs \to n'\eta's') = \frac{n_i}{32\pi^2\hbar^2}\frac{\varepsilon}{p_{n'}c^2}\left[1 + ss' + \frac{m^2c^4}{\varepsilon^2}(1 - ss')\right]$$

$$\cdot \int_{-\infty}^{\infty}\int_{-\infty}^{\infty} |U_q|^2\left\{\left[1 + ss' - \frac{1}{2}\frac{ss'c^2}{\varepsilon^2 - m^2c^4}(\eta'p_{n'} - p_z)^2\right](F^2_{n'n}(u) + F^2_{n'-1n-1}(u))\right.$$

$$- \frac{ss'u\hbar\omega_B mc^2}{\varepsilon^2 - m^2c^4}(F^2_{n'-1n}(u) + F^2_{n'n-1}(u))$$

$$\left. - \frac{sp_zc + s'\eta'p_{n'}c}{\sqrt{\varepsilon^2 - m^2c^4}}(F^2_{n'n}(u) - F^2_{n'-1n-1}(u))\right\} dq_y\, dq_x \tag{77}$$

using $dy_B' = \hbar dq_x / m\omega_B$.

As an example of how the transport coefficients are derived, consider only an electric field (other circumstances are a trivial generalization). In the steady state

$$-|e|E\,\frac{\partial f_{np_zs}}{\partial p_z} = \sum_{n's'\eta'} W(np_zs \to n'\eta's')(f_{n'\eta's'} - f_{np_zs}) \tag{78}$$

This can be solved by linearization. Assume $f_{np_zs} = f^0 + f^1_{np_zs}$ where f^0 is the equilibrium (Fermi-Dirac) distribution function, which depends only on the energy. Using $\partial f^0/\partial p_z = (p_zc^2/\varepsilon)\partial f^0/\partial\varepsilon$, equation (78) is to first order

$$\sum_{n's'\eta'} W(np_zs \to n'\eta's')(f^1_{n'\eta's'} - f^1_{np_zs}) = -|e|E\,\frac{p_zc^2}{\varepsilon}\frac{\partial f^0}{\partial\varepsilon} \tag{79}$$

This is a system of equations for the perturbations $f^1_{np_zs}$ from which the currents are determined.

The electric and thermal currents are

$$j_z = -\frac{|e|}{V}\sum_i v_z f^1_{np_zs} \tag{80}$$

$$F_z = \frac{1}{V}\sum_i (\varepsilon - \mu) v_z f^1_{np_zs} \tag{81}$$

where the sums are over n, p_z, s, y_B. Since the summand is independent of y_B, $\sum_i \to V(m\omega_B/4\pi^2\hbar^2)\sum_{n=0}^{\infty}\sum_{s=\pm1}\int_{-\infty}^{\infty} dp_z$. After algebra, using $v_z = p_z c^2/\varepsilon$, equations (80) and (81) become

$$j_z = -\frac{|e|m\omega_B c^2}{4\pi^2\hbar^2}\sum_{n=0}^{\infty}\sum_{s=\pm1}\int_0^{\infty}\frac{p_n}{\varepsilon}(f^1_{np_ns} - f^1_{n-p_ns})\,dp_n \tag{82}$$

$$F_z = \frac{m\omega_B c^2}{4\pi^2\hbar^2}\sum_{n=0}^{\infty}\sum_{s=\pm1}\int_0^{\infty}(\varepsilon - \mu)\frac{p_n}{\varepsilon}(f^1_{np_ns} - f^1_{n-p_ns})\,dp_n \tag{83}$$

Interchanging the sum over n and the integral over p_n, using $dp_n = \varepsilon d\varepsilon/p_n c^2$ gives

$$j_z = -\frac{|e|m\omega_B}{4\pi^2\hbar^2}\int_{mc^2}^{\infty}\sum_{n=0}^{n_{max}}\sum_{\eta=\pm1}\sum_{s=\pm1}\eta f^1_{n\eta s}\,d\varepsilon \tag{84}$$

$$F_z = \frac{m\omega_B}{4\pi^2\hbar^2}\int_{mc^2}^{\infty}(\varepsilon - \mu)\sum_{n=0}^{n_{max}}\sum_{\eta=\pm1}\sum_{s=\pm1}\eta f^1_{n\eta s}\,d\varepsilon \tag{85}$$

The sum over n is limited by $n_{max} = (\varepsilon^2 - m^2c^4)/2mc^2\hbar\omega_B$. In order to find the transport coefficients it is useful to define a dimensionless scattering rate $a(n\eta s \to n'\eta' s')$ and a dimensionless perturbation to the distribution function $\varphi_{n\eta s}$ by

$$W(n\eta s \rightarrow n'\eta's') = n_i |v_z| \sigma_0 a(n\eta s \rightarrow n'\eta's') \tag{86}$$

$$f^1_{n\eta s} = \eta \frac{|e|E}{\sigma_0 n_i} \frac{\partial f^0}{\partial \varepsilon} \varphi_{n\eta s} \tag{87}$$

where σ_0 is defined by equation (68) for e-ion scattering and by equation (71) for e-phonon scattering. Then relation (79) becomes a dimensionless system for $\varphi_{n\eta s}$

$$\sum_{n'=0}^{n_{max}} \sum_{\eta'=\pm1} \sum_{s'=\pm1} a(n\eta s \rightarrow n'\eta's') \left(\varphi_{n\eta s} - \frac{\eta'}{\eta} \varphi_{n'\eta's'} \right) = 1 \tag{88}$$

for $n = 0,1,2, \cdots n_{max}$, $\eta = \pm1$, $s = \pm1$. The transport coefficients are given by equations (84), (85), (87) and the general definitions (1) and (2). A procedure analogous to the one outlined above, taking into account temperature gradients, allows γ_{zz} to be found. The final result can be expressed in the form

$$\begin{pmatrix} \sigma_{zz} \\ \lambda_{zz} \\ \gamma_{zz} \end{pmatrix} = - \frac{2m\omega_B}{4\pi^2\hbar^2\sigma_0 n_i} \int_{mc^2}^{\infty} \frac{\partial f^0}{\partial \varepsilon} \begin{pmatrix} -|e|(\varepsilon-\mu)/T \\ e^2 \\ (\varepsilon-\mu)^2/T \end{pmatrix} \varphi(\nu,\beta)\, d\varepsilon \tag{89}$$

$$\varphi(\nu,\beta) = \frac{1}{2} \sum_{n=0}^{n_{max}} \sum_{\eta=\pm1} \sum_{s=\pm1} \varphi_{n\eta s} \tag{90}$$

where β and ν are defined in equations (32) and (64), respectively. Note that in definition (90) the term with $n=0$ has only the combinations $\eta=1, s=-1$ and $\eta=-1, s=1$ (see § III). Equations (89) are the quantum analogs of relations (6) along the field in the limit $\Omega\tau \gg 1$ (see the discussion at the end of § V).

The non-relativistic limit of these expressions is

$$\begin{pmatrix} \sigma_{zz} \\ \lambda_{zz} \\ \gamma_{zz} \end{pmatrix} = - \frac{2m\omega_B}{4\pi^2\hbar^2\sigma_0 n_i} \int_{0}^{\infty} \frac{\partial f^0}{\partial \varepsilon} \begin{pmatrix} -|e|(\varepsilon-\mu)/T \\ e^2 \\ (\varepsilon-\mu)^2/T \end{pmatrix} \varphi_{NR}\, d\varepsilon \tag{91}$$

It is possible to show that non-relativistically (e.g., Ventura 1973)

$f^1_{n\eta=-1s} = -f^1_{n\eta=+1s}$ (where s now denotes spin, and not helicity) implying that $\varphi_{n\,1s} = \varphi_{n\,-1s}$. Thus

$$\varphi_{NR} = \sum_{n=0}^{n_{max}} \sum_{s=\pm 1} \varphi_n^s \tag{92}$$

where $\eta = +1$ has been used. Furthermore spin-flip transitions are not important (Yakovlev 1980a,b, 1982) so that the system for φ_n^s can be written as

$$(2a_{nn}^- + \sum_{n' \neq n} (a_{nn'}^+ + a_{nn'}^-))\,\varphi_n^s - \sum_{n' \neq n} (a_{nn'}^+ - a_{nn'}^-)\,\varphi_{n'}^s = 1 \tag{93}$$

where $a_{nn'}^- = a(n\eta{=}1 \to n'\eta'{=}-1)$, $a_{nn'}^+ = a(n\eta{=}1 \to n'\eta'{=}1)$. The results (91)-(93) agree with those of Yakovlev (1980a, 1982).

The expressions (88)-(90) together with the relations defining $a(n\eta s \to n'\eta's')$, equations (77) and (86), are completely general, as long as the scattering is elastic. They are valid for arbitrary degree of degeneracy and scattering mechanism of interest. For the special cases of $|U_q|^2$ given in § VI the rates $a(n\eta s \to n'\eta's')$ are explicitly (for other $|U_q|^2$ see Kaminker and Yakovlev 1981)

$$a(n\eta s \to n'\eta's') = \frac{1}{4}\frac{\nu^2\beta^3}{q_{n'}q_n}\left[1 + ss' + \frac{1}{\beta^2\nu^2}(1 - ss')\right]\int_0^\infty h_n^{\eta'\eta}(u;\nu,\beta)\left\{\left[1 + ss'\right.\right.$$

$$\left.-\frac{1}{2}\frac{ss'}{\beta^2\nu^2 - 1}(\eta' q_{n'} - \eta q_n)^2\right](F^2_{n'n}(u) + F^2_{n'-1n-1}(u)) - \frac{ss'\beta}{\beta^2\nu^2 - 1}u(F^2_{n'-1n} + F^2_{n'n-1})$$

$$\left.-\frac{s\eta q_n + s'\eta' q_{n'}}{\sqrt{\beta^2\nu^2 - 1}}(F^2_{n'n}(u) - F^2_{n'-1n-1}(u))\right\}du \tag{94}$$

where $q_n = (\nu^2\beta^2 - 2n\beta - 1)^{1/2}$. Thus, $\varphi(\nu;\beta)$ is independent of σ_0 and, in particular, for the phonon case independent of u_{-2}. For electron-ion scattering $\varphi(\nu;\beta)$ depends weakly on the screening lengths through the function $h_n^{\eta'\eta}(u;\nu,\beta)$ (see

eq. [73]).

Two complications arise in the solution of the system of equations (88). The scattering rates $a(n\eta s \rightarrow n'\eta's')$ satisfy the two symmetry relations

$$a(n\eta s \rightarrow n'\eta's') = a(n'\eta's' \rightarrow n\eta s) \tag{95}$$

$$a(n\eta s \rightarrow n'\eta's') = a(n-\eta-s \rightarrow n'-\eta'-s') \tag{96}$$

The first follows from detailed balance and the second from time-reversal (these can be demonstrated explicitly from [94]). It is possible to show that these two conditions are sufficient to ensure that the system (88) is singular. Further, if the system is of dimension N the rank will be $N-1$. An additional relation between the $\varphi_{n\eta s}$ is required to close the system. This is provided by the requirement that the perturbation to the distribution function not change the number of particles in the system. In terms of $\varphi_{n\eta s}$ this gives

$$\sum_{n=0}^{n_{max}} \sum_{\eta=\pm1} \sum_{s=\pm1} \eta\varphi_{n\eta s} = 0 \tag{97}$$

Again only $\eta=1,s=-1$ and $\eta=-1,s=1$ are allowed for $n=0$. In practice this relation can be substituted for any one of the equations in the system (88) and it will no longer be singular.

The second potential problem involves the question of possible divergences in the integrals defining $a(n\eta s \rightarrow n'\eta's')$. That is, if $n = n'$ and $\eta = \eta'$ then $\xi_{nn}^{\eta\eta}(\nu,\beta) = 0$; thus for phonons $h_{nn}^{\eta\eta}(u;\nu,\beta) = 1/u$. Near the origin several of the terms in the integrand of equation (94) are divergent. However, it is easy to show that these difficulties do not enter into the solution of the system. To this end, equation (88) can be written

$$\sum_{\substack{n'=0\\n'\neq n}}^{n_{max}} \sum_{\eta'=\pm 1} \sum_{s'=\pm 1} a(n\eta s \to n'\eta' s') \left(\varphi_{n\eta s} - \frac{\eta'}{\eta}\varphi_{n'\eta' s'}\right) + a(n\eta s \to n\eta -s)(\varphi_{n\eta s} - \varphi_{n\eta -s})$$

$$+ a(n\eta s \to n -\eta s)(\varphi_{n\eta s} + \varphi_{n -\eta s}) + a(n\eta s \to n -\eta -s)(\varphi_{n\eta s} + \varphi_{n -\eta -s}) = 1 \qquad (98)$$

And, from relation (94) the coefficients $a(n\eta s \to n\eta -s)$ for phonon scattering can be found analytically

$$a(n\eta s \to n\eta -s) = \frac{\beta^2}{(\beta^2\nu^2 - 1)(\beta^2\nu^2 - 2n\beta - 1)} \quad (n \neq 0) \qquad (99)$$

using the symmetry and normalization of the $F^2_{n'n}$. For $n = n' = 0$, $\eta = \eta'$ is not allowed. Thus no divergent terms appear.

It is of interest to consider the completely degenerate limit ($T \to 0$) of the transport coefficients. Following the standard procedure the leading behavior of the expressions (89) is

$$\sigma_{zz} = \frac{2m\omega_B e^2}{\sigma_0 n_i 4\pi^2\hbar^2}\varphi(\zeta;\beta) + O(T^2) \qquad (100)$$

$$\lambda_{zz} = -\frac{m|e|k^2T}{6\sigma_0 n_i \hbar^3}\varphi'(\zeta;\beta) + O(T^3) \qquad (101)$$

$$\gamma_{zz} = \kappa_{zz} = \frac{\pi^2}{3}\frac{k^2T}{e^2}\sigma_{zz} \qquad (102)$$

where $\varphi'(\zeta;\beta) \equiv d\varphi/d\nu|_{\nu=\zeta}$. These are analogous to the components of expressions (8)-(10) along the field in the $\Omega\tau \gg 1$ limit. The Wiedemann-Franz law is again recovered. Unfortunately these expansions are not as useful as the expressions in the absence of a quantizing field. The higher order terms in equations (100)-(102) involve derivatives of φ which can be infinite due to jump discontinuities in φ (see examples in § X). Thus these expansions can be strongly violated for certain values of ζ.

VIII. Transport Perpendicular to $\vec{B}$-Dissipative Currents

This section will be concerned with the diagonal components of the transport coefficients, orthogonal to $\vec{B}$. Symmetry requires that the xx and yy components of the tensors be equal. As a result of the quantization of the electron motion perpendicular to $\vec{B}$ it is not possible to use a Boltzmann equation to derive the conductivities. The method of Zyryanov (Zyryanov and Guseva 1969; Zyryanov and Klinger 1976) is applicable. It relies on the continuity equations for charge and thermal energy density

$$\frac{\partial}{\partial t}(-|e|n_e) + \nabla\cdot\vec{j} = 0 \tag{103}$$

$$\frac{\partial W}{\partial t} + \nabla\cdot\vec{F} = 0 \tag{104}$$

As an example, consider chemical potential and temperature gradients along the y-axis: $\nabla\mu = \nabla_y\mu\hat{e}_y$, $\nabla T = \nabla_y T\hat{e}_y$. The number density is given in terms of the density matrix by

$$n_e = \sum_{\alpha\alpha'} \hat{n}_{\alpha\alpha'}\rho_{\alpha\alpha'} \tag{105}$$

where the sum is over all quantum numbers and the number density operator is

$$\hat{n}_{\alpha\alpha'} = \Psi_\alpha^\dagger\Psi_{\alpha'}\delta_{\alpha\alpha'} \tag{106}$$

Writing the spinors as $\Psi(\vec{r}) = e^{i(p_x x + p_z z)/\hbar}\psi(\xi)/\sqrt{L_x L_z}$ and in the continuum limit, $\sum_\alpha \to L_x L_z\,(m\omega_B/4\pi^2\hbar^2)\sum_{ns}\int_{-\infty}^{\infty}dp_z\int_{-\infty}^{\infty}dy_B$ gives

$$n_e = \frac{m\omega_B}{4\pi^2\hbar^2}\sum_{ns}\int_{-\infty}^{\infty}\int_{-\infty}^{\infty}\psi^\dagger(\xi)\psi(\xi)f_{ns}(p_z,y_B)dp_z\,dy_B \tag{107}$$

The diagonal components of the density matrix $\rho_{\alpha\alpha} = f_{ns}(p_z,y_B)$ serve as the

distribution function and evolve, due to collisions, according to (Zyryanov and Guseva 1969)

$$\frac{\partial f_{ns}}{\partial t}(p_z, y_B) = \sum_f W_{if}(f_{n's'}(p_z', y_B') - f_{ns}(p_z, y_B)) \tag{108}$$

where W_{if} is the scattering rate and the sum is over n', p_z', s', y_B'. Thus

$$\frac{\partial}{\partial t}(-|e|n_e) = -\frac{|e|m\omega_B}{4\pi^2\hbar^2}\sum_{ns}\sum_{n's'}\sum_{p_z' y_B'}\int_{-\infty}^{\infty}\int_{-\infty}^{\infty}\psi^\dagger(\xi)\psi(\xi)W_{if}$$

$$(f_{n's'}(p_z', y_B') - f_{ns}(p_z, y_B))\,dp_z\,dy_B \tag{109}$$

Linearization is now performed by substituting the local equilibrium distribution function for $f_{n's'}(p_z', y_B')$ and $f_{ns}(p_z, y_B)$. It can be shown that this is given by (Zyryanov and Guseva 1969)

$$f^0_{y_B}(\varepsilon) = \left[1 + \exp\left[\frac{\varepsilon - \mu(y_B)}{kT(y_B)}\right]\right]^{-1} \tag{110}$$

For sufficiently large magnetic fields $\psi^\dagger(\xi)\psi(\xi)$ will be non-zero only in a narrow range of ξ centered about ξ=0 and it is possible to ignore the distinction between y and y_B. Then, taking into account the normalization of $\psi^\dagger(\xi)\psi(\xi)$ and expanding the result in a series of $y_B' - y_B$ gives to lowest order

$$\frac{\partial}{\partial t}(-|e|n_e) = -\frac{\partial}{\partial y}\left[-\frac{|e|m\omega_B}{4\pi^2\hbar^2}\sum_{ns}\sum_{n's'}\sum_{p_z' y_B'}\int_{-\infty}^{\infty}\frac{(y_B' - y_B)^2}{2}\frac{\partial f^0}{\partial \varepsilon}\right.$$

$$\left.\left(\nabla_y\mu + \frac{\varepsilon - \mu}{T}\nabla_y T\right)W_{if}\,dp_z\right] \tag{111}$$

where f^0 is the equilibrium distribution function $f^0 = (1 + \exp((\varepsilon - \mu)/kT))^{-1}$, depending only on energy. Then relations (103) and (111) imply

$$j_y = -\frac{|e|m\omega_B}{4\pi^2\hbar^2}\sum_{ns}\sum_{n's'}\sum_{p_z'y_B'}\int_{-\infty}^{\infty}\frac{(y_B'-y_B)^2}{2}\frac{\partial f^0}{\partial\varepsilon}\left[\nabla_y\mu+\frac{\varepsilon-\mu}{T}\nabla_y T\right]W_{if}\,dp_z \qquad (112)$$

The derivation for the thermal energy current is completely analogous and gives

$$F_y = \frac{m\omega_B}{4\pi^2\hbar^2}\sum_{ns}\sum_{n's'}\sum_{p_z'y_B'}\int_{-\infty}^{\infty}\frac{(y_B'-y_B)^2}{2}\frac{\partial f^0}{\partial\varepsilon}(\varepsilon-\mu)\left[\nabla_y\mu+\frac{\varepsilon-\mu}{T}\nabla_y T\right]W_{if}\,dp_z \qquad (113)$$

From equations (1) and (2) the transport coefficients are

$$\begin{pmatrix}\sigma_{yy}\\ \lambda_{yy}\\ \gamma_{yy}\end{pmatrix} = -\frac{m\omega_B}{4\pi^2\hbar^2}\sum_{ns}\sum_{n's'}\sum_{p_z'y_B'}\int_{-\infty}^{\infty}\frac{(y_B'-y_B)^2}{2}\frac{\partial f^0}{\partial\varepsilon}W_{if}\begin{bmatrix}-|e|(\varepsilon-\mu)/T\\ (\varepsilon-u)^2/T\\ e^2\end{bmatrix}dp_z \qquad (114)$$

In this expression only W_{if} depends on s,s' and p_z'. Integrating the scattering rate (58) over p_z' and using $dy_B' = \hbar dq_x/m\omega_B$ gives

$$\sum_{ss'p_z'}W_{if} = \frac{n_i m^2c^2}{4\pi^2\hbar^2 p_n\varepsilon}\sum_{\eta'=\pm1}\int_{-\infty}^{\infty}|U_q|^2\left\{\left[\frac{\varepsilon^2}{m^2c^4}-\frac{(\eta'p_{n'}-p_z)^2}{4m^2c^2}\right]\right.$$

$$\left.(F^2_{n'n}(u)+F^2_{n'-1n-1}(u))-\frac{u}{2}\frac{\hbar\omega_B}{mc^2}(F^2_{n'-1n}(u)+F^2_{n'n-1}(u))\right\}dq_x\,dq_y \qquad (115)$$

Interchanging the integral over p_z and the sum over n in equation (114) (see eqs. [80]-[85]) and using $y_B' - y_B = \hbar q_x/m\omega_B$

$$\begin{pmatrix}\sigma_{yy}\\ \lambda_{yy}\\ \gamma_{yy}\end{pmatrix} = -\frac{1}{8\pi^2 m\omega_B c^2}\int_{mc^2}^{\infty}\frac{\partial f^0}{\partial\varepsilon}\begin{bmatrix}-|e|(\varepsilon-\mu)/T\\ (\varepsilon-\mu)^2/T\\ e^2\end{bmatrix}$$

$$\left[\sum_{n=0}^{n_{max}}\sum_{n'=0}^{n_{max}}\sum_{\eta=\pm1}\sum_{q_x}q_x^2\frac{\varepsilon}{p_n}\sum_{ss'p_z'}W_{if}\right]\Bigg|_{p_z=\eta p_n}d\varepsilon \qquad (116)$$

Finally, combining equations (115) and (116) and transforming the integral over $dq_x\,dq_y$ to one over du

$$\begin{pmatrix}\sigma_{yy}\\ \lambda_{yy}\\ \gamma_{yy}\end{pmatrix} = -\frac{n_i m^3 \omega_B}{16\pi^3\hbar^4}\int_{mc^2}^{\infty}\frac{\partial f^0}{\partial\varepsilon}\begin{pmatrix}-|e|(\varepsilon-\mu)/T\\ (\varepsilon-\mu)^2/T\end{pmatrix}\left\{\sum_{n=0}^{n_{max}}\sum_{n'=0}^{n_{max}}\sum_{\eta=\pm1}\sum_{\eta'=\pm1}\frac{1}{p_n p_{n'}}\int_0^{\infty} u\,|U_q|^2\right.$$

$$\left.\left[\left(\frac{\varepsilon^2}{m^2c^4}-\frac{(\eta' p_{n'}-\eta p_n)^2}{4m^2c^2}\right)(F^2_{n'n}+F^2_{n'-1n-1})-\frac{u}{2}\frac{\hbar\omega_B}{mc^2}(F^2_{n'-1n}+F^2_{n'n-1})\right]du\right\}d\varepsilon \quad (117)$$

The sums over n and n' are limited by $n_{max} = (\varepsilon^2 - m^2c^4)/2mc^2\hbar\omega_B$. This agrees with the result given by Kaminker and Yakovlev (1981) if we note that the summand of η and η' depends on η,η' only in the combination $(\eta' p_{n'} - \eta p_n)^2 = (p_{n'} - \eta\eta' p_n)^2$. (This is true of the scattering potentials given in § VI as well.) Then $\sum_{\eta=\pm1}\sum_{\eta'=\pm1} \to 2\sum_{(\eta\eta')=\pm1}$ and the previous result is recovered.

The non-relativistic limit of relation (117) is

$$\begin{pmatrix}\sigma_{yy}\\ \lambda_{yy}\\ \gamma_{yy}\end{pmatrix} = -\frac{n_i m^3 \omega_B}{16\pi^3\hbar^4}\int_0^{\infty}\frac{\partial f^0}{\partial\varepsilon}\begin{pmatrix}-|e|(\varepsilon-\mu)/T\\ (\varepsilon-\mu)^2/T\end{pmatrix}\left\{\sum_{n=0}^{n_{max}}\sum_{n'=0}^{n_{max}}\sum_{\eta=\pm1}\sum_{\eta'=\pm1}\frac{1}{p_n p_{n'}}\right.$$

$$\left.\int_0^{\infty} u\,|U_q|^2\,(F^2_{n'n}+F^2_{n'-1n-1})\,du\right\}d\varepsilon \quad (118)$$

This agrees with the non-relativistic result of Yakovlev (1980b) if we replace the sums over η and η' with a single sum over the product of η and η' as above.

The expressions (117) are completely general as long as the scattering is elastic. They are valid for any degree of degeneracy and scattering mechanism of interest. For the special cases given in § VI (see Kaminker and Yakovlev 1981 for others) equation (117) can be written in a more useful form in terms of dimensionless quantities. Let $\sum_{\eta=\pm1}\sum_{\eta'=\pm1} \to 2\sum_{\pm}$ where the plus sign denotes forward scattering ($\eta = \eta'$) and the minus sign denotes backward scattering ($\eta = -\eta'$). Then

$$\begin{pmatrix}\sigma_{yy}\\ \lambda_{yy}\\ \gamma_{yy}\end{pmatrix} = -\frac{n_i \sigma_0}{2\pi^2\hbar}\int_{mc^2}^{\infty}\frac{\partial f^0}{\partial\varepsilon}\begin{pmatrix}-|e|(\varepsilon-\mu)/T\\ (\varepsilon-\mu)^2/T\end{pmatrix} Q(\nu;\beta)\,d\varepsilon \quad (119)$$

where

$$Q(\nu;\beta) = \beta \sum_{n=0}^{n_{max}} \sum_{n'=0}^{n_{max}} \sum_{\pm} \frac{1}{\sqrt{\nu^2\beta^2 - 1 - 2n\beta}\sqrt{\nu^2\beta^2 - 1 - 2n'\beta}} \int_0^\infty u h^{\pm}_{n'n}(u;\nu,\beta)$$

$$[(\nu^2\beta^2 - \frac{1}{4}\xi^{\pm}_{n'n})(F^2_{n'n}(u) + F^2_{n'-1n-1}(u)) - \frac{u}{2}\beta(F^2_{n'-1n}(u) + F^2_{n'n-1}(u))]\,du \qquad (120)$$

$$h^{\pm}_{n'n}(u;\nu,\beta) = \begin{cases} 1/(u + \xi^{\pm}_{n'n}/2\beta + a_d)^2 & e\text{-ion} \\ 1/(u + \xi^{\pm}_{n'n}/2\beta) & e\text{-phonon} \end{cases} \qquad (121)$$

$$\xi^{\pm}_{n'n} = (\sqrt{\nu^2\beta^2 - 2n'\beta - 1} \mp \sqrt{\nu^2\beta^2 - 2n\beta - 1})^2 \qquad (122)$$

The quantity σ_0 is defined by relation (68) for e-ion scattering and by relation (71) for e-phonon scattering. Written in this form the function $Q(\nu;\beta)$ is independent of σ_0. In particular it does not depend on u_{-2} for e-phonon collisions and is only a weak function of the screening parameter a_d for e-ion collisions. The overall multiplicative factor of β in the definition of $Q(\nu;\beta)$ ensures that Q is independent of β in the non-relativistic limit. Relations (119) are analogous to the corresponding components of equation (6) in the limit $\Omega\tau \gg 1$.

A complication arises in the evaluation of $Q(\nu;\beta)$ and the subsequent integration over energy. In terms of ν and β, $n_{max} = (\nu^2\beta^2 - 1)/2\beta$. Whenever ν is such that $\nu = \sqrt{1+2n_{max}\beta}/\beta$ the terms in the sum over n,n' with $n = n_{max}$ and/or $n' = n_{max}$ will be singular. The terms with only $n = n_{max}$ or $n' = n_{max}$ do not cause difficulty because they are square-root type singularities and can be integrated. The terms with $n = n' = n_{max}$, however, cannot be handled and the integral over ε diverges logarithmically. The origin of these divergences can be understood as follows. The development has implicitly assumed that $\Omega\tau \gg 1$ (see end of § V). In this limit the components of the transport tensors under discussion $\sim 1/\tau$ (see § II). The magnitude of the electron momentum along the field is $p_n = \sqrt{\varepsilon^2 - m^2c^4 - 2n\hbar\omega_B mc^2}/c = mc\sqrt{\nu^2\beta^2 - 1 - 2n\beta}$. Electrons with

energy such that $\nu^2\beta^2 - 1 - 2n\beta \to 0$ will have vanishingly small velocity along the field and the collision time for these particles will go to zero. Physical quantities $\sim 1/\tau$ are then divergent. This is not a problem for transport along the field as these coefficients $\sim\tau$ (see § II). Thus the singularities are not physical but are a direct result of the approximation $\Omega\tau \gg 1$ breaking down.

The standard method for handling the divergences is to exclude the points $\varepsilon = \varepsilon_n = \sqrt{m^2c^4 + 2n\hbar\omega_B mc^2}$ from the integral (119) of the divergent terms (Kaminker and Yakovlev 1981; Yakovlev 1980b). That is, the integral of the divergent terms is written in the form $\sum_{n=0}^{\infty} \int_{\varepsilon_n+\gamma_n}^{\varepsilon_{n+1}} (\,) d\varepsilon$. The parameters γ_n, which cut off the integral and remove the singular behavior, are chosen on a physical basis. Several mechanisms have been proposed (for a thorough discussion see Kubo, Miyake, and Hashitsume 1965). For applications to neutron star matter the two most important factors in determining the γ_n are inelasticity of the electron collisions and collisional broadening of the Landau levels (Yakovlev 1980b). The appropriate value of γ_n is given by the mechanism with the larger cutoff energy (Kubo, Miyake, and Hashitsume 1965) and depends, in general, on density and temperature. The transport coefficients will also, then, depend weakly on the γ_n.

If inelasticity is the dominant cutoff mechanism γ_n is given by the mean energy transfer in a collision. For e-ion scattering this is, roughly (Yakovlev 1980b)

$$\gamma_n \sim \left(\frac{kT}{m_i}\right)^{1/2} 2p_F \tag{123}$$

As noted in § V this factor is $\ll kT$ in the liquid phase. To estimate the importance of this factor, set $p_F = p_{F_0}$ and use the degenerate relation of p_{F_0} to density (eq. [20]). Then, for iron

$$\gamma_n \sim 5.2\times10^{-11}\rho_6^{1/3}T_6^{1/2} \tag{124}$$

For electron-phonon collisions (Yakovlev 1980b)

$$\gamma_n \sim \hbar\omega_{p_i} \tag{125}$$

where ω_{p_i} is defined by equation (27). Again, if $Z = 26$, $A = 56$

$$\gamma_n \sim 5\times10^{-10}\rho_6^{1/2} \tag{126}$$

If collisional broadening of the Landau levels dominates, then γ_n is given by the standard expression in § III

$$\gamma_n \sim \hbar/\tau \tag{127}$$

As an estimate, the collision times (24), (25) can be used. In the liquid, assuming iron and $\Lambda_{ei} = 1$

$$\gamma_n \sim 4.8\times10^{-10}\sqrt{1 + .6\rho_6^{2/3}} \tag{128}$$

In the solid with $Z = 26$, $A = 56$, and $u_{-2} = 13$

$$\gamma_n \sim 3.4\times10^{-11}\rho_6^{-1/3}(1 + .3\rho_6^{2/3})(1 + .6\rho_6^{2/3})^{-1/2}T_6 \tag{129}$$

The approximate regions in the $\rho-T$ plane where each mechanism is more important are indicated in Figure 4, along with the melting curve (31).

Finally, it is again of interest to find the limiting ($T \to 0$) expressions for the transport coefficients. The leading behavior of equation (119) is

$$\sigma_{yy} = \frac{n_i\sigma_0 e^2}{2\pi^2\hbar}Q(\zeta;\beta) + O(T^2) \tag{130}$$

$$\lambda_{yy} = -\frac{n_i\sigma_0|e|k^2T}{6\hbar^2\omega_\beta}Q'(\zeta;\beta) + O(T^3) \tag{131}$$

$$\gamma_{yy} = \kappa_{yy} = \frac{\pi^2}{3}\frac{k^2 T}{e^2}\sigma_{yy} \tag{132}$$

where $Q'(\zeta;\beta) = dQ/d\nu|_{\nu=\zeta}$. These correspond to the appropriate cross-field components of equations (8)-(10) in the limit $\Omega\tau \gg 1$. The Wiedemann-Franz (132) is recovered. Again these are not as useful as relations (8)-(10) because of the singularities in $Q(\nu;\beta)$. Only if thermal smoothing is included do the divergences vanish. Note that in this limit the transport coefficients are independent of the γ_n.

IX. Transport Perpendicular to $\vec{B}$-Non-Dissipative Currents

In the limit $\Omega\tau \gg 1$ the off-diagonal components of the transport tensors are independent of the scattering mechanism (see § II) and hence are referred to as non-dissipative. Furthermore, only one of these is independent and can be taken to be the $y-x$ (positive) component. As in § VIII a method relying on a transport equation cannot be used. In addition, the effects of currents and heat fluxes associated with magnetization must be taken into account. Because these are solenoidal a derivation based on the continuity equations (103), (104) is also not possible. The method developed by Zyryanov (e.g., Zyryanov and Guseva 1969) for these components is applicable.

If scattering is neglected the density matrix is diagonal $\rho_{\alpha\alpha'} = f_\alpha \delta_{\alpha\alpha'}$ (Zyryanov and Guseva 1969) where f_α will play the role of a distribution function. In this approximation f_α will depend only on the constants of motion ε, p_z, and y_B (Zyryanov and Guseva 1969).

As an example, consider chemical potential and temperature gradients along the y-axis. $\nabla\mu = \nabla_y \mu \hat{e}_y$, $\nabla T = \nabla_y T \hat{e}_y$. The electric and thermal currents in the x-direction are given in terms of f_α by

$$\tilde{j}_x = -|e| \sum_\alpha (\hat{j}_x)_{\alpha\alpha} f_\alpha \tag{133}$$

$$\tilde{F}_x = \sum_a (\varepsilon - \mu)\,(\hat{j}_x)_{aa} f_a \tag{134}$$

where $(\hat{j}_x)_{aa}$ are the diagonal components of the probability current density operator (e.g., Berestetskii, Lifshitz, and Pitaevskii 1982)

$$(\hat{j}_x)_{aa} = c\,\Psi_a^\dagger \gamma^0 \gamma_x\, \Psi_a \tag{135}$$

In the standard representation

$$\gamma^0\gamma_x = \begin{pmatrix} 0 & \sigma_x \\ \sigma_x & 0 \end{pmatrix} = \begin{pmatrix} 0 & 0 & 0 & 1 \\ 0 & 0 & 1 & 0 \\ 0 & 1 & 0 & 0 \\ 1 & 0 & 0 & 0 \end{pmatrix} \tag{136}$$

From the definition of Ψ (eqs. [13]-[15]), relations (135) and (136) give

$$(\hat{j}_x)_{aa} = -\frac{c}{L_x L_z} \frac{\sqrt{2n\hbar\omega_B mc^2}}{\varepsilon} \tilde{H}_n(\xi)\tilde{H}_{n-1}(\xi) \tag{137}$$

Equations (133) and (134) are linearized by using the local equilibrium distribution function (110) for f_a. For weak gradients in μ and T this can be expanded

$$f_a = f^0 + (y - y_B)\,\frac{\partial f^0}{\partial \varepsilon}\left[\nabla_y \mu + \frac{\varepsilon - \mu}{T}\nabla_y T\right] + \cdots \tag{138}$$

where f^0 is the equilibrium distribution function $f^0 = (1 + \exp(\varepsilon - \mu)/kT)^{-1}$, depending only on energy. The function f^0 causes the currents to vanish as is easily verified by performing the integral over y_B in equations (133) and (134). Using $\sum_a \to (L_x L_z / 4\pi^2\hbar^2) m\omega_B \sum_{n\sigma} \int_{-\infty}^{\infty} dy_B \int_{-\infty}^{\infty} dp_z$ and the definitions (15) of ξ and $\tilde{H}_n(\xi)$

$$\tilde{j}_x = \frac{|e|mc^2\hbar\omega_B}{4\pi^2\hbar^2}\sum_{ns}\int_{-\infty}^{\infty}\frac{1}{\varepsilon}\frac{\partial f^0}{\partial\varepsilon}\left(\nabla_y\mu + \frac{\varepsilon-\mu}{T}\nabla_y T\right)\frac{1}{\sqrt{\pi}2^{n-1}(n-1)!}\cdot$$

$$\int_{-\infty}^{\infty}\xi e^{-\xi^2}H_n(\xi)H_{n-1}(\xi)d\xi\,dp_z \tag{139}$$

and similarly for $\tilde{F}_x$. As always the term with $n=0$ has spin degeneracy 1 while the other terms are doubly degenerate. The integral over ξ can be done by using the recursion relation for Hermite polynomials $\xi H_n(\xi) = \frac{1}{2}H_{n+1}(\xi) + nH_{n-1}(\xi)$, giving the factor $n\sqrt{\pi}2^{n-1}(n-1)!$. Thus

$$\tilde{j}_x = \frac{|e|mc^2}{4\pi^2\hbar^2}\sum_{ns}\int_{-\infty}^{\infty}\frac{n\hbar\omega_B}{\varepsilon}\frac{\partial f^0}{\partial\varepsilon}\left(\nabla_y\mu + \frac{\varepsilon-\mu}{T}\nabla_y T\right)dp_z \tag{140}$$

$$\tilde{F}_x = -\frac{mc^2}{4\pi^2\hbar^2}\sum_{ns}\int_{-\infty}^{\infty}\frac{n\hbar\omega_B}{\varepsilon}(\varepsilon-\mu)\frac{\partial f^0}{\partial\varepsilon}\left(\nabla_y\mu + \frac{\varepsilon-\mu}{T}\nabla_y T\right)dp_z \tag{141}$$

In order to relate these to the currents j_x and F_x defined by equations (1) and (2) it is necessary to account for magnetization effects (Zyryanov and Guseva 1969). The associated currents are

$$\vec{j}_m = c\,\nabla\times\vec{M} \tag{142}$$

$$\vec{F}_m = c\,\nabla\times\vec{L} \tag{143}$$

where $\vec{M}$ is the magnetization and $\vec{L}$ is defined analogously.

It can be shown that the appearance of magnetization currents is directly attributable to slight inaccuracies in the treatment of the density of states factor $\sum_a \to (L_x L_z/4\pi^2\hbar^2)m\omega_B\sum_{ns}\int_{-\infty}^{\infty}dy_B\int_{-\infty}^{\infty}dp_z$. That is, the spinors (13) are normalized in the finite volume $L_x L_y L_z$, whose dimensions are assumed to be much larger than any relevant physical dimensions in the system. Thus the integral over y_B in $\sum_a$ can be extended to $\pm\infty$, with negligible error in most cases.

However, Heuser and Hajdu (1974) have demonstrated in the non-relativistic case that it is precisely this approximation which leads to the appearance of surface effects in the calculation of transport coefficients. Furthermore, they have shown that a calculation correcting for magnetization currents (such as that presented here) leads to results equivalent with an exact treatment of the density of states factor.

The magnetization is most easily found from the thermodynamic relation $M_z = -(1/V)(\partial\Omega/\partial B)_{\mu,T}$ where Ω is the grand potential (e.g., Blandford and Hernquist 1982)

$$\Omega = -\frac{kTVm\omega_B}{4\pi^2\hbar^2}\sum_{ns}\int_{-\infty}^{\infty}\ln(1+e^{(\mu-\varepsilon_n)/kT})\,dp_z \tag{144}$$

Using relation (12), after an integration by parts

$$M_z = \frac{|e|mc}{4\pi^2\hbar^2}\sum_{ns}\int_{-\infty}^{\infty} f^0\frac{1}{\varepsilon}\left[\frac{p_z^2}{m} - n\hbar\omega_B\right]dp_z \tag{145}$$

But

$$(\nabla\times\vec{M})_x = \frac{\partial M_z}{\partial\mu}\nabla_y\mu + \frac{\partial M_z}{\partial T}\nabla_y T \tag{146}$$

There is no corresponding contribution in the y-direction. Thus

$$(j_m)_x = -\frac{|e|mc^2}{4\pi^2\hbar^2}\sum_{ns}\int_{-\infty}^{\infty}\frac{1}{\varepsilon}\left[\frac{p_z^2}{m} - n\hbar\omega_B\right]\frac{\partial f^0}{\partial\varepsilon}\left[\nabla_y\mu + \frac{\varepsilon-\mu}{T}\nabla_y T\right]dp_z \tag{147}$$

The thermal current is given similarly by

$$(F_m)_x = \frac{mc^2}{4\pi^2\hbar^2}\sum_{ns}\int_{-\infty}^{\infty}\frac{1}{\varepsilon}\left[\frac{p_z^2}{m} - n\hbar\omega_B\right](\varepsilon-\mu)\frac{\partial f^0}{\partial\varepsilon}\left[\nabla_y\mu + \frac{\varepsilon-\mu}{T}\nabla_y T\right]dp_z \tag{148}$$

These results must be subtracted from equations (140) and (141), respectively,

in order to extract the conduction currents (Zyryanov and Guseva 1969)

$$j_x = \frac{|e|mc^2}{4\pi^2\hbar^2}\sum_{ns}\int_{-\infty}^{\infty}\frac{1}{\varepsilon}\frac{p_z^2}{m}\frac{\partial f^0}{\partial\varepsilon}\left[\nabla_y\mu + \frac{\varepsilon-\mu}{T}\nabla_y T\right]dp_z \tag{149}$$

$$F_x = -\frac{mc^2}{4\pi^2\hbar^2}\sum_{ns}\int_{-\infty}^{\infty}\frac{1}{\varepsilon}\frac{p_z^2}{m}\frac{\partial f^0}{\partial\varepsilon}(\varepsilon-\mu)\left[\nabla_y\mu + \frac{\varepsilon-\mu}{T}\nabla_y T\right]dp_z \tag{150}$$

The transport coefficients can now be found from relations (1) and (2). After an integration by parts

$$\sigma_{xy} = -\sigma_{yx} = -\frac{e^2}{4\pi^2\hbar^2}\sum_{ns}\int_{-\infty}^{\infty} f^0 dp_z \tag{151}$$

Comparison with relation (33) gives

$$\sigma_{yx} = \frac{|e|c}{B}n_s \tag{152}$$

This agrees with the non-relativistic result in Zyryanov and Guseva (1969).

The entropy per unit volume is given by $S = (-1/V)(\partial\Omega/\partial T)_{\mu,B}$. Using equation (144), after an integration by parts

$$S = -\frac{m\omega_B}{4\pi^2\hbar^2}\sum_{ns}\int_{-\infty}^{\infty}\frac{p_z^2c^2}{\varepsilon}\frac{\varepsilon-\mu}{T}\frac{\partial f^0}{\partial\varepsilon}dp_z \tag{153}$$

From equation (149) it is deduced

$$\lambda_{yx} = -\frac{c}{B}S \tag{154}$$

This agrees with the non-relativistic result in Zyryanov and Guseva (1969).

The final transport coefficient is, from equation (150)

$$\gamma_{yx} = -\frac{mc^2}{4\pi^2\hbar^2}\sum_{ns}\int_{-\infty}^{\infty}\frac{1}{\varepsilon}\frac{p_z^2}{m}\frac{\partial f^0}{\partial\varepsilon}\frac{(\varepsilon-\mu)^2}{T}dp_z \tag{155}$$

This can also be written in terms of thermodynamic quantities. The identity

$$\frac{(\varepsilon-\mu)^2}{T^2}\frac{\partial f^0}{\partial \varepsilon} = \frac{\partial}{\partial T}\Big|_\mu \int_{-\infty}^{\mu} d\mu' \, \frac{\varepsilon-\mu'}{T}\frac{\partial f^0}{\partial \varepsilon}(\mu', T) \tag{156}$$

along with definition (153) enables relation (155) to be written as

$$\gamma_{yx} = \frac{1}{m\omega_B} T \, \frac{\partial}{\partial T}\Big|_\mu \int_{-\infty}^{\mu} S(\mu', T)\, d\mu' \tag{157}$$

This agrees with the non-relativistic result in Zyryanov and Guseva (1969). For computational purposes the form (155) is likely to be more useful.

In the $T \to 0$ limit the leading behavior of equations (152), (154), and (157) is

$$\sigma_{yx} = \frac{e^2 mc}{2\pi^2\hbar^2} \sum_{n=0}^{n_{max}} g_n \sqrt{\zeta^2\beta^2 - 1 - 2n\beta} + O(T^2) \tag{158}$$

$$\lambda_{yx} = -\frac{|e|\omega_B k^2 T}{6\hbar mc^3} \sum_{n=0}^{n_{max}} g_n \frac{\zeta}{\sqrt{\zeta^2\beta^2 - 1 - 2n\beta}} + O(T^3) \tag{159}$$

$$\gamma_{yx} = \kappa_{yx} = \frac{\pi^2}{3e^2} k^2 T \sigma_{yx} \tag{160}$$

The Wiedemann-Franz law (160) is valid to lowest order in T. These are not as useful as relations (8)-(10) because the higher order terms involve derivatives of $\sqrt{\beta^2\zeta^2 - 1 - 2n\beta}$ which can be singular.

X. Computation of Intermediate Functions

The relative compactness of the relations defining the transport coefficients (eqs. [89], [119], and associated expressions) tends to obscure the computational difficulty in actually evaluating them. In this case the major problem is not so much in performing the integrals, but in evaluating the integrands, even though numerical integration is required. For example, if longitudinal

conductivities are desired (eq. [89]) it is necessary to solve a linear system, in which the coefficient matrices themselves are defined in terms of integrals (eqs. [88], [94]), at each point that the integrand must be calculated. Only for the non-dissipative transverse transport properties (eqs. [152], [154], [157]) is this not a problem. If accurate fits to the functions $\varphi(\nu;\beta)$ and $Q(\nu;\beta)$ (eqs. [89], [119]) were available, the other components of the transport tensors would be of the same degree of computational difficulty.

There are additional motivations for presenting results in the form of fits to $\varphi(\nu;\beta)$ and $Q(\nu;\beta)$ rather than, say, fits to the transport coefficients themselves. Once $\varphi(\nu;\beta)$ and $Q(\nu;\beta)$ were known any of the conductivities could be evaluated. Secondly, the transport properties are, in general, functions of density, temperature, and magnetic field strength. The functions φ and Q, with carefully chosen approximations, depend only on the electron energy ,ν, and field ,β. For most applications the dependence on B is more in the form of a parameter. That is, most geometries assume a constant, uniform magnetic field. Thus it is sufficient to give results on a coarse grid of B for values of interest. Consequently, it is much easier to fit φ and Q accurately as functions of ν for fixed β, than it is to fit the dependence of the transport coefficients on temperature and density for fixed field.

Finally, many of the physical uncertainties present in the conductivities , such as the factor u_{-2} in the solid, do not enter into these functions. Moreover, φ and Q are only weakly dependent upon those physical quantities that do enter in, such as the screening lengths. Thus accurate fits (~10%) to φ and Q are justified, in spite of uncertainties in other factors. This is highly desirable because of the potential for numerical errors in evaluating φ and Q. Several technical issues that arose in making these calculations must now be addressed.

a) Screening Lengths

From the relations defining φ and Q (eqs. [88], [90], [94], and [120]) it is seen that there is a dependence on the screening length parameter a_d through the functions $h_n^{\eta'\eta}$ and $h_{n'n}^{\pm}$ (eqs. [73] and [121]) for e-ion scattering. Because this is a weak dependence, several simplifying approximations can be made. (The weak nature of this dependence has been demonstrated explicitly by Yakovlev 1980a,b, 1982.) For convenience the screening lengths in Yakovlev (1980a, 1982) will be used. These are

$$r_d^{-2} = r_i^{-2} + r_e^{-2} \tag{161}$$

$$r_i^2 = r_{D_i}^2 + a^2/6 \tag{162}$$

$$r_e^{-2} = 4\pi e^2 \frac{\partial}{\partial \mu} n_e(\mu) \tag{163}$$

where r_i is the ion screening length, r_e is the electron screening length, $r_{D_i} = (kT/m_i)^{1/2}/\omega_{p_i}$, and $a = (3/4\pi n_i)^{1/3}$. Quantum effects are negligible for r_i but will induce oscillations in r_e, in view of equation (33). As an estimate of the relative importance of the two screening mechanisms, take $\mu = \mu_0$ in relation (163). This gives , for iron, $r_e^{-2} \approx 4.9\times10^{18}\rho_6^{1/3}(1 + .6\rho_6^{2/3})^{1/2}$. The exact expression for r_i implies $r_i^{-2} \approx 7.6\times10^{19}\rho_6^{2/3}/(1 + 2/\Gamma)$, where Γ is given by equation (30). Thus it is valid to set $r_d \approx r_i$ in the calculations of φ and Q because of the weak dependence on this factor. Also $\Gamma \gg 1$ at the relevant densities implying

$$a_d = \frac{3\hbar}{m\omega_B}\left(\frac{4\pi}{3Z}\right)^{2/3} n_e^{2/3} \tag{164}$$

In relating n_e to chemical potential and magnetic field it is sufficient to use the $t=0$ expression (eq. [35]). This gives

$$a_d = \left[\frac{2\sqrt{6}}{\pi Z}\right]^{2/3} \left[\sum_{n=0}^{n_{max}} g_n \sqrt{(\beta^2\zeta^2 - 1)/2\beta - n}\right]^{2/3} \tag{165}$$

For $Z = 26$, $(2\sqrt{6}/\pi Z)^{2/3} \approx .15$.

Finally, one further approximation can be made. For degenerate gases, which are of most interest, the major contributions to the integrals defining the transport coefficients will be for values $\nu \approx \zeta$, because of the factor $\partial f^0/\partial\varepsilon$. Thus, for iron

$$a_d \approx .15\left[\sum_{n=0}^{n_{max}} g_n \sqrt{(\beta^2\nu^2 - 1)/2\beta - n}\right]^{2/3} \tag{166}$$

If this form is used for a_d then no additional dependences, such as temperature or density, will be introduced into either φ or Q.

b) Cutoff Parameters

As discussed in § VIII , the transverse dissipative conductivities are weak functions of the cutoff factors γ_n. (The weak nature of this dependence has been demonstrated explicitly by Yakovlev 1980b.) Strictly speaking it is the integrals themselves and not the integrands that depend on the γ_n. However, for purposes of producing results that are relatively easy to use, it is most convenient to absorb this dependence into $Q(\nu;\beta)$. This is accomplished by setting to zero the contribution to $Q(\nu;\beta)$ from the divergent pieces (terms with $n = n' = n_{max}$) in the interval $\varepsilon = \varepsilon_n \to \varepsilon_n + \gamma_n$, where ε_n is given by $\nu_n^2 = (1 + 2n_{max}\beta)/\beta^2$. Although straightforward enough, this would seem to introduce additional dependences into $Q(\nu;\beta)$. However, as with the screening lengths, it is possible to take advantage of the weak nature of the dependence on the γ_n and make

several simplifying approximations. It should also be noted that a precise calculation of the γ_n is not justified because of the crude way in which these quantities were derived.

As noted in § VIII , the γ_n in neutron star crusts will be determined by either inelasticity of collisions or collisional broadening of the Landau levels. Comparison of Figure 4 with the thermal structure calculations of Gudmundsson, Pethick, and Epstein (1983), allows the following simplification. In the liquid phase assume that γ_n is determined exclusively by collisional broadening and in the solid phase only by inelastic scattering. The advantage of this, as is seen from relations (126) and (128), is that the dependence on temperature vanishes. Then, in the liquid, using equations (20), (24), and (127)

$$\frac{\gamma_n}{\hbar\omega_B} = \frac{4}{3\pi}\alpha^2 Z\Lambda_{ei}\,\zeta_0 \tag{167}$$

where α is the fine structure constant. This is not quite correct as the γ_n should not include the rest mass. Thus, in equation (167) the replacement $\zeta_0 \rightarrow \zeta_0 - 1/\beta$ should be made. It is sufficient to use the $t=0$ relation of ζ_0 to ζ and β (eq. [35]). Furthermore, it can be assumed that $\zeta \approx \nu$ as was the case for the screening lengths, and that $\Lambda_{ei}Z$ can be set to a constant. For $Z = 26$ and the typical value $\Lambda_{ei} = 1$ (see § XI), subtracting the rest mass

$$\frac{\gamma_n}{\hbar\omega_B} \approx \frac{5.9\times10^{-4}}{\beta}\left\{\left[\left[\frac{3}{2}\beta\sum_{k=0}^{n} g_k\sqrt{\beta^2\nu^2 - 1 - 2k\beta}\right]^{2/3} + 1\right]^{1/2} - 1\right\} \tag{168}$$

In the solid, using equations (20), (27), and (125)

$$\frac{\gamma_n}{\hbar\omega_B} = \sqrt{4Zm\alpha/3\pi Am_p}\;\frac{1}{\beta}(\beta^2\zeta_0^2 - 1)^{3/4} \tag{169}$$

Making the same approximations that led to expression (168)

$$\frac{\gamma_n}{\hbar\omega_B} \approx 1.1\times10^{-3}\beta^{-1/2}\left[\sum_{k=0}^{n} g_k\sqrt{\beta^2\nu^2 - 1 - 2k\beta}\right]^{1/2} \tag{170}$$

Thus no additional dependences are introduced into $Q(\nu;\beta)$.

c) Computational Scheme

Some care must be taken in the computations because of the potential for numerical difficulties. The function $\varphi(\nu;\beta)$ is calculated from equation (90) where the individual terms $\varphi_{n\eta s}$ are the solutions to the system of equations (98), supplemented by condition (97). Naturally the system can only be solved numerically. The coefficient matrix is given by linear combinations of the scattering rate (94). In order to discuss the evaluation of $a(n\eta s \to n'\eta' s')$ it is convenient to define the following

$$I^{pl}_{n'n}(w) = \int_0^\infty \frac{u^p F^2_{n'n}(u)du}{(u+w)^l} \tag{171}$$

Then the scattering rate can be written, with $q_n = \sqrt{\nu^2\beta^2 - 2n\beta - 1}$

$$a(n\eta s \to n'\eta' s') = \frac{1}{4}\frac{\nu^2\beta^3}{q_n q_{n'}}\left[1 + ss' + \frac{1}{\beta^2\nu^2}(1 - ss')\right]$$

$$\left\{\left[1 + ss' - \frac{1}{2}\frac{ss'}{\beta^2\nu^2 - 1}(\eta' q_{n'} - \eta q_n)^2\right](I^{0l}_{n'n}(w_l) + I^{0l}_{n'-1n-1}(w_l)) - \frac{ss'\beta}{\beta^2\nu^2 - 1}\cdot\right.$$

$$\left.(I^{1l}_{n'-1n}(w_l) + I^{1l}_{n'n-1}(w_l)) - \frac{s\eta q_n + s'\eta' q_{n'}}{\sqrt{\beta^2\nu^2 - 1}}(I^{0l}_{n'n}(w_l) - I^{0l}_{n'-1n-1}(w_l))\right\} \tag{172}$$

where l = 1,2 for phonon and ion scattering, respectively and $w_1 = \xi^{\eta'\eta}_{n'n}/2\beta$, $w_2 = \xi^{\eta'\eta}_{n'n}/2\beta + a_d$, with $\xi^{\eta'\eta}_{n'n}$ given by relation (67).

The function $Q(\nu;\beta)$ is given by the sum (120) and relations (121), (122). The sum can be simplified by noting that the terms are symmetric in n and n'. Using equation (171)

$$Q(\nu;\beta) = \beta \sum_{\pm} \sum_{n=0}^{n_{max}} \sum_{n'=0}^{n} \frac{g_{n'n}}{q_n q_{n'}} \left\{ \left[\nu^2\beta^2 - \frac{1}{4}\xi^{\pm}_{n'n} \right] (I^{1l}_{n'n}(w_l) + \right.$$

$$\left. I^{1l}_{n'-1n-1}(w_l)) - \frac{\beta}{2}(I^{2l}_{n'-1n}(w_l) + I^{2l}_{n'n-1}(w_l)) \right\} \qquad (173)$$

where $l = 1,2$ for phonon and ion scattering, respectively, $w_1 = \xi^{\pm}_{n'n}/2\beta$, $w_2 = \xi^{\pm}_{n'n}/2\beta + \alpha_d$, and the factor $g_{n'n} = 2 - \delta_{n'n}$ ensures that the terms with $n = n'$ are not double-counted.

The computation of the integrals $I^{pl}_{n'n}(w)$ for $p = 0,1,2$ and $l = 1,2$ is reduced through use of the recursion relations

$$I^{11}_{n'n} = 1 - wI^{01}_{n'n}$$

$$I^{21}_{n'n} = n + n' + 1 - w + w^2 I^{01}_{n'n}$$

$$I^{02}_{n'n} = -\partial I^{01}_{n'n}/\partial w \qquad (174)$$

$$I^{12}_{n'n} = I^{01}_{n'n} - wI^{02}_{n'n}$$

$$I^{22}_{n'n} = 1 - 2wI^{01}_{n'n} + w^2 I^{02}_{n'n}$$

using $\int_0^\infty F^2_{n'n}du = 1$ and $\int_0^\infty uF^2_{n'n}du = n + n' + 1$. Thus all relevant $I^{pl}_{n'n}$ can be related to $I^{01}_{n'n}$.

In principle the integrals $I^{01}_{n'n}$ can be done analytically by using the polynomial representation for the Laguerre polynomials

$$L^{n-n'}_{n'}(u) = \sum_{m=0}^{n'} (-1)^m \binom{n}{n'-m} \frac{u^m}{m!} \qquad (175)$$

However, the resulting expressions are not generally reliable. For large argument and large order the form (175) is not suitable for the calculation of Laguerre polynomials. This is due to loss of precision as a result of large cancellations between the terms in relation (175). In order to avoid such difficulties the following was used to evaluate $L_n^{n-n'}$ (Abramowitz and Stegun 1972)

$$L_n^{n-n'}(u) = \binom{n}{n'} a_0(u) \tag{176}$$

where $a_0(u)$ is generated recursively according to

$$a_{m-1}(u) = 1 - \frac{n' - m + 1}{m(n - n' + m)} u a_m(u) \tag{177}$$

$$m = n', n'-1, \cdots, 2, 1; \quad a_{n'}(u) = 1$$

This representation is valid for all u and all order.

The integrals $I_{n'n}^{01}(w)$ were computed numerically for a grid of n, n', and w, making use of the symmetry $I_{n'n}^{01}(w) = I_{nn'}^{01}(w)$. The computations were performed for $0 \le n \le 30$, $0 \le n' \le n$, and $0 \le w \le w_{max}(n,n')$, where $(w_{max})_{phonons} = ((30-n')^{1/2} + (30-n)^{1/2})^2$; $(w_{max})_{ions} = (w_{max})_{phonons} + (a_d)_{max}$. If ν and β are restricted to values such that $n_{max} = 30$ then, from equation (166), $(a_d)_{max} \lesssim 5.5$. The grid in w was chosen to be sufficiently fine that numerical interpolation of relatively low order (6th order Lagrangian) could be used to provide the desired accuracy (<1%) for all relevant values of w.

d) Computations of $\varphi(\nu;\beta)$ and $Q(\nu;\beta)$

The functions $\varphi(\nu;\beta)$ and $Q(\nu;\beta)$ were calculated as functions of ν for values of β of interest, with the approximations described in the previous pages for

both e-ion and e-phonon scattering. All computations were performed to an accuracy of <1% in order to ensure that numerical errors did not affect the solutions. The functions were evaluated to allow up to 30 Landau levels to be populated. This should probably be sufficient for all conditions present in a neutron star crust.

Examples of φ and Q are given in Figures 5-8 for both e-ion and e-phonon scattering for a field strength $B = 10^{13}G$ ($\beta = .2266$). As can be seen from Figures 5 and 7 φ jumps discontinuously to zero at the points ν_n satisfying $\nu_n^2\beta^2 - 2n\beta - 1 = 0$. The function Q diverges at ν_n; however, due to the cutoff factors these are integrable singularities. Fits have been made to both φ and Q using piecewise continuous functions. For φ

$$\log_{10}\varphi = c_{0n} + c_{1n}\log_{10}(\nu - \nu_n) + c_{2n}(\log_{10}(\nu - \nu_n))^2 \qquad (178)$$

where $n = 0,1,2,\cdots 29$. In each interval $\nu_n \to \nu_{n+1}$ the fit is accurate to $\approx 10\%$ for $\nu_n + .01(\nu_{n+1} - \nu_n) \le \nu < \nu_{n+1}$. In the range $\nu_n \le \nu < \nu_n + .01(\nu_{n+1} - \nu_n)$, where φ is relatively small, the fit is not as good; however this is not a serious limitation. For the relevant degrees of degeneracy the function $\partial f^0/\partial\varepsilon$ will be sufficiently wide that the dominant contribution to the integrals (89) will never come from this interval. Thus, errors in this range will have a negligible influence ($\ll$10%) on the conductivities.

The fits to $Q(\nu;\beta)$ are somewhat more complicated because this function is divergent at $\nu = \nu_n$ and relatively large contributions to the integrals (119) are made for $\nu \approx \nu_n$. The following form, accurate to $\approx 10\%$ over each interval $\nu_n \to \nu_{n+1}$, explicitly demonstrates the integrable nature of the singularities, when cutoffs are accounted for

$$\log_{10}Q = d_{0n} + d_{1n}\log_{10}(\nu - \nu_n) \qquad \nu_n \le \nu < \nu_n^*$$

$$\log_{10}Q = e_{0n} + e_{1n}\log_{10}(\nu - \nu_n) + e_{2n}(\log_{10}(\nu - \nu_n))^2 \qquad \nu_n^* \le \nu < \nu_{n+1} \quad (179)$$

Tabulations of the c_{kn}, d_{kn}, and e_{kn} are given in the appendices. The values of ν_n^* are presented in the form $\nu_n^* = \nu_n + f_n(\nu_{n+1} - \nu_n)$, with the f_n tabulated. The corresponding field strengths are summarized in Table 1.

Table 1. Index to the Appendices

Ap.	B (G)	β	Ap.	B (G)	β	Ap.	B (G)	β
A	10^{10}	.0002266	D	3×10^{11}	.006797	G	10^{13}	.2266
B	3×10^{10}	.0006797	E	10^{12}	.02266	H	3×10^{13}	.6797
C	10^{11}	.002266	F	3×10^{12}	.06797	I	10^{14}	2.266

Fits to φ and Q for both e-ion and e-phonon scattering are given in each appendix.

XI. Calculation of Transport Properties

Given the results of § X , it is now relatively easy to generate accurate values for the transport properties from equations (89) and (119). In order to demonstrate the usefulness and validity of the fits to φ and Q several examples of transport coefficients have been computed. The results are expressed in a form similar to that of Yakovlev (1980a,b, 1982). It is most instructive to present the conductivities in terms of the corresponding quantities in the absence of a quantizing magnetic field. For large quantum numbers these ratios should tend to unity. Also this has the advantage of eliminating the dependence on factors which are uncertain, such as u_{-2}. Of course, in an actual application this problem persists and this, along with other similar considerations, will be addressed in § XII .

In all examples the gas is assumed to be degenerate because this is the situation of most interest. The conductivities neglecting quantum effects are given to lowest order by equations (8)-(10), with the tensor (7) in the limit $\Omega_0\tau_0 \gg 1$ (see § V). The relaxation times (24) and (25) are assumed and the choice of what to use for Λ_{ei} will be discussed later in this section. It is also useful to express the ratios in terms of the dimensionless quantities defined by relation (32). It should be emphasized that the calculations presented in this section are not intended to be used in applications. The form that they are given in would make this impractical. The question of how to best use the results in § X will be discussed in the conclusions.

In order to express the thermoelectric coefficient, $\vec{\lambda}$, in terms of its limit in the absence of a quantizing field, $\vec{\lambda}_0$, repeated use is made of $\partial\tau_0/\partial\mu_0$. From equations (24) and (25)

$$\frac{\partial\tau_0}{\partial\mu_0} = -\frac{\tau_0}{\mu_0} \quad (e\text{-ion}) \tag{180}$$

$$\frac{\partial\tau_0}{\partial\mu_0} = \frac{\tau_0}{\mu_0} m^2c^4 \left[\frac{3\mu_0^2 - m^2c^4}{\mu_0^4 - m^4c^8}\right] \quad (e\text{-phonon}) \tag{181}$$

assuming constant values for Z, A, and Λ_{ei}.

Finally the cross-sections σ_0 appearing in the conductivities (89) and (119) are given by equations (68) and (71).

a) Longitudinal Transport Coefficients

From equation (89) and the definitions mentioned previously, after algebra, for electron-ion scattering

$$\frac{\sigma_{zz}}{(\sigma_0)_{zz}} = \frac{6\zeta_0^2\beta^6\Lambda_{ei}L_0(\zeta,t,\beta)}{t(\beta^2\zeta_0^2-1)^3(\beta\zeta-1)}$$

$$\frac{\lambda_{zz}}{(\lambda_0)_{zz}} = \frac{18\zeta_0^3\beta^8\Lambda_{ei}L_1(\zeta,t,\beta)}{\pi^2t^3(\beta^2\zeta_0^2+2)(\beta\zeta-1)^3(\beta^2\zeta_0^2-1)^2} \tag{182}$$

$$\frac{\gamma_{zz}}{(\gamma_0)_{zz}} = \frac{18\zeta_0^2\beta^8\Lambda_{ei}L_2(\zeta,t,\beta)}{\pi^2t^3(\beta^2\zeta_0^2-1)^3(\beta\zeta-1)^3}$$

and for electron-phonon scattering

$$\frac{\sigma_{zz}}{(\sigma_0)_{zz}} = \frac{3\beta^3(\beta^2\zeta_0^2+1)L_0(\zeta,t,\beta)}{t(\beta^2\zeta_0^2-1)^2(\beta\zeta-1)}$$

$$\frac{\lambda_{zz}}{(\lambda_0)_{zz}} = \frac{9\beta^3(\beta^2\zeta_0^2+1)^2L_1(\zeta,t,\beta)}{2\pi^2t^3\zeta_0(\beta^2\zeta_0^2+3)(\beta^2\zeta_0^2-1)(\beta\zeta-1)^3} \tag{183}$$

$$\frac{\gamma_{zz}}{(\gamma_0)_{zz}} = \frac{9\beta^5(\beta^2\zeta_0^2+1)L_2(\zeta,t,\beta)}{\pi^2t^3(\beta\zeta-1)^3(\beta^2\zeta_0^2-1)^2}$$

The dimensionless integrals $L_n(\zeta,t,\beta)$ are

$$L_n(\zeta,t,\beta) = \int_{1/\beta}^{\infty}(\nu-\zeta)^n\,\frac{e^{(\nu-\zeta)\beta/t(\beta\zeta-1)}}{(1+e^{(\nu-\zeta)\beta/t(\beta\zeta-1)})^2}\varphi(\nu;\beta)\,d\nu \tag{184}$$

In the limit $t \to 0$ for both scattering processes

$$\frac{\gamma_{zz}}{(\gamma_0)_{zz}} = \frac{\sigma_{zz}}{(\sigma_0)_{zz}} \tag{185}$$

and for electron-ion collisions

$$\frac{\sigma_{zz}}{(\sigma_0)_{zz}} = \frac{6\beta^5\zeta_0^2\Lambda_{ei}\varphi(\zeta;\beta)}{(\zeta_0^2\beta^2-1)^3}$$

$$\frac{\lambda_{zz}}{(\lambda_0)_{zz}} = \frac{6\beta^5\zeta_0^3\Lambda_{ei}\varphi'(\zeta;\beta)}{(\beta^2\zeta_0^2-1)^2(\beta^2\zeta_0^2+2)} \tag{186}$$

while for electron-phonon scattering

$$\frac{\sigma_{zz}}{(\sigma_0)_{zz}} = \frac{3\beta^2(\zeta_0^2\beta^2 + 1)\varphi(\zeta;\beta)}{(\zeta_0^2\beta^2 - 1)^2}$$

$$\frac{\lambda_{zz}}{(\lambda_0)_{zz}} = \frac{3}{2}\frac{(\beta^2\zeta_0^2 + 1)^2\varphi'(\zeta;\beta)}{\zeta_0(\zeta_0^2\beta^2 - 1)(\zeta_0^2\beta^2 + 3)} \tag{187}$$

As noted in § VII the $t=0$ expressions are not as useful as the corresponding quantities in the absence of a quantizing magnetic field. This assertion will be demonstrated by comparing examples of relations (182)-(184) with relations (185)-(187).

b) Transverse, Dissipative Transport Coefficients

Using equation (119) and the same procedure, for electron-ion collisions

$$\frac{\sigma_{yy}}{(\sigma_0)_{yy}} = \frac{3}{8}\frac{1}{t}\frac{T_0(\zeta,t,\beta)}{\beta\Lambda_{ei}\zeta_0^2(\beta\zeta - 1)}$$

$$\frac{\lambda_{yy}}{(\lambda_0)_{yy}} = \frac{9}{8\pi^2}\frac{\beta}{t^3}\frac{(\beta^2\zeta_0^2 - 1)T_1(\zeta,t,\beta)}{(\beta\zeta - 1)^3\Lambda_{ei}\zeta_0(5\beta^2\zeta_0^2 - 2)} \tag{188}$$

$$\frac{\gamma_{yy}}{(\gamma_0)_{yy}} = \frac{9}{8\pi^2 t^3}\frac{\beta T_2(\zeta,t,\beta)}{\Lambda_{ei}\zeta_0^2(\beta\zeta - 1)^3}$$

and for electron-phonon collisions

$$\frac{\sigma_{yy}}{(\sigma_0)_{yy}} = \frac{3}{4}\frac{1}{t}\frac{\beta^2 T_0(\zeta,t,\beta)}{(\beta^4\zeta_0^4 - 1)(\beta\zeta - 1)}$$

$$\frac{\lambda_{yy}}{(\lambda_0)_{yy}} = \frac{9}{16\pi^2 t^3}\frac{T_1(\zeta,t,\beta)}{(\beta\zeta - 1)^3\zeta_0^3} \tag{189}$$

$$\frac{\gamma_{yy}}{(\gamma_0)_{yy}} = \frac{9}{4\pi^2 t^3} \frac{\beta^4 T_2(\zeta,t,\beta)}{(\beta\zeta - 1)^3(\beta^4\zeta_0^4 - 1)}$$

The dimensionless integrals $T_n(\zeta,t,\beta)$ are

$$T_n(\zeta,t,\beta) = \int_{\nu\beta}^{\infty} (\nu - \zeta)^n \frac{e^{(\nu-\zeta)\beta/t(\beta\zeta-1)}}{(1 + e^{(\nu-\zeta)\beta/t(\beta\zeta-1)})^2} Q(\nu;\beta)\, d\nu \tag{190}$$

In the limit $t \to 0$ for both scattering processes

$$\frac{\gamma_{yy}}{(\gamma_0)_{yy}} = \frac{\sigma_{yy}}{(\sigma_0)_{yy}} \tag{191}$$

and for electron-ion scattering

$$\frac{\sigma_{yy}}{(\sigma_0)_{yy}} = \frac{3}{8} \frac{1}{\beta^2} \frac{Q(\zeta;\beta)}{\zeta_0^2 \Lambda_{ei}}$$

$$\frac{\lambda_{yy}}{(\lambda_0)_{yy}} = \frac{3}{8} \frac{1}{\beta^2 \Lambda_{ei}} \frac{(\beta^2\zeta_0^2 - 1)Q'(\zeta;\beta)}{\zeta_0(5\zeta_0^2\beta^2 - 2)} \tag{192}$$

while for electron-phonon scattering

$$\frac{\sigma_{yy}}{(\sigma_0)_{yy}} = \frac{3}{4}\beta \frac{Q(\zeta;\beta)}{\beta^4\zeta_0^4 - 1}$$

$$\frac{\lambda_{yy}}{(\lambda_0)_{yy}} = \frac{3}{16} \frac{1}{\beta^3\zeta_0^3} Q'(\zeta;\beta) \tag{193}$$

Again, as noted in § VIII , the $t \to 0$ forms are not as useful as the corresponding quantities if quantum effects are neglected. This will also be demonstrated by comparing examples of relations (188)-(190) with relations (191)-(193).

c) Transverse, Non-Dissipative Transport Coefficients

From equations (152), (154), and (155)

$$\sigma_{yx} = (\sigma_0)_{yx}$$

$$\frac{\lambda_{yx}}{(\lambda_0)_{yx}} = \frac{3}{2\pi^2}\frac{\beta^2}{t^3}\frac{N_1(\zeta,t,\beta)}{\zeta_0(\zeta_0^2\beta^2-1)^{1/2}(\beta\zeta-1)^3} \tag{194}$$

$$\frac{\gamma_{yx}}{(\gamma_0)_{yx}} = \frac{9}{2\pi^2}\frac{\beta^4}{t^3}\frac{N_2(\zeta,t,\beta)}{(\beta^2\zeta_0^2-1)^{3/2}(\beta\zeta-1)^3}$$

where

$$N_p(\zeta,t,\beta) = \int_{1/\beta}^{\infty}(\nu-\zeta)^p\,\frac{e^{(\nu-\zeta)\beta/t(\beta\zeta-1)}}{(1+e^{(\nu-\zeta)\beta/t(\beta\zeta-1)})^2}\left[\sum_{n=0}^{n_{max}} g_n\sqrt{\nu^2\beta^2-1-2n\beta}\right]d\nu \tag{195}$$

The first relation in equations (194) is a consequence of the fact that σ_{yx} depends on the chemical potential only through n_s and hence does not suffer quantum effects (treating density as the independent variable).

In the $t \to 0$ limit $\sigma_{yx} = (\sigma_0)_{yx}$ and

$$\frac{\lambda_{yx}}{(\lambda_0)_{yx}} = \frac{\beta}{2\zeta_0(\zeta_0^2\beta^2-1)^{1/2}}\sum_{n=0}^{n_{max}} g_n\,\zeta(\zeta^2\beta^2-1-2n\beta)^{-1/2}$$

$$\gamma_{yx} = (\gamma_0)_{yx} \tag{196}$$

The second relation in equations (196) follows from relation (35) and the Wiedemann-Franz law.

d) Numerical Examples

The ratios defined in the preceding equations depend only on the three dimensionless parameters ζ, β, t. The factor ζ_0 is related to ζ, β, t through relation (33) in the general case, and relation (35) in the limit $t \to 0$. For e-ion scattering the ratios also depend on the Coulomb logarithm, Λ_{ei}, which is a slowly varying function of temperature and density. There is some uncertainty in the form for Λ_{ei}. Recently Itoh, *et al.* (1983) have computed conductivities in the liquid phase, neglecting magnetic effects. The results are expressed in a form identical to that given by Yakovlev and Urpin (1980). Residual discrepancies ($\sim 10-30\%$ for iron) are absorbed in the Coulomb logarithm and are principally accounted for by the fact that Yakovlev and Urpin neglected electron screening in their estimates. The expressions for Λ_{ei} given in Yakovlev (1980a,b, 1982) include electron screening. However the values derived from these formulae do not agree with those of Yakovlev and Urpin (1980) if only ion screening is assumed.

As the results presented in this section are intended to be illustrative and not definitive, it is not appropriate to discuss the relative merits of the calculations of Λ_{ei} . Thus, in the computations of the ratios (182), (186), (188), and (192), the constant value $\Lambda_{ei} = 1$ has been assumed. This is representative of the conditions in neutron star crusts (see Itoh ,*et al.* 1983). In view of this approximation, which involves errors $\lesssim 30\%$, it should not be surprising that the ratios for e-ion scattering do not precisely approach unity when a large number of Landau levels are populated.

For convenience, and in order to be able to compare these results to those of Yakovlev (1980a,b, 1982), the ratios of the transport coefficients were computed for fixed β and t as functions of ζ. In this form the quantum oscillations and thermal damping are most visible. The integrals (184) and (190) were

performed numerically, breaking the interval of integration into a sum of subintervals, defined by the discontinuities in φ and Q. Because φ and Q have been tabulated only up to a finite value of ν, the conductivities can be calculated only out to a corresponding finite value of ζ. For degenerate gases ($t \ll 1$) the remainder of the integrands of equations (184) and (190) is sharply peaked so this should not be a serious limitation.

Results are given for the field strengths $B = 10^{11}G$ and $B = 10^{13}G$, corresponding to $\beta = .002266$ and $\beta = .2266$, respectively. Comparisons between the fully degenerate limit ($t = 0$) and the more general case are made for $t = .025$, which is typical of neutron star crusts. The longitudinal properties are given in Figures 9-12 for $B = 10^{11}G$ and Figures 13-16 for $B = 10^{13}G$. The transverse, dissipative coefficients are shown in Figures 17-20 for $B = 10^{11}G$ and Figures 21-24 for $B = 10^{13}G$. Finally, examples of the transverse, non-dissipative conductivities are given in Figures 25 and 26. All calculations have been performed using the fits to $\varphi(\nu;\beta)$ and $Q(\nu;\beta)$ given in the appendices.

e) Discussion

The results for $B = 10^{11}\,G$ ($\beta = .002266$) are in good agreement with the non-relativistic calculations of Yakovlev (1980a,b, 1982). Small numerical differences in the ratios $\sigma_{zz}/(\sigma_0)_{zz}$, $\gamma_{zz}/(\gamma_0)_{zz}$ for e-ion scattering are explained by the approximation $\Lambda_{ei} = 1$ made in this paper. The convergence of $\varphi(\nu;\beta)$ was further checked by explicitly solving the non-relativistic system of Yakovlev (1980a, 1982). For the field strength $B = 10^{10}\,G$, the relativistic and non-relativistic calculations agreed to $<2\%$.

The tendency of the electrical and thermal conductivity ratios to approach unity for large ζ is a check on the numerical accuracy of the calculations of $\varphi(\nu;\beta)$ and $Q(\nu;\beta)$. Also, the approximations described in § X (screening lengths and cutoff factors) are justified. Again, small deviations ($\sim$30%) from unity of the ratios for e-ion scattering are due to the uncertainty in Λ_{ei}.

The behavior of the thermoelectric coefficient for large ζ is somewhat surprising. For e-phonon scattering the ratios converge rapidly to 1 (Figs. 12,16,20,24). However, for e-ion scattering the ratios appear to approach 1 only asymptotically. The large deviations ($\lesssim$ a factor of 10) cannot be attributed to either the uncertainty in Λ_{ei} or numerical problems. The most likely explanation is that $\varphi(\nu;\beta)$ and $Q(\nu;\beta)$ have not been calculated for sufficiently large ν to ensure that the ratios have converged. However, further analysis may be required to show that the expected limit is attained as the number of levels populated becomes infinite.

The importance of thermal effects is clearly demonstrated by these calculations. For non-zero t the oscillations are damped and the Wiedemann-Franz law is not satisfied. Furthermore, it is not a good approximation to assume the $t = 0$ values for the conductivities, especially for transport perpendicular to B. The divergences in the cross-field conductivities are removed when thermal smoothing is included.

The oscillations in the $y-x$ components of the transport tensors (Figs. 25,26) are relatively unimportant because these elements are independent of the collision time. Again, the $t = 0$ limit is not a good approximation.

XII. Conclusions

A complete treatment of electron transport in a quantizing magnetic field has been presented, with allowance for relativistic electrons and arbitrary degree of degeneracy. The work of Yakovlev (1980a,b, 1982) has been extended and generalized. The analytic results are valid for any scattering potential as long as the collisions are elastic. Numerical results have been given for e-ion and e-phonon collisions, which are the most important scattering mechanisms in neutron star crusts. Electron-electron scattering will be unimportant unless low Z ions ($Z \lesssim 10$) are present. Impurity effects are not likely to be significant because the matter in the crust is believed to be rather pure (in any case, as mentioned earlier, it is easy to extend the present analysis to handle impurity scattering). The numerical results are presented in a form which will allow the transport coefficients to be more easily evaluated. The analytic expressions and computations agree in detail with Yakovlev (1980a,b, 1982) in the non-relativistic limit.

Although the fitting formulae for $\varphi(\nu;\beta)$ and $Q(\nu;\beta)$ reduce the difficulty of evaluating the transport coefficients, several complications remain. The integrals defining the conductivities must be done numerically. Because of the discontinuities in the integrand this can be time-consuming. Also, in an actual application it would be necessary to invert the relation between density and chemical potential. A possible solution would be to calculate the transport coefficients on a grid of values and then interpolate. Alternatively, because the deviation of ζ from ζ_0 is small, it should be a good approximation to use the unmagnetized relation of density to chemical potential for all but the lowest densities (see Fig. 2). If only one Landau level is occupied the $t = 0$ relation between ζ and ζ_0 is strongly satisfied and can easily be inverted.

Finally, values must be assumed for the factors Λ_{ei} and u_{-2} in order to compute the transport tensors. The existing calculations of Λ_{ei} agree to within $\lesssim 30\%$. This should not be critical as other uncertainties will almost certainly be more significant. The estimates for u_{-2}, on the other hand, differ by factors ~ 3. Thus the conductivities in the solid are subject to similar errors. Since the transport coefficients scale simply with u_{-2} , however, the present conclusions will remain valid if further research leads to a definitive value for this factor.

Acknowledgments

I would like to thank Roger Blandford and Jim Applegate for valuable discussions and guidance throughout. Also I thank Peter Goldreich for providing badly needed computing resources. This work was supported by the National Science Foundation under grants AST82-13001 and AST83-13725.

Appendix A

Coefficients in the fits to $\varphi(\nu;\beta)$ and $Q(\nu;\beta)$ (eqs. [178] and [179]) for $B = 10^{10}$ G ($\beta = 2.266\times10^{-4}$) .

Table 2. Ion Scattering

n	c_{0n}	c_{1n}	c_{2n}	d_{0n}	d_{1n}	e_{0n}	e_{1n}	e_{2n}	f_n
0	1.084	2.683	.2289	.0000	.0000	-.3194	-1.342	-.0318	.0001
1	1.689	2.266	.6325	-.3863	-.4920	-.0810	-1.120	-.0110	.0004
2	2.066	1.723	.4676	-.0930	-.4901	.0482	-.7729	.0482	.0010
3	2.351	1.340	.3666	-.0639	-.4871	.1166	-.6192	.0711	.0010
4	2.564	1.066	.2147	-.0499	-.4819	.1622	-.5189	.0873	.0020
5	2.760	.9278	.1761	-.0515	-.4794	.1948	-.4510	.0960	.0020
6	2.929	.8251	.1474	-.0554	-.4772	.2193	-.4010	.1017	.0020
7	3.078	.7454	.1253	-.0419	-.4699	.2364	-.3684	.1019	.0040
8	3.211	.6816	.1078	-.0462	-.4678	.2508	-.3377	.1037	.0040
9	3.332	.6293	.0936	-.0506	-.4659	.2629	-.3122	.1047	.0040
10	3.441	.5855	.0819	-.0550	-.4641	.2732	-.2909	.1051	.0040
11	3.543	.5484	.0720	-.0592	-.4624	.2823	-.2725	.1052	.0040
12	3.636	.5162	.0636	-.0631	-.4607	.2904	-.2567	.1051	.0040
13	3.723	.4881	.0563	-.0380	-.4508	.2937	-.2712	.0851	.0080
14	3.805	.4635	.0499	-.0406	-.4490	.3003	-.2593	.0845	.0080
15	3.881	.4416	.0444	-.0430	-.4473	.3063	-.2488	.0838	.0080
16	3.953	.4220	.0395	-.0453	-.4457	.3116	-.2394	.0831	.0080
17	4.022	.4043	.0351	-.0475	-.4440	.3164	-.2308	.0824	.0080
18	4.086	.3882	.0312	-.0496	-.4426	.3209	-.2230	.0816	.0080
19	4.148	.3736	.0276	-.0516	-.4411	.3249	-.2161	.0808	.0080
20	4.207	.3603	.0245	-.0535	-.4397	.3287	-.2095	.0801	.0080
21	4.263	.3480	.0216	-.0553	-.4383	.3323	-.2032	.0794	.0080
22	4.317	.3367	.0189	-.0569	-.4370	.3357	-.1976	.0787	.0080
23	4.368	.3262	.0165	-.0585	-.4357	.3388	-.1924	.0780	.0080
24	4.418	.3164	.0142	-.0600	-.4345	.3417	-.1875	.0773	.0080
25	4.466	.3073	.0122	-.0614	-.4333	.3443	-.1829	.0767	.0080
26	4.512	.2988	.0103	-.0628	-.4321	.3469	-.1787	.0760	.0080
27	4.556	.2909	.0085	-.0641	-.4310	.3493	-.1747	.0753	.0080
28	4.599	.2833	.0069	-.0653	-.4298	.3515	-.1709	.0746	.0080
29	4.641	.2763	.0053	-.0665	-.4288	.3537	-.1675	.0739	.0080

Table 3. Phonon Scattering

n	c_{0n}	c_{1n}	c_{2n}	d_{0n}	d_{1n}	e_{0n}	e_{1n}	e_{2n}	f_n
0	.3819	1.840	.1379	.0000	.0000	-.2364	-1.162	-.0285	.0020
1	.8607	1.422	.2692	.1054	-.4929	.3682	-.9242	.0237	.0080
2	1.117	1.036	.1756	.5766	-.4866	.6938	-.7515	.0333	.0200
3	1.313	.8264	.1237	.7835	-.4808	.9021	-.6411	.0431	.0200
4	1.471	.6947	.0911	.9160	-.4759	1.053	-.5658	.0493	.0200
5	1.604	.6036	.0688	1.033	-.4657	1.169	-.5320	.0299	.0400
6	1.718	.5363	.0527	1.113	-.4611	1.265	-.4902	.0317	.0400
7	1.819	.4846	.0406	1.179	-.4571	1.346	-.4564	.0330	.0400
8	1.909	.4429	.0309	1.236	-.4534	1.416	-.4291	.0336	.0400
9	1.989	.4088	.0232	1.285	-.4500	1.477	-.4058	.0341	.0400
10	2.063	.3806	.0171	1.329	-.4469	1.531	-.3856	.0345	.0400
11	2.131	.3564	.0118	1.369	-.4440	1.581	-.3685	.0345	.0400
12	2.194	.3355	.0074	1.405	-.4413	1.625	-.3532	.0345	.0400
13	2.252	.3173	.0037	1.438	-.4387	1.660	-.4548	-.1423	.0400
14	2.307	.3013	.0005	1.469	-.4363	1.698	-.4360	-.1319	.0400
15	2.358	.2870	-.0023	1.497	-.4339	1.734	-.4190	-.1228	.0400
16	2.406	.2743	-.0048	1.524	-.4317	1.767	-.4038	-.1148	.0400
17	2.452	.2627	-.0069	1.549	-.4296	1.798	-.3900	-.1077	.0400
18	2.495	.2523	-.0089	1.573	-.4276	1.827	-.3774	-.1013	.0400
19	2.537	.2427	-.0106	1.595	-.4257	1.854	-.3659	-.0955	.0400
20	2.576	.2341	-.0121	1.616	-.4238	1.880	-.3551	-.0903	.0400
21	2.613	.2261	-.0134	1.637	-.4220	1.905	-.3453	-.0855	.0400
22	2.649	.2186	-.0147	1.656	-.4203	1.928	-.3363	-.0812	.0400
23	2.684	.2117	-.0158	1.674	-.4186	1.950	-.3278	-.0773	.0400
24	2.717	.2053	-.0168	1.692	-.4170	1.972	-.3199	-.0736	.0400
25	2.748	.1994	-.0178	1.709	-.4154	1.992	-.3125	-.0702	.0400
26	2.779	.1938	-.0186	1.726	-.4139	2.012	-.3055	-.0671	.0400
27	2.809	.1886	-.0194	1.741	-.4124	2.030	-.2989	-.0642	.0400
28	2.837	.1837	-.0201	1.757	-.4110	2.049	-.2928	-.0615	.0400
29	2.865	.1791	-.0208	1.771	-.4096	2.066	-.2869	-.0589	.0400

Appendix B

Coefficients in the fits to $\varphi(\nu;\beta)$ and $Q(\nu;\beta)$ (eqs. [178] and [179]) for $B = 3\times10^{10}$ G ($\beta = 6.797\times10^{-4}$).

Table 4. Ion Scattering

n	c_{0n}	c_{1n}	c_{2n}	d_{0n}	d_{1n}	e_{0n}	e_{1n}	e_{2n}	f_n
0	1.084	2.683	.2290	.0000	.0000	-.3192	-1.342	-.0318	.0001
1	1.690	2.267	.6327	-.3862	-.4920	-.0807	-1.120	-.0109	.0004
2	2.067	1.724	.4678	-.0927	-.4901	.0486	-.7725	.0483	.0010
3	2.351	1.401	.3668	-.0635	-.4871	.1173	-.6187	.0712	.0010
4	2.564	1.066	.2149	-.0494	-.4819	.1631	-.5183	.0874	.0020
5	2.760	.9286	.1763	-.0509	-.4794	.1960	-.4503	.0961	.0020
6	2.929	.8259	.1476	-.0546	-.4771	.2207	-.4003	.1019	.0020
7	3.077	.7462	.1255	-.0409	-.4699	.2380	-.3676	.1021	.0040
8	3.210	.6825	.1080	-.0451	-.4678	.2526	-.3368	.1039	.0040
9	3.331	.6302	.0938	-.0493	-.4659	.2650	-.3113	.1049	.0040
10	3.440	.5864	.0821	-.0535	-.4641	.2755	-.2899	.1053	.0040
11	3.541	.5493	.0722	-.0576	-.4624	.2849	-.2714	.1055	.0040
12	3.634	.5171	.0638	-.0614	-.4607	.2933	-.2556	.1053	.0040
13	3.721	.4890	.0565	-.0360	-.4507	.2967	-.2700	.0854	.0080
14	3.803	.4644	.0502	-.0385	-.4489	.3036	-.2581	.0847	.0080
15	3.879	.4425	.0446	-.0407	-.4473	.3098	-.2475	.0841	.0080
16	3.951	.4229	.0397	-.0429	-.4456	.3153	-.2381	.0834	.0080
17	4.019	.4052	.0353	-.0449	-.4440	.3204	-.2295	.0827	.0080
18	4.083	.3891	.0314	-.0468	-.4425	.3251	-.2217	.0819	.0080
19	4.145	.3745	.0279	-.0486	-.4410	.3294	-.2147	.0811	.0080
20	4.203	.3612	.0247	-.0504	-.4396	.3334	-.2081	.0804	.0080
21	4.259	.3489	.0218	-.0519	-.4382	.3373	-.2018	.0797	.0080
22	4.313	.3376	.0191	-.0534	-.4369	.3408	-.1961	.0790	.0080
23	4.364	.3271	.0167	-.0548	-.4356	.3442	-.1909	.0783	.0080
24	4.414	.3173	.0145	-.0562	-.4343	.3473	-.1859	.0776	.0080
25	4.461	.3082	.0124	-.0574	-.4331	.3502	-.1813	.0769	.0080
26	4.507	.2997	.0105	-.0586	-.4320	.3530	-.1771	.0763	.0080
27	4.551	.2918	.0088	-.0598	-.4308	.3556	-.1730	.0756	.0080
28	4.594	.2842	.0071	-.0608	-.4297	.3582	-.1693	.0749	.0080
29	4.635	.2772	.0056	-.0618	-.4286	.3606	-.1658	.0742	.0080

Table 5. Phonon Scattering

n	c_{0n}	c_{1n}	c_{2n}	d_{0n}	d_{1n}	e_{0n}	e_{1n}	e_{2n}	f_n
0	.3820	1.840	.1380	.0000	.0000	-.2364	-1.163	-.0289	.0010
1	.8609	1.423	.2692	.1055	-.4929	.3684	-.9238	.0238	.0080
2	1.117	1.036	.1757	.5676	-.4893	.6956	-.7388	.0439	.0080
3	1.313	.8268	.1237	.7837	-.4808	.9026	-.6406	.0433	.0200
4	1.471	.6952	.0912	.9163	-.4759	1.054	-.5651	.0495	.0200
5	1.603	.6041	.0689	1.014	-.4717	1.172	-.5099	.0533	.0200
6	1.718	.5368	.0528	1.091	-.4680	1.268	-.4675	.0557	.0200
7	1.818	.4851	.0407	1.160	-.4571	1.347	-.4556	.0333	.0400
8	1.908	.4434	.0310	1.236	-.4534	1.417	-.4283	.0339	.0400
9	1.989	.4093	.0233	1.286	-.4500	1.478	-.4050	.0344	.0400
10	2.062	.3811	.0172	1.330	-.4469	1.533	-.3848	.0348	.0400
11	2.130	.3569	.0119	1.370	-.4440	1.582	-.3676	.0348	.0400
12	2.193	.3361	.0076	1.406	-.4412	1.627	-.3523	.0348	.0400
13	2.251	.3179	.0038	1.439	-.4386	1.668	-.3388	.0348	.0400
14	2.305	.3018	.0006	1.470	-.4362	1.706	-.3267	.0347	.0400
15	2.356	.2876	-.0022	1.499	-.4339	1.742	-.3157	.0346	.0400
16	2.404	.2748	-.0047	1.525	-.4317	1.775	-.3057	.0345	.0400
17	2.450	.2633	-.0068	1.551	-.4296	1.805	-.2966	.0342	.0400
18	2.493	.2528	-.0087	1.574	-.4275	1.829	-.3774	-.1010	.0400
19	2.534	.2433	-.0104	1.597	-.4256	1.857	-.3658	-.0952	.0400
20	2.573	.2347	-.0119	1.618	-.4237	1.883	-.3551	-.0900	.0400
21	2.610	.2266	-.0133	1.639	-.4219	1.908	-.3452	-.0852	.0400
22	2.646	.2191	-.0146	1.658	-.4202	1.931	-.3362	-.0809	.0400
23	2.680	.2123	-.0157	1.677	-.4185	1.954	-.3277	-.0770	.0400
24	2.713	.2059	-.0167	1.695	-.4169	1.975	-.3198	-.0733	.0400
25	2.745	.1999	-.0177	1.712	-.4153	1.996	-.3123	-.0699	.0400
26	2.775	.1944	-.0185	1.728	-.4137	2.016	-.3053	-.0668	.0400
27	2.805	.1891	-.0193	1.744	-.4123	2.035	-.2988	-.0639	.0400
28	2.833	.1842	-.0200	1.760	-.4108	2.053	-.2926	-.0612	.0400
29	2.861	.1796	-.0207	1.775	-.4094	2.070	-.2867	-.0587	.0400

Appendix C

Coefficients in the fits to $\varphi(\nu;\beta)$ and $Q(\nu;\beta)$ (eqs. [178] and [179]) for $B = 10^{11}$ G ($\beta = 2.266\times10^{-3}$) .

Table 6. Ion Scattering

n	c_{0n}	c_{1n}	c_{2n}	d_{0n}	d_{1n}	e_{0n}	e_{1n}	e_{2n}	f_n
0	1.085	2.684	.2294	.0000	.0000	-.3185	-1.342	-.0317	.0001
1	1.691	2.269	.6333	-.3858	-.4920	-.0799	-1.119	-.0107	.0004
2	2.068	1.727	.4685	-.0919	-.4901	.0503	-.7712	.0486	.0010
3	2.352	1.404	.3675	-.0622	-.4871	.1197	-.6171	.0716	.0010
4	2.567	1.079	.2164	-.0476	-.4819	.1663	-.5163	.0879	.0020
5	2.759	.9313	.1768	-.0486	-.4794	.2000	-.4480	.0966	.0020
6	2.927	.8287	.1482	-.0518	-.4771	.2256	-.3977	.1024	.0020
7	3.076	.7491	.1261	-.0375	-.4698	.2437	-.3646	.1028	.0040
8	3.208	.6854	.1086	-.0411	-.4677	.2591	-.3336	.1047	.0040
9	3.327	.6332	.0945	-.0449	-.4657	.2723	-.3079	.1056	.0040
10	3.436	.5894	.0827	-.0485	-.4639	.2837	-.2863	.1060	.0040
11	3.536	.5523	.0729	-.0521	-.4622	.2939	-.2676	.1062	.0040
12	3.629	.5201	.0644	-.0552	-.4605	.3031	-.2516	.1061	.0040
13	3.715	.4920	.0572	-.0292	-.4505	.3071	-.2660	.0863	.0080
14	3.796	.4674	.0509	-.0311	-.4487	.3148	-.2540	.0857	.0080
15	3.871	.4455	.0453	-.0327	-.4470	.3218	-.2433	.0850	.0080
16	3.942	.4259	.0404	-.0343	-.4454	.3282	-.2337	.0844	.0080
17	4.010	.4082	.0360	-.0357	-.4437	.3341	-.2250	.0836	.0080
18	4.073	.3922	.0321	-.0372	-.4422	.3396	-.2171	.0829	.0080
19	4.134	.3776	.0286	-.0384	-.4407	.3446	-.2100	.0820	.0080
20	4.192	.3642	.0254	-.0395	-.4393	.3495	-.2033	.0813	.0080
21	4.247	.3519	.0225	-.0405	-.4379	.3542	-.1969	.0807	.0080
22	4.300	.3406	.0199	-.0415	-.4366	.3585	-.1911	.0799	.0080
23	4.351	.3301	.0174	-.0423	-.4353	.3627	-.1858	.0792	.0080
24	4.399	.3203	.0152	-.0430	-.4340	.3666	-.1808	.0786	.0080
25	4.446	.3112	.0132	-.0437	-.4327	.3703	-.1761	.0779	.0080
26	4.491	.3027	.0113	-.0444	-.4315	.3738	-.1718	.0772	.0080
27	4.534	.2947	.0095	-.0449	-.4304	.3773	-.1676	.0765	.0080
28	4.576	.2871	.0079	-.0454	-.4293	.3806	-.1638	.0758	.0080
29	4.617	.2801	.0063	-.0458	-.4282	.3838	-.1603	.0751	.0080

Table 7. Phonon Scattering

n	c_{0n}	c_{1n}	c_{2n}	d_{0n}	d_{1n}	e_{0n}	e_{1n}	e_{2n}	f_n
0	.3826	1.841	.1382	.0000	.0000	-.2357	-1.162	-.0287	.0010
1	.8617	1.424	.2695	.1018	-.4941	.3686	-.9271	.0211	.0040
2	1.118	1.038	.1759	.5682	-.4893	.6968	-.7371	.0445	.0080
3	1.313	.8283	.1240	.7710	-.4849	.9062	-.6220	.0582	.0080
4	1.470	.6968	.0915	.9003	-.4811	1.058	-.5439	.0665	.0080
5	1.603	.6057	.0693	1.015	-.4717	1.174	-.5075	.0542	.0200
6	1.716	.5386	.0531	1.093	-.4679	1.271	-.4649	.0566	.0200
7	1.816	.4869	.0410	1.157	-.4646	1.353	-.4307	.0582	.0200
8	1.905	.4452	.0314	1.212	-.4615	1.423	-.4030	.0590	.0200
9	1.986	.4112	.0237	1.261	-.4586	1.485	-.3795	.0595	.0200
10	2.059	.3830	.0175	1.303	-.4560	1.540	-.3593	.0598	.0200
11	2.126	.3588	.0123	1.374	-.4438	1.588	-.3646	.0359	.0400
12	2.188	.3379	.0079	1.410	-.4410	1.634	-.3492	.0359	.0400
13	2.246	.3198	.0042	1.444	-.4384	1.676	-.3356	.0359	.0400
14	2.299	.3037	.0010	1.475	-.4360	1.714	-.3234	.0358	.0400
15	2.350	.2895	-.0018	1.504	-.4336	1.750	-.3123	.0357	.0400
16	2.397	.2767	-.0043	1.531	-.4314	1.783	-.3023	.0355	.0400
17	2.442	.2652	-.0064	1.557	-.4293	1.815	-.2932	.0353	.0400
18	2.485	.2547	-.0084	1.581	-.4272	1.844	-.2848	.0351	.0400
19	2.525	.2452	-.0101	1.604	-.4253	1.872	-.2770	.0349	.0400
20	2.564	.2365	-.0116	1.626	-.4234	1.899	-.2698	.0347	.0400
21	2.600	.2285	-.0129	1.647	-.4215	1.924	-.2631	.0345	.0400
22	2.636	.2210	-.0142	1.667	-.4198	1.948	-.2569	.0342	.0400
23	2.669	.2141	-.0154	1.686	-.4181	1.971	-.2511	.0340	.0400
24	2.702	.2077	-.0164	1.704	-.4164	1.993	-.2456	.0337	.0400
25	2.733	.2017	-.0173	1.721	-.4149	2.009	-.3118	-.0690	.0400
26	2.762	.1962	-.0182	1.738	-.4133	2.029	-.3048	-.0658	.0400
27	2.791	.1909	-.0189	1.755	-.4118	2.049	-.2982	-.0630	.0400
28	2.819	.1860	-.0197	1.771	-.4103	2.068	-.2920	-.0603	.0400
29	2.846	.1814	-.0203	1.786	-.4089	2.086	-.2861	-.0577	.0400

Appendix D

Coefficients in the fits to $\varphi(\nu;\beta)$ and $Q(\nu;\beta)$ (eqs. [178] and [179]) for $B = 3\times10^{11}$ G ($\beta = 6.797\times10^{-3}$).

Table 8. Ion Scattering

n	c_{0n}	c_{1n}	c_{2n}	d_{0n}	d_{1n}	e_{0n}	e_{1n}	e_{2n}	f_n
0	1.088	2.687	.2304	.0000	.0000	-.3167	-1.340	-.0314	.0001
1	1.696	2.275	.6349	-.3846	-.4919	-.0774	-1.117	-.0102	.0004
2	2.072	1.735	.4704	-.0895	-.4900	.0549	-.7676	.0495	.0010
3	2.355	1.413	.3696	-.0585	-.4870	.1264	-.6127	.0726	.0010
4	2.564	1.076	.2168	-.0425	-.4818	.1754	-.5106	.0893	.0020
5	2.723	.8769	.1553	-.0421	-.4792	.2114	-.4417	.0980	.0020
6	2.924	.8365	.1497	-.0439	-.4769	.2392	-.3907	.1039	.0020
7	3.070	.7571	.1277	-.0278	-.4695	.2597	-.3565	.1047	.0040
8	3.201	.6934	.1103	-.0300	-.4674	.2773	-.3250	.1066	.0040
9	3.318	.6412	.0962	-.0323	-.4654	.2927	-.2988	.1076	.0040
10	3.425	.5975	.0845	-.0345	-.4636	.3063	-.2767	.1080	.0040
11	3.523	.5604	.0747	-.0365	-.4619	.3187	-.2576	.1082	.0040
12	3.614	.5282	.0662	-.0096	-.4519	.3254	-.2691	.0895	.0080
13	3.698	.5001	.0590	-.0102	-.4500	.3358	-.2554	.0888	.0080
14	3.776	.4755	.0527	-.0106	-.4481	.3456	-.2431	.0881	.0080
15	3.850	.4535	.0471	-.0107	-.4464	.3547	-.2321	.0875	.0080
16	3.919	.4339	.0422	-.0108	-.4447	.3632	-.2223	.0868	.0080
17	3.984	.4161	.0379	-.0107	-.4430	.3711	-.2134	.0860	.0080
18	4.046	.4000	.0340	-.0107	-.4415	.3786	-.2052	.0852	.0080
19	4.105	.3854	.0304	-.0104	-.4400	.3857	-.1980	.0844	.0080
20	4.161	.3719	.0273	-.0101	-.4385	.3926	-.1911	.0837	.0080
21	4.214	.3596	.0244	-.0096	-.4371	.3993	-.1844	.0830	.0080
22	4.265	.3482	.0217	-.0090	-.4357	.4056	-.1785	.0822	.0080
23	4.314	.3376	.0193	-.0084	-.4344	.4117	-.1730	.0815	.0080
24	4.360	.3277	.0171	-.0077	-.4330	.4176	-.1679	.0808	.0080
25	4.405	.3185	.0150	-.0070	-.4318	.4232	-.1630	.0801	.0080
26	4.448	.3100	.0131	-.0061	-.4305	.4287	-.1586	.0794	.0080
27	4.490	.3019	.0113	-.0053	-.4294	.4340	-.1543	.0787	.0080
28	4.530	.2943	.0097	-.0044	-.4282	.4392	-.1503	.0780	.0080
29	4.569	.2871	.0081	.0535	-.4103	.4397	-.1736	.0568	.0200

Table 9. Phonon Scattering

n	c_{0n}	c_{1n}	c_{2n}	d_{0n}	d_{1n}	e_{0n}	e_{1n}	e_{2n}	f_n
0	.3843	1.843	.1389	.0000	.0000	-.2335	-1.159	-.0274	.0004
1	.8639	1.427	.2701	.1029	-.4940	.3710	-.9237	.0222	.0040
2	1.119	1.041	.1766	.5699	-.4893	.7004	-.7324	.0462	.0080
3	1.313	.8325	.1248	.7736	-.4848	.9111	-.6166	.0600	.0080
4	1.469	.7012	.0923	.9037	-.4810	1.065	-.5379	.0684	.0080
5	1.600	.6104	.0701	.9994	-.4777	1.185	-.4804	.0736	.0080
6	1.713	.5433	.0541	1.098	-.4677	1.280	-.4578	.0590	.0200
7	1.811	.4918	.0420	1.164	-.4643	1.364	-.4232	.0606	.0200
8	1.899	.4502	.0323	1.220	-.4612	1.436	-.3951	.0614	.0200
9	1.977	.4161	.0247	1.269	-.4583	1.499	-.3714	.0619	.0200
10	2.049	.3880	.0185	1.313	-.4556	1.556	-.3508	.0623	.0200
11	2.114	.3638	.0133	1.353	-.4531	1.608	-.3333	.0622	.0200
12	2.175	.3430	.0089	1.389	-.4507	1.655	-.3178	.0621	.0200
13	2.231	.3248	.0052	1.422	-.4485	1.698	-.3040	.0619	.0200
14	2.283	.3088	.0020	1.489	-.4354	1.736	-.3147	.0386	.0400
15	2.332	.2945	-.0008	1.520	-.4330	1.773	-.3035	.0385	.0400
16	2.378	.2817	-.0033	1.548	-.4307	1.808	-.2933	.0383	.0400
17	2.421	.2701	-.0054	1.575	-.4285	1.841	-.2841	.0381	.0400
18	2.462	.2597	-.0074	1.600	-.4264	1.872	-.2755	.0378	.0400
19	2.501	.2501	-.0091	1.624	-.4244	1.902	-.2677	.0376	.0400
20	2.538	.2414	-.0106	1.647	-.4225	1.930	-.2603	.0374	.0400
21	2.573	.2333	-.0120	1.669	-.4206	1.956	-.2535	.0372	.0400
22	2.607	.2258	-.0133	1.690	-.4188	1.982	-.2473	.0368	.0400
23	2.639	.2188	-.0144	1.710	-.4171	2.006	-.2413	.0366	.0400
24	2.670	.2124	-.0154	1.729	-.4154	2.030	-.2358	.0363	.0400
25	2.699	.2064	-.0164	1.748	-.4138	2.052	-.2306	.0361	.0400
26	2.728	.2007	-.0172	1.766	-.4122	2.074	-.2256	.0358	.0400
27	2.755	.1954	-.0180	1.784	-.4106	2.095	-.2210	.0355	.0400
28	2.781	.1905	-.0188	1.801	-.4091	2.115	-.2166	.0353	.0400
29	2.807	.1858	-.0194	1.817	-.4077	2.135	-.2124	.0350	.0400

Appendix E

Coefficients in the fits to $\varphi(\nu;\beta)$ and $Q(\nu;\beta)$ (eqs. [178] and [179]) for $B = 10^{12}$ G ($\beta = .02266$) .

Table 10. Ion Scattering

n	c_{0n}	c_{1n}	c_{2n}	d_{0n}	d_{1n}	e_{0n}	e_{1n}	e_{2n}	f_n
0	1.096	2.698	.2339	.0000	.0000	-.3102	-1.335	-.0304	.0001
1	1.710	2.297	.6404	-.3804	-.4918	-.0688	-1.110	-.0084	.0004
2	2.085	1.763	.4765	-.0812	-.4899	.0708	-.7555	.0525	.0010
3	2.364	1.443	.3762	-.0458	-.4868	.1493	-.5983	.0758	.0010
4	2.587	1.231	.3083	-.0250	-.4814	.2060	-.4925	.0935	.0020
5	2.752	.9631	.1830	-.0199	-.4788	.2492	-.4216	.1024	.0020
6	2.912	.8609	.1545	.0010	-.4713	.2836	-.3716	.1069	.0040
7	3.052	.7815	.1326	.0043	-.4688	.3116	-.3318	.1102	.0040
8	3.176	.7178	.1152	.0067	-.4665	.3360	-.2990	.1121	.0040
9	3.288	.6653	.1010	.0090	-.4645	.3579	-.2717	.1131	.0040
10	3.389	.6213	.0893	.0113	-.4626	.3779	-.2487	.1134	.0040
11	3.481	.5839	.0795	.0136	-.4608	.3966	-.2286	.1135	.0040
12	3.566	.5513	.0710	.0461	-.4505	.4079	-.2398	.0959	.0080
13	3.644	.5228	.0637	.0499	-.4485	.4241	-.2257	.0951	.0080
14	3.717	.4977	.0574	.0538	-.4466	.4396	-.2130	.0943	.0080
15	3.785	.4754	.0518	.0578	-.4448	.4542	-.2017	.0935	.0080
16	3.849	.4553	.0468	.0618	-.4431	.4680	-.1917	.0927	.0080
17	3.909	.4371	.0424	.0659	-.4413	.4812	-.1825	.0918	.0080
18	3.966	.4206	.0384	.0700	-.4397	.4938	-.1742	.0909	.0080
19	4.019	.4055	.0349	.0741	-.4381	.5059	-.1667	.0899	.0080
20	4.070	.3916	.0316	.0782	-.4366	.5176	-.1597	.0890	.0080
21	4.119	.3788	.0287	.0824	-.4351	.5290	-.1530	.0882	.0080
22	4.165	.3670	.0259	.0866	-.4337	.5400	-.1470	.0873	.0080
23	4.209	.3560	.0234	.0908	-.4323	.5506	-.1414	.0865	.0080
24	4.251	.3457	.0211	.0950	-.4309	.5609	-.1362	.0857	.0080
25	4.292	.3361	.0190	.0992	-.4296	.5708	-.1313	.0849	.0080
26	4.331	.3271	.0171	.1611	-.4118	.5732	-.1572	.0640	.0200
27	4.368	.3186	.0152	.1660	-.4103	.5825	-.1530	.0632	.0200
28	4.404	.3106	.0135	.1709	-.4089	.5916	-.1492	.0625	.0200
29	4.438	.3031	.0119	.1759	-.4076	.6004	-.1457	.0616	.0200

Table 11. Phonon Scattering

n	c_{0n}	c_{1n}	c_{2n}	d_{0n}	d_{1n}	e_{0n}	e_{1n}	e_{2n}	f_n
0	.3899	1.851	.1412	.0000	.0000	-.2273	-1.152	-.0258	.0004
1	.8714	1.437	.2723	.1030	-.4950	.3781	-.9185	.0221	.0020
2	1.124	1.054	.1790	.5693	-.4910	.7138	-.7107	.0557	.0040
3	1.314	.8461	.1274	.7825	-.4846	.9283	-.5985	.0659	.0080
4	1.466	.7156	.0950	.9157	-.4807	1.087	-.5181	.0744	.0080
5	1.592	.6252	.0730	1.015	-.4772	1.212	-.4591	.0797	.0080
6	1.699	.5584	.0570	1.094	-.4742	1.316	-.4136	.0830	.0080
7	1.793	.5070	.0449	1.160	-.4714	1.404	-.3770	.0852	.0080
8	1.876	.4655	.0353	1.246	-.4603	1.478	-.3705	.0687	.0200
9	1.949	.4313	.0276	1.299	-.4573	1.546	-.3462	.0690	.0200
10	2.016	.4031	.0215	1.346	-.4545	1.608	-.3251	.0693	.0200
11	2.077	.3788	.0163	1.389	-.4519	1.665	-.3070	.0691	.0200
12	2.132	.3578	.0119	1.429	-.4495	1.717	-.2911	.0688	.0200
13	2.184	.3395	.0081	1.465	-.4471	1.765	-.2770	.0684	.0200
14	2.231	.3232	.0048	1.500	-.4449	1.809	-.2644	.0680	.0200
15	2.276	.3087	.0020	1.532	-.4427	1.851	-.2530	.0675	.0200
16	2.317	.2957	-.0005	1.603	-.4288	1.887	-.2678	.0456	.0400
17	2.356	.2839	-.0027	1.633	-.4265	1.924	-.2585	.0451	.0400
18	2.393	.2731	-.0047	1.661	-.4243	1.959	-.2499	.0447	.0400
19	2.428	.2633	-.0064	1.689	-.4222	1.993	-.2420	.0443	.0400
20	2.461	.2543	-.0079	1.715	-.4202	2.025	-.2346	.0440	.0400
21	2.492	.2460	-.0094	1.740	-.4183	2.056	-.2279	.0436	.0400
22	2.521	.2382	-.0108	1.764	-.4164	2.085	-.2217	.0431	.0400
23	2.549	.2310	-.0119	1.787	-.4146	2.114	-.2158	.0427	.0400
24	2.576	.2242	-.0130	1.810	-.4128	2.141	-.2103	.0423	.0400
25	2.602	.2179	-.0140	1.831	-.4111	2.167	-.2052	.0419	.0400
26	2.626	.2120	-.0149	1.852	-.4094	2.192	-.2003	.0415	.0400
27	2.650	.2065	-.0158	1.873	-.4078	2.217	-.1957	.0411	.0400
28	2.673	.2012	-.0166	1.893	-.4063	2.241	-.1914	.0408	.0400
29	2.695	.1963	-.0173	1.912	-.4047	2.264	-.1873	.0404	.0400

Appendix F

Coefficients in the fits to $\varphi(\nu;\beta)$ and $Q(\nu;\beta)$ (eqs. [178] and [179]) for $B = 3\times10^{12}$ G ($\beta = .06797$) .

Table 12. Ion Scattering

n	c_{0n}	c_{1n}	c_{2n}	d_{0n}	d_{1n}	e_{0n}	e_{1n}	e_{2n}	f_n
0	1.119	2.729	.2434	.0000	.0000	-.2925	-1.320	-.0276	.0001
1	1.750	2.354	.6540	-.3686	-.4915	-.0456	-1.091	-.0038	.0004
2	2.119	1.831	.4911	-.0582	-.4895	.1132	-.7256	.0598	.0010
3	2.387	1.516	.3911	-.0020	-.4838	.2124	-.5513	.0895	.0020
4	2.596	1.305	.3229	.0217	-.4806	.2835	-.4513	.1025	.0020
5	2.767	1.153	.2740	.0378	-.4778	.3427	-.3776	.1112	.0020
6	2.881	.9132	.1638	.0704	-.4700	.3927	-.3224	.1173	.0040
7	3.008	.8320	.1416	.0839	-.4672	.4343	-.2813	.1202	.0040
8	3.119	.7665	.1239	.0958	-.4649	.4714	-.2475	.1218	.0040
9	3.217	.7121	.1094	.1070	-.4628	.5052	-.2196	.1222	.0040
10	3.306	.6661	.0973	.1178	-.4608	.5362	-.1963	.1221	.0040
11	3.388	.6270	.0872	.1589	-.4505	.5575	-.2029	.1071	.0080
12	3.462	.5923	.0784	.1705	-.4483	.5840	-.1878	.1056	.0080
13	3.530	.5621	.0708	.1815	-.4463	.6091	-.1742	.1042	.0080
14	3.593	.5353	.0642	.1923	-.4443	.6331	-.1621	.1029	.0080
15	3.652	.5113	.0583	.2029	-.4425	.6557	-.1513	.1017	.0080
16	3.708	.4897	.0531	.2132	-.4407	.6770	-.1418	.1004	.0080
17	3.760	.4700	.0484	.2233	-.4389	.6973	-.1332	.0992	.0080
18	3.808	.4521	.0442	.2329	-.4372	.7167	-.1254	.0979	.0080
19	3.855	.4357	.0404	.2425	-.4356	.7352	-.1186	.0966	.0080
20	3.899	.4204	.0369	.2518	-.4341	.7530	-.1122	.0954	.0080
21	3.940	.4065	.0338	.2609	-.4326	.7702	-.1060	.0943	.0080
22	3.980	.3934	.0309	.2698	-.4312	.7868	-.1006	.0931	.0080
23	4.018	.3813	.0282	.3378	-.4134	.7911	-.1306	.0725	.0200
24	4.054	.3699	.0257	.3472	-.4118	.8061	-.1262	.0714	.0200
25	4.089	.3593	.0235	.3565	-.4103	.8207	-.1220	.0704	.0200
26	4.122	.3493	.0213	.3655	-.4088	.8347	-.1183	.0694	.0200
27	4.154	.3399	.0194	.3742	-.4074	.8484	-.1147	.0684	.0200
28	4.185	.3310	.0175	.3829	-.4060	.8616	-.1114	.0674	.0200
29	4.215	.3226	.0158	.3914	-.4047	.8743	-.1087	.0663	.0200

Table 13. Phonon Scattering

n	c_{0n}	c_{1n}	c_{2n}	d_{0n}	d_{1n}	e_{0n}	e_{1n}	e_{2n}	f_n
0	.4056	1.871	.1477	.0000	.0000	-.2100	-1.133	-.0213	.0002
1	.8910	1.465	.2778	.1135	-.4949	.4005	-.8910	.0299	.0020
2	1.135	1.085	.1848	.5862	-.4907	.7483	-.6746	.0660	.0040
3	1.313	.8794	.1334	.7978	-.4869	.9776	-.5475	.0837	.0040
4	1.453	.7494	.1012	.9498	-.4799	1.148	-.4705	.0881	.0080
5	1.567	.6589	.0791	1.057	-.4763	1.285	-.4098	.0929	.0080
6	1.663	.5917	.0631	1.144	-.4731	1.401	-.3631	.0956	.0080
7	1.745	.5396	.0509	1.219	-.4701	1.501	-.3257	.0973	.0080
8	1.817	.4972	.0412	1.315	-.4585	1.584	-.3187	.0824	.0200
9	1.880	.4620	.0334	1.375	-.4554	1.663	-.2947	.0820	.0200
10	1.936	.4328	.0271	1.430	-.4525	1.734	-.2739	.0815	.0200
11	1.988	.4074	.0217	1.480	-.4497	1.800	-.2564	.0807	.0200
12	2.034	.3853	.0171	1.526	-.4471	1.860	-.2410	.0798	.0200
13	2.077	.3659	.0132	1.570	-.4447	1.917	-.2274	.0789	.0200
14	2.116	.3485	.0097	1.611	-.4424	1.969	-.2155	.0779	.0200
15	2.152	.3330	.0067	1.649	-.4402	2.019	-.2047	.0770	.0200
16	2.186	.3190	.0041	1.729	-.4257	2.058	-.2236	.0561	.0400
17	2.217	.3062	.0017	1.764	-.4233	2.102	-.2152	.0552	.0400
18	2.247	.2945	-.0005	1.798	-.4211	2.143	-.2074	.0543	.0400
19	2.275	.2837	-.0024	1.831	-.4189	2.183	-.2003	.0534	.0400
20	2.301	.2739	-.0041	1.862	-.4169	2.221	-.1937	.0527	.0400
21	2.326	.2647	-.0057	1.892	-.4149	2.258	-.1877	.0519	.0400
22	2.349	.2559	-.0072	1.921	-.4130	2.292	-.1823	.0511	.0400
23	2.372	.2479	-.0085	1.949	-.4111	2.326	-.1771	.0503	.0400
24	2.393	.2404	-.0097	1.976	-.4094	2.358	-.1723	.0496	.0400
25	2.413	.2333	-.0108	2.002	-.4076	2.389	-.1678	.0489	.0400
26	2.433	.2267	-.0118	2.027	-.4060	2.419	-.1636	.0482	.0400
27	2.451	.2204	-.0128	2.051	-.4043	2.448	-.1597	.0475	.0400
28	2.469	.2145	-.0137	2.075	-.4027	2.476	-.1560	.0469	.0400
29	2.486	.2088	-.0145	2.098	-.4012	2.468	-.2752	-.0447	.0400

Appendix G

Coefficients in the fits to $\varphi(\nu;\beta)$ and $Q(\nu;\beta)$ (eqs. [178] and [179]) for $B = 10^{13}$ G ($\beta = .2266$).

Table 14. Ion Scattering

n	c_{0n}	c_{1n}	c_{2n}	d_{0n}	d_{1n}	e_{0n}	e_{1n}	e_{2n}	f_n
0	1.193	2.824	.2725	.0000	.0000	-.2384	-1.275	-.0194	.0001
1	1.861	2.509	.6867	-.3293	-.4907	.0237	-1.041	.0079	.0004
2	2.205	2.000	.5218	.0141	-.4885	.2341	-.6544	.0755	.0010
3	2.435	1.681	.4192	.1011	-.4823	.3763	-.4684	.1068	.0020
4	2.607	1.459	.3478	.1505	-.4789	.4798	-.3685	.1178	.0020
5	2.744	1.297	.2962	.2081	-.4709	.5709	-.2851	.1293	.0040
6	2.858	1.170	.2563	.2427	-.4677	.6438	-.2345	.1321	.0040
7	2.900	.9203	.1537	.2728	-.4650	.7056	-.1950	.1335	.0040
8	2.987	.8477	.1349	.2992	-.4627	.7603	-.1629	.1337	.0040
9	3.065	.7866	.1193	.3542	-.4524	.8013	-.1579	.1233	.0080
10	3.135	.7347	.1064	.3779	-.4501	.8442	-.1404	.1205	.0080
11	3.199	.6906	.0956	.3995	-.4480	.8842	-.1251	.1179	.0080
12	3.257	.6511	.0860	.4203	-.4458	.9209	-.1127	.1153	.0080
13	3.311	.6166	.0778	.4396	-.4439	.9555	-.1015	.1131	.0080
14	3.362	.5859	.0706	.4580	-.4419	.9880	-.0915	.1110	.0080
15	3.409	.5584	.0643	.4755	-.4401	1.018	-.0828	.1091	.0080
16	3.454	.5335	.0586	.4922	-.4384	1.047	-.0751	.1072	.0080
17	3.495	.5110	.0536	.5081	-.4366	1.074	-.0681	.1055	.0080
18	3.535	.4903	.0490	.5231	-.4350	1.099	-.0619	.1037	.0080
19	3.573	.4715	.0450	.5376	-.4335	1.123	-.0566	.1020	.0080
20	3.608	.4539	.0412	.5516	-.4320	1.146	-.0516	.1004	.0080
21	3.643	.4379	.0378	.6271	-.4143	1.149	-.0886	.0799	.0200
22	3.675	.4228	.0346	.6411	-.4127	1.170	-.0847	.0785	.0200
23	3.707	.4088	.0317	.6546	-.4111	1.189	-.0812	.0770	.0200
24	3.737	.3958	.0291	.6677	-.4096	1.208	-.0781	.0756	.0200
25	3.765	.3836	.0266	.6803	-.4081	1.226	-.0750	.0744	.0200
26	3.793	.3721	.0244	.6924	-.4067	1.244	-.0723	.0731	.0200
27	3.820	.3613	.0222	.7042	-.4053	1.261	-.0697	.0719	.0200
28	3.846	.3510	.0202	.7157	-.4040	1.277	-.0675	.0708	.0200
29	3.871	.3414	.0184	.7269	-.4027	1.292	-.0657	.0695	.0200

Table 15. Phonon Scattering

n	c_{0n}	c_{1n}	c_{2n}	d_{0n}	d_{1n}	e_{0n}	e_{1n}	e_{2n}	f_n
0	.4566	1.936	.1673	.0000	.0000	-.1577	-1.083	-.0106	.0002
1	.9442	1.539	.2912	.1489	-.4945	.4734	-.8128	.0507	.0020
2	1.155	1.164	.1976	.6430	-.4898	.8575	-.5812	.0903	.0040
3	1.299	.9565	.1458	.8782	-.4857	1.119	-.4527	.1056	.0040
4	1.407	.8225	.1130	1.054	-.4781	1.320	-.3666	.1136	.0080
5	1.491	.7272	.0901	1.181	-.4744	1.483	-.3092	.1155	.0080
6	1.561	.6550	.0733	1.286	-.4710	1.620	-.2660	.1157	.0080
7	1.620	.5982	.0604	1.376	-.4679	1.739	-.2321	.1151	.0080
8	1.671	.5514	.0501	1.489	-.4556	1.836	-.2287	.1012	.0200
9	1.715	.5117	.0415	1.563	-.4525	1.929	-.2089	.0989	.0200
10	1.755	.4787	.0346	1.629	-.4495	2.014	-.1917	.0967	.0200
11	1.790	.4497	.0286	1.690	-.4468	2.091	-.1778	.0944	.0200
12	1.822	.4243	.0236	1.746	-.4442	2.162	-.1656	.0923	.0200
13	1.852	.4019	.0192	1.798	-.4417	2.228	-.1549	.0902	.0200
14	1.879	.3816	.0153	1.892	-.4272	2.276	-.1788	.0699	.0400
15	1.904	.3636	.0119	1.939	-.4247	2.334	-.1710	.0681	.0400
16	1.928	.3472	.0089	1.984	-.4222	2.387	-.1641	.0663	.0400
17	1.950	.3321	.0062	2.026	-.4200	2.438	-.1581	.0646	.0400
18	1.970	.3183	.0038	2.066	-.4178	2.486	-.1525	.0630	.0400
19	1.990	.3057	.0016	2.105	-.4157	2.531	-.1474	.0615	.0400
20	2.009	.2942	-.0003	2.141	-.4136	2.575	-.1425	.0603	.0400
21	2.026	.2833	-.0021	2.176	-.4117	2.616	-.1382	.0590	.0400
22	2.042	.2729	-.0038	2.210	-.4098	2.655	-.1345	.0577	.0400
23	2.058	.2635	-.0053	2.242	-.4080	2.693	-.1308	.0565	.0400
24	2.074	.2546	-.0067	2.273	-.4063	2.657	-.3132	-.0519	.0400
25	2.088	.2463	-.0080	2.303	-.4046	2.693	-.3053	-.0493	.0400
26	2.102	.2385	-.0092	2.332	-.4030	2.727	-.2979	-.0469	.0400
27	2.115	.2311	-.0103	2.360	-.4014	2.761	-.2910	-.0447	.0400
28	2.128	.2241	-.0113	2.387	-.3999	2.793	-.2844	-.0426	.0400
29	2.141	.2175	-.0122	2.413	-.3984	2.824	-.2781	-.0406	.0400

Appendix H

Coefficients in the fits to $\varphi(\nu;\beta)$ and $Q(\nu;\beta)$ (eqs. [178] and [179]) for $B = 3\times10^{13}$ G ($\beta = .6797$) .

Table 16. Ion Scattering

n	c_{0n}	c_{1n}	c_{2n}	d_{0n}	d_{1n}	e_{0n}	e_{1n}	e_{2n}	f_n
0	1.370	3.035	.3329	.0000	.0000	-.1235	-1.186	-.0036	.0001
1	2.066	2.767	.7259	-.2343	-.4892	.1613	-.9658	.0241	.0004
2	2.337	2.239	.5502	.1653	-.4871	.4519	-.5605	.0927	.0010
3	2.497	1.891	.4409	.2927	-.4807	.6468	-.3697	.1227	.0020
4	2.608	1.640	.3645	.3698	-.4774	.7822	-.2765	.1300	.0020
5	2.734	1.530	.3363	.4501	-.4691	.9034	-.1903	.1413	.0040
6	2.773	1.309	.2673	.5006	-.4660	.9949	-.1448	.1418	.0040
7	2.837	1.191	.2339	.5432	-.4634	1.072	-.1092	.1417	.0040
8	2.808	.9246	.1401	.6119	-.4531	1.132	-.0946	.1351	.0080
9	2.864	.8552	.1238	.6457	-.4508	1.188	-.0788	.1307	.0080
10	2.915	.7963	.1102	.6765	-.4485	1.238	-.0654	.1268	.0080
11	2.964	.7463	.0990	.7040	-.4466	1.285	-.0535	.1234	.0080
12	3.008	.7014	.0889	.7301	-.4445	1.327	-.0443	.1201	.0080
13	3.050	.6624	.0804	.7539	-.4426	1.367	-.0356	.1173	.0080
14	3.089	.6277	.0730	.7763	-.4408	1.404	-.0279	.1147	.0080
15	3.126	.5966	.0664	.7975	-.4390	1.439	-.0211	.1124	.0080
16	3.161	.5686	.0606	.8173	-.4373	1.471	-.0152	.1103	.0080
17	3.195	.5433	.0554	.8362	-.4356	1.501	-.0099	.1082	.0080
18	3.227	.5200	.0507	.8539	-.4340	1.529	-.0053	.1062	.0080
19	3.258	.4989	.0464	.9350	-.4166	1.528	-.0501	.0856	.0200
20	3.287	.4792	.0425	.9523	-.4149	1.553	-.0472	.0836	.0200
21	3.316	.4612	.0391	.9688	-.4133	1.577	-.0439	.0820	.0200
22	3.343	.4444	.0358	.9847	-.4117	1.599	-.0410	.0804	.0200
23	3.369	.4288	.0328	1.000	-.4101	1.621	-.0387	.0788	.0200
24	3.395	.4143	.0301	1.015	-.4086	1.641	-.0367	.0773	.0200
25	3.419	.4007	.0276	1.029	-.4072	1.661	-.0345	.0760	.0200
26	3.443	.3879	.0252	1.043	-.4058	1.680	-.0327	.0746	.0200
27	3.466	.3759	.0231	1.056	-.4044	1.698	-.0310	.0733	.0200
28	3.488	.3645	.0210	1.068	-.4031	1.715	-.0296	.0720	.0200
29	3.510	.3539	.0191	1.081	-.4019	1.732	-.0287	.0707	.0200

Table 17. Phonon Scattering

n	c_{0n}	c_{1n}	c_{2n}	d_{0n}	d_{1n}	e_{0n}	e_{1n}	e_{2n}	f_n
0	.5780	2.079	.2078	.0000	.0000	-.0411	-.9775	.0112	.0002
1	1.032	1.663	.3078	.2368	-.4937	.6369	-.6763	.0829	.0020
2	1.167	1.278	.2114	.7730	-.4885	1.079	-.4444	.1200	.0040
3	1.249	1.056	.1576	1.058	-.4806	1.388	-.3086	.1382	.0080
4	1.308	.9085	.1230	1.249	-.4763	1.615	-.2439	.1364	.0080
5	1.354	.8014	.0987	1.397	-.4725	1.799	-.1984	.1336	.0080
6	1.392	.7191	.0806	1.519	-.4692	1.953	-.1645	.1305	.0080
7	1.425	.6540	.0667	1.659	-.4569	2.076	-.1590	.1180	.0200
8	1.454	.6003	.0556	1.752	-.4535	2.191	-.1421	.1133	.0200
9	1.479	.5543	.0463	1.835	-.4504	2.293	-.1286	.1091	.0200
10	1.502	.5162	.0388	1.909	-.4476	2.385	-.1166	.1056	.0200
11	1.523	.4827	.0324	2.021	-.4335	2.452	-.1427	.0855	.0400
12	1.543	.4535	.0269	2.085	-.4306	2.528	-.1358	.0820	.0400
13	1.562	.4276	.0222	2.144	-.4278	2.598	-.1297	.0788	.0400
14	1.579	.4043	.0180	2.200	-.4252	2.663	-.1245	.0760	.0400
15	1.595	.3837	.0144	2.251	-.4228	2.724	-.1196	.0735	.0400
16	1.610	.3649	.0112	2.300	-.4205	2.781	-.1152	.0712	.0400
17	1.625	.3477	.0083	2.346	-.4182	2.835	-.1114	.0690	.0400
18	1.639	.3320	.0057	2.389	-.4161	2.886	-.1079	.0670	.0400
19	1.652	.3176	.0033	2.431	-.4141	2.934	-.1046	.0652	.0400
20	1.665	.3045	.0013	2.470	-.4121	2.850	-.3658	-.0618	.0400
21	1.677	.2922	-.0006	2.508	-.4102	2.896	-.3547	-.0583	.0400
22	1.689	.2806	-.0024	2.544	-.4084	2.940	-.3447	-.0552	.0400
23	1.700	.2698	-.0041	2.578	-.4066	2.983	-.3351	-.0523	.0400
24	1.711	.2599	-.0055	2.611	-.4049	3.023	-.3262	-.0496	.0400
25	1.722	.2505	-.0069	2.643	-.4033	3.062	-.3178	-.0472	.0400
26	1.732	.2417	-.0082	2.674	-.4017	3.099	-.3099	-.0449	.0400
27	1.742	.2334	-.0093	2.703	-.4001	3.135	-.3025	-.0428	.0400
28	1.751	.2256	-.0104	2.732	-.3986	3.170	-.2955	-.0409	.0400
29	1.761	.2183	-.0114	2.760	-.3972	3.204	-.2888	-.0390	.0400

Appendix I

Coefficients in the fits to $\varphi(\nu;\beta)$ and $Q(\nu;\beta)$ (eqs. [178] and [179]) for $B = 10^{14}$ G ($\beta = 2.266$).

Table 18. Ion Scattering

n	c_{0n}	c_{1n}	c_{2n}	d_{0n}	d_{1n}	e_{0n}	e_{1n}	e_{2n}	f_n
0	1.801	3.485	.4464	.0000	.0000	.1078	-1.023	.0229	.0001
1	2.388	3.078	.7318	-.0117	-.4847	.4159	-.8553	.0475	.0008
2	2.504	2.473	.5430	.4517	-.4832	.8286	-.4052	.1242	.0020
3	2.557	2.080	.4330	.6026	-.4795	1.046	-.2689	.1327	.0020
4	2.591	1.799	.3576	.7208	-.4712	1.228	-.1510	.1478	.0040
5	2.624	1.592	.3040	.7948	-.4681	1.357	-.0947	.1476	.0040
6	2.653	1.428	.2623	.8547	-.4651	1.462	-.0539	.1468	.0040
7	2.433	.9681	.1302	.9043	-.4626	1.550	-.0218	.1457	.0040
8	2.576	.9870	.1370	.9810	-.4522	1.617	-.0103	.1392	.0080
9	2.610	.9105	.1211	1.019	-.4500	1.678	.0008	.1341	.0080
10	2.642	.8456	.1078	1.054	-.4478	1.733	.0104	.1297	.0080
11	2.675	.7907	.0968	1.084	-.4459	1.784	.0193	.1259	.0080
12	2.704	.7413	.0870	1.113	-.4439	1.829	.0256	.1222	.0080
13	2.733	.6985	.0787	1.139	-.4420	1.872	.0320	.1191	.0080
14	2.761	.6605	.0714	1.163	-.4402	1.912	.0376	.1163	.0080
15	2.789	.6265	.0649	1.186	-.4385	1.949	.0425	.1138	.0080
16	2.815	.5958	.0592	1.208	-.4368	1.983	.0468	.1115	.0080
17	2.841	.5681	.0541	1.294	-.4197	1.976	-.0048	.0913	.0200
18	2.866	.5431	.0495	1.315	-.4179	2.005	-.0028	.0890	.0200
19	2.890	.5197	.0453	1.334	-.4162	2.031	-.0015	.0866	.0200
20	2.913	.4981	.0415	1.352	-.4145	2.057	.0000	.0846	.0200
21	2.935	.4786	.0381	1.370	-.4129	2.082	.0022	.0829	.0200
22	2.957	.4602	.0349	1.387	-.4113	2.106	.0039	.0812	.0200
23	2.978	.4433	.0320	1.403	-.4098	2.128	.0052	.0795	.0200
24	2.999	.4275	.0293	1.419	-.4082	2.150	.0062	.0780	.0200
25	3.019	.4127	.0268	1.434	-.4068	2.170	.0076	.0766	.0200
26	3.039	.3989	.0245	1.448	-.4054	2.189	.0084	.0752	.0200
27	3.058	.3859	.0224	1.462	-.4041	2.208	.0093	.0738	.0200
28	3.077	.3736	.0204	1.476	-.4028	2.226	.0099	.0725	.0200
29	3.095	.3619	.0185	1.489	-.4016	2.243	.0100	.0711	.0200

Table 19. Phonon Scattering

n	c_{0n}	c_{1n}	c_{2n}	d_{0n}	d_{1n}	e_{0n}	e_{1n}	e_{2n}	f_n
0	.8729	2.383	.2832	.0000	.0000	.1964	-.8025	.0404	.0001
1	1.154	1.819	.3126	.4389	-.4928	.9562	-.4955	.1172	.0020
2	1.149	1.397	.2130	1.029	-.4872	1.458	-.2911	.1440	.0040
3	1.142	1.149	.1586	1.350	-.4792	1.808	-.1656	.1582	.0060
4	1.140	.9829	.1237	1.563	-.4750	2.052	-.1219	.1504	.0080
5	1.141	.8621	.0991	1.759	-.4633	2.244	-.0984	.1408	.0200
6	1.145	.7694	.0809	1.895	-.4593	2.403	-.0828	.1322	.0200
7	1.150	.6960	.0669	2.010	-.4557	2.541	-.0702	.1253	.0200
8	1.157	.6356	.0557	2.110	-.4524	2.661	-.0605	.1192	.0200
9	1.163	.5841	.0463	2.242	-.4387	2.745	-.0900	.0995	.0400
10	1.171	.5415	.0388	2.323	-.4355	2.839	-.0852	.0944	.0400
11	1.179	.5042	.0323	2.397	-.4324	2.924	-.0826	.0895	.0400
12	1.187	.4715	.0268	2.465	-.4296	3.002	-.0795	.0854	.0400
13	1.195	.4429	.0221	2.527	-.4269	3.075	-.0766	.0819	.0400
14	1.203	.4170	.0179	2.585	-.4244	3.142	-.0742	.0786	.0400
15	1.211	.3942	.0142	2.639	-.4220	3.204	-.0716	.0758	.0400
16	1.220	.3735	.0110	2.690	-.4197	3.032	-.4519	-.0780	.0400
17	1.227	.3545	.0081	2.737	-.4175	3.094	-.4348	-.0730	.0400
18	1.235	.3373	.0055	2.783	-.4154	3.153	-.4191	-.0684	.0400
19	1.243	.3215	.0032	2.826	-.4134	3.208	-.4047	-.0643	.0400
20	1.251	.3072	.0011	2.866	-.4114	3.261	-.3910	-.0605	.0400
21	1.259	.2937	-.0008	2.905	-.4096	3.310	-.3787	-.0571	.0400
22	1.266	.2810	-.0026	2.943	-.4078	3.358	-.3675	-.0541	.0400
23	1.273	.2693	-.0042	2.978	-.4060	3.403	-.3569	-.0513	.0400
24	1.280	.2585	-.0057	3.012	-.4044	3.446	-.3470	-.0487	.0400
25	1.287	.2483	-.0071	3.045	-.4027	3.488	-.3376	-.0463	.0400
26	1.294	.2388	-.0083	3.077	-.4011	3.528	-.3288	-.0441	.0400
27	1.301	.2298	-.0095	3.107	-.3996	3.566	-.3207	-.0421	.0400
28	1.308	.2214	-.0106	3.137	-.3981	3.603	-.3129	-.0402	.0400
29	1.315	.2134	-.0116	3.166	-.3967	3.639	-.3055	-.0383	.0400

References

Abramowitz, M. and Stegun I. A. 1972, *Handbook of Mathematical Functions*, Dover, New York.

Berestetskii, V. R., Lifshitz, E. M., and Pitaevskii, L. P. 1982, *Quantum Electrodynamics*, Pergamon Press, Oxford.

Blandford, R. D., DeCampli, W. M., and Königl, A. 1979, *Bull. Am. Astr. Soc.* **11**, 703.

Blandford, R. D. and Hernquist, L. 1982, *J. Phys. C: Solid State Phys.* **15**, 6233.

Blandford, R. D., Applegate, J. H., and Hernquist, L. 1983, *Mon. Not. R. astr. Soc.* **204**, 1025.

Canuto, V. and Chiu, H.-Y. 1969. *Phys. Rev.* **188**, 2446.

Canuto, V. and Chiuderi, C. 1970, *Phys. Rev. D* **1**, 2219.

Canuto, V. and Ventura, J. 1977, *Fund. of Cosmic Phys.* **2**, 203.

Flowers, E. and Itoh, N. 1976, *Ap. J.* **206**, 218.

Glen, G. and Sutherland, P. G. 1980, *Ap. J.* **239**, 671.

Gudmundsson, E. H., Pethick, C. and Epstein, R. I. 1983, *Ap. J.* **272**, 286.

ter Haar, D. 1961, *Rept. Prog. Phys.* **24**, 304.

Heuser, M. and Hajdu, J. 1974, *Z. Physik* **270**, 289.

Itoh, N., Mitake, S. Iyetomi, H., and Ichimaru, S. 1983, *Ap. J.* **273**, 774.

Kahn, A. H. and Frederikse, H. P. R. 1959, *Solid State Phys.* **9**, 257.

Kaminker, A. D. and Yakovlev, D. G. 1981, *Theor.* and *Math. Phys.* **49**, 1012.

Kohn W. and Luttinger, J. M. 1957, *Phys. Rev.* **108**, 590.

Kubo, R., Yokota, M., and Nakajima, S. 1957, *J. Phys. Soc. of Japan* **12**, 1203.

Kubo, R., Miyake, S. J., and Hashitsume, N. 1965, *Solid State Phys.* **17**, 269.

Lampe, M. 1968, *Phys. Rev.* **170**,306.

Landau, L. D. and Lifshitz, E. M. 1960, *Electrodynamics of Continuous Media*, Pergamon Press, Oxford.

Langer, S. H. 1981, *Phys. Rev. D* **23**,328.

Luttinger, J. M. 1964, *Phys. Rev.* **135**,A1505.

Nomoto, K. and Tsuruta, S. 1981, *Ap. J. Lett.* **250**,L19.

Pavlov, G. G. and Yakovlev, D. G. 1976, *Sov. Phys. JETP* **43**,389.

Pollock, E. L. and Hansen, J. P. 1973, *Phys. Rev. A* **8**,3110.

Richardson, M. B., Van Horn, H. M., Ratcliff, K. F. and Malone, R. C. 1982, *Ap. J.* **255**,624.

Slattery, W. L., Doolen, G. D., and DeWitt, H. E. 1980, *Phys. Rev. A* **21**,2087.

Stinchcombe, R. B. 1961, *Proc. Phys. Soc.* **78**,275.

Stinchcombe, R. B. 1974, in *Lecture Notes in Physics: Transport Phenomena*, ed. Kirczenow, G. and Morro, J., Springer-Verlag, Berlin.

Tsuruta, S. 1979, *Phys. Rept.* **56**,237.

Urpin, V. A. and Yakovlev, D. G. 1980a, *Soviet Astronomy* **24**,126.

Urpin, V. A. and Yakovlev, D. G. 1980b, *Soviet Astronomy* **24**,425.

Van Riper, K. A. and Lamb, D. Q. 1981, *Ap. J. Lett.* **244**,L13.

Ventura, J. 1973, *Phys. Rev. A* **8**,3021.

Yakovlev, D. G. and Urpin, V. A. 1980, *Soviet Astronomy* **24**,303.

Yakovlev, D. G. 1980a, Preprint No. 678, A.F. Ioffe Institute of Physics and Technology, Leningrad.

Yakovlev, D. G. 1980b, Preprint No. 679, A.F. Ioffe Institute of Physics and Technology, Leningrad.

Yakovlev, D. G. 1982, *Ast. Zh.* **59**,683.

Zyryanov, P. S. and Guseva, G. I. 1969, *Soviet Physics Uspekhi* 11 ,538.

Zyryanov, P. S. and Klinger, M. I. 1976, *Quantum Theory of Electron Transport Phenomena in Crystallized Semiconductors*, Nauka, Moscow.

Figure Captions

Figure 1.

Approximate region (cross-hatched) in the $\rho - T$ plane in which quantum effects on electron transport can be significant, for a field strength of $B = 10^{13} G$. Also shown is the sensitivity strip of Gudmundsson, Pethick, and Epstein (1983) (dotted region), in which the cooling calculations depend most strongly on the thermal conductivity.

Figure 2.

The relation of the chemical potential ($\zeta = \mu / \hbar\omega_B$) to the chemical potential in the absence of a quantizing field ($\zeta_0 = \mu_0 / \hbar\omega_B$) for a field strength $B = 10^{13} G$. Two degrees of degeneracy are shown: $t = 0$ (solid line) and $t = .05$ (dashed line). The effects of thermal smoothing indicate that only in the limit of one Landau level being occupied does μ differ appreciably from μ_0. Furthermore, the $t = 0$ relation of ζ to ζ_0 is strongly satisfied when only one level is populated.

Figure 3.

At a given density the influence of the magnetic field on physical conditions is indicated. Shown are the approximate boundaries at which the gas can be considered to be ideal, completely ionized, non-relativistic, or degenerate. The final condition is indicated for the temperatures $T = 10^6, 10^7$ K. Also shown is the limit in which only one Landau level is occupied ($n_{max} = 0$). Only in this limit are the boundaries significantly shifted as a result of the deviation of μ from μ_0.

Figure 4.

The regions in the $\rho-T$ plane in which the cutoff factors γ_n are determined by inelastic scattering of the electrons or by collisional broadening of the Landau levels.

Figure 5.

The function $\varphi(\nu;\beta)$ for e-ion scattering and $B = 10^{13}G$ ($\beta = .2266$).

Figure 6.

The function $Q(\nu;\beta)$ for e-ion scattering and $B = 10^{13}G$ ($\beta = .2266$).

Figure 7.

The function $\varphi(\nu;\beta)$ for e-phonon scattering and $B = 10^{13}G$ ($\beta = .2266$).

Figure 8.

The function $Q(\nu;\beta)$ for e-phonon scattering and $B = 10^{13}G$ ($\beta = .2266$).

Figure 9.

The ratios $\sigma_{zz}/(\sigma_0)_{zz}$ (dashed line) and $\gamma_{zz}/(\gamma_0)_{zz}$ (dotted-dashed line) as functions of ζ for e-ion scattering, $t = .025$, and $B = 10^{11}$ G ($\beta = .002266$). In the $t = 0$ limit (solid line) the two ratios are equal.

Figure 10.

The ratios $\sigma_{zz}/(\sigma_0)_{zz}$ (dashed line) and $\gamma_{zz}/(\gamma_0)_{zz}$ (dotted-dashed line) as functions of ζ for e-phonon scattering, $t = .025$, and $B = 10^{11}$ G ($\beta = .002266$). In the $t = 0$ limit (solid line) the two ratios are equal.

Figure 11.

The ratio $\lambda_{zz}/(\lambda_0)_{zz}$ (dashed line) as a function of ζ for e-ion scattering, $t = .025$, and $B = 10^{11}$ G ($\beta = .002266$). The $t = 0$ limit (solid line) is also indicated.

Figure 12.

The ratio $\lambda_{zz}/(\lambda_0)_{zz}$ (dashed line) as a function of ζ for e-phonon scattering, $t = .025$, and $B = 10^{11}$ G ($\beta = .002266$). The $t = 0$ limit (solid line) is also indicated.

Figure 13.

The ratios $\sigma_{zz}/(\sigma_0)_{zz}$ (dashed line) and $\gamma_{zz}/(\gamma_0)_{zz}$ (dotted-dashed line) as functions of ζ for e-ion scattering, $t = .025$, and $B = 10^{13}$ G ($\beta = .2266$). In the $t = 0$ limit (solid line) the two ratios are equal.

Figure 14.

The ratios $\sigma_{zz}/(\sigma_0)_{zz}$ (dashed line) and $\gamma_{zz}/(\gamma_0)_{zz}$ (dotted-dashed line) as functions of ζ for e-phonon scattering, $t = .025$, and $B = 10^{13}$ G ($\beta = .2266$). In the $t = 0$ limit (solid line) the two ratios are equal.

Figure 15.

The ratio $\lambda_{zz}/(\lambda_0)_{zz}$ (dashed line) as a function of ζ for e-ion scattering, $t = .025$, and $B = 10^{13}$ G ($\beta = .2266$). The $t = 0$ limit (solid line) is also indicated.

Figure 16.

The ratio $\lambda_{zz}/(\lambda_0)_{zz}$ (dashed line) as a function of ζ for e-phonon scattering, $t = .025$, and $B = 10^{13}$ G ($\beta = .2266$). The $t = 0$ limit (solid line) is also indicated.

Figure 17.

The ratios $\sigma_{yy}/(\sigma_0)_{yy}$ (dashed line) and $\gamma_{yy}/(\gamma_0)_{yy}$ (dotted-dashed line) as functions of ζ for e-ion scattering, $t = .025$, and $B = 10^{11}$ G ($\beta = .002266$). In the $t = 0$ limit (solid line) the two ratios are equal.

Figure 18.

The ratios $\sigma_{yy}/(\sigma_0)_{yy}$ (dashed line) and $\gamma_{yy}/(\gamma_0)_{yy}$ (dotted-dashed line) as functions of ζ for e-phonon scattering, $t = .025$, and $B = 10^{11}$ G ($\beta = .002266$). In the $t = 0$ limit (solid line) the two ratios are equal.

Figure 19.

The ratio $\lambda_{yy}/(\lambda_0)_{yy}$ (dashed line) as a function of ζ for e-ion scattering, $t = .025$, and $B = 10^{11}$ G ($\beta = .002266$). The $t = 0$ limit (solid line) is also indicated.

Figure 20.

The ratio $\lambda_{yy}/(\lambda_0)_{yy}$ (dashed line) as a function of ζ for e-phonon scattering, $t = .025$, and $B = 10^{11}$ G ($\beta = .002266$). The $t = 0$ limit (solid line) is also indicated.

Figure 21.

The ratios $\sigma_{yy}/(\sigma_0)_{yy}$ (dashed line) and $\gamma_{yy}/(\gamma_0)_{yy}$ (dotted-dashed line) as functions of ζ for e-ion scattering, $t = .025$, and $B = 10^{13}$ G ($\beta = .2266$). In the $t = 0$ limit the two ratios are equal.

Figure 22.

The ratios $\sigma_{yy}/(\sigma_0)_{yy}$ (dashed line) and $\gamma_{yy}/(\gamma_0)_{yy}$ (dotted-dashed line) as functions of ζ for e-phonon scattering, $t = .025$, and $B = 10^{13}$ G ($\beta = .2266$). In the

$t = 0$ limit the two ratios are equal.

Figure 23.

The ratio $\lambda_{yy} / (\lambda_0)_{yy}$ (dashed line) as a function of ζ for e-ion scattering, $t = .025$, and $B = 10^{13}$ G ($\beta = .2266$). The $t = 0$ limit (solid line) is also indicated.

Figure 24.

The ratio $\lambda_{yy} / (\lambda_0)_{yy}$ (dashed line) as a function of ζ for e-phonon scattering, $t = .025$, and $B = 10^{13}$ G ($\beta = .2266$). The $t = 0$ limit (solid line) is also indicated.

Figure 25.

The ratios $\lambda_{yx} / (\lambda_0)_{yx}$ (dashed line) and $\gamma_{yx} / (\gamma_0)_{yx}$ (dotted-dashed line) as functions of ζ for $t = .025$ and $B = 10^{11}$ G ($\beta = .002266$). The $t = 0$ limit of $\lambda_{yx} / (\lambda_0)_{yx}$ (solid line) is also indicated.

Figure 26.

The ratios $\lambda_{yx} / (\lambda_0)_{yx}$ (dashed line) and $\gamma_{yx} / (\gamma_0)_{yx}$ (dotted-dashed line) as functions of ζ for $t = .025$ and $B = 10^{13}$ G ($\beta = .2266$). The $t = 0$ limit of $\lambda_{yx} / (\lambda_0)_{yx}$ (solid line) is also indicated.

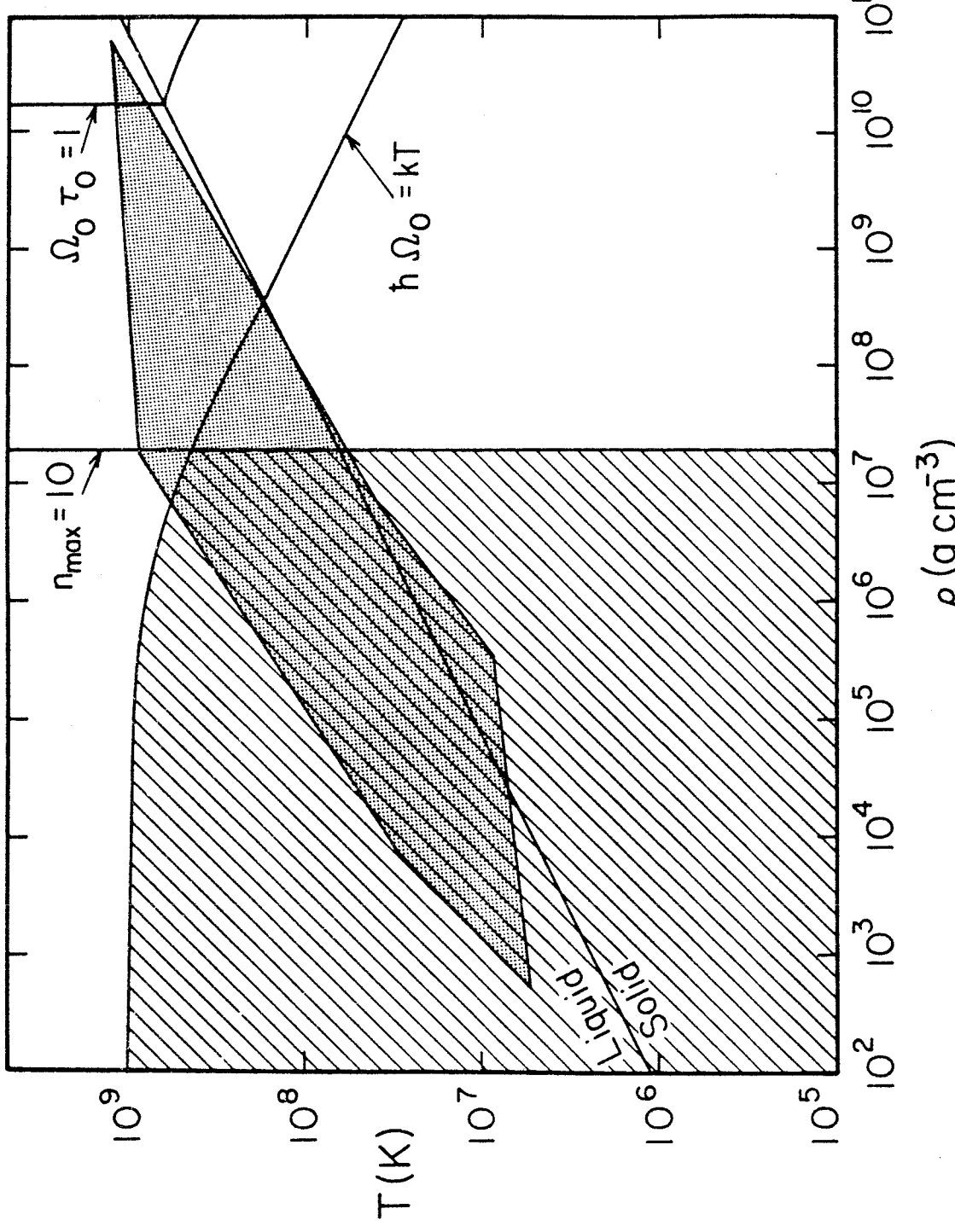
$\Omega_0 \tau_0 = 1$
$h\Omega_0 = kT$
$n_{max} = 10$
Liquid
Solid
T(K)
ρ (g cm^{-3})
10^9
10^8
10^7
10^6
10^5
10^2
10^3
10^4
10^5
10^6
10^7
10^8
10^9
10^{10}
10^{11}

Figure 1

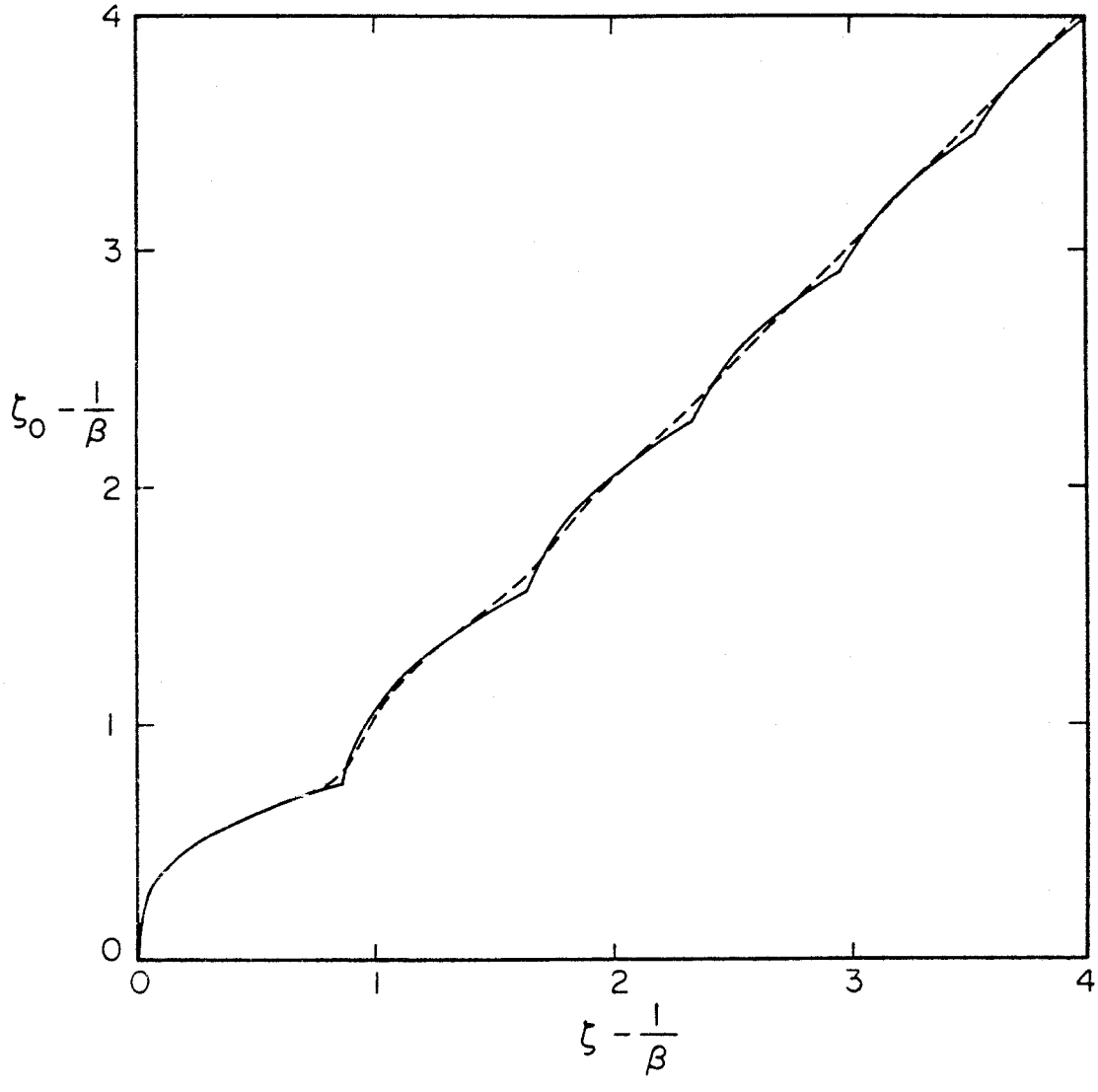

Figure 2

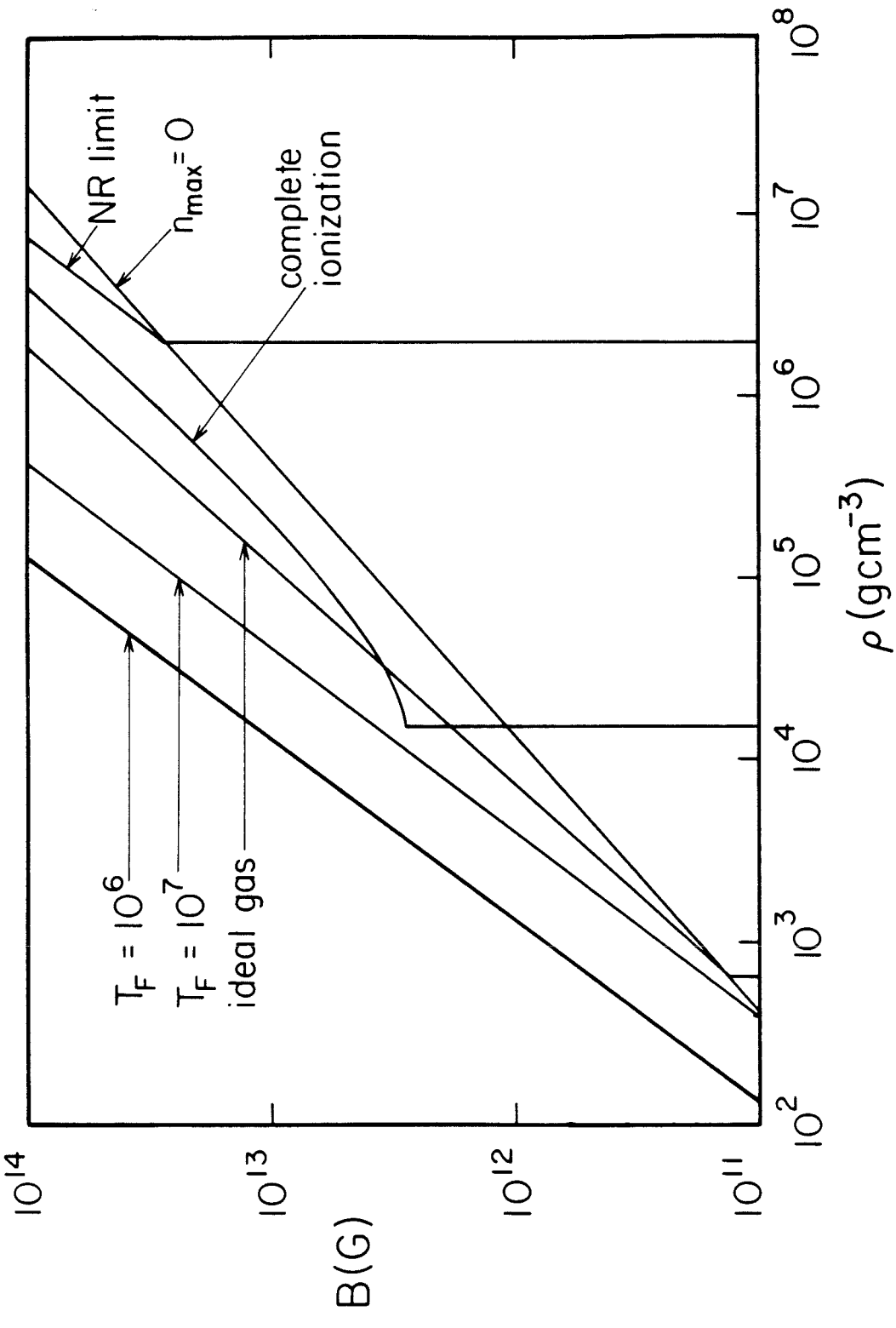
NR limit
$n_{max}=0$
complete ionization
$T_F = 10^6$
$T_F = 10^7$
ideal gas
B(G)
10^{14}
10^{13}
10^{12}
10^{11}
10^2
10^3
10^4
10^5
10^6
10^7
10^8
$\rho\,(gcm^{-3})$

Figure 3

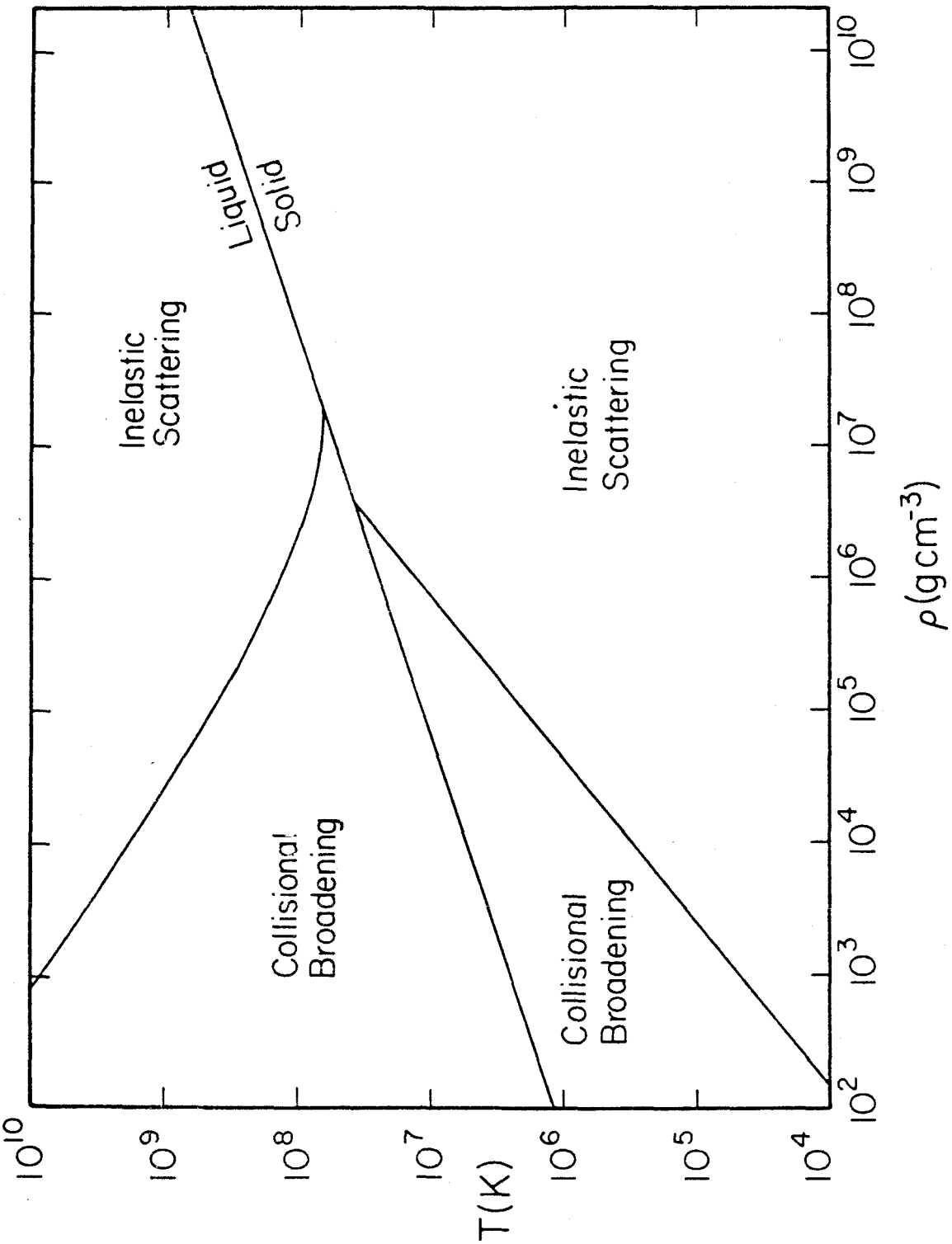
Inelastic Scattering
Liquid
Solid
Collisional Broadening
Collisional Broadening
Inelastic Scattering
T(K)
ρ(g cm⁻³)
10¹⁰
10⁹
10⁸
10⁷
10⁶
10⁵
10⁴
10²
10³
10⁴
10⁵
10⁶
10⁷
10⁸
10⁹
10¹⁰

Figure 4

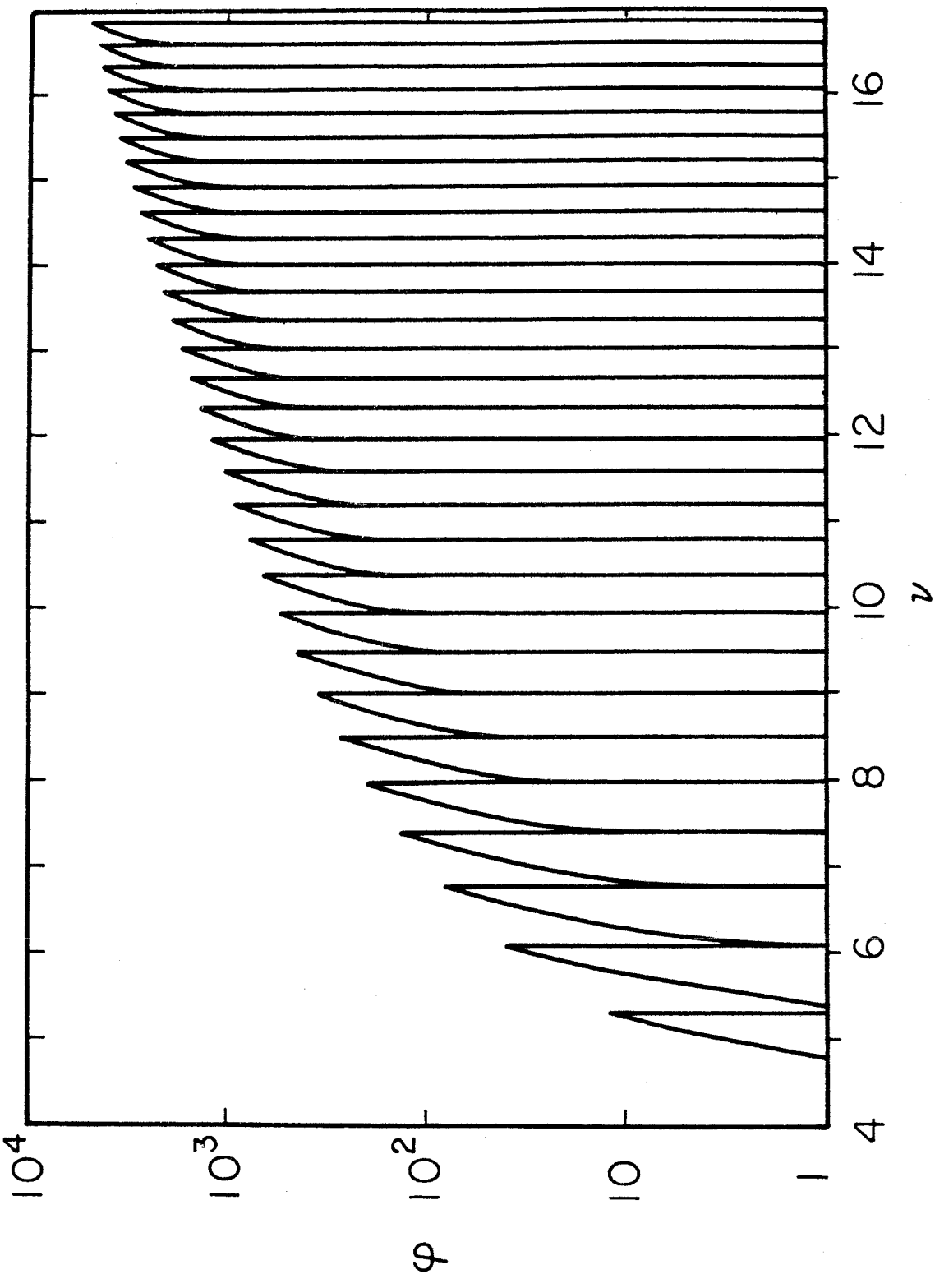

Figure 5

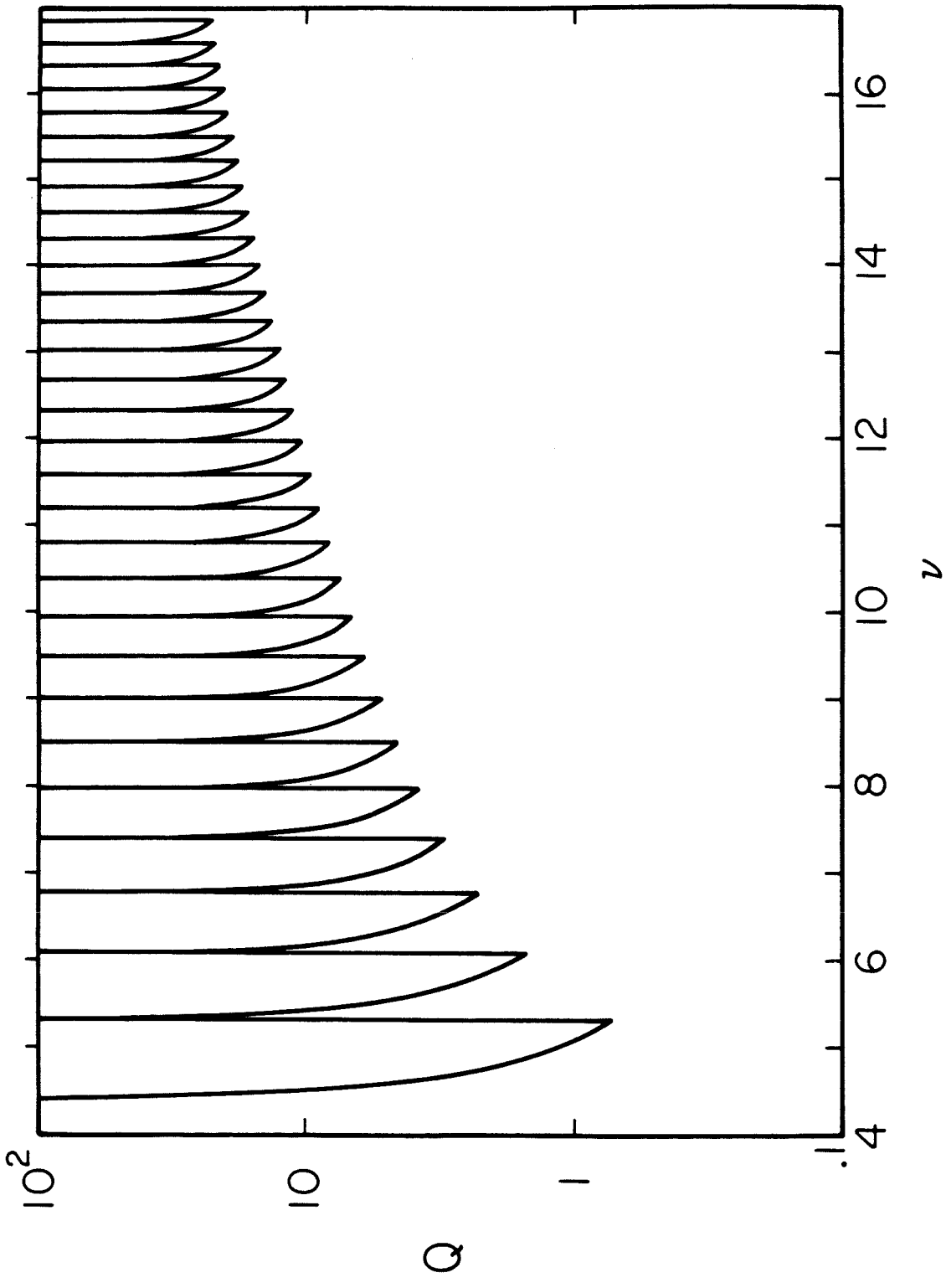

Figure 6

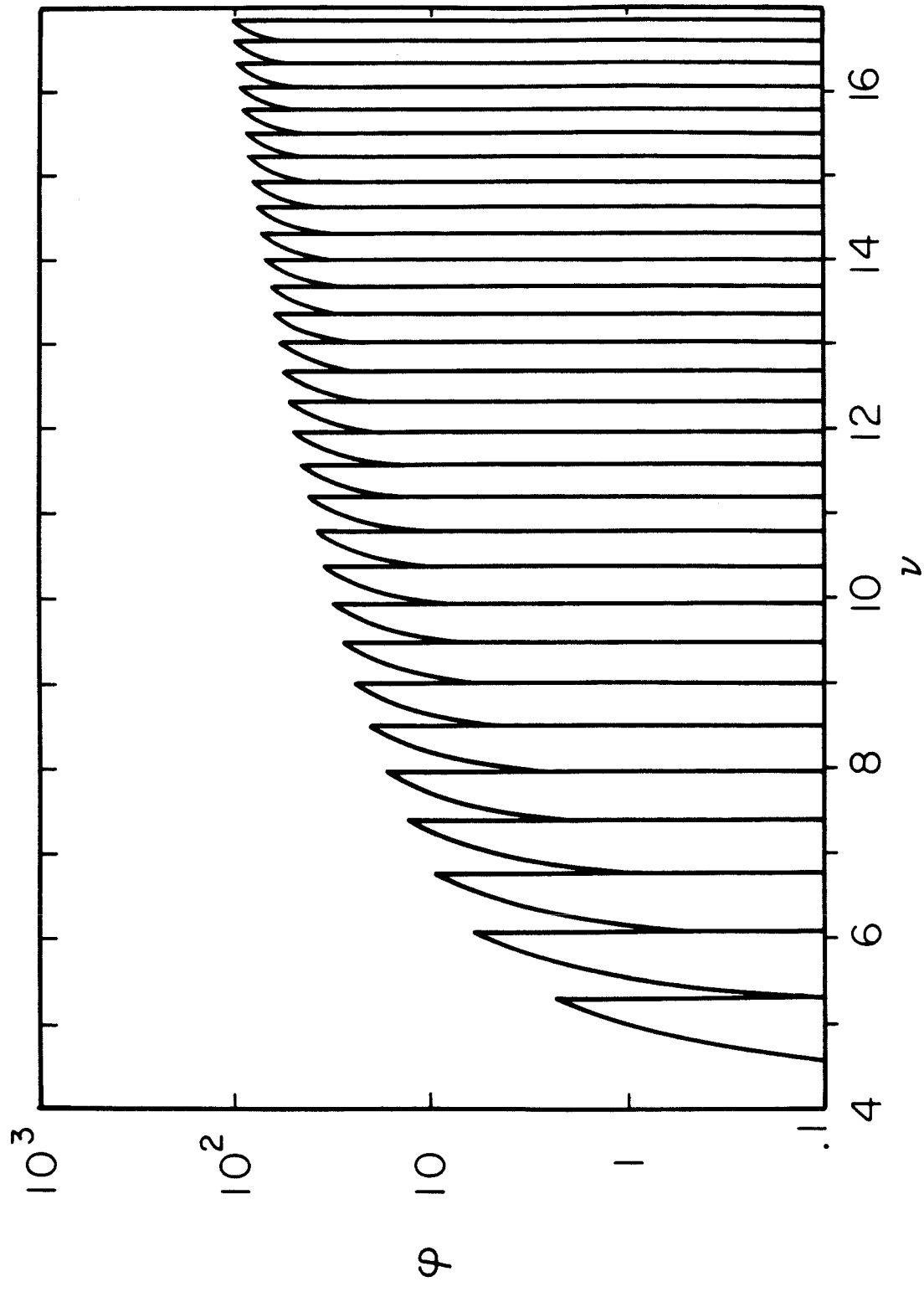

Figure 7

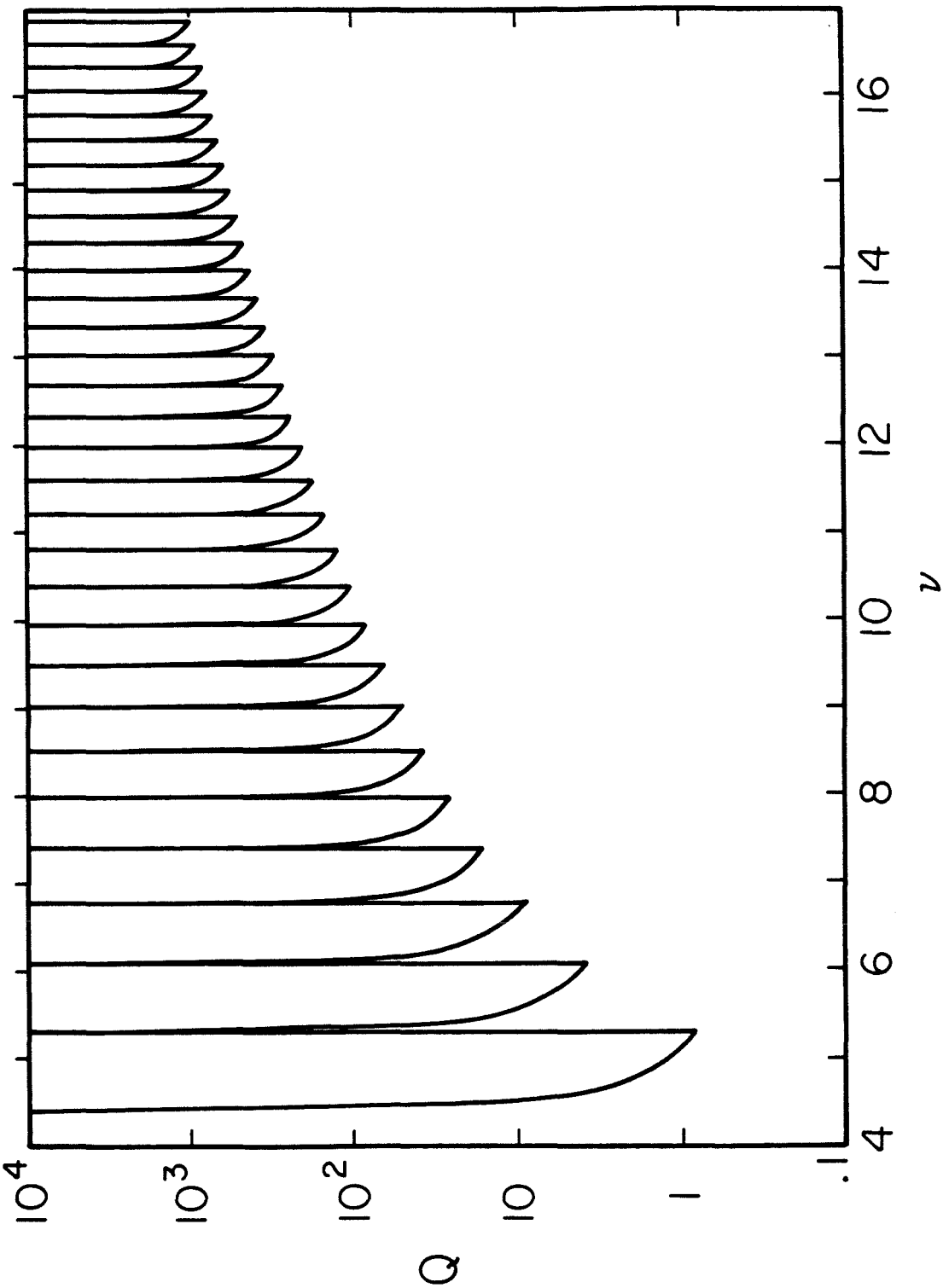

Figure 8

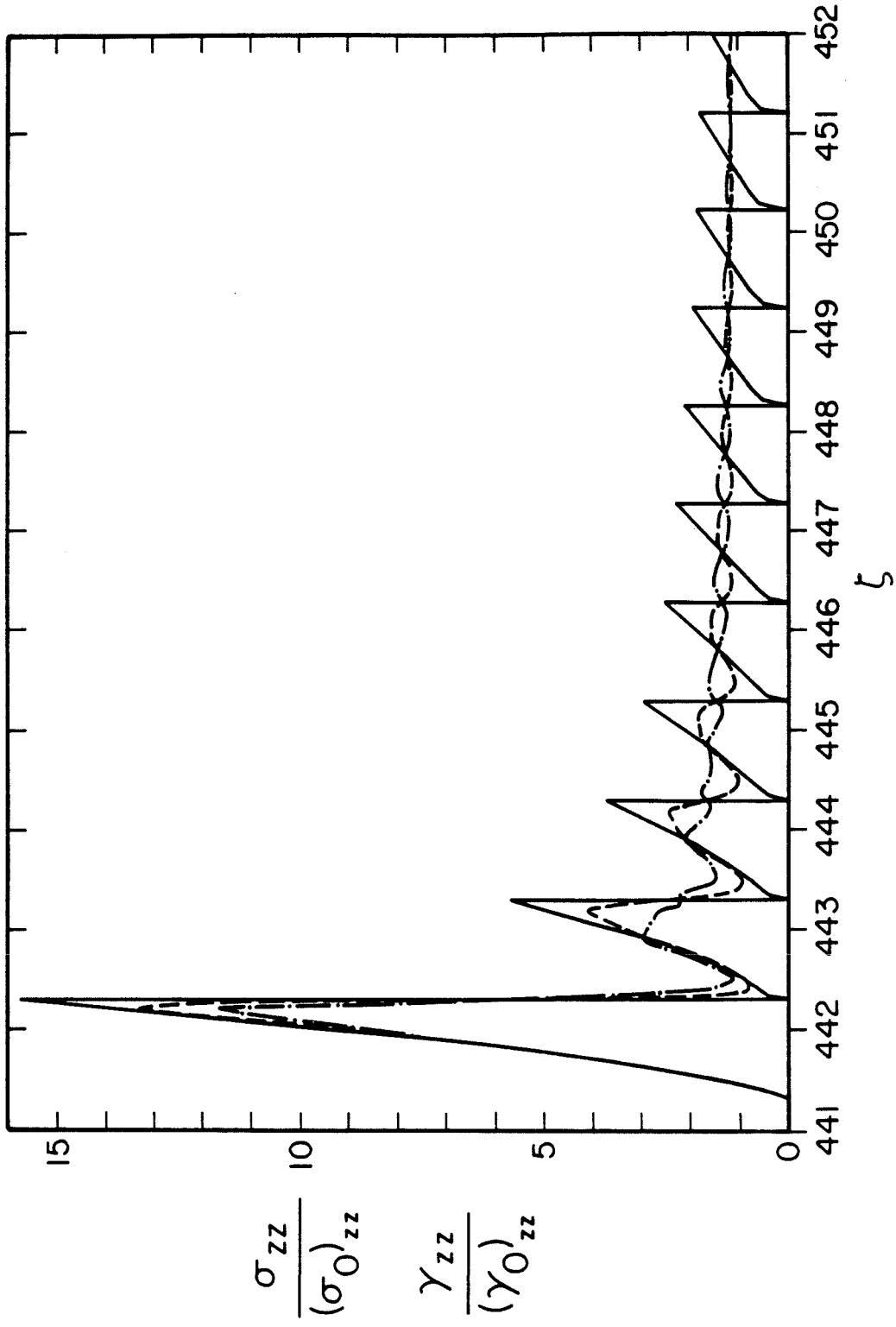
15
10
5
0
441
442
443
444
445
446
447
448
449
450
451
452
ζ
$\frac{\sigma_{zz}}{(\sigma_0)_{zz}}$
$\frac{\gamma_{zz}}{(\gamma_0)_{zz}}$

Figure 9

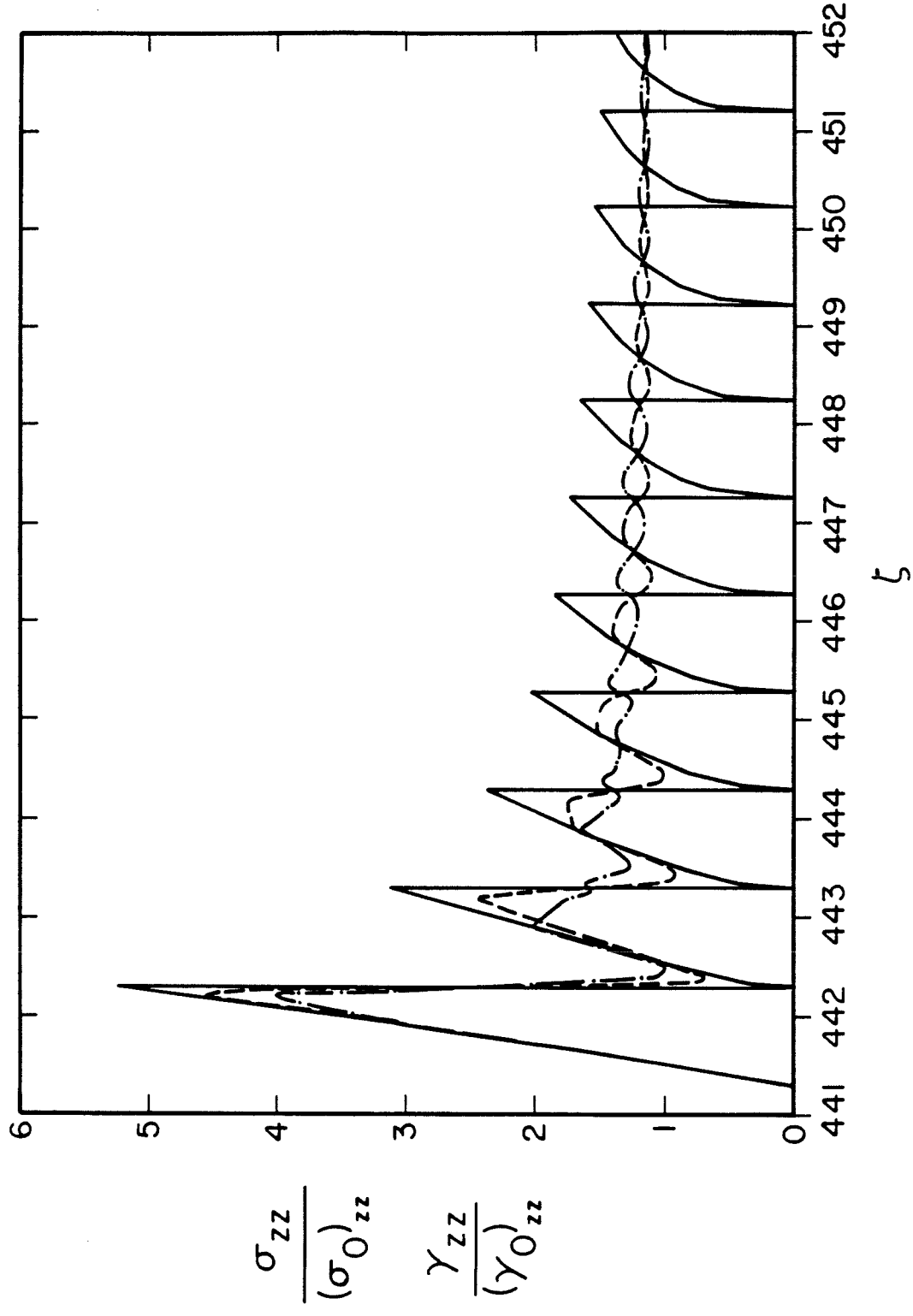
0
1
2
3
4
5
6
441
442
443
444
445
446
447
448
449
450
451
452
ζ
$\frac{\sigma_{zz}}{(\sigma_0)_{zz}}$
$\frac{\gamma_{zz}}{(\gamma_0)_{zz}}$

Figure 10

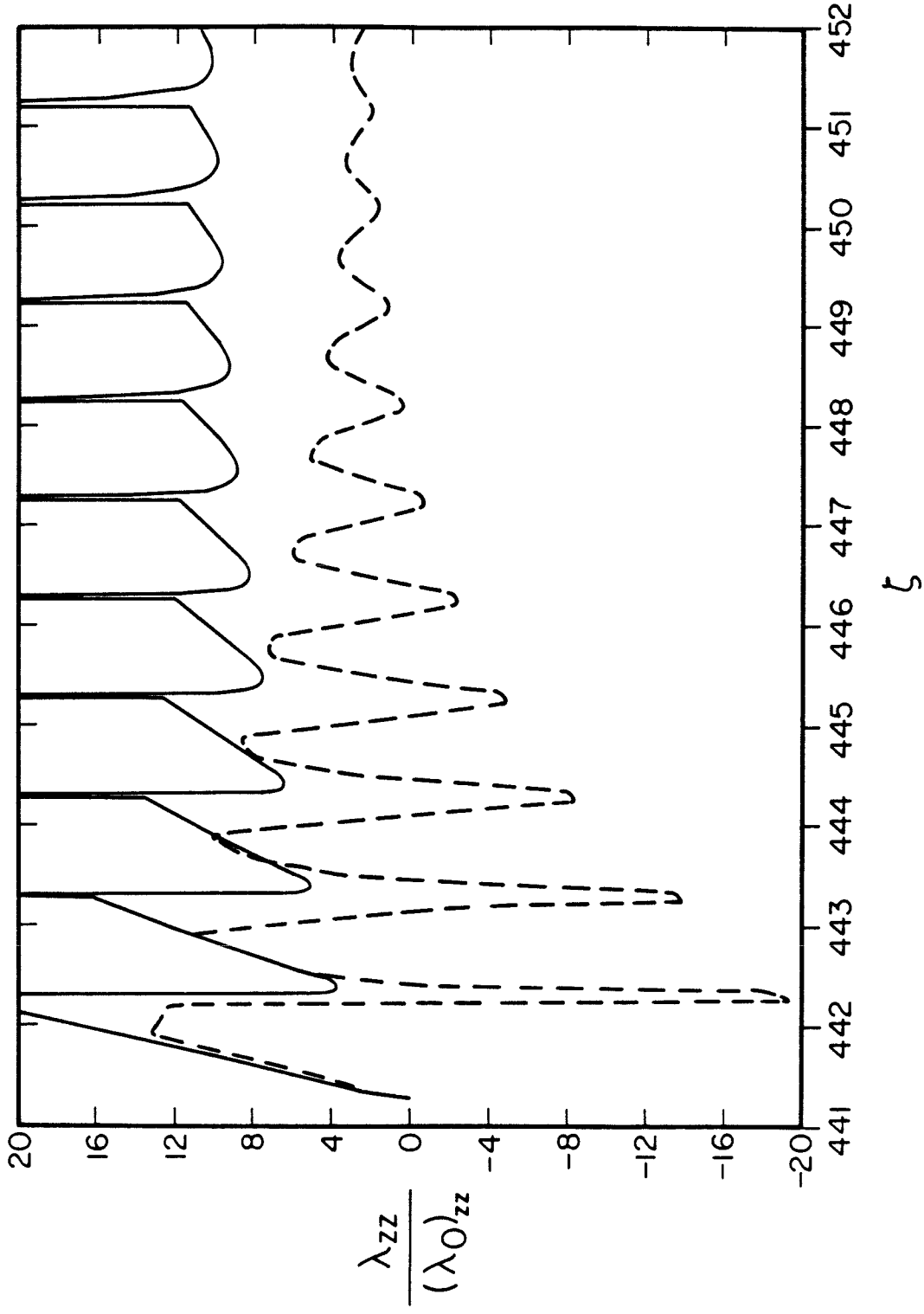
20
16
12
8
4
0
-4
-8
-12
-16
-20
441
442
443
444
445
446
447
448
449
450
451
452
ζ
$\frac{\lambda_{zz}}{(\lambda_0)_{zz}}$

Figure 11

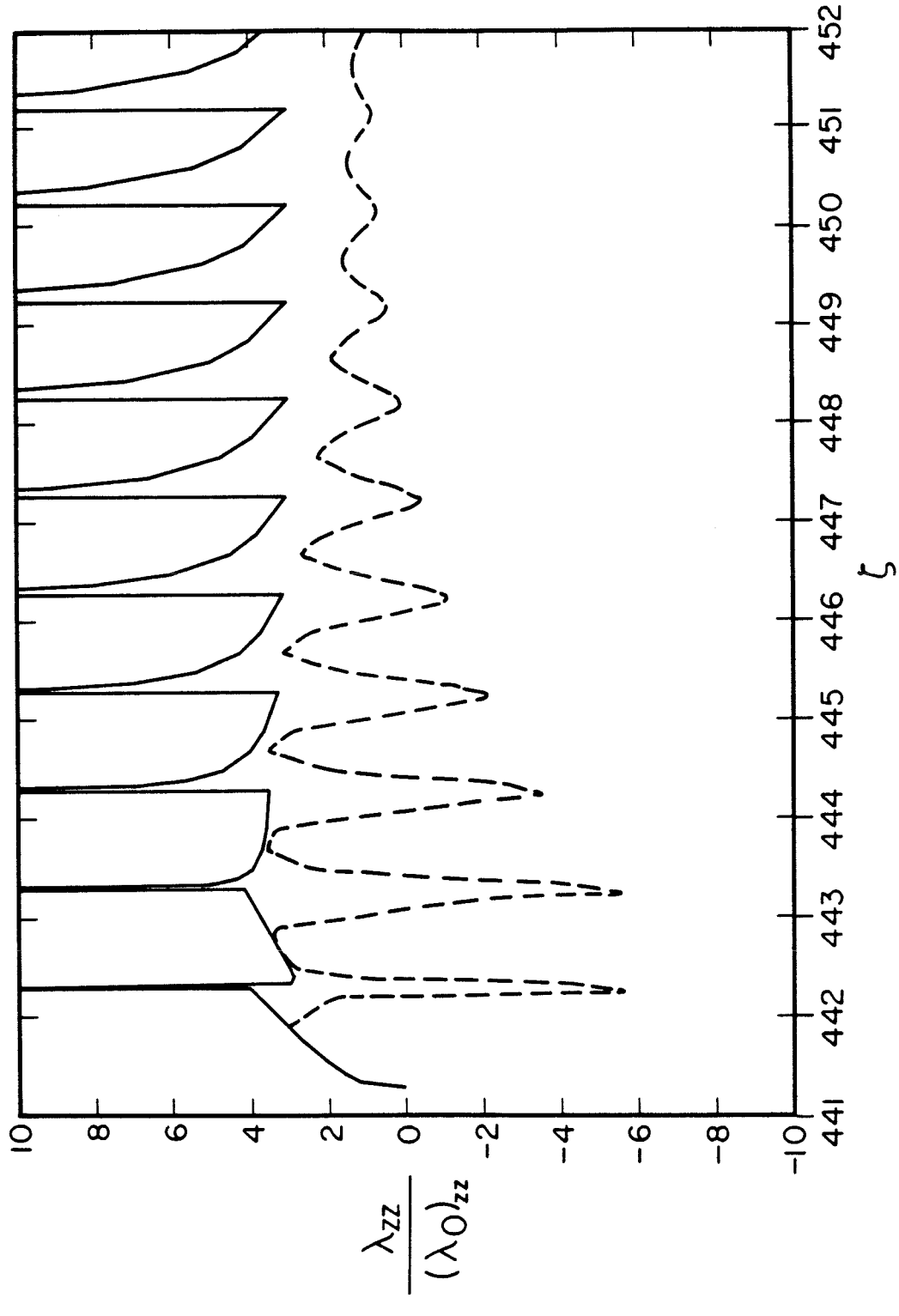
10
8
6
4
2
0
-2
-4
-6
-8
-10
441
442
443
444
445
446
447
448
449
450
451
452
ζ
$\frac{\lambda_{zz}}{(\lambda_0)_{zz}}$

Figure 12

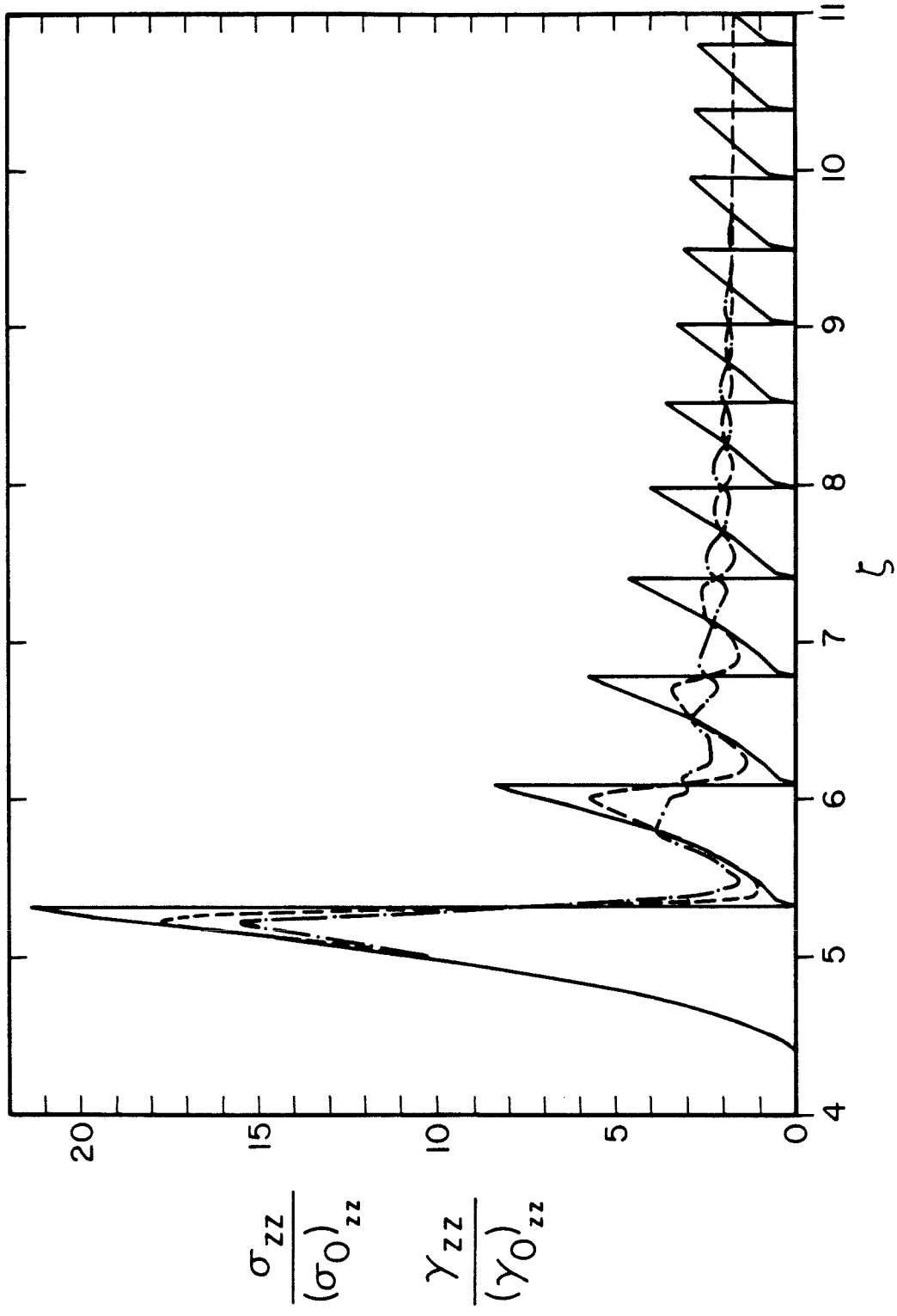
20
15
10
5
0
4
5
6
7
8
9
10
11
ζ
$\frac{\sigma_{zz}}{(\sigma_0)_{zz}}$
$\frac{\gamma_{zz}}{(\gamma_0)_{zz}}$

Figure 13

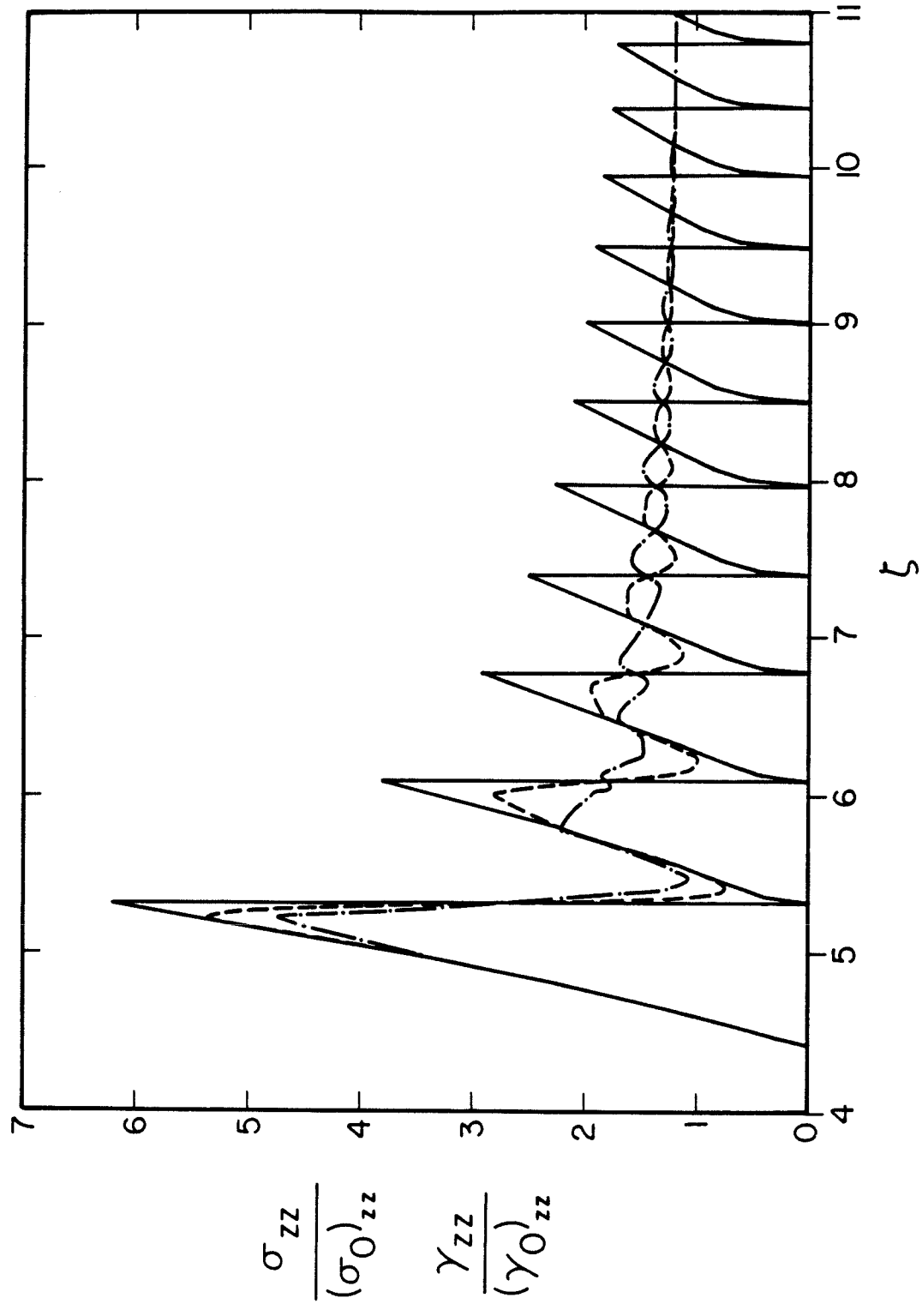
7
6
5
4
3
2
1
0
4
5
6
7
8
9
10
11
ζ
$\frac{\sigma_{zz}}{(\sigma_0)_{zz}}$
$\frac{\gamma_{zz}}{(\gamma_0)_{zz}}$

Figure 14

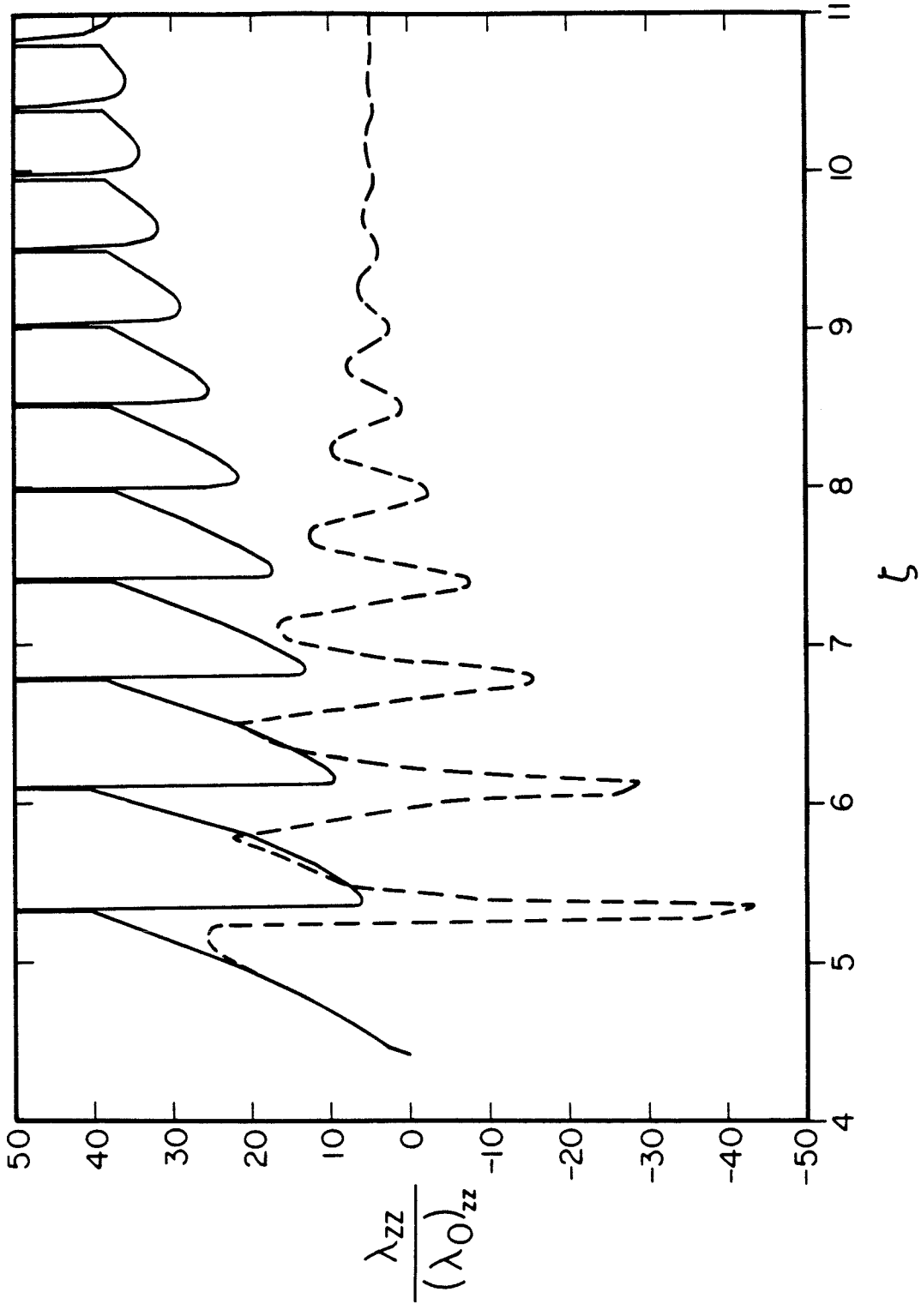
50
40
30
20
10
0
-10
-20
-30
-40
-50
4
5
6
7
8
9
10
11
ζ
$\frac{\lambda_{zz}}{(\lambda_0)_{zz}}$

Figure 15

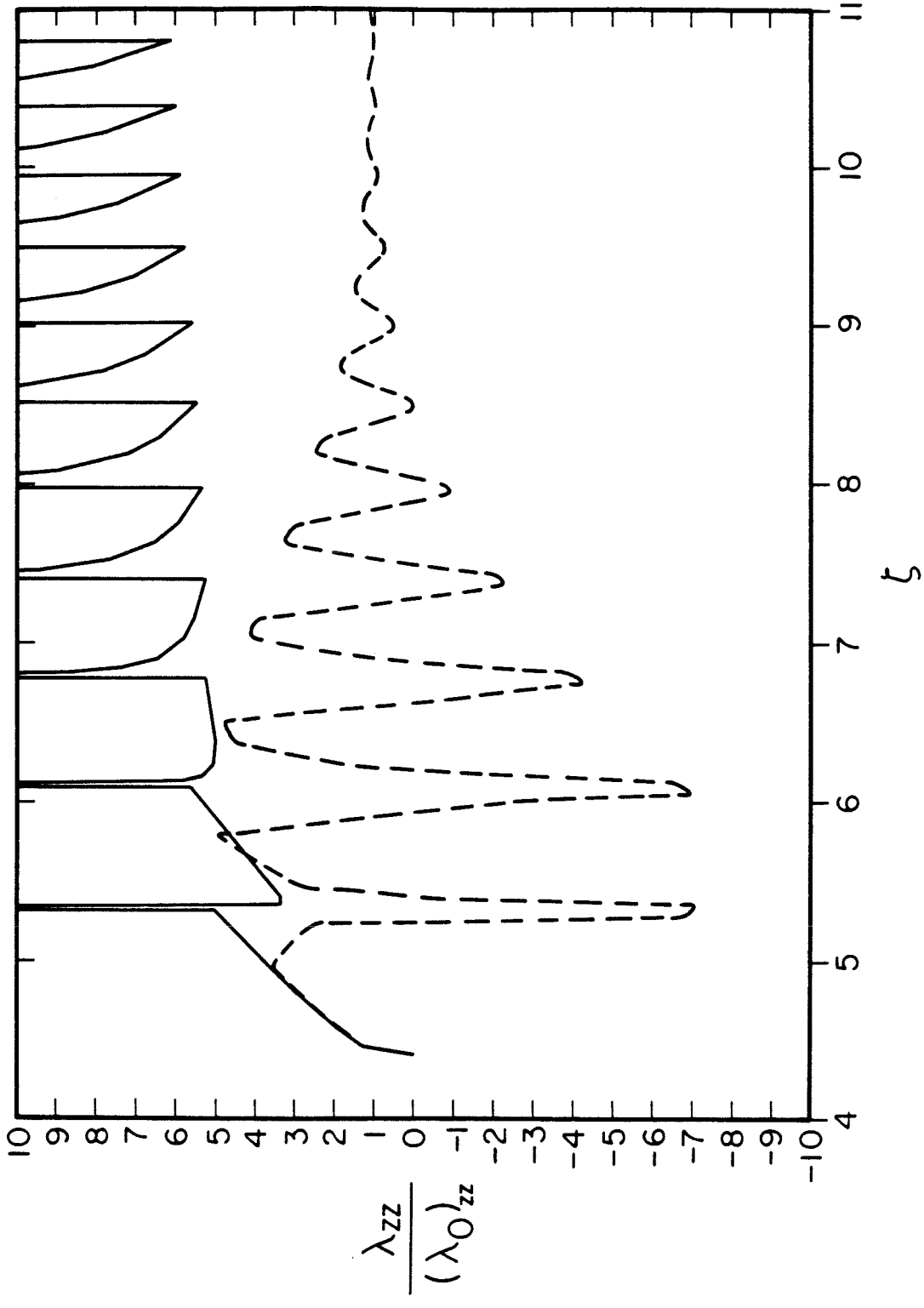
$\frac{\lambda_{zz}}{(\lambda_0)_{zz}}$
10 9 8 7 6 5 4 3 2 1 0 -1 -2 -3 -4 -5 -6 -7 -8 -9 -10
4 5 6 7 8 9 10 11
ζ

Figure 16

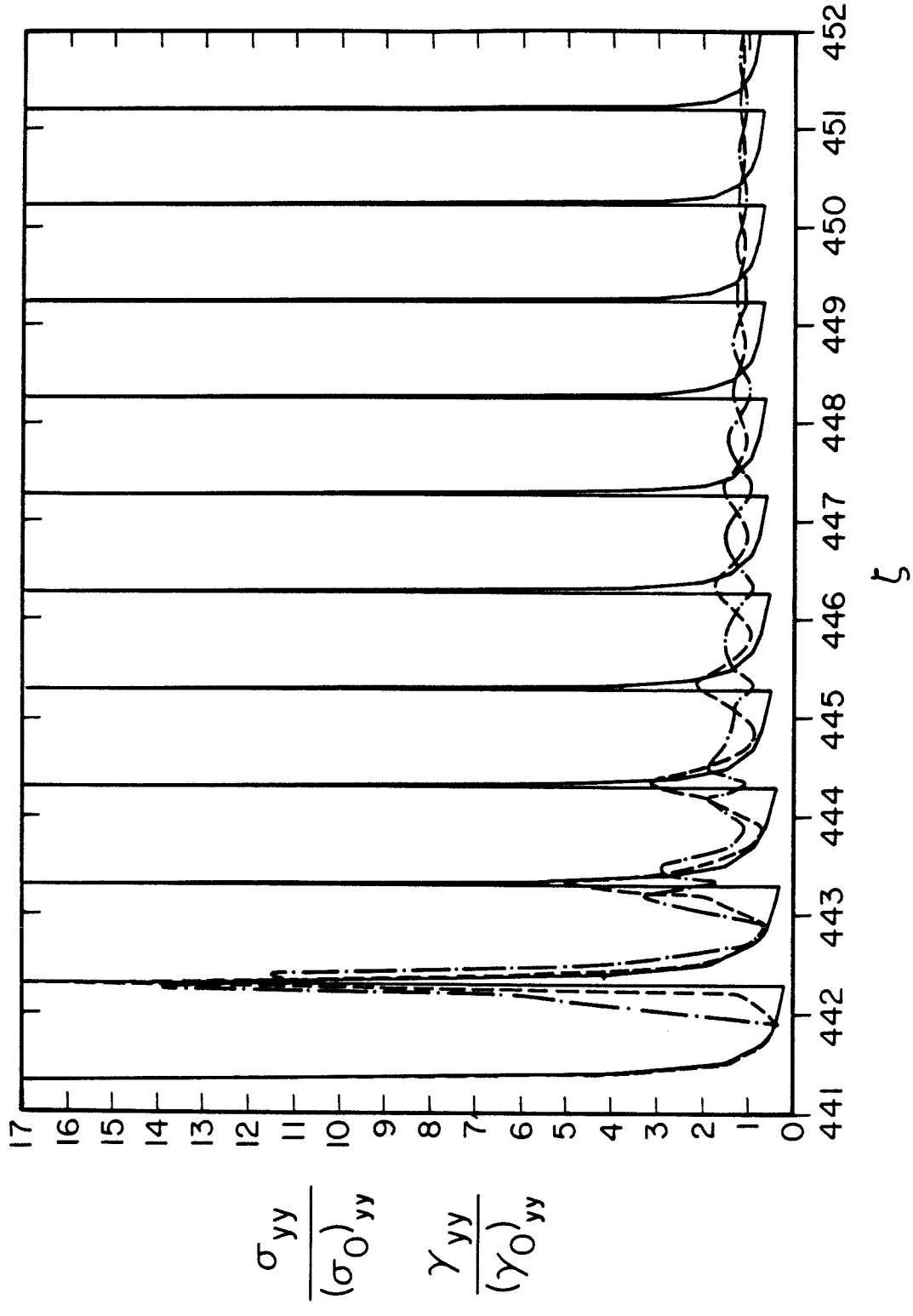
17
16
15
14
13
12
11
10
9
8
7
6
5
4
3
2
1
0
441
442
443
444
445
446
447
448
449
450
451
452
ζ
$\frac{\sigma_{yy}}{(\sigma_0)_{yy}}$
$\frac{\gamma_{yy}}{(\gamma_0)_{yy}}$

Figure 17

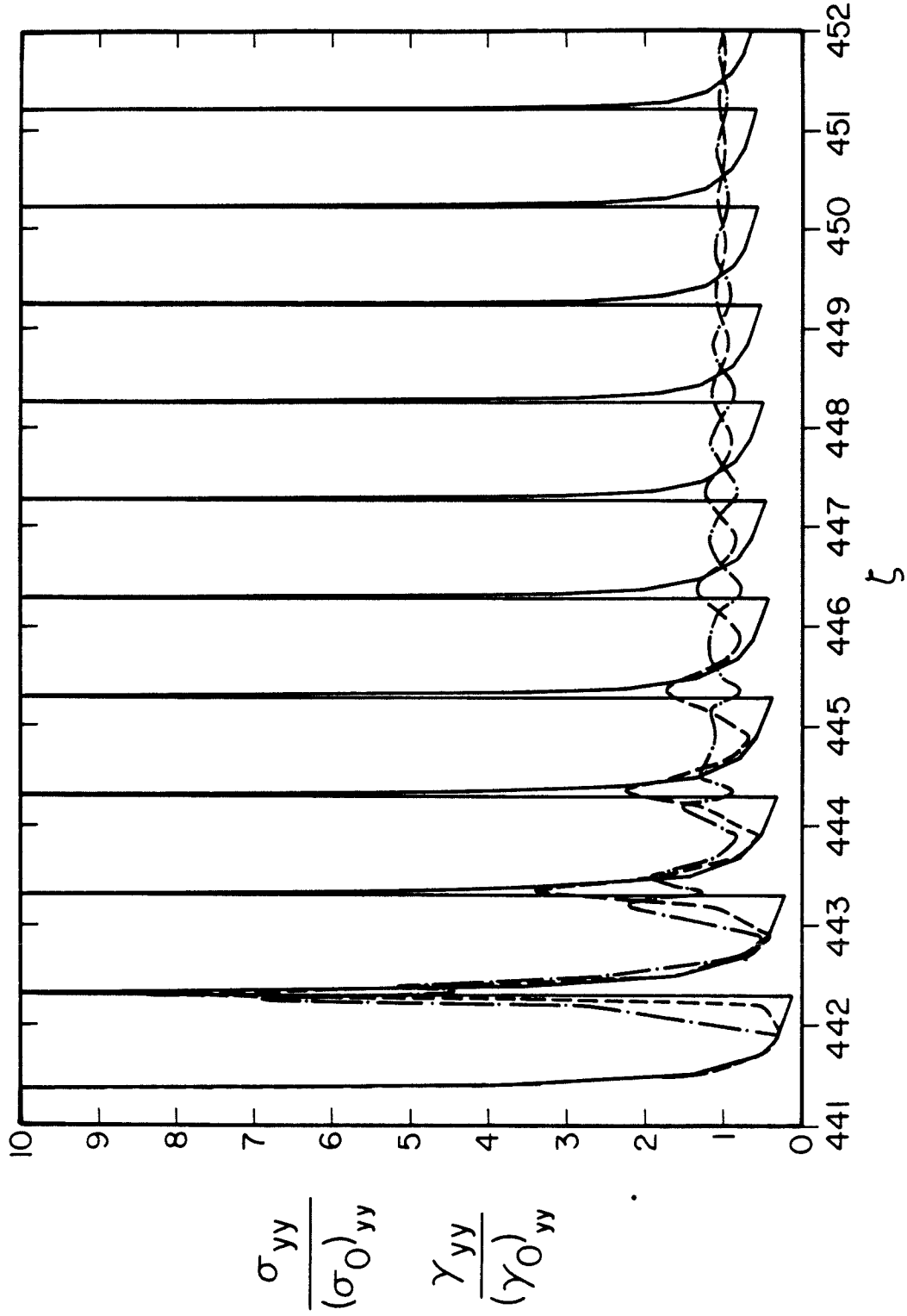
441
442
443
444
445
446
447
448
449
450
451
452
ζ
0
1
2
3
4
5
6
7
8
9
10
$\frac{\gamma_{yy}}{(\gamma_0)_{yy}}$
$\frac{\sigma_{yy}}{(\sigma_0)_{yy}}$

Figure 18

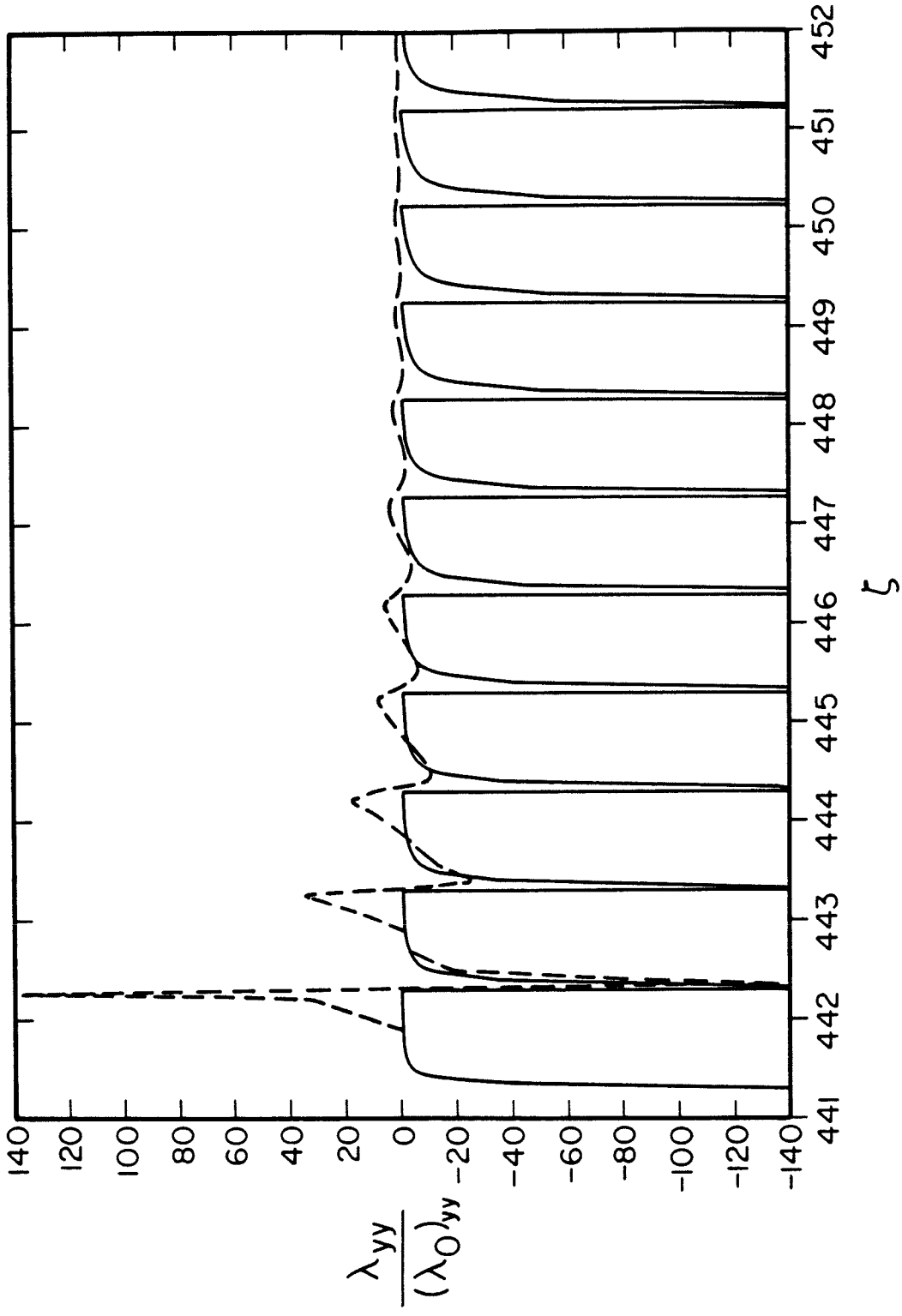
140
120
100
80
60
40
20
0
-20
-40
-60
-80
-100
-120
-140
441
442
443
444
445
446
447
448
449
450
451
452
ζ
$\frac{\lambda_{yy}}{(\lambda_0)_{yy}}$

Figure 19

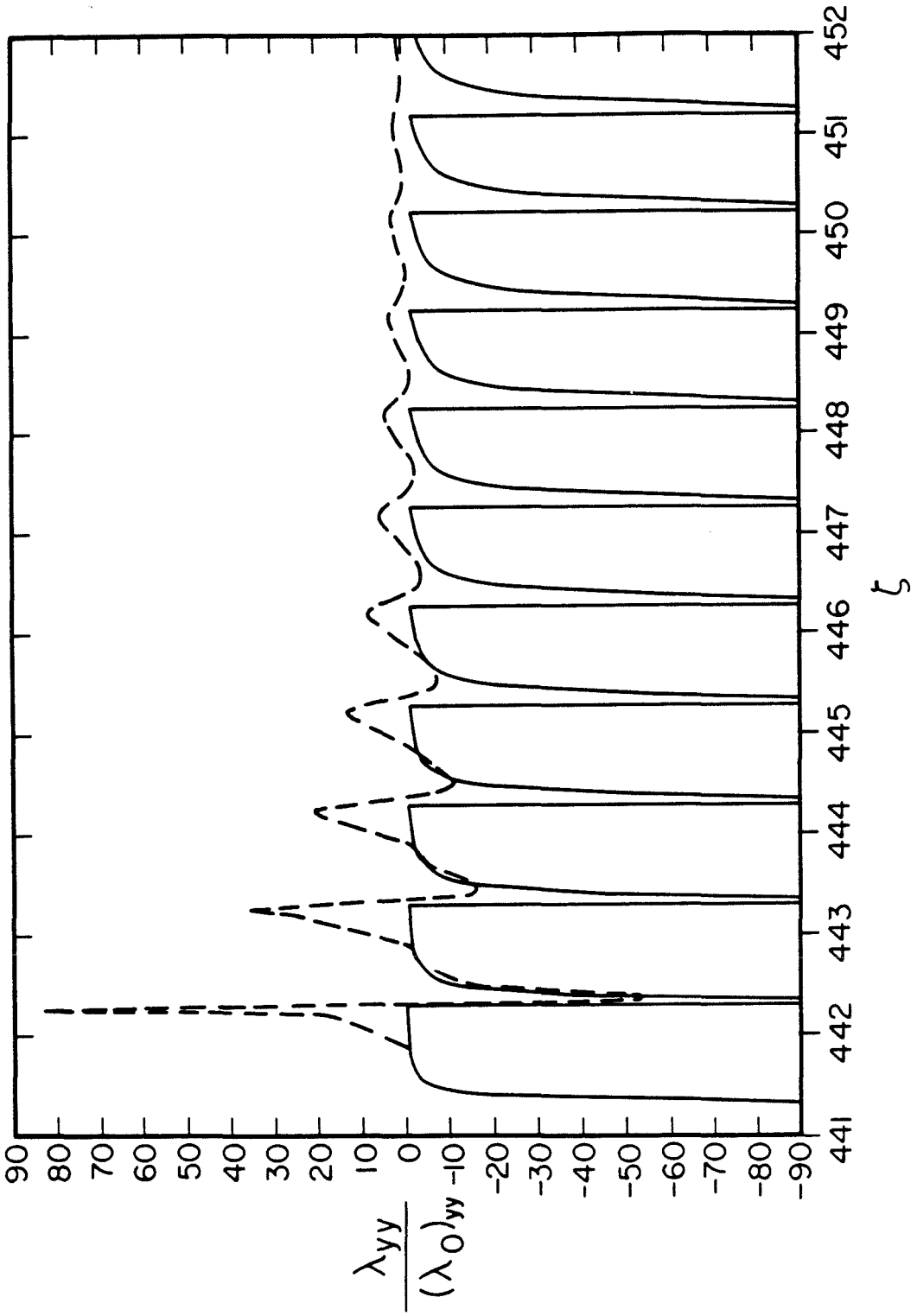
90
80
70
60
50
40
30
20
10
0
-10
-20
-30
-40
-50
-60
-70
-80
-90
$\frac{\lambda_{yy}}{(\lambda_0)_{yy}}$
441
442
443
444
445
446
447
448
449
450
451
452
ζ

Figure 20

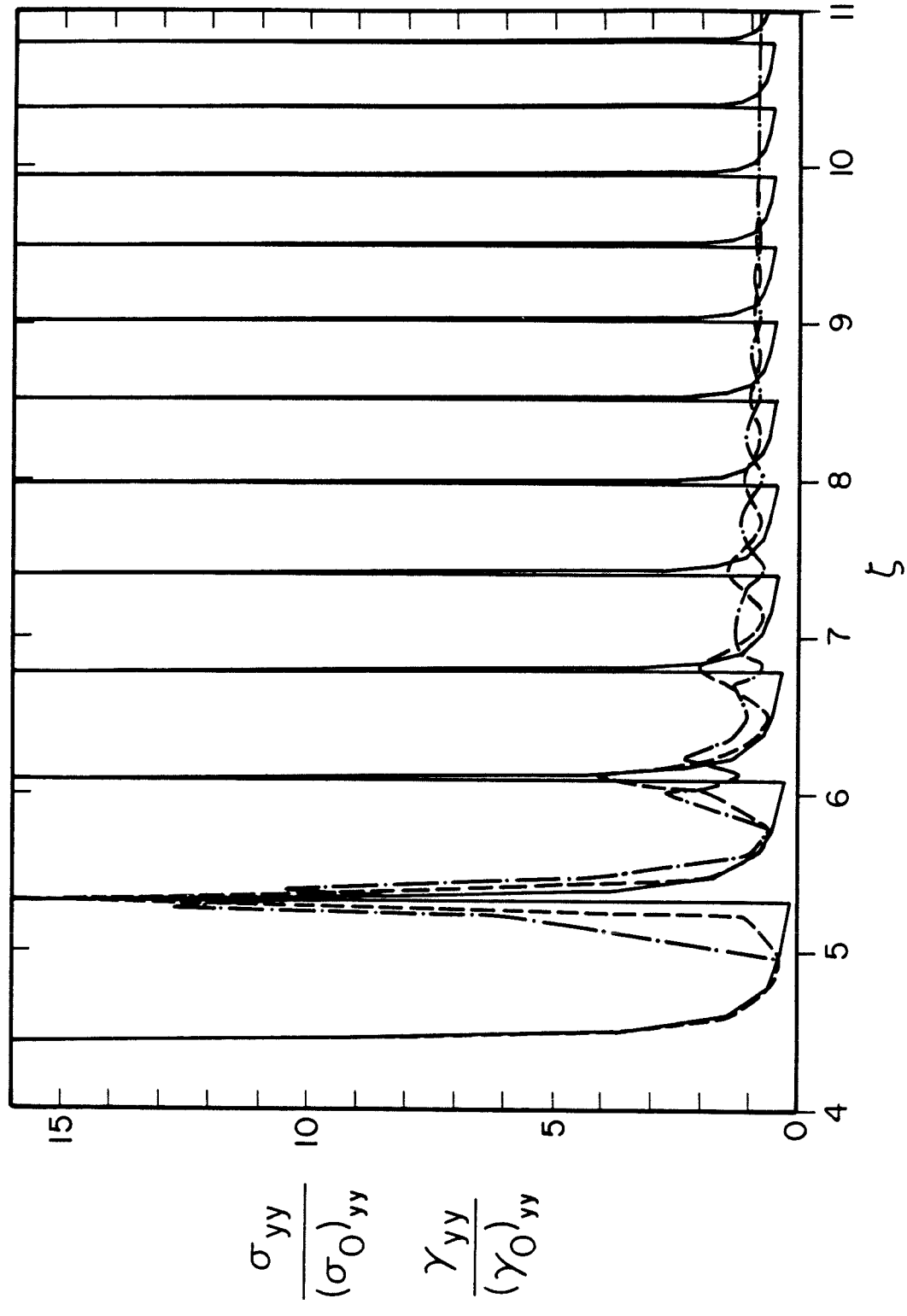
15
10
5
0
4
5
6
7
8
9
10
11
ζ
$\frac{\sigma_{yy}}{(\sigma_0)_{yy}}$
$\frac{\gamma_{yy}}{(\gamma_0)_{yy}}$

Figure 21

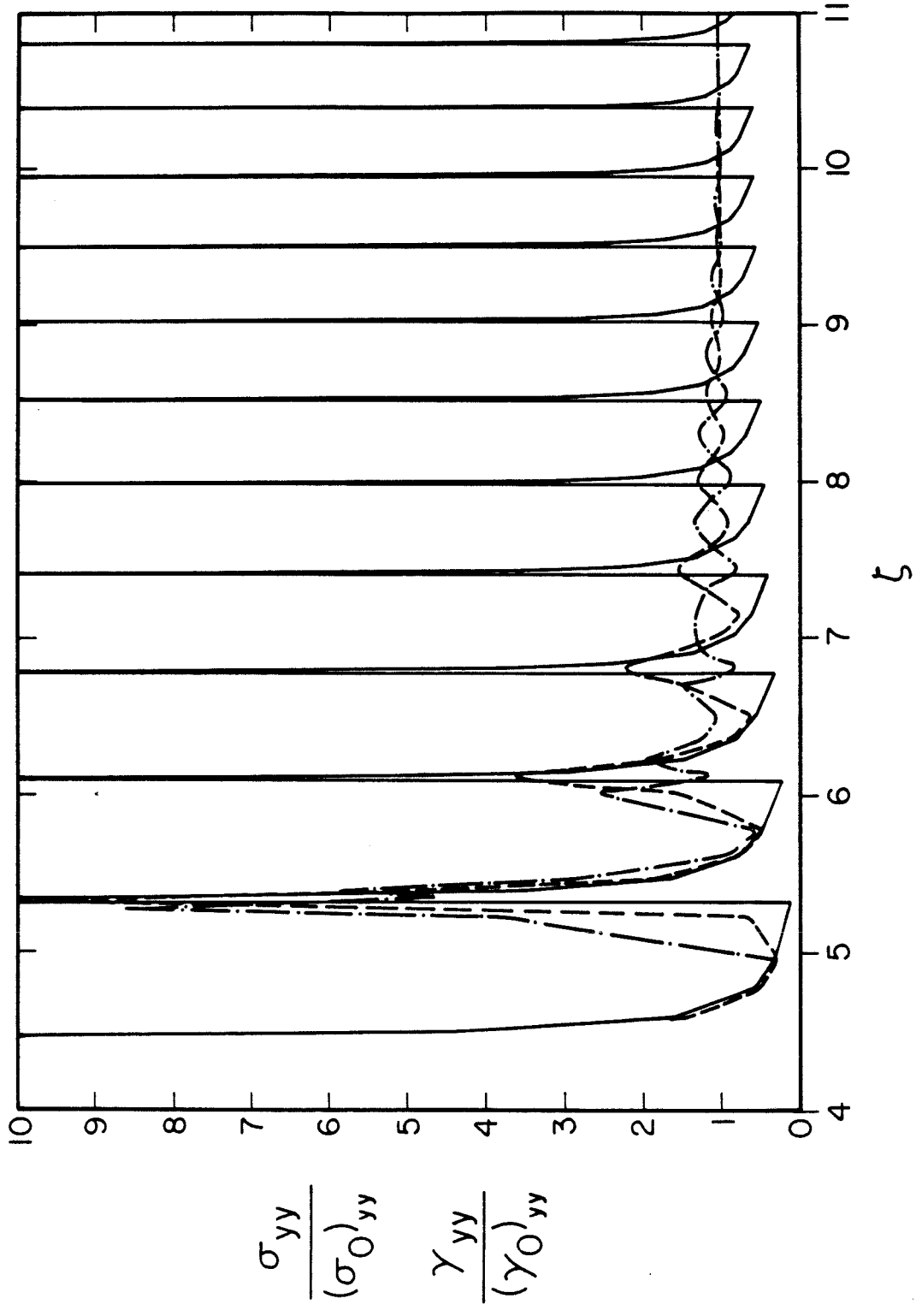
10
9
8
7
6
5
4
3
2
1
0
$\frac{\sigma_{yy}}{(\sigma_0)_{yy}}$
$\frac{\gamma_{yy}}{(\gamma_0)_{yy}}$
4
5
6
7
8
9
10
11
ζ

Figure 22

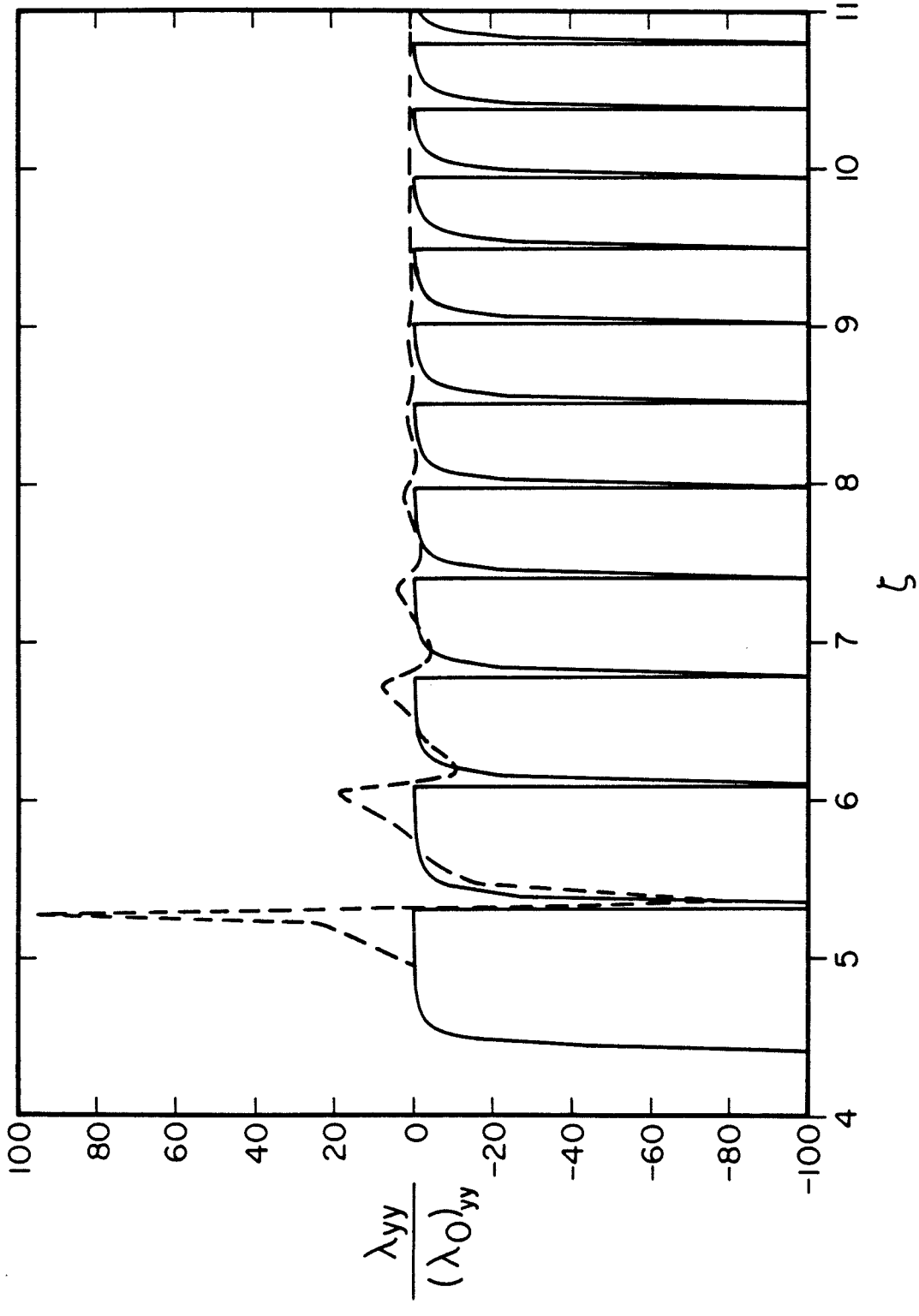
100
80
60
40
20
0
-20
-40
-60
-80
-100
$\frac{\lambda_{yy}}{(\lambda_0)_{yy}}$
4
5
6
7
8
9
10
11
ζ

Figure 23

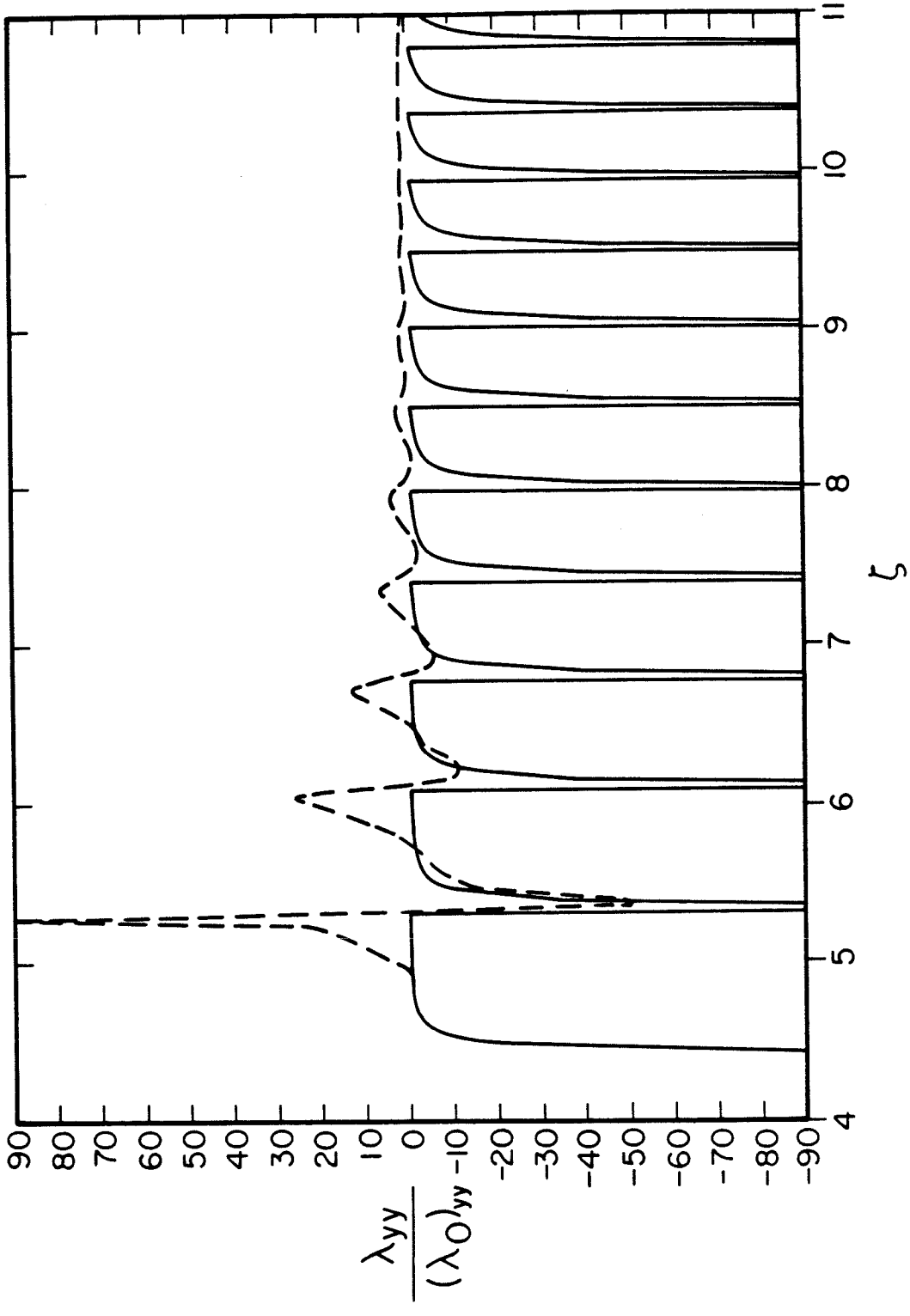
90
80
70
60
50
40
30
20
10
0
-10
-20
-30
-40
-50
-60
-70
-80
-90
$\frac{\lambda_{yy}}{(\lambda_O)_{yy}}$
4
5
6
7
8
9
10
11
ζ

Figure 24

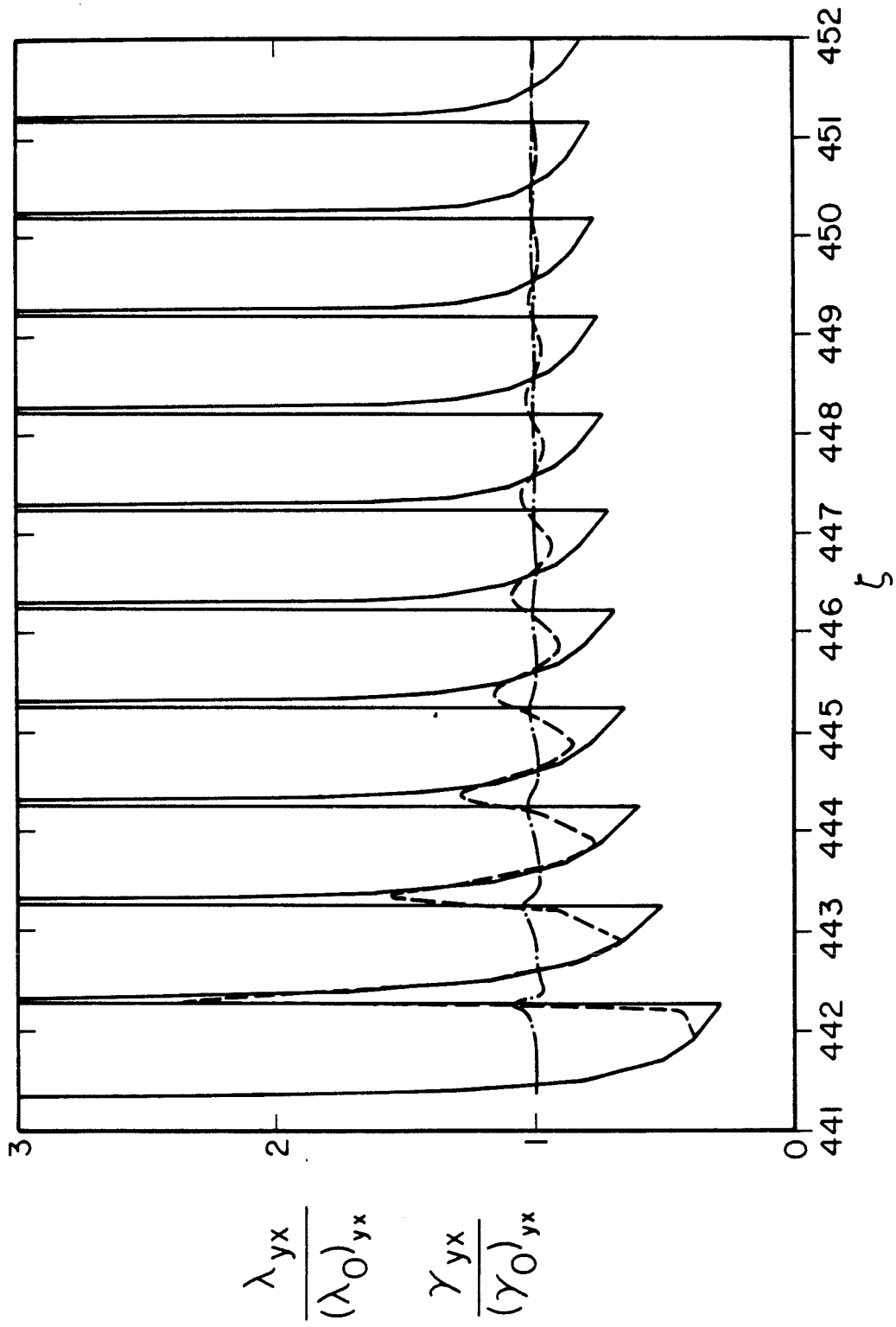
3
2
1
0
441
442
443
444
445
446
447
448
449
450
451
452
ζ
$\frac{\lambda_{yx}}{(\lambda_0)_{yx}}$
$\frac{\gamma_{yx}}{(\gamma_0)_{yx}}$

Figure 25

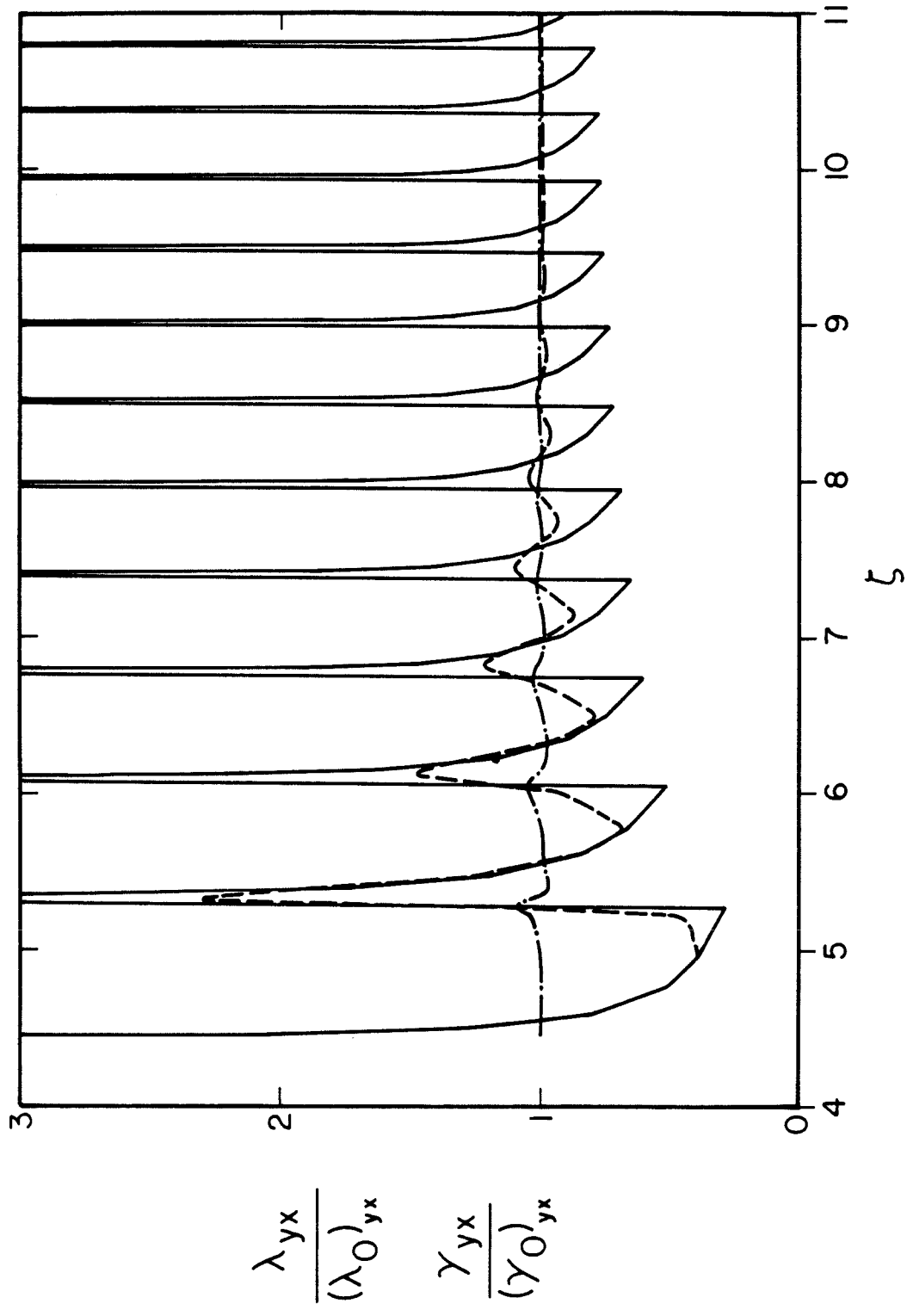

Figure 26

CHAPTER 5

Analytical Models of Neutron Star Envelopes

Lars Hernquist and James Applegate

To be published in

The Astrophysical Journal,

1984 Dec 1.

Analytical Models of Neutron Star Envelopes

Lars Hernquist and James H. Applegate

Theoretical Astrophysics, California Institute of Technology

ABSTRACT

The thermal structure of neutron star envelopes is investigated using approximate analytical formulae. In the degenerate layers the thermal structure equation is solved exactly for electron-dominated heat transport. In the non-degenerate layers it is shown that if the opacity is a power law function of density and temperature, then the $T(\rho)$ profiles lie along curves of constant thermal conductivity. The two solutions are matched at intermediate densities to give an approximate relation between the heat flux and the core temperature of the neutron star. The dependence on various uncertain factors is found explicitly, allowing a detailed understanding of the physical processes that control the heat flux. The possible significance of the results to cooling calculations that take into account strong magnetic fields is discussed.

I. Introduction

The prospect of detecting thermal x-rays from the surfaces of young neutron stars has motivated considerable interest in theoretical studies of neutron star cooling. The link between observation and theory can provide insight into the internal structure of the core, physical processes in the crust, and global properties of the magnetic field. To date, the majority of cooling calculations (e.g., Tsuruta 1974, 1975, 1979; Maxwell 1979; Glen and Sutherland 1980; Nomoto and Tsuruta 1981; Van Riper and Lamb 1981; Richardson *et al.* 1982) have concentrated primarily on the sensitivity of the overall results to effects at high densities ($\rho \gtrsim 10^{11}$ gm cm^{-3}). This is not surprising in view of the large uncertainties in the physics of the core region. A consensus on the importance to neutron star cooling of superfluidity, pion condensation, and the possible appearance of free quarks has not yet been reached. In contrast, the relevant physical processes in the crust are well-established, although numerical calculations (primarily of the opacity) do not agree in detail. Thus, it is of interest to investigate the dependence of neutron star thermal structure on effects at low ($\rho \lesssim 10^{11}$ gm cm^{-3}) densities.

As has been emphasized in the recent work by Gudmundsson and coauthors (Gudmundsson 1981; Gudmundsson, Pethick, and Epstein 1982, 1983; Epstein, Gudmundsson, and Pethick 1983) the thermal structures of the crust and core evolve essentially independently during the epoch of neutrino cooling. This is expected to be true of neutron stars associated with galactic supernova remnants (ages $\lesssim 10^4$ years). In this approximation the core is assumed to be isothermal and to contain all of the star's mass and thermal energy. The temperature of the core is regulated by the loss of neutrinos which do not interact with the crust. The surrounding crust acts as a thin insulating envelope with no sources or sinks of energy and contains all of the temperature gradient. Thus,

for a given core temperature, the heat flux through the crust is constant and the effective surface temperature is determined entirely by processes within the crust. This method was used by Gudmundsson in numerical calculations to obtain accurate temperature-density profiles and to examine the sensitivity of the $F-T_c$ relation to uncertainties in the physics of the crust. It was found that this relation depends strongly on variations in the opacity only in a narrow strip in the $T-\rho$ plane (Fig. 1), which throttles the heat flux through the crust.

In this paper approximate analytical expressions are derived which relate the flux to the core temperature. The dependence on various uncertain factors is found explicitly, allowing a more detailed understanding of the sensitivity strip found numerically by Gudmundsson. General arguments of this type, though not intended to supplant more accurate numerical computations, which they corroborate, provide constraints on future results if refinements are made to existing opacity calculations.

More significantly, a physical understanding of the importance of the various processes in the crust to the $F-T_c$ relation is extremely useful if the influence of a strong magnetic field is taken into account. In §5 we argue that the insensitivity of this relation to the photon thermal conductivity results from the extreme sensitivity of the photon thermal conductivity to temperature and density ($\propto T^{6.5}\rho^{-2}$) for a Kramers opacity, as compared to the relative insensitivity of the electron thermal conductivity in the liquid metal phase to temperature and density ($\propto T\rho$ for non-relativistic electrons and $\propto T\rho^{1/3}$ for highly relativistic electrons). Furthermore, we argue that the photon processes of greatest importance are those of relevance near the point at which the photon and electron thermal conductivities are equal; this means that free-free is more important than bound-free or bound-bound opacity. Therefore, since the free-free conductivity in a strong magnetic field behaves roughly as $T^{4.5}\rho^{-2}$ (Silant'ev

and Yakovlev 1980) we expect that the $F-T_c$ relation for strongly magnetized neutron stars will be insensitive to the photon thermal conductivity. Accurate expressions for bound-bound and bound-free absorption (which, for non-zero field, do not exist and will be difficult to obtain) are not required. On the other hand, reliable calculations of free-free absorption (Silant'ev and Yakovlev 1980) and electron thermal conductivity (Hernquist 1984a) are available; hence meaningful cooling calculations with magnetic fields should be possible.

A similar analysis was performed by Urpin and Yakovlev (1980c) for the degenerate layers of neutron star crusts. However, the influence of the photons was not taken into account self-consistently and a sensitivity analysis was not performed. As a result the subsequent cooling calculation (Yakovlev and Urpin 1981) improperly accounted for the effect of the magnetic field on the conductivities (see Hernquist 1984b and Applegate, Blandford, and Hernquist 1984 for a discussion).

In the following section the thermal structure of the degenerate layers is found for the region in which heat transport is dominated by electron conduction. In §3 general relations are derived for the temperature distribution in the non-degenerate layers for a restricted form of the radiative opacity. The two solutions are matched and a sensitivity analysis is presented in §4. A physical interpretation of the results is discussed in §5, along with implications for future calculations.

II. Degenerate Regime

Because the neutron star crust is assumed to be thin and to contain negligible mass and no sources or sinks of energy, the general relativistic equations of stellar structure simplify enormously and can be conveniently summarized as (Gudmundsson, Pethick, and Epstein 1983)

$$\frac{dT}{dP} = \frac{3}{16\sigma}\frac{\tilde{\kappa}}{T^3}\frac{F}{g_s} \tag{2.1}$$

where F is the heat flux, g_s is the surface gravity, and the opacity, $\tilde{\kappa}$, is related to the thermal conductivity, κ, by

$$\tilde{\kappa} = \frac{16\sigma}{3}\frac{T^3}{\rho\kappa} \tag{2.2}$$

The relation of T to the general relativistic depth coordinate, z, is given by (Gudmundsson, Pethick, and Epstein 1983)

$$\frac{dT}{dz} = \frac{3}{16\sigma}\frac{\tilde{\kappa}\rho}{T^3}F \tag{2.3}$$

In the following discussion it is convenient to use the electron chemical potential, μ, as an independent variable. (Throughout μ will include the electron rest mass, mc^2 .) If the pressure is assumed to be given entirely by the electronic contribution and the thermodynamic identities $n_e = (\partial P_e/\partial\mu)_T$, $S_e = (\partial P_e/\partial T)_\mu$ are used, the thermal structure equations become

$$\frac{dT}{d\mu} = \frac{F}{g_s}\frac{Z}{Am_p}\frac{1}{\kappa}\frac{1}{1-(FS_e/g_s\rho\kappa)} \tag{2.4}$$

$$\frac{d\mu}{dz} = \frac{Am_p}{Z}g_s\left[1-\frac{F}{g_s}\frac{S_e}{\rho\kappa}\right] \tag{2.5}$$

where Z is the number of conduction electrons per ion, A is the ion mass, and S_e is the entropy per unit volume of the electrons. In the degenerate layers the thermal corrections are negligible and (2.4), (2.5) become

$$\frac{dT}{d\mu} = \frac{F}{g_s}\frac{Z}{Am_p}\frac{1}{\kappa} \tag{2.6}$$

$$\frac{d\mu}{dz} = \frac{Am_p}{Z}g_s \tag{2.7}$$

(Throughout the remainder of this paper it will be assumed that relations accurate to ~ 10–20% are desired, and approximations will be made accordingly.)

For a degenerate gas μ is related to the electron number density by

$$n_e = \frac{1}{3\pi^2\hbar^3 c^3}\left(\mu^2 - m^2c^4\right)^{3/2} \tag{2.8}$$

For the case of fully ionized iron

$$\frac{\mu}{mc^2} = \left(1 + .61\rho_6^{2/3}\right)^{1/2} \tag{2.9}$$

where ρ_6 is the density in units of 10^6 gm cm^{-3}. The curve $kT = \mu - mc^2$, which gives, roughly, the transition between the degenerate and non-degenerate regimes is shown in Fig. 1.

If A and Z are treated as constants, (2.7) can be integrated immediately. The constant of integration can be evaluated by noting that in the limit $z \to 0$, μ must tend to mc^2 in the degenerate approximation. Thus

$$\frac{\mu}{mc^2} = 1 + \frac{m_p}{mc^2}\frac{A}{Z} g_s\, z \tag{2.10}$$

(See also Blandford and Hernquist 1982.) If $A = 56$, $Z = 26$

$$z = 2.27\times10^3\, g_{s_{14}}{}^{-1}\left[(1 + .61\rho_6^{2/3})^{1/2} - 1\right] \text{ cm} \tag{2.11}$$

where $g_{s_{14}}$ is the surface gravity in units of 10^{14} cm sec^{-2}.

In order to integrate the thermal structure equation, an expression for the conductivity is required. For simplicity it will be assumed that electron conduction dominates at the densities for which the degenerate form (2.6) is a good approximation. (See Fig. 1 and the relevant discussion in §4.) In the liquid phase the dominant scattering mechanism is electron-ion scattering, while

electron-phonon collisions are most important in the solid phase. Electron-electron scattering will generally be negligible unless low Z ($\lesssim 10$) ions are present (Urpin and Yakovlev 1980a). The thermal conductivity in the liquid phase has been calculated by Flowers and Itoh (1976), Yakovlev and Urpin (1980), Urpin and Yakovlev (1980b), and Itoh *et al.* (1983). The original calculations of Flowers and Itoh (1976) and Yakovlev and Urpin (1980) differed by factors ~ 3 with essentially the same density and temperature dependence (Blandford, Applegate, and Hernquist, 1983). In the recent work of Itoh *et al.* (1983) the thermal conductivity is expressed in a form identical to that of Yakovlev and Urpin (1980), with residual discrepancies ($\sim 10-30\%$ for iron) absorbed in the Coulomb logarithm. In terms of the chemical potential

$$\kappa_{e-ion} = \eta_{ei} \frac{\pi k^2 c}{12 e^4 \Lambda_{ei} Z} T \frac{(\mu^2 - m^2c^4)^{3/2}}{\mu^2} \tag{2.12}$$

where Λ_{ei} is the Coulomb logarithm and η_{ei} is a dimensionless scale factor. Henceforth, due to the uncertainty in the Coulomb logarithm, the slow density dependence of Λ_{ei} will be neglected and the constant value $\Lambda_{ei} = 1$ will be assumed.

Considerable disagreement (factors $\sim$ 3) still exists between the calculations of the conductivity due to e-phonon scattering (Flowers and Itoh 1976; Yakovlev and Urpin 1980). (For a critique see Blandford, Applegate, and Hernquist 1983). As the Flowers and Itoh results are not given in an analytic form, the Yakovlev and Urpin (1980) expression will be used. In terms of μ

$$\kappa_{e-phonon} = \eta_{ep} \frac{k}{9e^2\hbar} \frac{1}{u_{-2}} \frac{(\mu^2 - m^2c^4)^2}{\mu^2 + m^2c^4} \tag{2.13}$$

where η_{ep} is a dimensionless scale factor and $u_{-2} = \langle \omega^{-2}(k)/\omega_p{}^{-2} \rangle$. In the definition of u_{-2} the brackets denote an average over the phonon spectrum of

the solid and ω_p is the ion plasma frequency. Henceforth the value $u_{-2} = 13$ (Pollock and Hansen 1973) used by Yakovlev and Urpin (1980) will be assumed.

The melting curve is given by

$$T_m = \frac{Z^2 e^2}{a} \frac{1}{k\Gamma_m}; \quad a = (3/4\pi n_{i,m})^{1/3} \tag{2.14}$$

where T_m is the melting temperature and $n_{i,m}$ is the ion number density at the melt surface. Estimates for the melting parameter, Γ_m , range from $\sim 150-170$ (Pollock and Hansen 1973; Slattery, Doolen, and DeWitt 1980). Unless otherwise stated, the value $\Gamma_m = 160$ will be used in numerical examples throughout. The boundary between the liquid and solid phases is shown in Fig. 1 for $\Gamma_m = 160$. In terms of μ

$$T_m = \left[\frac{4}{9\pi}\right]^{1/3} \frac{Z^{5/3}}{k\Gamma_m} \frac{e^2}{\hbar c} (\mu_m{}^2 - m^2c^4)^{1/2} \tag{2.15}$$

where μ_m is the chemical potential at the melt.

The thermal structure equation thus is

$$\text{Liquid:} \quad \frac{dT}{d\mu} = \frac{12e^4}{\pi k^2 c m_p} \frac{1}{\eta_{ei}} \frac{Z^2}{A} \frac{F}{g_s} \frac{1}{T} \frac{\mu^2}{(\mu^2 - m^2c^4)^{3/2}} \tag{2.16}$$

$$\text{Solid:} \quad \frac{dT}{d\mu} = \frac{9\hbar e^2}{k m_p} \frac{Z}{A} \frac{F}{g_s} \frac{13}{\eta_{ep}} \frac{\mu^2 + m^2c^4}{(\mu^2 - m^2c^4)^2} \tag{2.17}$$

These can be integrated analytically if the slow density variations of A and Z are neglected. Integrating (2.16) from an initial point (T_i,μ_i) to an arbitrary point in the liquid (T,μ) gives

$$T^2 = T_i^2 + \frac{24e^4}{\pi k^2 c m_p \eta_{ei}} \frac{Z^2}{A} \frac{F}{g_s} \left[- \frac{\mu / mc^2}{\left((\mu / mc^2)^2 - 1\right)^{1/2}} + \ln\left(\frac{\mu}{mc^2} + \left((\mu / mc^2)^2 - 1\right)^{1/2} \right) \right.$$

$$\left. + \frac{\mu_i / mc^2}{\left((\mu_i / mc^2)^2 - 1\right)^{1/2}} - \ln\left(\mu_i / mc^2 + \left((\mu_i / mc^2)^2 - 1\right)^{1/2} \right) \right] \qquad (2.18)$$

A similar result was derived by Urpin and Yakovlev (1980c) for the density-dependent form of Λ_{ei} in Yakovlev and Urpin (1980). Integrating (2.17) from the melt surface (T_m, μ_m) to an arbitrary point in the solid (T, μ)

$$T = T_m + \frac{9\hbar e^2}{k m_p} \frac{Z}{A} \frac{F}{g_s} \frac{13}{\eta_{ep}} \left[- \frac{\mu}{\mu^2 - m^2c^4} + \frac{\mu_m}{\mu_m^2 - m^2c^4} \right] \qquad (2.19)$$

This agrees with the result of Urpin and Yakovlev (1980c). The relation of flux to core temperature is found by evaluating (2.19) at the core boundary (T_c, μ_c). Using (2.15)

$$T_c = \left[\frac{4}{9\pi} \right]^{1/3} \frac{Z^{5/3}}{k \Gamma_m} \frac{e^2}{\hbar c} (\mu_m^2 - m^2c^4)^{1/2}$$

$$+ \frac{9\hbar e^2}{k m_p} \frac{Z}{A} \frac{F}{g_s} \frac{13}{\eta_{ep}} \left[- \frac{\mu_c}{\mu_c^2 - m^2c^4} + \frac{\mu_m}{\mu_m^2 - m^2c^4} \right] \qquad (2.20)$$

The factor μ_m is found from the intersection of (2.15) and (2.18)

$$\left[\frac{4}{9\pi} \right]^{2/3} \frac{Z^{10/3}}{k^2 \Gamma_m^2} \frac{e^4}{\hbar^2 c^2} (\mu_m^2 - m^2c^4) = T_i^2 + \frac{24e^4 Z^2}{\pi k^2 c m_p A} \frac{1}{\eta_{ei}} \frac{F}{g_s} \left[- \frac{\mu_m / mc^2}{\left((\mu_m / mc^2)^2 - 1\right)^{1/2}} \right.$$

$$+ \ln\left(\mu_m / mc^2 + \left((\mu_m / mc^2)^2 - 1\right)^{1/2} \right) + \frac{\mu_i / mc^2}{\left((\mu_i / mc^2)^2 - 1\right)^{1/2}}$$

$$\left. - \ln\left(\mu_i / mc^2 + \left((\mu_i / mc^2)^2 - 1\right)^{1/2} \right) \right] \qquad (2.21)$$

This is a non-linear equation which can be solved numerically to find μ_m for

given T_i, μ_i, and F/g_s .

In the derivation of (2.20) and (2.21) Z and A have been treated as constants. For the equilibrium nuclei present in the crust (Baym, Pethick, and Sutherland 1971) this is not strictly true. However, although the analysis could be extended to allow for variations in Z and A, it will be demonstrated in §4 that these relations are dominated by effects in the liquid phase. At these densities it is possible to treat Z and A as constants with negligible error in the flux- T_c relation.

An explicit relation between F and T_c can now be found from (2.20), (2.21) if several approximations are made. As the star is isothermal at densities $\rho > 10^{10}$ gm cm^{-3} for all but the highest surface temperatures of interest it is possible to choose the core boundary such that $\mu_c \gg \mu_m$ and neglect the term involving μ_c in (2.20). Next, of the two terms involving μ_i in (2.21), the logarithmic term can generally be neglected because the electrons are non-relativistic at the transition between photon-dominated and electron-dominated heat transport. For example, if $\rho_i = 4\times10^4$ gm cm^{-3} (which is appropriate for $T_s = 10^6 K$ --see §4) then from (2.9) $\mu_i/mc^2 \approx 1.035$ and the two terms are in the ratio 15:1 .

The relations can be further simplified by considering two separate regimes. First, assume $\mu_m{}^2 \gg m^2c^4$. For $T_s = 10^6 K$, the density at the melt will turn out to be $\rho_m \approx 9\times10^7$ gm cm^{-3} implying $\mu_m{}^2/m^2c^4 \approx 13$. The term involving μ_m on the left hand side of (2.21) will be a factor ≈ 5 larger than the μ_m- dependent terms on the right hand side of (2.21), for $T_s = 10^6 K$. Neglecting the smaller terms, (2.21) can be solved for μ_m

$$\mu_m = 6\left(\frac{3}{2\pi}\right)^{1/6} \frac{\hbar c^{1/2}\Gamma_m}{Z^{2/3}A^{1/2}m_p^{1/2}\eta_{ei}{}^{1/2}} \left(\frac{F}{g_s}\right)^{1/2} \frac{(\mu_i/mc^2)^{1/2}}{((\mu_i/mc^2)^2-1)^{1/4}} M^{1/2}(\mu_i, T_i, F/g_s) \quad (2.22)$$

where

$$M(\mu_i, T_i, F/g_s) = 1 + \frac{\pi k^2 c m_p}{24 e^4} \frac{A}{Z^2} \eta_{ei} \frac{T_i^2}{F/g_s} \frac{((\mu_i/mc^2)^2 - 1)^{1/2}}{\mu_i/mc^2} \quad (2.23)$$

The core temperature is then

$$T_c = \left[\frac{24}{\pi}\right]^{1/2} \frac{e^2}{k(m_p c)^{1/2}} \frac{Z}{A^{1/2}} \frac{1}{\eta_{ei}^{1/2}} \left[\frac{F}{g_s}\right]^{1/2} \frac{(\mu_i/mc^2)^{1/2}}{((\mu_i/mc^2)^2 - 1)^{1/4}} \left[M^{1/2}(\mu_i, T_i, F/g_s) \right.$$

$$\left. + 9\left[\frac{4}{9\pi}\right]^{1/3} \frac{\pi}{24} Z^{2/3} \frac{13\eta_{ei}}{\eta_{ep}\Gamma_m} \frac{((\mu_i/mc^2)^2 - 1)^{1/2}}{\mu_i/mc^2} M^{-1/2}(\mu_i, T_i, F/g_s) \right] \quad (2.24)$$

The second term in (2.24) is generally small compared with the first one. For example, if $\mu_i/mc^2 = 1.035$ and $T_i = 5.5\times10^6 K$ (appropriate for $T_s = 10^6 K$ --see §4) then the two terms are in the ratio 9:1 . The second term has been retained in order to show the dependence on the melting parameter, Γ_m , and the electron conductivity in the solid, which scales as η_{ep}.

The other limiting case for which (2.20), (2.21) can be solved explicitly is $\mu_m \approx mc^2$. Write

$$\mu_m = \tilde{\mu}_m + mc^2 \quad (2.25)$$

with $\tilde{\mu}_m \ll mc^2$. Relations (2.20), (2.21) become, to lowest order

$$T_c = \left[\frac{4}{9\pi}\right]^{1/3} \frac{Z^{5/3}}{k\Gamma_m} \frac{e^2}{\hbar c} (2mc^2)^{1/2} \tilde{\mu}_m^{1/2} + \frac{4.5\hbar e^2}{k m_p} \frac{Z}{A} \frac{F}{g_s} \frac{13}{\eta_{ep}} \frac{1}{\tilde{\mu}_m} \quad (2.26)$$

$$\left[\frac{4}{9\pi}\right]^{2/3} \frac{Z^{10/3}}{k^2\Gamma_m^2} \frac{2me^4}{\hbar^2} \tilde{\mu}_m = T_i^2 + \frac{24e^4}{\pi k^2 c m_p} \frac{1}{\eta_{ei}} \frac{Z^2}{A} \frac{F}{g_s} \left[-\left[\frac{mc^2}{2\tilde{\mu}_m}\right]^{1/2} \right.$$

$$\left. + \ln(1 + (2\tilde{\mu}_m/mc^2)^{1/2}) + \frac{\mu_i/mc^2}{((\mu_i/mc^2)^2 - 1)^{1/2}} \right] \quad (2.27)$$

For a surface temperature $T_s = 10^{5.5}$, the melting density will turn out to be, roughly, $\rho_m = 2\times10^5$ gm cm^{-3}, corresponding to a chemical potential $\tilde{\mu}_m / mc^2 \approx .1$. The term linear in $\tilde{\mu}_m$ in (2.27) will exceed the non-linear terms by a factor ~ 4 . Thus the non-linear terms can be neglected and

$$\tilde{\mu}_m = \left(\frac{9\pi}{4}\right)^{2/3} \frac{12}{\pi} \frac{\hbar^2}{mcm_p} \frac{\Gamma_m{}^2}{AZ^{4/3}\eta_{ei}} \frac{F}{g_s} \frac{\mu_i / mc^2}{((\mu_i / mc^2)^2 - 1)^{1/2}} M(\mu_i, T_i, F/g_s) \quad (2.28)$$

where $M(\mu_i, T_i, F/g_s)$ is defined by (2.23). From (2.26) and (2.28)

$$T_c = \left(\frac{24}{\pi}\right)^{1/2} \frac{e^2}{k(m_p c)^{1/2}} \frac{Z}{A^{1/2}} \frac{1}{\eta_{ei}{}^{1/2}} \left(\frac{F}{g_s}\right)^{1/2} \frac{(\mu_i / mc^2)^{1/2}}{((\mu_i / mc^2)^2 - 1)^{1/4}} \Big[M^{1/2}(\mu_i, T_i, F/g_s)$$

$$+ \frac{\pi}{24}\left(\frac{3}{2\pi}\right)^{1/6} \frac{m m_p{}^{1/2} c^{3/2} A^{1/2} Z^{4/3}}{\hbar \Gamma_m{}^2 (F/g_s)^{1/2}} \frac{13\eta_{ei}}{\eta_{ep}} \frac{((\mu_i / mc^2)^2 - 1)^{3/4}}{(\mu_i / mc^2)^{3/2}} M^{-1}(\mu_i, T_i, F/g_s) \Big] \quad (2.29)$$

Again the second term in (2.29) is generally small compared with the first one. For example, if $\mu_i / mc^2 = 1.005$ and $T_i = 1.1\times10^6\, K$ (appropriate for $T_s = 10^{5.5}\, K$ --see §4) then the two terms are in the ratio 12:1 . Thus (2.29) is essentially the same solution as for the $\mu_m{}^2 \gg m^2c^4$ limit (2.24) with slightly different dependences on the factors in the solid phase.

For a given heat flux (2.20) and (2.21) determine T_c, if μ_i and T_i are known. The quantities μ_i and T_i are determined by the solution to the thermal structure equation at low densities and an approximate method for estimating them will be discussed in the following section. However, it is already possible to make general statements about the sensitivity of the results to the physical parameters in the degenerate layers which are independent of the uncertainties in the determination of μ_i and T_i . From (2.24), (2.29) it is obvious that T_c, for a given F/g_s, is much more sensitive to the conductivity in the liquid phase ($\sim\eta_{ei}$) than in the solid phase ($\sim\eta_{ep}$) . The dependence on Γ_m is also weak, of the same order as the conductivity in the solid. Finally, the results are rather

insensitive to an exact determination of μ_i, T_i and it is apparent that the photons will be less important than the electrons in determining T_c. A more precise demonstration of these assertions will be given in §4.

III. Non-Degenerate Regime

In order to estimate μ_i and T_i, and examine the sensitivity of the results to photon conduction we consider the non-degenerate layers in detail. (As is seen in Fig. 1, photons dominate the heat transport in the non-degenerate regime.) The thermal structure equation for neutron star envelopes is given by (2.1). In terms of the thermal conductivity

$$\frac{dT}{dP} = \frac{F}{g_s}\frac{1}{\rho\kappa} \tag{3.1}$$

This has been derived from the general relativistic equations of stellar structure for neutron star envelopes (Gudmundsson, Pethick, and Epstein, 1983) but is also valid for non-relativistic stellar atmospheres (from the equation of hydrostatic equilibrium with constant gravitational acceleration and the heat flux equation).

Consider a conductivity of power law form

$$\kappa = \kappa_0 \frac{T^\beta}{\rho^\alpha} \tag{3.2}$$

This is often the situation of interest as any opacity of Kramers form, $\tilde{\kappa} \propto \rho / T^{3.5}$, will translate into a conductivity (3.2), with $\beta = 6.5$ and $\alpha = 2$. For a non-degenerate gas the electron pressure is

$$P = n_e kT = \frac{Z}{Am_p}\rho kT \tag{3.3}$$

From (3.1), (3.2), and (3.3)

$$\frac{dT}{dP} = \frac{F}{g_s}\frac{1}{\kappa_0}\left(\frac{Am_p}{Zk}\right)^{\alpha-1}\frac{P^{\alpha-1}}{T^{\alpha+\beta-1}} \tag{3.4}$$

If the gradients in A and Z are neglected, (3.4) can be integrated. Furthermore, because of the rapid convergence of the radiative zero solution to the exact solution in the non-degenerate layers (Schwarzschild 1958) the constant of integration can be set to zero. It then follows that

$$\kappa = \frac{\alpha+\beta}{\alpha}\frac{F}{g_s}\frac{Zk}{Am_p} \tag{3.5}$$

Thus we arrive at the rather remarkable conclusion that the $T(\rho)$ solutions will follow paths such that the conductivity is a constant. This is generally true for a non-degenerate gas with a power law opacity as long as gradients in Z and A are small and the radiation pressure is negligible. For the case of a Kramers opacity $T \propto \rho^{2/6.5}$ and the opacity along a solution is $\tilde{\kappa} \propto \rho^{-1/13}$. Thus the opacity is also nearly a constant, being a very slowly decreasing function of the density. The relation between T and ρ is given by (3.2) and (3.5)

$$T = \left(\frac{\alpha+\beta}{\alpha}\frac{F}{g_s}\frac{Zk}{Am_p}\frac{1}{\kappa_0}\right)^{1/\beta}\rho^{\alpha/\beta} \tag{3.6}$$

The variation of T and ρ with the general relativistic depth coordinate, z, can also be obtained. As the heat flux through the crust is assumed to be constant, (3.5) and the heat flux equation

$$\frac{dT}{dz} = \frac{F}{\kappa} \tag{3.7}$$

imply that the temperature gradient is also constant along a solution. Thus, from (3.5) and (3.7), neglecting gradients in A and Z

$$T = \frac{\alpha}{\alpha+\beta}g_s\frac{Am_p}{Zk}z \tag{3.8}$$

$$\rho = \left(\frac{\kappa_0}{F/g_s}\right)^{1/\alpha} g_s^{\beta/\alpha} \left(\frac{\alpha}{\alpha+\beta}\frac{Am_p}{Zk}\right)^{(\beta+1)/\alpha} z^{\beta/\alpha} \tag{3.9}$$

where the radiative zero boundary conditions have been assumed.

For further analysis it is useful to assume that the opacity is of Kramers form; this leads to a thermal conductivity

$$\kappa = \eta_r \kappa_0 \frac{T^{6.5}}{\rho^2} \text{erg cm}^{-2}\text{s}^{-1}\text{K}^{-1} \tag{3.10}$$

We choose κ_0 to be that appropriate for free-free absorption, and allow for a dimensionless scale factor, η_r. The non-degenerate, non-relativistic form of κ_0 is approximately (Cox and Giuli 1968)

$$\kappa_0 = \frac{16\sigma}{3}\frac{196.5}{24.59} m_p \frac{A^2}{Z^3} \tag{3.11}$$

The solution (3.5) then implies

$$T = \left(\frac{4.25Zk}{\kappa_0 Am_p}\right)^{1/6.5} \left(\frac{F}{g_s}\right)^{1/6.5} \frac{1}{\eta_r^{1/6.5}} \rho^{2/6.5} \tag{3.12}$$

Numerically, for iron

$$T = 2.75\times10^5 \left(\frac{F}{g_s}\right)^{1/6.5} \frac{1}{\eta_r^{1/6.5}} \rho^{2/6.5} \tag{3.13}$$

Similarly, if $A = 56$, $Z = 26$ then (3.8) and (3.9) give

$$T = 6.14\times10^5 g_{s,14} z \tag{3.14}$$

$$\rho = 13.6 \frac{1}{(F/g_s)^{1/2}} g_{s,14}^{3.25} z^{3.25} \text{ gm cm}^{-3} \tag{3.15}$$

A comparison with the Los Alamos radiative opacities (Huebner, *et al.*, 1977; Gudmundsson, 1981) indicates that the free-free opacity is not an

accurate approximation to the total opacity throughout the non-degenerate layers. However, as the gas becomes increasingly ionized, free-free absorption will become the dominant source of opacity and (3.10) should be a good approximation to the radiative opacity as the gas starts to become degenerate. Because of the rapid convergence of the radiative zero solution to the correct solution, errors in the total conductivity at low densities should be unimportant to the $T(\rho)$ curve at densities where free-free dominates. Thus it should be possible to approximate T_i and μ_i using (3.12).

Finally, we note that the numerical calculations of $T(\rho)$ made by Gudmundsson, Pethick, and Epstein (1983) are well fit by power laws $T \propto \rho^{\gamma}$ in the non-degenerate layers. The exponent is approximately $\gamma = 0.31$, appropriate for a Kramers opacity. This is perhaps not too surprising since the important opacity mechanisms (bound-free, free-free) are individually of the Kramers form $\tilde{\kappa} \propto \rho / T^{3.5}$.

IV. Sensitivity Analysis

In order to investigate the sensitivity of the flux- core temperature relation to the uncertain factors, it is necessary to match the degenerate and non-degenerate solutions at some point. It is a reasonable approximation to do this along the curve $\kappa_{electron} = \kappa_{photon}$. This curve lies within a region in which the gas is mildly degenerate (Fig. 1). Thus some error will be introduced in using the non-degenerate solution to find μ_i and T_i . However, since T_c is relatively insensitive to the exact numerical values assumed for μ_i, T_i this procedure is justified. Probably the major source of error introduced into the $F-T_c$ relation is the underestimate of the total conductivity in the transition zone between photon-dominated and electron-dominated heat transport.

Assuming a Kramers opacity, the radiative conductivity (3.10) is numerically, for iron

$$\kappa_{rad} = .72\eta_r \frac{T_6^{8.5}}{\rho_6^2} \text{ erg cm}^{-2}\text{s}^{-1}\text{K}^{-1} \tag{4.1}$$

In terms of density the thermal conductivity due to electron-ion scattering (2.12) is, for iron

$$\kappa_{elec} = 4.19\times10^{13}\, T_6\eta_{ei} \frac{\rho_6}{1 + .61\rho_6^{2/3}} \text{ erg cm}^{-2}\text{s}^{-1}\text{K}^{-1} \tag{4.2}$$

Equating (4.1) and (4.2) (shown in Fig. 1)

$$T_6 = 3.18\left[\frac{\eta_{ei}}{\eta_r}\right]^{1/5.5} \frac{\rho_6^{3/5.5}}{(1 + .61\rho_6^{2/3})^{1/5.5}} \tag{4.3}$$

The non-degenerate solution will intersect this curve at the point given by equating (3.13) and (4.3). Identifying this with the point (ρ_i, T_i)

$$\frac{\rho_{i,6}}{(1 + .61\rho_{i,6}^{2/3})^{.765}} = 7.63\times10^{-6}\left[\frac{F}{g_s}\right]^{.647} \frac{\eta_r^{.118}}{\eta_{ei}^{.765}} \tag{4.4}$$

For the purposes of producing approximate relations for ρ_i and T_i to be used in (2.24) and (2.29) it is sufficient to take

$$\rho_{i,6} = 7.6\times10^{-6}\left[\frac{F}{g_s}\right]^{.647} \frac{\eta_r^{.118}}{\eta_{ei}^{.765}} \tag{4.5}$$

The corresponding temperature is

$$T_{i,6} = .51\left[\frac{F}{g_s}\right]^{.353} \frac{1}{\eta_{ei}^{.235}\eta_r^{.118}} \tag{4.6}$$

Thus it is seen that the extreme insensitivity of the core temperature to the photon conductivity (scale factor η_r) enters into this solution because of the

large power of T in κ_{rad} and the cancellation of the terms involving η_r in (3.13) and (4.3).

Using (4.5) and (4.6) the relations (2.24) and (2.29) become, respectively, for iron

$$T_c = 5.8\times10^5\left[\frac{F}{g_s}\right]^{.392}\frac{1}{\eta_{ei}^{.373}\eta_r^{.02}}\left[M^{1/2}(\eta_{ei},\eta_r,F/g_s)\right.$$

$$\left. + 6.7\times10^{-3}\,\frac{1}{\eta_{ep}}\left[\frac{160}{\Gamma_m}\right]\eta_r^{.04}\eta_{ei}^{.745}\left[\frac{F}{g_s}\right]^{.218}M^{-1/2}(\eta_{ei},\eta_r,F/g_s)\right] \qquad (4.7)$$

$$T_c = 5.8\times10^5\left[\frac{F}{g_s}\right]^{.392}\frac{1}{\eta_{ei}^{.373}\eta_r^{.02}}\left[M^{1/2}(\eta_{ei},\eta_r,F/g_s)\right.$$

$$\left. + .37\,\eta_{ei}^{.617}\,\frac{1}{\eta_{ep}}\left[\frac{160}{\Gamma_m}\right]^2\frac{\eta_r^{.06}}{(F/g_s)^{.176}}M^{-1}(\eta_{ei},\eta_r,F/g_s)\right] \qquad (4.8)$$

where

$$M(\eta_{ei},\eta_r,F/g_s) = 1 + .79\,\frac{\eta_{ei}^{.275}}{(F/g_s)^{.078}\eta_r^{.20}} \qquad (4.9)$$

It is now possible to investigate the sensitivity of T_c to variations in the conductivities and the melting parameter. In order to compare these results with the calculations of Gudmundsson (1981) relation (4.7) has been evaluated for $T_s = 10^{6.5}, 10^{6.375}$, and 10^6 and relation (4.8) has been evaluated for $T_s = 10^{5.5}$. In addition, the "exact" expressions (2.20), (2.21), (4.3), and (4.4) have been evaluated for the same conditions to determine the numerical accuracy of the approximate relations (4.7)-(4.9). The results are summarized in Tables 1-4 (see Appendix) for various values of Γ_m, the radiative conductivity ($\propto\eta_r$), the e-ion conductivity ($\propto\eta_{ei}$), and the e-phonon conductivity ($\propto\eta_{ep}$). The core temperatures derived from the approximate expressions (4.7)-(4.9) (T_c^a) and those

derived from the "exact" relations (2.20), (2.21), (4.3), (4.4) ($T_c^{\,e}$) are given. The ratios of the core temperatures ($T_c^{\,a}$ or $T_c^{\,e}$) in each case to the core temperatures (($T_c^{\,a}$)$_s$ or ($T_c^{\,e}$)$_s$) found with the "standard" values of the parameters ($\eta_r = 1$, $\eta_{ei} = 1$, $\eta_{ep} = 1$, and $\Gamma_m = 160$) are also shown. In (2.20) and (2.21) the core boundary has been taken to be $\rho_c = 10^{10}\,\mathrm{gm\,cm^{-3}}$ for compatibility with Gudmundsson (1981). Finally, the $T(\rho)$ profiles implied by (2.18), (2.19), and (3.6) are indicated in Fig. 1 assuming $A = 56$, $Z = 26$ and the "standard" set of parameters for $T_s = 10^{6.5}, 10^{6}$, and $10^{5.5}$. All numerical calculations have used $g_s = 10^{14}$.

A comparison can be made to the numerical calculations in Gudmundsson (1981) for $\Gamma_m = 158$ and $g_s = 10^{14}$. The relevant results are reproduced in Table 5. The core temperature has been calculated for a standard set of the parameters, a reduction of the radiative conductivity by a factor of 2, a reduction of the electron conductivity by a factor of 2, and a reduction of both conductivities by a factor of 2. These can be compared with cases 1,5,10, and 15, respectively, in Tables 1-4. Furthermore, Gudmundsson (1981) indicates that T_c varies by $\lesssim 2\%$ if $\Gamma_m = 100$ or 200 are assumed.

Several conclusions can be drawn from the results in the Appendix. First, it is apparent that the approximate relations for T_c, (2.24) and (2.29), are in good agreement with the "exact" relations, (2.20) and (2.21). Significant differences ($\lesssim 20\%$) are noted only for the largest surface temperatures ($T_s = 10^{6.5}$). This is not surprising because the terms that were neglected in (2.21) are not necessarily small for $T_s = 10^{6.5}$. In addition, the relative importance of variations in Γ_m and the e-phonon conductivity are overestimated by (2.24) for high surface temperatures. Again, this is to be expected since (2.24) assumes a core density $\gg 10^{10}\,\mathrm{gm\,cm^{-3}}$. As is seen in Fig. 1 the $T(\rho)$ solution corresponding to $T_s = 10^{6.5}$ crosses the melting curve at $\rho > 10^{10}$. However, the sensitivity of (2.24) to the

total electron conductivity (e-ion and e-phonon) is in good agreement with the "exact" solution.

The agreement between the "exact" analytical results and the numerical calculations of Gudmundsson (1981) is quite good. The core temperatures agree to $\lesssim$5% for $T_s \geq 10^6$. Only for the lowest surface temperatures ($T_s = 10^{5.5}$) does the analytical solution deviate significantly. The source of this discrepancy is not difficult to trace and will be discussed in the following section.

In general, the flux- core temperature relation is strongly sensitive to the electron conductivity in the liquid phase, much less sensitive to the electron conductivity in the solid phase and the melting parameter Γ_m, and virtually independent of the photon conductivity, in agreement with Gudmundsson (1981).

V. Conclusions

An approximate analytical method for investigating the sensitivity of the flux- core temperature relation in neutron star crusts to variations in uncertain factors has been presented. The results are in good agreement with the accurate numerical calculations of Gudmundsson (1981) and Gudmundsson, Pethick, and Epstein (1983). Although the formulae have used the specialized forms for the electron conductivities of Yakovlev and Urpin (1980), it is clear that the method could be applied to conductivities with sufficiently simple, yet arbitrary temperature and density dependences.

Because of the good agreement between the results in Table 1 and the sensitivity analysis of Gudmundsson (1981), it is now possible to understand the sensitivity zone of Gudmundsson, Pethick, and Epstein (1983) in detail. The lack of dependence on the photons will be maintained as long as the conductivity is such a strong function of temperature ($\propto T^{6.5}$) . Physically this is realized

through the rapid convergence of the radiative zero result to the correct solution. Because of the strong temperature dependence of the radiative conductivity the solution will converge to the correct $T(\rho)$ curve, even if large errors are made in κ_{rad} . Thus it is to be expected that the layers in which photon conduction dominates will always be unimportant in determining the heat flux for a given core temperature. These expectations are confirmed by the sharp low-density cutoff to the sensitivity zone of Gudmundsson, Pethick, and Epstein (1983) along the curve where electron conduction begins to dominate (Fig. 1).

In the degenerate layers the conductivity in the solid phase and the melting factor Γ_m are relatively less important than the conductivity in the liquid. From (4.7) and (4.8) it is seen that the terms involving η_{ep} and Γ_m are generally small. Physically this is because the temperature gradient in the solid phase of the crust is much smaller than in the liquid phase (except for the highest surface temperatures). Thus, it is not surprising that the high-density cutoff to the sensitivity zone of Gudmundsson, Pethick, and Epstein (1983) roughly follows the melting curve (Fig. 1). Consequently, the thermal conductivity in the liquid phase must dominate the flux- core temperature relation. The temperature gradient is still relatively large and the e-ion conductivity is a relatively weak function of temperature ($\propto T$) . Thus, if large errors are made in κ_{e-ion} the solution will not be as efficient in converging to the correct $T(\rho)$ curve as in the non-degenerate layers and the derived core temperature will be inaccurate. However, it should be noted that the insensitivity of the high T_s solutions to the e-phonon conductivity is an artifact of the choice of $\rho_{core} = 10^{10}\,\mathrm{gm\,cm^{-3}}$ (Fig. 1). If the core boundary had been at a much higher density the solution would have had roughly the same sensitivity to the e-ion and e-phonon conductivities (see Sec. 4).

As discussed earlier the present work deviates significantly (~30% higher core temperature) from the numerical calculations of Gudmundsson (1981) at low surface temperatures, $T_s = 10^{5.5}$. Our analytical model has assumed the Yakovlev and Urpin e-ion conductivity (2.12) throughout the liquid phase. However, the results of Gudmundsson (1981) have used these conductivities only for $(\mu - mc^2)/kT > 10$. At low densities ($(\mu - mc^2)/kT < 1$) the electron thermal conductivities of the Los Alamos group (Huebner, *et al.* 1977) were used. At intermediate values of $(\mu - mc^2)/kT$, Gudmundsson (1981) found κ_{e-ion} by linearly interpolating (on a log-log scale) between the Los Alamos and Yakovlev and Urpin conductivities. This difference will affect the low T_s solutions to a greater extent as the boundary between photon-dominated and electron-dominated heat transport and the degeneracy curve ($(\mu - mc^2)/kT = 1$) converge at low temperatures (Fig. 1). The Yakovlev and Urpin form (2.12) underestimates the thermal conductivity at low densities, relative to the expressions used by Gudmundsson (1981). As a result, the local temperature gradient is overestimated and the resulting core temperature is too high. For $T_s = 10^{5.5}$ the conductivity (2.12) is roughly a factor of 2 smaller than that of Gudmundsson, averaged over the sensitivity strip. From Table 4, multiplying κ_{e-ion} by 2 would give $T_{c_8} \approx .17$, roughly 8% higher than the Gudmundsson result. This is further evidence that the $F - T_c$ relation is dominated by the e-ion conductivity in the liquid phase.

As a final note in this regard, it is not objectively clear that the interpolation performed by Gudmundsson (1981) should give the most reliable results. For $\rho = 10^{3.3}$ gm cm^{-3} and $T = 10^7 K$ (equal to ρ_i and T_i, respectively, for $T_s = 10^{5.5}$) the e-ion opacity used by Gudmundsson (1981) is roughly 5.4 times smaller than the e-ion opacity of Yakovlev and Urpin (1980). (This has assumed the Yakovlev and Urpin form for Λ_{ei} .) At this density and temperature

(Gudmundsson, 1981) partial ionization can account for only a few percent of the discrepancy as the thermal conductivity in the liquid for non-relativistic electrons depends only logarithmically on Z (see Yakovlev and Urpin 1980). We believe that the Yakovlev and Urpin (1980) result is more accurate even though the degeneracy parameter ($(\mu - mc^2)/kT$) at this density and temperature is only 2.8 . The Yakovlev and Urpin (1980) e-ion opacity can be compared with the numerical calculations of Hubbard and Lampe (1969). These earlier computations, performed for arbitrary degree of degeneracy, are still thought to be reliable as long as the gas is non-relativistic and $\Gamma = Z^2e^2/kTa < 10$ (where a is defined in [2.14]). For $\rho = 10^{3.3}$gm cm^{-3} , $T = 10^7$ K, and carbon composition, corresponding to $(\mu - mc^2)/kT = 2.74$, the Yakovlev and Urpin (1980) and Hubbard and Lampe (1969) results agree to $\sim 50\%$, with Yakovlev and Urpin giving the higher value of the opacity. As the degeneracy is increased the two calculations agree more accurately until $\Gamma \sim 10$, when the Hubbard and Lampe results are no longer reliable. Thus we conclude that the Gudmundsson (1981) e-ion opacities underestimate the true e-ion opacity by a factor ~ 4 under these conditions and that the resulting core temperatures for low T_s ($\sim 10^{5.5}$ K) are probably too small (by $\sim$ 10--15%).

The detailed agreement between the analytical results and those of Gudmundsson, Pethick, and Epstein (1983) indicates that to ~10% accuracy the $F-T_c$ relation is completely insensitive to effects at low densities. Corrections to the free electron equation of state and to the radiative free-free opacity are negligible. In addition, partial ionization is unimportant. Naturally, however, the $T(\rho)$ profiles will be inaccurate at low densities (as is seen by comparing Fig. 1 to the corresponding curves in Gudmundsson, Pethick, and Epstein (1983)). At high densities the results are insensitive to the slow variation of A and Z.

The preceding discussion has useful implications for cooling calculations which take into account strong magnetic fields. The magnetized free-free photon conductivity has been calculated for a non-degenerate, non-relativistic gas by Pavlov and Yakovlev (1977) and Silant'ev and Yakovlev (1980). For large values of the parameter $b = \hbar\omega_b / 7kT \approx 2B_{12}T_7^{-1}$, where $10^{12}B_{12}$ is the field strength in Gauss, the conductivity is roughly isotropic and increases as b^2 . At small values of b the conductivity tends to its zero field value. Thus the extreme temperature dependence of the photon conductivity is preserved and it seems likely that the electron conductivity in the liquid phase will again be the dominant factor (contrary to the assumption made by Yakovlev and Urpin 1981). This is significant because the bound-bound and bound-free contributions to the photon conductivity in a strong magnetic field have not been calculated, while relatively accurate expressions for the magnetized electron conductivity (Hernquist 1984a) are available.

Finally, it should be emphasized that κ_{e-ion} is still the greatest remaining uncertainty in the thermal structure of unmagnetized neutron star envelopes, as noted by Gudmundsson, Pethick, and Epstein (1983). The relatively large discrepancies in $\kappa_{e-phonon}$ (Yakovlev and Urpin 1980; Flowers and Itoh 1976) are unimportant except, perhaps, at the highest surface temperatures of interest. The agreement between the recent work of Itoh, *et al.*, (1983) and Yakovlev and Urpin (1980) on the calculation of κ_{e-ion} indicates that a consensus on the thermal structure of unmagnetized neutron star envelopes may soon be reached.

Acknowledgments

We thank Roger Blandford for guidance and encouragement. This work was supported by the National Science Foundation under grants AST82-13001 and AST83-13725. JHA acknowledges the support of a Bantrell Fellowship at Caltech.

Appendix

The sensitivity of the flux- core temperature relation to variations in Γ_m , the radiative conductivity ($\propto\eta_r$), the e-ion conductivity ($\propto\eta_{ei}$), and the e-phonon conductivity ($\propto\eta_{ep}$) is summarized in Tables 1-4 for $T_s = 10^{6.5}, 10^{6.375}, 10^{6}$, and $10^{5.5}$. Similar results from the numerical computations of Gudmundsson (1981) are given in Table 5.

Table 1. $T_s = 10^{6.5}$

Case	η_r	η_{ei}	η_{ep}	Γ_m	$T_{c_8}{}^a$	$T_c{}^a/(T_c{}^a)_s$	$T_{c_8}{}^e$	$T_c{}^e/(T_c{}^e)_s$
1	1	1	1	160	8.78	1.	10.4	1.
2	1	1	1	200	8.42	.96	10.4	1.
3	1	1	1	100	9.89	1.13	10.4	1.
4	2	1	1	160	8.66	.98	10.2	.98
5	.5	1	1	160	8.92	1.02	10.5	1.01
6	100	1	1	160	8.14	.93	9.55	.92
7	.01	1	1	160	10.0	1.14	11.7	1.13
8	1	.5	1	160	10.3	1.17	13.8	1.33
9	1	2	1	160	7.79	.89	7.80	.75
10	1	.5	.5	160	11.7	1.33	13.8	1.33
11	1	2	2	160	6.62	.75	7.80	.75
12	1	1	.5	160	10.6	1.21	10.4	1.
13	1	1	2	160	6.99	.80	10.4	1.
14	2	2	2	160	6.51	.74	7.67	.74
15	.5	.5	.5	160	11.9	1.36	14.0	1.35

Table 2. $T_s = 10^{6.375}$

Case	η_r	η_{ei}	η_{ep}	Γ_m	$T_{c_8}{}^a$	$T_c{}^a/(T_c{}^a)_s$	$T_{c_8}{}^e$	$T_c{}^e/(T_c{}^e)_s$
1	1	1	1	160	5.36	1.	6.30	1.
2	1	1	1	200	5.91	.97	6.30	1.
3	1	1	1	100	5.18	1.10	6.34	1.01
4	2	1	1	160	5.27	.98	6.21	.98
5	.5	1	1	160	5.46	1.02	6.40	1.02
6	100	1	1	160	4.89	.91	5.79	.92
7	.01	1	1	160	6.23	1.16	7.13	1.13
8	1	.5	1	160	6.39	1.19	8.39	1.33
9	1	2	1	160	4.66	.87	4.79	.76
10	1	.5	.5	160	7.11	1.33	8.38	1.33
11	1	2	2	160	4.08	.76	4.73	.75
12	1	1	.5	160	6.27	1.17	6.30	1.
13	1	1	2	160	4.91	.92	6.30	1.
14	2	2	2	160	4.00	.75	4.66	.74
15	.5	.5	.5	160	7.21	1.35	8.49	1.35

Table 3. $T_s = 10^6$

Case	η_r	η_{ei}	η_{ep}	Γ_m	$T_{c_8}{}^a$	$T_c{}^a/(T_c{}^a)_s$	$T_{c_8}{}^e$	$T_c{}^e/(T_c{}^e)_s$
1	1	1	1	160	1.29	1.	1.37	1.
2	1	1	1	200	1.27	.98	1.37	1.
3	1	1	1	100	1.35	1.05	1.38	1.01
4	2	1	1	160	1.26	.97	1.33	.97
5	.5	1	1	160	1.32	1.02	1.40	1.02
6	100	1	1	160	1.13	.88	1.20	.88
7	.01	1	1	160	1.58	1.22	1.66	1.21
8	1	.5	1	160	1.59	1.23	1.76	1.28
9	1	2	1	160	1.07	.83	1.10	.80
10	1	.5	.5	160	1.67	1.30	1.81	1.32
11	1	2	2	160	1.00	.77	1.04	.76
12	1	1	.5	160	1.40	1.08	1.45	1.06
13	1	1	2	160	1.24	.96	1.33	.97
14	2	2	2	160	.98	.76	1.01	.74
15	.5	.5	.5	160	1.71	1.33	1.85	1.35

Table 4. $T_s = 10^{5.5}$

Case	η_r	η_{ei}	η_{ep}	Γ_m	$T_{c_8}{}^a$	$T_c{}^a/(T_c{}^a)_s$	$T_{c_8}{}^e$	$T_c{}^e/(T_c{}^e)_s$
1	1	1	1	160	.213	1.	.205	1.
2	1	1	1	200	.210	.99	.204	1.
3	1	1	1	100	.229	1.08	.216	1.05
4	2	1	1	160	.207	.97	.199	.97
5	.5	1	1	160	.219	1.03	.212	1.03
6	100	1	1	160	.183	.86	.171	.83
7	.01	1	1	160	.273	1.28	.267	1.30
8	1	.5	1	160	.265	1.24	.253	1.23
9	1	2	1	160	.173	.81	.172	.84
10	1	.5	.5	160	.274	1.29	.261	1.27
11	1	2	2	160	.167	.79	.162	.79
12	1	1	.5	160	.223	1.05	.218	1.06
13	1	1	2	160	.208	.97	.199	.97
14	2	2	2	160	.162	.76	.157	.76
15	.5	.5	.5	160	.280	1.32	.270	1.32

Table 5. Sensitivity Tests of Gudmundsson (1981)

$\log T_s$	T_{c_8}	$T_c(.5\kappa_{rad})/T_c$	$T_c(.5\kappa_{elec})/T_c$	$T_c(.5\kappa_{tot})/T_c$
6.5	10.5	--	--	--
6.375	6.26	1.02	1.34	1.37
6	1.29	1.03	1.33	1.37
5.5	.158	1.02	1.35	1.38

References

Applegate, J., Blandford, R., and Hernquist, L. 1984, in preparation.

Baym, G., Pethick, C., and Sutherland, P. 1971, *Ap.J.* **170**,299.

Blandford, R. and Hernquist, L. 1982, *J. Phys. C: Solid State Phys.* **15**,6233.

Blandford, R., Applegate, J., and Hernquist, L. 1983, *M.N.R.A.S.* **204**, 1025.

Cox, J. and Giuli, R. 1968, *Principles of Stellar Structure*, (New York: Gordon and Breach)

Epstein, R., Gudmundsson, E., and Pethick, C. 1983, *M.N.R.A.S.* **204**, 471.

Flowers, E. and Itoh, N. 1976, *Ap.J.* **206**,218.

Glen, G. and Sutherland, P. 1980, *Ap.J.* **239**,671.

Gudmundsson, E. 1981, licentiate thesis, University of Copenhagen.

Gudmundsson, E., Pethick, C., and Epstein, R. 1982, *Ap.J.* (*Letters*) **259**, L19.

Gudmundsson, E., Pethick, C., and Epstein, R. 1983, *Ap.J.* **272**,286.

Hernquist, L. 1984a, *Ap.J. Suppl.*, submitted.

Hernquist, L. 1984b, in preparation.

Hubbard, W. and Lampe, M. 1969, *Ap.J. Suppl.* **18**,297.

Huebner, W., Merts, A., Magee, N., Jr., and Argo, M. 1977, *Astrophysical Opacity Library*, Rept. No. LA 6760M, Los Alamos Scientific Lab.

Itoh, N., Mitake, S., Iyetomi, H., and Ichimaru, S. 1983, *Ap.J.* **273**,774.

Maxwell, O. 1979, *Ap.J.* **231**,201.

Nomoto, K. and Tsuruta, S. 1981, *Ap.J.* (*Letters*) **250**,L19.

Pavlov, G. and Yakovlev, D. 1977, *Astrophysics* **13**,89.

Pollock, E. and Hansen, J. 1973, *Phys. Rev.* **A8**,3110.

Richardson, M., Van Horn, H., Ratcliff, K., and Malone, R. 1982, *Ap.J.* **255,** 624.

Schwarzschild, M. 1958, *Structure* and *Evolution of the Stars*, (Princeton: Princeton University Press)

Silant'ev, N. and Yakovlev, D. 1980, *Ap.* and *Sp. Sci.* **71** ,45.

Slattery, W., Doolen, G., and DeWitt, H. 1980, *Phys. Rev.* **A21** ,2087.

Tsuruta, S. 1974, in *IAU Symposium* 53: *The Physics of Dense Matter*, ed. C. Hansen, (Dordrecht: Reidel).

Tsuruta, S. 1975, *Ap.* and *Sp. Sci.* **34** ,199.

Tsuruta, S. 1979, *Phys. Rept.* **56** ,237.

Urpin, V. and Yakovlev, D. 1980a, *Soviet Astr.* **24** ,126.

Urpin, V. and Yakovlev, D. 1980b, *Soviet Astr.* **24** ,425.

Urpin, V. and Yakovlev, D. 1980c, *Astrophysics* **15** ,429.

Van Riper, K. and Lamb., D. 1981, *Ap.J.* (*Letters*) **244** ,L13.

Yakovlev, D. and Urpin, V. 1980, *Soviet Astr.* **24** ,303.

Yakovlev, D. and Urpin, V. 1981, *Soviet Astr.* (*Letters*) **7** ,88.

Figure Captions

Figure 1.

Relevant physical conditions in neutron star envelopes. Shown are the melting curve, approximate boundary between the non-degenerate and degenerate regimes, and the transition between photon-dominated and electron-dominated heat transport. The sensitivity zone (dotted region) of Gudmundsson, Pethick, and Epstein (1983) is also indicated. Superimposed are approximate $T(\rho)$ profiles for $T_s = 10^{6.5}, 10^{6}$, and $10^{5.5}$.

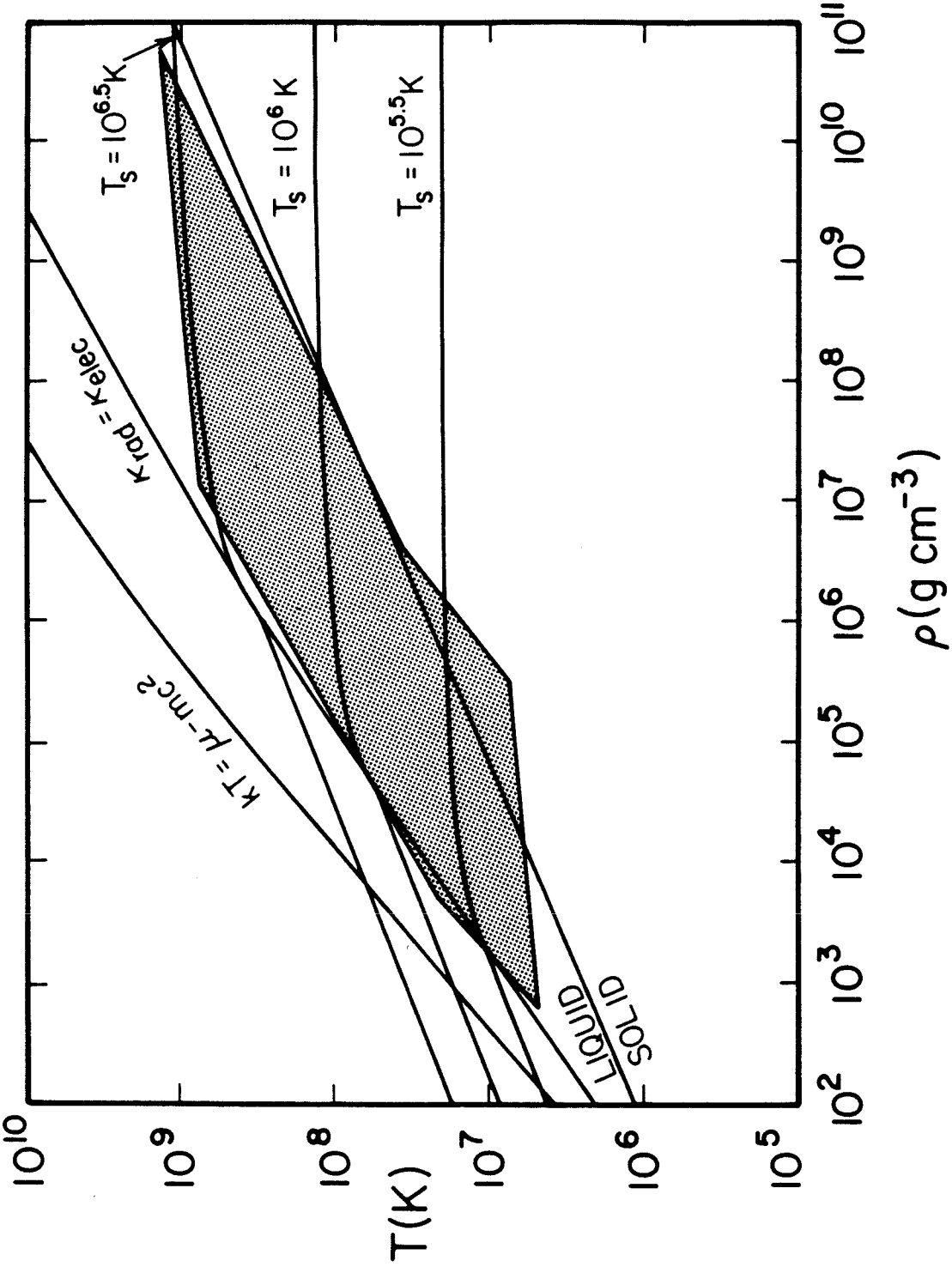
$T_s = 10^{6.5}$K
$T_s = 10^{6}$ K
$T_s = 10^{5.5}$K
$\kappa_{rad} = \kappa_{elec}$
$kT = \mu - mc^2$
LIQUID
SOLID
T(K)
ρ(g cm^{-3})
10^{10}
10^{9}
10^{8}
10^{7}
10^{6}
10^{5}
10^{2}
10^{3}
10^{4}
10^{5}
10^{6}
10^{7}
10^{8}
10^{9}
10^{10}
10^{11}

Figure 1

CHAPTER 6

Thermal Structure of Magnetized Neutron Star Envelopes

Lars Hernquist

Submitted for publication,

Monthly Notices of the Royal Astronomical Society.

Thermal Structure of Magnetized Neutron Star Envelopes

Lars Hernquist

Theoretical Astrophysics, California Institute of Technology

ABSTRACT

The influence of a strong magnetic field ($B \sim 10^{10} - 10^{14}\ G$) on the thermal structure of neutron star envelopes is investigated using the most recent calculations of radiative and electronic thermal conductivities. In particular, the relation between the core temperature, T_c, and the heat flux, F, is considered for effective surface temperatures in the range $T_s = 10^{5.5} - 10^{6.5}\ K$. For a purely vertical magnetic field it is found that quantum effects will enhance (relative to the zero field case) the heat flux, for a fixed core temperature, by a factor $\lesssim 3$. It is further argued that the anisotropic nature of electron transport in a magnetic field will suppress the heat flux for a more realistic field geometry by a factor $\lesssim 3$. Thus the magnetic field is expected to have only a minor effect on neutron star cooling. This conclusion differs substantially from those of earlier magnetized cooling calculations and a comparison is performed to isolate sources of discrepancy. (It is argued that the disagreement results primarily from inaccurate approximations to the electronic thermal conductivity used in past calculations.) The sensitivity of the flux- core temperature relation to variations in the input physics is studied in a manner analogous

to Gudmundsson, *et al.* The results of the sensitivity analysis are used to argue that disagreements among the existing calculations of the conductivity will not alter the basic conclusion that magnetic effects on the flux- core temperature relation are relatively unimportant.

1. Introduction

Substantial evidence exists to support the view that most observable neutron stars have strong surface magnetic fields in the range $B \sim 10^9$ to 10^{13} G (for a summary see Blandford, Applegate, and Hernquist 1983). The standard models of radio pulsars and pulsating x-ray sources incorporate magnetized neutron stars in order to account for the periodicity of the emission and to provide efficient mechanisms for the production of radiation. Timing observations of most radio pulsars are well fit by a narrow distribution of field strengths ($\propto (P\dot{P})^{1/2}$) in the range $1-5\times10^{12}$ G (e.g., Manchester 1981). In addition, cyclotron lines have been observed in the x-ray spectra of pulsating x-ray sources and γ-ray bursters. Fields $\sim 1-5\times10^{12}$ G are required if the features originate from electron transitions between the two lowest Landau levels.

Neutron stars are expected to be intense sources of thermal x-ray radiation. However, attempts to observe unpulsed point sources in young galactic supernova remnants have largely been unsuccessful (for a recent review see Helfand and Becker 1984). Furthermore, in those cases for which there is evidence for a point source (the Crab, Vela, RCW103, 3C58, and CTB80 remnants) it is not possible to determine the surface x-ray flux unambiguously. The implied upper limits for the surface temperatures of the neutron stars are marginally consistent with standard, unmagnetized cooling calculations (e.g., Nomoto and Tsuruta 1981; Van Riper and Lamb 1981). However, a number of theoretical issues are unsettled, and it may be necessary to invoke rapid cooling due to uncertain phenomena in the core (e.g., pion condensation) if future observations lower the derived surface temperatures.

Magnetic fields of the strength associated with neutron stars can significantly influence the physical conditions and transport properties in neutron star envelopes (e.g., Hernquist 1984; Yakovlev 1984). Thus, it has been

generally assumed that neutron star cooling could be similarly affected. However, previous magnetized thermal structure calculations (Tsuruta, *et al.* 1972; Tsuruta 1974,1975,1979; Glen and Sutherland 1980; Nomoto and Tsuruta 1981; Van Riper and Lamb 1981; Yakovlev and Urpin 1981) have not been completely satisfactory. The thermal conductivities which have been used are not accurate and geometrical effects have not been included. In the present work it is argued that the influence of the magnetic field on neutron star cooling has been greatly overestimated and that magnetic effects are likely to be unimportant.

As has been emphasized in the recent work of Gudmundsson and co-authors (Gudmundsson 1981; Gudmundsson, Pethick, and Epstein 1982,1983; Epstein, Gudmundsson, and Pethick 1983) the thermal structures of the envelope and core evolve independently during the epoch of neutrino cooling. In this approximation the core is assumed to be isothermal and to contain all of the star's mass and thermal energy. The temperature of the core is regulated by the loss of neutrinos which do not interact with the crust. The surrounding crust acts as a thin insulating envelope with no sources or sinks of energy and contains all of the temperature gradient. Thus, for a given core temperature, the heat flux through the crust is constant and the effective surface temperature is determined entirely by processes within the crust. This is an ideal method with which to study the effects of a magnetic field on neutron star thermal structure because the dominant influence of the field is confined to the envelope.* (Indeed, in some models, e.g., Blandford, Applegate, and Hernquist 1983, it is further assumed that the field does not penetrate the core.) In addition, the relevant equations are relatively simple and, most importantly, it is possible to determine the sensitivity of the results to each physical input (Gudmundsson,

*A possible effect of the magnetic field on the core could be to reduce the neutrino luminosities (e.g., Tsuruta 1979), although a rigorous calculation has yet to confirm this.

Pethick, and Epstein 1983; Hernquist and Applegate 1984).

In this paper the thermal structure of magnetized neutron star envelopes is investigated using the method due to Gudmundsson, Pethick, and Epstein (1983) and the most recent calculations of radiative and electronic thermal conductivities. A number of simplifying assumptions are made which allow the dominant effects to be isolated. In the following section the effects of a quantizing magnetic field on the thermodynamic properties of the matter are discussed. Section 3 contains a summary of the relevant calculations of the thermal conductivity. The form of the thermal structure equation which has been used is given in Section 4. Numerical solutions are presented in Section 5 along with an analysis of the sensitivity of the results to various physical inputs. In Section 6 a comparison is made to previous calculations and possible sources of discrepancy are discussed. Finally, conclusions and remaining uncertainties are summarized in Section 7.

2. Thermodynamic Relations

2.1 QUANTIZATION OF ELECTRON ORBITS

For sufficiently strong magnetic fields the classical description of electron orbits is no longer valid and quantum effects must be included. In order to derive the local thermodynamic and transport properties it is sufficient to consider a free electron gas in a uniform, homogeneous magnetic field B. The Dirac equation can be solved exactly (e.g., Berestetskii, *et al.* 1982) to give the energy

spectrum

$$\varepsilon = (p_{\|}^2 c^2 + m^2 c^4 + 2n\hbar\omega_B mc^2)^{1/2} \tag{2.1}$$

where $p_{\|}$ is the momentum along the field. The energy levels, which are known as Landau levels, are doubly degenerate for $n \neq 0$ and non-degenerate for $n = 0$. Note that the quantity ω_B is not the relativistic gyrofrequency $\Omega = |e|Bc/\varepsilon$ but is

$$\omega_B = |e|B/mc \tag{2.2}$$

Quantum effects are generally significant only when the gas as a whole occupies a small number of Landau levels. The highest level populated, n_{max}, in a non-degenerate gas is given roughly by

$$n_{max} = kT/\hbar\omega_B \tag{2.3}$$

and in a degenerate gas by (e.g., Blandford and Hernquist 1982)

$$n_{max} = (\mu^2 - m^2c^4)/2mc^2\hbar\omega_B \tag{2.4}$$

where μ is the electron chemical potential including rest mass. Note that (2.3) and (2.4) yield the same result for $\mu - mc^2 = kT$, in the non-relativistic approximation (the gas is always non-relativistic in the non-degenerate regime). Thus the number of Landau levels is continuously increasing through the crust. A rough estimate of the relation of n_{max} to density can be obtained from the unmagnetized, degenerate expression for chemical potential

$$\mu_0^2 = p_{F_0}^2 c^2 + m^2 c^4 \tag{2.5}$$

$$p_{F_0} = \hbar(3\pi^2)^{1/3} n_e^{1/3} \tag{2.6}$$

$$n_e = Z\rho/Am_p \tag{2.7}$$

where n_e is the electron number density, A is the ion mass, Z is the number of conduction electrons per ion, and m_p is the proton mass. (Throughout, the subscript zero will be used to denote a quantity in the absence of a quantizing magnetic field.) Equation (2.7) is valid only if a single ion species is present, as will always be assumed. From (2.5)-(2.7) for $A = 56$, $Z = 26$

$$n_{max} = .74\, T_8 / B_{12} \qquad \text{(non-degenerate)} \tag{2.8a}$$

$$n_{max} = 1.3 \rho_8^{2/3} / B_{13} \qquad \text{(degenerate)} \tag{2.8b}$$

(The notation X_p will be used to indicate a quantity in units of 10^p and cgs units are assumed throughout.)

2.2 THE CHEMICAL POTENTIAL

As a result of the quantization of the density of states the thermodynamic properties of the electron gas are modified (e.g., Hernquist 1984; Yakovlev 1984). It is useful to define the dimensionless parameters

$$\eta = (\mu - mc^2)/kT \tag{2.9}$$

$$\beta = \hbar\omega_B / mc^2 \tag{2.10}$$

Thus η is a measure of the degree of degeneracy and β is the field strength in units of 4.414×10^{13} G. The magnetized relation of electron chemical potential to density is

$$n_e = \frac{m\omega_B}{(2\pi\hbar)^2} \sum_{n=0}^{\infty} g_n \int_{-\infty}^{\infty} \frac{dp_\parallel}{1 + \exp((\varepsilon_n - \mu)/kT)} \tag{2.11}$$

where the ε_n are given by (2.1) and the factor $g_n = 2 - \delta_{n0}$ accounts for spin degeneracy. In the non-degenerate, non-relativistic limit (2.11) becomes

$$\frac{\mu - mc^2}{kT} = -\ln\left[\left(\frac{mkT}{2\pi\hbar^2}\right)^{3/2} \frac{1}{n_e} \frac{\hbar\omega_B}{kT} \sum_{n=0}^{\infty} g_n\, e^{-n\hbar\omega_B/kT}\right] \tag{2.12}$$

The relation corresponding to (2.11) in the absence of a quantizing field is

$$n_e = \frac{1}{\pi^2\hbar^3} \int_0^{\infty} \frac{p_0^2\, dp_0}{1 + \exp((\varepsilon_0 - \mu_0)/kT)} \tag{2.13}$$

where $\varepsilon_0^2 = p_0^2c^2 + m^2c^4$.

In the integration of the thermal structure equation (see Section 4) the partial derivatives $\partial\rho/\partial\mu)_{T,B}$ and $\partial\rho/\partial T)_{\mu,B}$ are required. From (2.11), transforming to integrals over energy and interchanging the sums and integrals (e.g., Hernquist 1984)

$$\left.\frac{\partial\rho}{\partial\mu}\right)_{T,B} = -\frac{m\omega_B A m_p}{2\pi^2\hbar^2 cZ} \int_{mc^2}^{\infty} \varepsilon \frac{\partial f}{\partial\varepsilon} \sum_{n=0}^{n_{max}} \frac{g_n}{(\varepsilon^2 - m^2c^4 - 2n\hbar\omega_B mc^2)^{1/2}}\, d\varepsilon \tag{2.14a}$$

$$\left.\frac{\partial\rho}{\partial T}\right)_{\mu,B} = -\frac{m\omega_B A m_p}{2\pi^2\hbar^2 cTZ} \int_{mc^2}^{\infty} \varepsilon(\varepsilon - \mu) \frac{\partial f}{\partial\varepsilon} \sum_{n=0}^{n_{max}} \frac{g_n}{(\varepsilon^2 - m^2c^4 - 2n\hbar\omega_B mc^2)^{1/2}}\, d\varepsilon \tag{2.14b}$$

where the sums are bounded by $n_{max} = (\varepsilon^2 - m^2c^4)/2\hbar\omega_B mc^2$ and $f = (1 + \exp(\varepsilon - \mu)/kT)^{-1}$ is the Fermi-Dirac function. In the non-degenerate, non-relativistic limit, from (2.12)

$$\left.\frac{\partial\rho}{\partial\mu}\right)_{T,B} = \frac{Am_p}{Z}\left(\frac{\pi}{2mkT}\right)^{1/2} \frac{\beta e^{\eta} m^3c^2}{2\pi^2\hbar^3} \sum_{n=0}^{\infty} g_n\, e^{-n\hbar\omega_B/kT} \tag{2.15a}$$

$$\left.\frac{\partial\rho}{\partial T}\right)_{\mu,B} = -\frac{Am_p}{Z}\left(\frac{\pi k}{2mT}\right)^{1/2} \frac{\beta e^{\eta} m^3c^2}{2\pi^2\hbar^3} \sum_{n=0}^{\infty} g_n\, e^{-n\hbar\omega_B/kT} \left(\eta - \frac{n\hbar\omega_B}{kT} - \frac{1}{2}\right) \tag{2.15b}$$

The completely degenerate forms of (2.14a) and (2.14b) are not useful because of the singularities (square root, integrable) in the integrands. Thus it is necessary to use (2.14a) and (2.14b) when the gas is no longer non-degenerate. The analogs of (2.14a) and (2.14b) in the absence of a quantizing field are

$$\left.\frac{\partial \rho}{\partial \mu_0}\right)_T = -\frac{Am_p}{Z}\frac{1}{\pi^2\hbar^3c^3}\int_{mc^2}^{\infty}\varepsilon_0(\varepsilon_0^2 - m^2c^4)^{1/2}\frac{\partial f}{\partial \varepsilon_0}d\varepsilon_0 \qquad (2.16a)$$

$$\left.\frac{\partial \rho}{\partial T}\right)_{\mu_0} = -\frac{Am_p}{Z}\frac{1}{\pi^2\hbar^3c^3T}\int_{mc^2}^{\infty}\varepsilon_0(\varepsilon_0 - \mu_0)(\varepsilon_0^2 - m^2c^4)^{1/2}\frac{\partial f}{\partial \varepsilon_0}d\varepsilon_0 \qquad (2.16b)$$

In the non-degenerate, non-relativistic limit (2.16a) and (2.16b) become

$$\left.\frac{\partial \rho}{\partial \mu_0}\right)_T = \frac{2Am_p}{ZkT}\left(\frac{mkT}{2\pi\hbar^2}\right)^{3/2}e^{\eta_0} \qquad (2.17a)$$

$$\left.\frac{\partial \rho}{\partial T}\right)_{\mu_0} = \frac{Am_p}{Z}\left(\frac{mkT}{2\pi\hbar^2}\right)^{3/2}\frac{1}{T}(3 - 2\eta_0)e^{\eta_0} \qquad (2.17b)$$

and in the completely degenerate ($T = 0$) limit become

$$\left.\frac{\partial \rho}{\partial \mu_0}\right)_T = \frac{Am_p}{Z}\frac{1}{\pi^2\hbar^3c^3}\mu_0(\mu_0^2 - m^2c^4)^{1/2} \qquad (2.18a)$$

$$\left.\frac{\partial \rho}{\partial T}\right)_{\mu_0} = \frac{Am_p}{Z}\frac{k^2T}{3\hbar^3c^3}\frac{2\mu_0^2 - m^2c^4}{(\mu_0^2 - m^2c^4)^{1/2}} \qquad (2.18b)$$

2.3 THE EQUATION OF STATE

Hernquist and Applegate (1984) have demonstrated that in the unmagnetized case corrections to the free electron equation of state (ionic, radiative, and electrostatic) have a negligible influence on the relation between the flux, F, and the core temperature, T_c, of the neutron star. This follows from the rapid convergence of the radiative zero solution when the heat conduction is by photons and the prevailing conditions (i.e., ideal gas) at the transition between radiation and electron dominated heat transport. Furthermore, partial ionization is also negligible in determining the $F-T_c$ relation because of the high degree of ionization (e.g., Gudmundsson 1981) at the transition. It will be assumed that the

same approximation is valid in the presence of a quantizing magnetic field (Hernquist and Applegate 1984). The validity of this assumption is confirmed by the sensitivity analysis in Section 5.

In the presence of a magnetic field (Blandford and Hernquist 1982) the thermodynamic pressure is isotropic and is given by

$$P = \frac{m\omega_B}{(2\pi\hbar)^2}\sum_{n=0}^{\infty} g_n \int_{-\infty}^{\infty} \frac{p_\parallel^2 c^2}{\varepsilon_n}\frac{dp_\parallel}{1+\exp((\varepsilon_n-\mu)/kT)} \tag{2.19}$$

(Magnetization effects are negligible.) In the non-degenerate, non-relativistic limit, using (2.12)

$$P = n_e kT \tag{2.20}$$

which is identical to the unmagnetized form.

The entropy per unit volume of the electrons, which is required in the integration of the thermal structure equation, is given by the thermodynamic identity $S_e = \partial P/\partial T)_\mu$. Using (2.19)

$$S_e = -\frac{m\omega_B}{2\pi^2\hbar^2 c}\int_{mc^2}^{\infty}\frac{\varepsilon-\mu}{T}\frac{\partial f}{\partial\varepsilon}\sum_{n=0}^{n_{max}} g_n(\varepsilon^2 - m^2c^4 - 2n\hbar\omega_B mc^2)^{1/2}\,d\varepsilon \tag{2.21}$$

In the non-degenerate, non-relativistic limit (2.21) becomes

$$S_e = \left[\frac{mkT}{2\pi\hbar^2}\right]^{3/2}\frac{mc^2}{T}\beta e^{\eta}\sum_{n=0}^{\infty} g_n\, e^{-n\hbar\omega_B/kT}\left[\frac{3}{2}+\frac{n\hbar\omega_B-(\mu-mc^2)}{kT}\right] \tag{2.22}$$

2.4 THE STATE OF THE MATTER

2.4.1 *Surface conditions*

It has been suggested (e.g., Ruderman 1974; Chen, *et al.* 1974; Flowers, *et al.* 1977) that the physical structure of the neutron star surface could be altered by the magnetic field, through the formation of linear chains of atoms. However, the most recent calculations (Müller 1984) indicate that the chains are not stable for iron, which is the equilibrium nuclear species at these densities (Baym, Pethick, and Sutherland 1971). In this paper it is assumed that the surface layers are composed of iron and that magnetic condensation does not occur. As noted by Hernquist and Applegate (1984) surface effects should not influence the flux- core temperature relation because of the rapid convergence of the radiative zero solution in the photon dominated regime. The only exception would be if the density distribution was terminated by magnetic effects at a point where the heat transport was by electron conduction. The results of Müller (1984) (low binding energies for helium) indicate that this is unlikely to occur even if the surface is composed of elements other than iron.

2.4.2 *Crystallization*

The ions are non-relativistic and non-degenerate and the state of the matter is determined by the parameter

$$\Gamma = Z^2 e^2 / kTa \qquad ; a = (3/4\pi n_i)^{1/3} \tag{2.23}$$

where n_i is the ion number density. The liquid-solid phase transition occurs at $\Gamma = \Gamma_m$, with the matter being liquid for $\Gamma < \Gamma_m$ and solid for $\Gamma > \Gamma_m$. Estimates for Γ_m, neglecting magnetic effects, are in the range $\sim 150-170$ (e.g., Pollock and Hansen 1973; Slattery, Doolen, and DeWitt 1980). It will be assumed that the

magnetic field does not affect the ions, in accordance with the calculations of thermal conductivity (Hernquist 1984; Yakovlev 1984). This requires, roughly, that $\omega_{B_i} = Z|e|B/m_i c < \omega_{p_i} = (4\pi Z^2 e^2 n_i / m_i)^{1/2}$ or $B_{14} < \rho_6^{1/2} G$ (e.g., Yakovlev 1984; Usov, *et al.* 1980). Another restriction on the strength of the field in the solid is provided by the condition that the magnetostrictive stresses not exceed the yield stress of the lattice. This gives, roughly (Blandford and Hernquist 1982) $B_{13} < (1 + .6\rho_6^{2/3})\varepsilon_{-2}$, where $\varepsilon = 10^{-2}\varepsilon_{-2}$ is the maximum allowed strain angle.

3. Thermal Conductivities

3.1 PHOTON CONDUCTION

At low densities heat is conducted almost entirely by photons. Several authors have calculated photon conductivities for a non-degenerate, non-relativistic plasma in the presence of a strong magnetic field (e.g., Canuto 1970; Canuto, *et al.* 1971; Lodenquai, *et al.* 1974; Pavlov and Panov 1976; Pavlov and Yakovlev 1977; Silant'ev and Yakovlev 1980). Difficulties with the earliest calculations have been noted by Silant'ev and Yakovlev (1980). In this paper, which assumes a purely vertical field geometry, the tabulated results of Silant'ev and Yakovlev (1980) are used for both Thomson scattering and free-free absorption. (Thomson scattering was found to be negligible at the relevant densities and temperatures.) Other sources of opacity (bound-free and bound-bound absorption) are ignored. As noted by Hernquist and Applegate (1984) in the unmagnetized case, corrections to the free-free thermal conductivity have a negligible influence on the flux- core temperature relation. This results from the rapid convergence of the radiative zero solution in the region where heat transport is

by photons and the dominance of free-free absorption at the transition to electron-dominated heat transport. These conditions should also hold in the magnetized case (Hernquist and Applegate 1984) and the insensitivity of the results to the photon conductivity is confirmed in Section 5. (The temperature distributions are, however, not accurate at low densities where bound-free and bound-bound absorption may be important.)

The magnetized conductivities in Silant'ev and Yakovlev (1980) are presented in the form of zero field conductivities multiplied by a function of B and temperature. The zero field free-free conductivity in Silant'ev and Yakovlev (1980) leads to an opacity which differs from the corresponding relation in Cox and Giuli (1968) by a factor ≈ 3 . The discrepancy can be entirely attributed to differences in the frequency-dependent Gaunt factors. Silant'ev and Yakovlev (1980) assume the form $g_{ff} = \frac{3^{1/2}}{\pi}\exp(h\nu/kT)K_0(h\nu/kT)$, where $K_0(z)$ is a modified Bessel function, which has been calculated in the Born approximation using free electron wave functions (Pavlov and Kaminker 1975). A more exact treatment (Karzas and Latter 1961) , taking into account Coulomb effects on the electron wave functions, shows that for iron at the relevant temperatures $g_{ff} \approx 1$, independent of frequency. When the two forms are averaged over frequency a factor ≈ 3 difference results. In this paper the approximation $g_{ff} = 1$ is made, although the sensitivity analysis presented in Section 5 indicates that deviations in the photon conductivity of this magnitude have a negligible influence on the flux- core temperature relation.

Finally, the conductivities of Silant'ev and Yakovlev (1980) are calculated for $b = \hbar\omega_B/kT \approx 1.3B_{12}/T_8 \leq 1000$. At higher values of b (near the surface) the conductivity was found by extrapolation. Although this is undoubtedly not accurate the flux-core temperature relation will not be affected because errors in the conductivity at low densities are not relevant (Hernquist and Applegate

1984).

3.2 ELECTRON CONDUCTION

3.2.1 *Unmagnetized calculations*

In the liquid phase the dominant scattering mechanism is electron-ion scattering, while electron-phonon collisions are most important in the solid phase. Electron-electron scattering will generally be negligible unless low-Z ions ($Z \lesssim 10$) are present (Urpin and Yakovlev 1980a). The thermal conductivity of the degenerate electrons in the liquid phase has been calculated by Flowers and Itoh (1976), Yakovlev and Urpin (1980), Urpin and Yakovlev (1980b), Itoh, *et al.* (1983), and Nandkumar and Pethick (1984). The original calculations of Flowers and Itoh (1976) and Yakovlev and Urpin (1980) differed by factors ~ 3 with essentially the same density and temperature dependence (Blandford, Applegate, and Hernquist 1983). In the recent work of Itoh, *et al.* (1983) and Nandkumar and Pethick (1984) the thermal conductivity is expressed in a form identical to that of Yakovlev and Urpin (1980), with residual discrepancies ($\sim$ 10–30% for iron, with Itoh, *et al.* (1983) and Nandkumar and Pethick (1984) giving the larger values of the thermal conductivity) absorbed in the Coulomb logarithm. In terms of density and temperature

$$\kappa_0{}^{e-ion} = \frac{\pi^3 \hbar^3 k^2}{4e^4 m^2 m_p} \frac{\rho T}{A \Lambda_{ei}} \left[1 + \left(\frac{\hbar}{mc} \right)^2 \left(\frac{3\pi^2 Z}{A m_p} \right)^{2/3} \rho^{2/3} \right]^{-1} \qquad (3.1)$$

where Λ_{ei} is the Coulomb logarithm. In this paper, when zero field conductivities are required, the approximation $\Lambda_{ei} = 1$ is made and $\kappa_0{}^{e-ion}$ is assumed to be uncertain to $\approx 30\%$.

The thermal conductivity in the solid phase due to e-phonon scattering has been calculated by Flowers and Itoh (1976), Yakovlev and Urpin (1980), Raikh and Yakovlev (1982), and near the melting point by Itoh, *et al.* (1984). Considerable disagreement (factors ~ 3) still exists between the various calculations. (For a critique see Blandford, Applegate, and Hernquist 1983.) For convenience the analytical expression in Yakovlev and Urpin (1980) has been used and $\kappa_0^{e-phonon}$ is assumed to be uncertain to a factor of 3 . (The sensitivity tests in Section 5 demonstrate explicitly that this is not a serious consideration in determining the flux-core temperature relation.) In terms of density and temperature

$$\kappa_0^{e-phonon} = \frac{(3\pi^2)^{1/3}\pi^2\hbar^3 k}{6m^2e^2u_{-2}}\left(\frac{Z\rho}{Am_p}\right)^{4/3}\left[1+\frac{1}{2}\left(\frac{\hbar}{mc}\right)^2\left(\frac{3\pi^2 Z}{Am_p}\right)^{2/3}\rho^{2/3}\right]^{-1} \tag{3.2}$$

where the factor u_{-2} is related to the mean square thermal displacement of the ions, $\overline{\xi^2}$, by

$$\overline{\xi^2} = \frac{3kT}{m_i\omega_{p_i}{}^2}u_{-2} \tag{3.3}$$

$$\omega_{p_i}{}^2 = \frac{4\pi Z^2e^2n_i}{m_i} \tag{3.4}$$

Henceforth the value $u_{-2} = 13$ (Pollock and Hansen 1973) used by Yakovlev and Urpin (1980) will be assumed.

3.2.2 *Magnetized conductivities*

The thermal conductivity due to relativistic electrons in a quantizing magnetic field has recently been calculated by Hernquist (1984) and Yakovlev (1984) in the field-parallel case, and by Kaminker and Yakovlev (1981) and Hernquist

(1984) in the field-perpendicular case. Difficulties with previous calculations (e.g., Canuto and Chiu 1969; Canuto and Chiuderi 1970; Ventura 1973; Canuto and Ventura 1977) have been noted by Yakovlev (1980ab,1982) in his treatment of non-relativistic electron transport. In particular, large errors can be introduced if the completely degenerate limit ($T = 0$) is assumed, because of the sensitivity of the flux- core temperature relation to the electron thermal conductivity. Thermal effects smooth and damp the quantum oscillations and are responsible for the breakdown of the Wiedemann-Franz law (Hernquist 1984; Yakovlev 1984).

For the vertical field geometry assumed in this paper the transport coefficients can be written as

$$\begin{Bmatrix} \sigma_{\parallel} \\ \lambda_{\parallel} \\ \gamma_{\parallel} \end{Bmatrix} = -\frac{2m\omega_B}{4\pi^2\hbar^2\sigma_0 n_i} \int_{mc^2}^{\infty} \frac{\partial f^0}{\partial \varepsilon} \begin{Bmatrix} e^2 \\ -|e|(\varepsilon-\mu)/T \\ (\varepsilon-\mu)^2/T \end{Bmatrix} \varphi(\varepsilon,B)\, d\varepsilon \tag{3.5}$$

where $\sigma_0 = \pi Z^2 e^4/\hbar^2\omega_B{}^2$ for e-ion scattering and $\sigma_0 = me^2kT\,u_{-2}/2\hbar^3\omega_B n_i$ for e-phonon scattering. The thermal conductivity $\kappa_{\parallel}$ is obtained from the relation

$$\kappa_{\parallel} = \gamma_{\parallel} - T\lambda_{\parallel}{}^2/\sigma_{\parallel} \tag{3.6}$$

(e.g., Hernquist 1984; Yakovlev 1984). Fits to the function $\varphi(\varepsilon,B)$ have been given by Hernquist (1984) for selected field strengths and with allowance for up to 30 Landau levels to be populated. Fits are provided for both e-ion and e-phonon scattering. The results of Yakovlev (1984) are expressed in a form identical to (3.5) but with a factor of 2β absorbed in the normalization of $\varphi(\varepsilon,B)$ rather than multiplying the integral in (3.5). That is, $\varphi(H) = \varphi(Y)/2\beta$. (The normalization of $\varphi(\varepsilon,B)$ in Hernquist (1984) ensures that φ is independent of B in the limit $B \to 0$.) Values of $\varphi(\varepsilon,B)$ are tabulated by Yakovlev (1984) for selected field strengths, both e-ion scattering and e-phonon scattering, and with

allowance for up to 6 Landau levels to be populated. The two calculations in the solid phase agree to within the accuracy of the fits in Hernquist (1984) and the stated accuracy of the numerical results in Yakovlev (1984). The two calculations in the liquid phase agree away from the zeros of φ (see Hernquist 1984). Near the zeros of φ the calculations disagree by up to $\approx 50\%$, with Hernquist (1984) giving the larger values. This will lead to differences $\lesssim 30\%$ in the conductivity when φ is used to calculate κ_{e-ion} from (3.5). The numerical differences are directly attributable to assumptions made about the screening length, r_d, used in the calculations. The expression for r_d used by Hernquist (1984) differs from that used by Yakovlev (1984) by a numerical factor of 1.64 (that is, $r_d(Y) = 1.64 r_d(H)$). The form of r_d used in Hernquist (1984) was chosen for consistency with the non-relativistic calculation of Yakovlev (1980ab,1982). As the resulting conductivities are in substantial agreement ($\sim 30\%$ difference in κ_{e-ion} at high densities) it is not appropriate to debate the relative merits of one choice of r_d over the other. The Hernquist (1984) calculation of the conductivity is used in this paper (because of the allowance for a greater number of Landau levels) and κ_{e-ion} is assumed to be uncertain to $\approx 30\%$ (entirely consistent with the uncertainties in the unmagnetized case). The two calculations of $\kappa_{e-phonon}$, which are in complete agreement, will be assumed to be uncertain to a factor ~ 3, in accordance with the unmagnetized calculations.*

3.2.3 *Magnetized conductivities at low densities*

The fits to φ_{e-ion} given by Hernquist (1984) and the tabulations of φ_{e-ion} given by Yakovlev (1984) both assume forms for the screening length which are

*The linear systems in Hernquist (1984) and Yakovlev (1984) used to find $\varphi(\varepsilon, B)$ differ by virtue of a symmetry relation. For the scattering potentials of interest it is possible to show that $\varphi_{n\eta s} = \varphi_{n-\eta-s}$ (in the notation of Hernquist 1984). If this relation is applied to the system in Hernquist (1984) it simplifies to the form of Yakovlev (1984). For more general scattering potentials, however, the system of Hernquist (1984) is necessary.

valid only in the degenerate limit. Typically the transition from photon-dominated to electron-dominated heat transport occurs when the gas is not highly degenerate. At these densities φ_{e-ion} is not accurately represented by the numerical calculations of Hernquist (1984) or Yakovlev (1984). However, it is possible to avoid difficulties by noting that the gas in the non-degenerate regime always occupies only the lowest Landau level whenever quantum effects have a significant effect on the flux-core temperature relation. In this limit ($n_{max} = 0$) it is possible to find φ analytically (e.g., Yakovlev 1984). With $\varphi(\varepsilon,B)$ normalized according to Hernquist (1984) this gives

$$\varphi_{e-phonon} = -\frac{1}{8} w(\beta,\nu) \left[\exp(w(\beta,\nu)) \, \mathrm{Ei}(-w(\beta,\nu)) \right]^{-1} \tag{3.7}$$

$$\varphi_{e-ion} = \frac{1}{8} w(\beta,\nu) \left[\exp(w(\beta,\nu) + a_d) \, \mathrm{Ei}(-w(\beta,\nu) - a_d) + \frac{1}{w(\beta,\nu) + a_d} \right]^{-1} \tag{3.8}$$

where $\nu = \varepsilon / \hbar\omega_B$, $w(\beta,\nu) = 2(\beta^2\nu^2 - 1)/\beta$, Ei is an exponential integral (Gradshteyn and Ryzhik 1980), and the dimensionless screening length parameter a_d is related to the screening length r_d by

$$a_d = \frac{1}{2\beta} \left(\frac{\hbar}{mc} \right)^2 \frac{1}{r_d^{\,2}} \tag{3.9}$$

For compatibility with Hernquist (1984) the screening lengths of Yakovlev (1980ab,1982) are used. The exact relations are

$$r_d^{\,-2} = r_i^{\,-2} + r_e^{\,-2} \tag{3.10a}$$

$$r_i^{\,2} = r_{D_i}^{\,2} + \frac{a^2}{6} \tag{3.10b}$$

$$r_e^{\,-2} = 4\pi e^2 \frac{\partial}{\partial \mu} n_e(\mu) \tag{3.10c}$$

where r_{D_i} is related to density and temperature by $r_{D_i} = (kT/4\pi Z^2 e^2 n_i)^{1/2}$, a is defined by (2.23), and $\partial n_e/\partial\mu)_T$ is obtained from (2.14a). Relations (3.7) and (3.8), along with (3.10a)-(3.10c), are used to calculate φ in the limit $n_{max} = 0$ in order to avoid numerical problems. At higher densities ($n_{max} > 0$) the fits given in Hernquist (1984) are used to compute φ.

4. Thermal Structure Equation

In general the problem of heat transport in a magnetic field is significantly more difficult than the unmagnetized case because the heat flux equation is a vector equation and the conductivity is a tensor. If, however, the field is vertical throughout the crust then $\nabla T \parallel \vec{B}$ and the familiar scalar equations can be used. This assumption will be made in this paper and, consequently, the results will represent the maximum amount by which the heat flux can be enhanced by quantum effects. (Geometrical effects are discussed briefly in Section 5, and more fully in Applegate, Blandford, and Hernquist 1984).

For a thin crust with negligible mass and no sources or sinks of energy the general relativistic equations of stellar structure can be written as (Gudmundsson, Pethick, and Epstein 1983)

$$\frac{dT}{dP} = \frac{F}{g_s}\frac{1}{\rho\kappa} \tag{4.1}$$

where F is the heat flux, g_s is the surface gravity, and κ is related to the opacity, $\tilde{\kappa}$, by

$$\kappa = \frac{16\sigma}{3}\frac{T^3}{\rho\tilde{\kappa}} \tag{4.2}$$

For a field geometry in which $\nabla T \parallel \vec{B}$, (4.1) is valid and $\kappa \to \kappa_{\parallel}$. However, (4.1) is

not the most convenient form of the thermal structure equation if magnetic effects are included. The transport coefficients (3.5) are expressed as functions of μ and T. Thus, if (4.1) were used it would be necessary to numerically invert (2.19) at each step in the numerical integration. In addition, it is desirable to solve for the temperature distribution as a function of density directly, rather than pressure. One possibility would be to write the thermal structure equation as a total derivative of the temperature with respect to the electron chemical potential (e.g., Hernquist and Applegate 1984) and then find the corresponding density from (2.11). However, it is possible to show that in the non-degenerate layers μ does not always increase monotonically along a solution and, therefore, is not suitable as the independent integration variable.

It is most convenient to use density as the independent variable and, furthermore, to solve for the chemical potential simultaneously rather than by inverting (2.11). This is accomplished by writing the thermal structure equation as two coupled differential equations for temperature and electron chemical potential. Using the identities $dP = \partial P/\partial\mu)_T\, d\mu + \partial P/\partial T)_\mu\, dT$ and $d\rho = \partial\rho/\partial\mu)_T\, d\mu + \partial\rho/\partial T)_\mu\, dT$, from (4.1)

$$\frac{dT}{d\rho} = \left[\left.\frac{\partial\rho}{\partial T}\right|_\mu + \left(\frac{Am_p}{Z}\frac{\kappa}{F/g_s} - \frac{S_e}{n_e} \right) \left.\frac{\partial\rho}{\partial\mu}\right|_T \right]^{-1} \tag{4.3}$$

$$\frac{d\mu}{d\rho} = \frac{1}{\partial\rho/\partial\mu)_T} \left[1 - \left.\frac{\partial\rho}{\partial T}\right|_\mu \frac{dT}{d\rho} \right] \tag{4.4}$$

where $S_e = \partial P/\partial T)_\mu$ is the entropy per unit volume of the electrons, the thermodynamic identity $n_e = \partial P/\partial\mu)_T$ has been used, and the right hand sides of both (4.3) and (4.4) are expressed entirely as functions of μ and T.

The thermal distribution is obtained by simultaneous numerical integration of (4.3) and (4.4) from an initial point (T_s, ρ_s, μ_s) to the core boundary. For a

given effective surface temperature (i.e., a fixed heat flux $F = \sigma T_s^4$) the initial density is found from the usual condition (e.g., Gudmundsson, Pethick, and Epstein 1983)

$$P_s = \frac{2}{3}\frac{g_s}{\bar{\kappa}_s} \tag{4.5}$$

The point (T_s, ρ_s, μ_s) always lies in the non-degenerate layers where the opacity is dominated by the photons. In this region the magnetized equation of state is identical to the unmagnetized form (2.20). Furthermore, because the flux- core temperature relation is completely insensitive to the surface boundary condition it is sufficient to use the free- free conductivity of Silant'ev and Yakovlev (1980) in (4.5). (See the relevant discussion in Hernquist and Applegate 1984.) Using the Cox and Giuli form of the unmagnetized free-free opacity, for fully ionized iron

$$\rho_s = .06\, g_{s_{14}}^{1/2}\, T_{s_6}^{1.25}\, \zeta_{\|}^{1/2}(\hbar\omega_B / kT_s) \tag{4.6}$$

where $\zeta_{\|}(\hbar\omega_B / kT)$ is the enhancement in the thermal conductivity when magnetic fields are included and is tabulated in Silant'ev and Yakovlev (1980). For pure free-free absorption $\zeta_{\|}$ increases monotonically from unity at $B = 0$ to 1.97×10^3 when $\hbar\omega_B / kT = 1000$. Thus the effective surface density lies at a higher density than in the unmagnetized case because of the increased transparency of the surface layers.

The initial chemical potential, μ_s, is obtained from (2.12) in the magnetized case and from the familiar corresponding relation in the unmagnetized case.

The numerical results confirm that the magnetized relation between the flux and core temperature is completely insensitive to the surface boundary condition. As in the $B = 0$ case (e.g., Hernquist and Applegate 1984) this results

from the rapid convergence of the radiative zero solution in the layers in which photons dominate the heat transport. Thus, as is seen from (4.3) and (4.4) the core temperature will depend on the surface gravity and effective surface temperature only in the combination T_s^4/g_s (in agreement with the $B = 0$ calculation-- see Gudmundsson, Pethick, and Epstein 1983). Therefore it is sufficient to vary only one of the two parameters in the numerical computations.

5. Numerical Calculations

5.1 PROCEDURE

The thermal structure equations (4.3) and (4.4) were integrated numerically, using a 5th and 6th order Runge-Kutta-Verner scheme, from the initial point (T_s, ρ_s, μ_s) to the core boundary (T_c, ρ_c, μ_c). For compatibility with Gudmundsson, Pethick, and Epstein (1983) the core boundary was taken to be at a density $\rho_c = 10^{10}$ gm cm^{-3}. Quantum effects were included up to the point at which 30 Landau levels ($n_{max} = 29$) were populated. At each step in the numerical integration, the electron thermal conductivity was given by (3.6) and a numerical integration of the transport coefficients (3.5) for $n_{max} \leq 29$, and by (3.1) or (3.2) for $n_{max} > 29$. The photon radiative thermal conductivity of Silant'ev and Yakovlev (1980) was used throughout. The functions $\partial\rho/\partial T)_\mu$, $\partial\rho/\partial\mu)_T$, and S_e (all functions of μ and T) were given by numerical integrations of the appropriate magnetized and unmagnetized relations in Section 2. In the nondegenerate regime the expansions for $\partial\rho/\partial\mu)_T$, $\partial\rho/\partial T)_\mu$, and S_e in Section 2 were found to be adequate. In the degenerate regime the Sommerfeld expansions for the unmagnetized forms were used (but not for the magnetized relations--see Section 2). Finally, the local values of Z and A were assumed to

be given by the equilibrium composition (Baym, Pethick, and Sutherland 1971), although it was found that it would have been sufficient to use $Z = 26$ and $A = 56$ throughout (see Hernquist and Applegate 1984).

5.2 RESULTS

The integration was performed for the field strengths for which the conductivities have been calculated (see Table 1) and for eleven different heat fluxes (values of F corresponding to the effective surface temperatures $\log T_s = 5.5 - 6.5$, in increments of $\Delta \log T_s = .1$). The range of values for T_s was chosen for compatibility with Gudmundsson, Pethick, and Epstein (1983). The surface gravity $g_s = 10^{14}$ cm s^{-2} was used in each calculation. However, in view of the scaling relation of the $F - T_c$ relation with T_s^4 / g_s (see Section 4) this is not a limitation.

5.2.1 *Flux – core temperature relation*

The values of the core temperature, T_c, are given in Table 1 (see Appendix) for the field strengths and surface temperatures used in the calculation. In Table 2 (see Appendix) the ratio of the zero field core temperature to T_c is given for each set of T_s and B. In each case the core temperature is lower than the zero field value, but the maximum effect is only $\approx 60\%$. The relation between $T_s / g_{s_{14}}$ and T_c is shown in Figure 1 for the field strengths $B = 0$, 10^{12}, 10^{13}, and 10^{14} G. It is also seen that the effect of the field on the flux- core temperature relation does not necessarily increase monotonically with increasing field strength. This is due to the quantum oscillations of the electronic conductivity and can be understood in terms of the sensitivity of the flux to κ_{elec} (see Section 5.4).

5.2.2 *Thermal structure*

Temperature-density profiles are given in Figures 2, 3, and 4 for the surface temperatures $T_s = 10^{5.5}$, 10^6, and $10^{6.5}$, respectively. In each figure the $T(\rho)$ curves are given for the field strengths $B = 0$, 10^{12}, 10^{13}, and 10^{14} G. As noted in Section 3 the temperature-density profiles are not accurate at very low densities where bound-bound and bound-free opacity are important. Thus the curves in Figures 2, 3, and 4 have been terminated at $\rho = 10^2$ gm cm^{-3}. In the non-degenerate regime the relation of log T to log ρ is roughly linear, in agreement with the analysis of Hernquist and Applegate (1984). The magnetized curves are, of course, not precisely linear because the free-free opacity in this case is only approximately a power law function of density and temperature.

5.2.3 *Physical conditions*

The approximate physical conditions along each solution plotted in Figures 2, 3, and 4 are given in Table 3. Tabulated are the densities corresponding to the crystallization point ($\Gamma = 160$), the approximate transition from photon-dominated to electron-dominated heat transport ($\kappa_{rad} = \kappa_{elec}$), and the approximate transition from the non-degenerate to degenerate regimes ($\mu - mc^2 = kT$). The density at which 30 Landau levels are occupied is given roughly by (2.8b) with $n_{max} = 29$.

5.2.4 *Thermodynamic variables*

An example of the solution for the electron chemical potential (in units of mc^2) is shown in Figure 5 for the surface temperature $T_s = 10^6$ and the field strengths $B = 0$, 10^{12}, 10^{13}, and 10^{14} G. At low densities the chemical potential is dominated by the rest mass contribution and the curves for the different field strengths are indistinguishable. At much greater densities the curves are again

indistinguishable as μ is independent of T for a highly degenerate gas. The ripples in the $\mu(\rho)$ profiles for $B = 10^{13}$ and 10^{14} G are due to the quantization of the electron orbits.

In Figure 6 the entropy per electron (in units of k) is shown for the same surface temperature and field strengths. Although the quantum oscillations are rather large their influence on the thermal structure is not significant because thermal corrections are small in the degenerate regime. Small jumps in the curves are due to the use of asymptotic expansions to calculate the entropy per unit volume at low densities (in the non-degenerate regime) and the appearance of new equilibrium nuclear species at high densities (Baym, Pethick, and Sutherland 1971).

Finally, the partial derivatives $\partial\rho/\partial\mu)_T$ and $\partial\rho/\partial T)_\mu$ (not plotted) also show large amplitude quantum oscillations. This is especially true of $\partial\rho/\partial T)_\mu$ which has not converged to the zero field limit even when $n_{max} = 29$ (oscillations about the zero field value of amplitude ~ 10 times the zero field value are noted at the largest fields and lowest temperatures). However, the neglect of quantum effects for n_{max} >29 does not affect the thermal structure because thermal corrections (i.e., $\partial\rho/\partial T)_\mu$) are not important in the degenerate regime.

5.2.5 *Thermal conductivity*

The total thermal conductivity (radiative + electronic) is given in Figures 7, 8, and 9 for the surface temperatures $T_s = 10^{5.5}$, 10^6, and $10^{6.5}$, respectively. In each figure $\kappa(\rho)$ is shown for $B = 0$, 10^{12}, 10^{13}, and 10^{14} G. At low densities the conductivity is roughly constant along a solution. This follows from the magnetized form of the equation of state in the non-degenerate phase (2.20) and the simple theory presented in Hernquist and Applegate (1984). Furthermore, the conductivity along a solution at low densities is independent of field strength, as

expected. (According to Hernquist and Applegate (1984) the conductivity along a solution depends only on the ratio F/g_s , even if magnetic effects are included.) The conductivity is not precisely a constant because the opacity is only approximately of power law form. At greater densities the quantum oscillations of the electronic conductivity are clearly visible although they are significantly damped by thermal effects along the high surface temperature solutions.

The discontinuous jumps in the conductivity at the melting point and at the cutoff points $n_{max}=29$ in the liquid phase (for a discussion of the origin of the discontinuities see Yakovlev 1984) do not represent a serious problem. In general the points at which $n_{max}=29$ lie in the solid phase except for the high surface temperature solutions (which are less sensitive to magnetic effects). (Note that the points at which $n_{max}=29$ are not given precisely by (2.8b) for the high T_s solutions because of thermal effects.) In addition, the discontinuities usually appear at such high densities that the flux- core temperature relation is not affected (see Section 5.4).

5.3 GEOMETRICAL EFFECTS

The results thus far have assumed a completely vertical field geometry ($\nabla T \parallel \vec{B}$) . If the field has a horizontal component then the results will overestimate the flux for a given core temperature. Although the radiative conductivity is roughly isotropic (to within a factor ~ 2-- see Silant'ev and Yakovlev 1980), the electronic conductivity is highly anisotropic. Direct electron transport perpendicular to $\vec{B}$ is reduced by $\sim O(1/(\Omega\tau)^2)$ and Hall transport is reduced by $\sim O(1/(\Omega\tau))$, where Ω is the relativistic gyrofrequency and τ is the collision time. As the electron conductivity is the factor which controls the heat flow (Section 5.4) it is apparent that geometrical effects can significantly alter the

heat flux. The product $\Omega\tau$ can be estimated from zero field values. Using the Yakovlev and Urpin (1980) form for τ_0, in the liquid

$$\Omega_0 \tau_0 \sim 40 B_{12} (1 + .6\rho_8^{2/3})^{-1} \tag{5.1}$$

and in the solid

$$\Omega_0 \tau_0 \sim 10 B_{12} T_8^{-1} \rho_8^{1/3} (2 + .6\rho_8^{2/3})^{-1} \tag{5.2}$$

where $Z = 26$, $A = 56$, $\Lambda_{ei} = 1$, $u_{-2} = 13$, and the fully degenerate limit have been assumed. Thus, for the relevant field strengths the cross-field heat flow is much smaller than that along the field.

It is possible to obtain a rough estimate of the overall effect of the anisotropic heat flow in the limit $\Omega\tau \to \infty$. Consider a slab of material with a uniform field inclined to the vertical axis by an angle α . The vertical heat flux in the $\Omega\tau \to \infty$ limit is then

$$F_z = -\kappa_{||} \frac{dT}{dz} \cos^2\alpha \tag{5.3}$$

where $\kappa_{||}$ is the conductivity along the field. Thus the effect of a more realistic field geometry on the heat flux can be estimated by averaging the factor $\cos^2\alpha$ factor over a sphere. For a uniformly magnetized sphere $<\cos^2\alpha> = 1/3$, while for a pure dipole field $<\cos^2\alpha> = 1/3.8$ (see Applegate, Blandford, and Hernquist 1984). Thus the net effect of the anisotropy of the heat flow is to reduce the flux by a factor $\sim 3-4$ in the infinite field limit. This is clearly an upper limit as photon conduction will be effective, to some degree, at transporting heat across the field. For small fields the anisotropy vanishes and the heat flux is unaffected by geometrical considerations.

For a fixed core temperature and a vertical field the effect of the quantum conductivities is to increase (relative to the zero field case) the heat flux by a

factor $\lesssim 3$. (The maximum effect is a factor of 3 at the highest field strengths while the magnetic influence vanishes at low field strengths -- see Table 1.) Thus it is concluded that the enhancement in the heat flux due to quantum effects will be canceled by the suppression of the heat flux due to the overall field geometry. Indeed, it is likely that for moderate fields $\sim 10^{12}\ G$ and high surface temperatures $T_s > 10^6\ K$ the geometrical effect will be more important. The result of this would be to reduce the flux relative to the zero field value and extend the epoch of neutrino cooling. (See Applegate, Blandford, and Hernquist 1984 for a thorough discussion.)

5.4 SENSITIVITY TESTS

The sensitivity of the flux- core temperature relation to variations in the radiative conductivity, electronic conductivity, and melting parameter was investigated in a manner analogous to Gudmundsson (1981). It was found that the sensitivity to the inputs in the magnetized case was almost the same as that in the unmagnetized case, in agreement with the discussion in Hernquist and Applegate (1984). In general the $F - T_c$ relation is most sensitive to variations in κ_{e-ion} , less sensitive to variations in $\kappa_{e-phonon}$ and the melting parameter Γ , and virtually independent of variations in κ_{rad} . Thus the sensitivity zone of Gudmundsson, Pethick, and Epstein (1983) is generalized to the magnetic case. The low-density boundary lies along the transition from photon-dominated to electron-dominated heat transport while the high-density boundary results from the conductivity being so large that the star is nearly isothermal (usually near the melt surface). (See also Hernquist and Applegate 1984.) The edges of the sensitivity zone are somewhat less precise than in the unmagnetized case because of the quantum oscillations in the thermal conductivity. However, resonant phenomena (examples are given below) will influence the neutron star

only over a small portion of its thermal history and hence will have a negligible influence on cooling. (An exception to the coincidence of the high-density edge of the sensitivity zone with the melt surface occurred for the conditions $T_s = 10^{5.5}$, $B = 10^{14}$. In this case the density at the melt was lower than that of the transition from photon-dominated to electron-dominated heat transport.)

The flux- core temperature relation was found to be highly insensitive to large variations in the radiative conductivity, κ_{rad} , in agreement with the discussion in Hernquist and Applegate (1984). Changes in κ_{rad} by factors of 2 altered the core temperature, for a given surface temperature, by $\approx 2\%$. (An exception was the case $B = 10^{14}$ G , $T_s = 10^{5.5}$ which had changes in T_c of $\approx 10\%$. At such low temperatures and high field strengths the transition from photon to electron dominated heat transport occurs at densities approaching the high-density cutoff to the sensitivity zone. Thus the photons should have a greater influence.) A factor of 10 change in κ_{rad} typically altered the core temperature by $\lesssim 10\%$.

Variations in the melting parameter, Γ, were also found to be relatively insignificant. Thermal structure curves were generated for $\Gamma = 100$ and 200 , along with the standard value $\Gamma = 160$. The core temperature was typically affected by $\lesssim 5\%$. Resonant effects are possible, however, because of the discontinuity in the magnetized thermal conductivity across the melt interface (see Yakovlev 1984 for a discussion of the discontinuity). For example, at $B = 10^{13}G$ and $T_s = 10^{5.5}$ the use of $\Gamma = 100$ led to a core temperature 36% higher than that using $\Gamma = 160$. However, it was typically found that resonant phenomena could only reduce the overall effect of the magnetic field on the flux- core temperature relation because the melt occurred at such a high density (effectively at the high-density edge of the sensitivity zone) with $\Gamma = 160$. (The effect of the magnetic field on the thermal conductivity in the liquid is more severe than in

the solid. See Hernquist 1984 or Yakovlev 1984.)

Finally, it was found that the $F - T_c$ relation depended most strongly on the electronic thermal conductivity and, in particular, was most sensitive to κ_{e-ion}. Variations in κ_{e-ion} by factors of 2 typically changed T_c by $\sim 25\%$ while identical variations in $\kappa_{e-phonon}$ changed T_c by $\sim 5\%$. (As noted previously, the low surface temperature ($T_s = 10^{5.5}$), high field ($> 10^{13}$) cases were exceptional because of the location of the melting point and were most sensitive to $\kappa_{e-phonon}$.)

It is now possible to understand the result that the flux- core temperature relation is not dramatically affected at the highest field strengths. In the limit that the electron gas occupies only a fraction of the lowest Landau level, for a degenerate gas, κ_{elec} is actually reduced relative to the zero field conductivity (e.g., Hernquist 1984). Thus, although the amplitudes of the oscillations grow with increasing field strength, the overall change in κ_{elec}, averaged over the sensitivity strip, is not severe. Indeed, the effect of the field on the $F - T_c$ relation should not necessarily be monotonic because of the sensitivity of the results to the oscillating conductivity.

It is also possible to use the sensitivity analysis to discuss the influence of the uncertainties in the conductivities on the flux- core temperature relation. As expected (Hernquist and Applegate 1984) it is a good approximation to assume that the photon conductivity is given entirely by the free-free contribution. Because of the rapid convergence of the radiative zero solution in the photon-dominated region the flux- core temperature relation is sensitive to the photon conductivity only at densities near the transition to electron-dominated heat transport. Even if κ_{rad} were in error by a factor of 10 at this point (which is unlikely at these high densities) the core temperature would be affected by $\lesssim 10\%$.

Disagreements among the calculations of the electronic thermal conductivity will not alter the conclusion that magnetic effects on neutron star cooling are relatively unimportant. As noted in Section 3 the magnetized and unmagnetized calculations of κ_{e-ion} and $\kappa_{e-phonon}$ are subject to the same uncertainty. In addition, the response of the flux- core temperature relation to variations in κ_{e-ion} and $\kappa_{e-phonon}$ is, in general, not strongly dependent on the field strength. Thus, the uncertainty induced in the $F-T_c$ relation by disagreements in κ_{elec} tends to cancel when magnetized and unmagnetized calculations are compared. The maximum enhancement in the heat flux (relative to the zero field case) for a purely vertical field geometry was always found to be a factor ≈ 3, even with allowance for uncertainties in κ_{e-ion} and $\kappa_{e-phonon}$ as discussed in Section 3. This enhancement is expected to be completely canceled by geometrical effects (Section 5.3).

6. Comparison to Previous Calculations

6.1 ZERO FIELD RESULTS

The values of T_c and the sensitivity of the flux- core temperature relation to the various inputs are in good agreement with the simple analytical model of Hernquist and Applegate (1984). The core temperatures are also in good agreement (to a few percent) with the numerical calculations of Gudmundsson, Pethick, and Epstein (1983) for high surface temperatures ($T_s \geq 10^6\ K$) . At lower T_s the present results and those of Gudmundsson, Pethick, and Epstein (1983) differ somewhat (at $T_s = 10^{5.5}\ K$ the value of $T_c = 2\times10^7\ K$ is roughly 25% higher than the corresponding result in Gudmundsson, Pethick, and Epstein 1983). As discussed in Hernquist and Applegate (1984) this can be attributed to

differences in the assumed e-ion conductivity at low densities. The actual core temperature probably lies between the two extremes. The sensitivity tests, however, are in good agreement with Gudmundsson, Pethick, and Epstein (1983) for all surface temperatures.

6.2 MAGNETIZED CALCULATIONS

The effect of a strong magnetic field on neutron star cooling has been considered by a number of authors (Tsuruta, *et al.* 1972; Tsuruta 1974, 1975,1979; Nomoto and Tsuruta 1981; Glen and Sutherland 1980; Van Riper and Lamb 1981; Yakovlev and Urpin 1981). The present conclusion that the magnetic field will have a relatively minor influence on neutron star cooling differs considerably from the previous belief that magnetic effects can be quite significant. It is not possible to compare the results of Section 5 directly with all of the existing cooling curves because of attempts to include magnetic effects in the core (e.g., Tsuruta, *et al.* 1972; Tsuruta 1974,1975,1979 suppress the URCA neutrino luminosity in the magnetic case). However, the relation of surface to core temperature, which isolates effects in the envelope, is given in Tsuruta (1979), Glen and Sutherland (1980), Van Riper and Lamb (1981), and Yakovlev and Urpin (1981). It is useful to consider these results in detail.

The calculations of Tsuruta (1979) are based on the earlier work of Tsuruta, *et al.* (1972); Tsuruta (1974,1975). The relation of surface to core temperature is given for a neutron star of mass .476 $M_\odot$ and radius 10.9 km and the field strengths B = 0, 10^{12}, 4.4×10^{12}, and 4.4×10^{13} G . For the field strength 10^{12} G the predicted enhancement in the surface flux is a factor ~ 2 at $T_c = 10^8$ and a factor ~ 10 at $T_c = 2\times10^7$. For $B = 4.4\times10^{12}$ G the flux enhancements are ~ 10 at $T_c = 10^8$ and ~ 50 at $T_c = 2\times10^7$ K. At the same core temperatures the enhancements are ~ 100 and ~ 300, respectively, for $B = 4.4\times10^{13}$ G. From

Figure 1 the predicted enhancement in the surface flux due to quantum effects alone is at $T_c = 10^8$ ~ 1.5 for $B = 10^{12}$, ~ 2.3 for $B = 10^{13}$, and ~ 2.7 for $B = 10^{14}$ G. At $T_s = 2\times10^7$ the enhancement is ~ 2.3, essentially independent of B. (As mentioned previously it is further expected that the enhancement will be completely canceled by geometrical effects.)

Glen and Sutherland (1980) give the surface- core temperature relation for two equations of state ($M = 1.25M_\odot$, R = 8.13 km and $M = 1.25M_\odot$, R = 16 km) and the field strengths $B = 0$ and 10^{12} G. At $T_c = 10^8$ the flux enhancement is ~ 2 for both models and at $T_c = 2\times10^7$ it is a factor ~ 10 for both models. (As predicted by the theory in this paper the enhancement in the flux due to effects in the crust should be independent of the surface gravity.)

Van Riper and Lamb (1981) give the luminosity at infinity as a function of core temperature for the field strengths $B = 0$ and 4.4×10^{12} G. The predicted enhancements in the flux (which are the same as the luminosity enhancement) are factors ~ 10 at $T_c = 10^8$ and ~ 50 at $T_c = 2\times10^7$ for all stellar models tested.

Finally, the relation of surface to core temperature is given by Yakovlev and Urpin (1981) for the model $M = 1M_\odot$, R = 10 km and the field strengths $B = 0$ and 10^{13} G. The flux enhancements are ~ 10 at $T_c = 10^8$ and ~ 100 at $T_c = 2\times10^7$.

The discrepancy between the previous calculations and the present results can be directly attributed to differences in assumptions about the input physics. The calculations of Tsuruta (1979), Glen and Sutherland (1980), and Van Riper and Lamb (1981) have relied on the method developed by Tsuruta, *et al.* (1972) and Tsuruta (1974,1975). The influence of the magnetic field on the photon conductivity was taken into account by applying a correction factor to the zero field cross-sections of the form $\sigma_\omega(B) = (\omega/\omega_B)^2\,\sigma_\omega(0)$, where ω_B is given by (2.2) and ω is the photon frequency. This approximation is based on the work of Canuto (1970); Canuto, Lodenquai, and Ruderman (1970); and Lodenquai, *et al.* (1974).

The Rosseland mean was then taken to give an opacity of the form $\tilde{\kappa}_r(B) = a_r \tilde{\kappa}_r(0)$. (See Glen and Sutherland (1980) for an explicit form of a_r.) Silant'ev and Yakovlev (1980) have shown that this results in a poor approximation to the free-free conductivity. Large discrepancies are noted for $b = \hbar\omega_B / kT > 1$ and the tensor nature of the photon transport has been ignored. However, the results summarized in Section 5.4 show that the flux-core temperature relation is highly insensitive to the photon conductivity and errors in the radiative opacity are relatively unimportant.

Another effect that has been considered at low densities is the possible formation of linear chains of atoms (see Section 2.4), which was included in Tsuruta (1975) and Van Riper and Lamb (1981). It is undoubtedly true that this contributes to the discrepancies between the present work and that of Van Riper and Lamb (1981). However, the fact that the predicted flux enhancements of Tsuruta (1979) and Glen and Sutherland (1980) are in reasonably good agreement with those of Van Riper and Lamb (1981) indicates that this is a minor effect.

A more important issue, in view of the discussion in Section 5.4, is the effect of the magnetic field on the electronic thermal conductivity. In the work of Tsuruta, *et al.* (1972), and in all subsequent calculations (with the exception of Yakovlev and Urpin 1981), magnetic effects have been taken into account by applying a correction factor to the zero field conductive opacities of the form $\tilde{\kappa}_c(B) = a_c \tilde{\kappa}_c(0)$. The function a_c was found from the calculation of Canuto and Chiu (1969) for electron transport along the field. An average over the quantum oscillations in the completely degenerate limit ($T = 0$) was performed to give the form of a_c plotted in Tsuruta (1974). A number of objections can be raised with regard to this procedure. Yakovlev (1980a,1982) has shown that the results of Canuto and Chiu (1969) are not reliable. Furthermore, as emphasized by

Hernquist (1984) and Yakovlev (1984) the completely degenerate limit ($T = 0$) is not a good approximation. Thermal effects smooth and damp the oscillations and are responsible for the violation of the Wiedemann-Franz law (the Wiedemann-Franz law was assumed in the calculation of Canuto and Chiu 1969). In addition, the results of Canuto and Chiu (1969) are valid only for e-ion scattering, which would tend to overestimate the effect of the magnetic field. Finally, and most importantly, the average over the oscillations gives a form of the conductivity which is seriously in error at low densities. In the limit that the electrons occupy only a fraction of the lowest Landau level, for a degenerate gas, the conductivity is actually reduced below the zero field result. Thus, as discussed in Section 5.4, the influence of the magnetic field of the flux- core temperature relation does not necessarily increase monotonically with increasing field strength. This is especially true at lower core temperatures when the sensitivity zone lies at low densities. The form of α_c given in Tsuruta (1974), however, decreases monotonically with decreasing density (i.e., a monotonically increasing conductivity). Thus the previous results should differ from the present calculation most strongly at high field strengths and low surface temperatures, as is the case. (See also the relevant discussions in Hernquist 1984 and Hernquist and Applegate 1984.)

The calculation of Yakovlev and Urpin (1981) included magnetic fields by assuming that the conductivity would be enhanced to such a degree as to isothermalize the neutron star at densities $\rho < 3\times10^6$ gm cm^{-3} . At higher densities magnetic effects were neglected. This is obviously not a good approximation and it is not surprising that the present results differ considerably from those of Yakovlev and Urpin (1981).

None of the previous calculations have made a reasonable attempt to include geometrical effects. Tsuruta (1974) tried to take into account the

angular dependence of the photon opacity by applying the magnetic correction factor over only a fraction of the stellar surface. However, the fact that $\tilde{\kappa}_{rad}$ is roughly isotropic (to within a factor of 2) and the insensitivity of the flux- core temperature relation to the radiation implies that the anisotropy of the photon transport is irrelevant. The dominant geometrical effect is associated with the tensor nature of the electron transport and will reduce the surface flux by a factor $\lesssim 3$ (see Applegate, Blandford, and Hernquist 1984).

Finally, the relative insensitivity of the results to variations in the B implies that the possible dependence of the field strength on the depth (e.g., Tsuruta, *et al.* 1972) is not important and will, in the worst case, lead to resonance phenomena.

7. Conclusions

The thermal structure of magnetized neutron star envelopes has been investigated using the method of Gudmundsson, *et al.* (Gudmundsson 1981; Gudmundsson, Pethick, and Epstein 1983) and the most recent calculations of radiative and electronic thermal conductivities. Magnetic effects were found to be substantially less important than in previous calculations. The maximum enhancement in the flux, for a given core temperature, due to quantum effects is a factor ~ 3. It has been further argued (see Applegate, Blandford, and Hernquist 1984 for a complete discussion) that the anisotropy in the electron transport will reduce the heat flux by a factor ~ 3 . For a realistic geometry the two effects will not cancel exactly but the flux probably will not differ much from the zero field case.

Disagreements among the existing calculations of the thermal conductivity do not affect the conclusion that the magnetic field will have only a minor

influence on the heat flux. In general, the sensitivity of the flux- core temperature relation to variations in the conductivity does not depend strongly on the magnetic field. Thus, the resulting uncertainty in the flux, for a given core temperature, tends to cancel when magnetized and unmagnetized results are compared. In addition, the sensitivity analysis confirms that large variations in the radiative conductivity are not significant, justifying the approximations made in the non-degenerate regime (neglecting bound-bound and bound-free opacity).

The state of the matter near the surface of a magnetized neutron star is uncertain. Surface effects have been neglected in this calculation and are likely to be unimportant unless the stellar surface is terminated at a density such that the electronic heat transport dominates throughout the crust.

The magnetic field is thus expected to play only a minor role in the thermal evolution of a neutron star. This has significant implications for attempts to observe thermal x-rays from neutron stars and models of phenomena which rely on enhanced cooling due to magnetic effects. For example, it may be necessary to invoke pion condensation in order to account for the internal temperatures of Vela and other pulsars predicted by the vortex creep theory of glitches (Alpar, *et al.* 1984a,b; Alpar, Nandkumar, and Pines 1984). (See Applegate, Blandford, and Hernquist 1984 for a discussion of the observational consequences of the current results.)

Finally, it is worth noting that the role of the heat flux in the magnetic evolution of a neutron star is not minor (Blandford, Applegate, and Hernquist 1983) and may provide a crucial link in our attempt to understand these objects.

Acknowledgments

I thank Jim Applegate and Roger Blandford for valuable discussions and encouragement. This work was supported by the National Science Foundation under grant AST82-13001.

Appendix

Table 1. Values of the core temperature (in units of 10^7 K).

	log T_s										
B	5.5	5.6	5.7	5.8	5.9	6.	6.1	6.2	6.3	6.4	6.5
0	2.01	2.88	4.15	6.06	8.92	13.3	19.9	30.0	45.6	69.1	103.6
10^{10}	2.01	2.88	4.15	6.06	8.92	13.3	19.9	30.0	45.6	69.1	103.6
3×10^{10}	1.95	2.86	4.15	6.06	8.92	13.3	19.9	30.0	45.6	69.1	103.6
10^{11}	1.77	2.65	3.95	5.93	8.88	13.3	19.9	30.0	45.6	69.1	103.6
3×10^{11}	1.57	2.37	3.61	5.52	8.44	12.9	19.7	29.9	45.6	69.1	103.6
10^{12}	1.39	2.05	3.10	4.79	7.50	11.8	18.5	28.9	44.8	68.8	103.5
3×10^{12}	1.40	2.00	2.89	4.26	6.49	10.2	16.4	26.3	41.8	65.7	101.1
10^{13}	1.49	2.02	2.90	4.19	6.13	9.21	14.1	22.4	36.1	58.2	91.4
3×10^{13}	1.58	2.14	2.91	4.18	6.08	8.98	13.4	20.2	31.3	50.2	79.0
10^{14}	1.35	2.11	2.97	4.03	5.80	8.58	12.7	18.8	28.1	42.9	65.6

Table 2. Ratio of the zero field core temperature to T_c.

	log T_s										
B	5.5	5.6	5.7	5.8	5.9	6.	6.1	6.2	6.3	6.4	6.5
0	1.	1.	1.	1.	1.	1.	1.	1.	1.	1.	1.
10^{10}	1.	1.	1.	1.	1.	1.	1.	1.	1.	1.	1.
3×10^{10}	1.03	1.01	1.	1.	1.	1.	1.	1.	1.	1.	1.
10^{11}	1.14	1.09	1.05	1.02	1.	1.	1.	1.	1.	1.	1.
3×10^{11}	1.28	1.22	1.15	1.10	1.06	1.03	1.01	1.	1.	1.	1.
10^{12}	1.45	1.40	1.34	1.27	1.19	1.13	1.08	1.04	1.02	1.	1.
3×10^{12}	1.44	1.44	1.44	1.42	1.37	1.30	1.21	1.14	1.09	1.05	1.02
10^{13}	1.35	1.43	1.43	1.45	1.46	1.44	1.41	1.34	1.26	1.19	1.13
3×10^{13}	1.27	1.35	1.43	1.45	1.47	1.48	1.49	1.49	1.46	1.38	1.31
10^{14}	1.49	1.36	1.40	1.50	1.54	1.55	1.57	1.60	1.62	1.61	1.58

Table 3. Physical conditions along selected solutions.

T_s	B	$\rho(\kappa_{rad} = \kappa_{elec})$	$\rho(\mu - mc^2 = kT)$	$\rho(\Gamma = 160)$
$10^{5.5}$	0	2.1×10^{3}	6.2×10^{2}	4.3×10^{5}
$10^{5.5}$	10^{12}	8.4×10^{2}	3.6×10^{3}	9.3×10^{4}
$10^{5.5}$	10^{13}	4.8×10^{3}	3.7×10^{4}	1.0×10^{5}
$10^{5.5}$	10^{14}	7.1×10^{4}	3.9×10^{5}	$< 10^{2}$
10^{6}	0	2.0×10^{5}	4.2×10^{3}	8.5×10^{7}
10^{6}	10^{12}	9.8×10^{3}	6.8×10^{3}	5.5×10^{7}
10^{6}	10^{13}	4.5×10^{4}	7.8×10^{4}	2.0×10^{7}
10^{6}	10^{14}	2.9×10^{5}	8.8×10^{5}	1.9×10^{7}
$10^{6.5}$	0	1.4×10^{6}	4.1×10^{4}	$> 10^{10}$
$10^{6.5}$	10^{12}	1.3×10^{6}	4.0×10^{4}	$> 10^{10}$
$10^{6.5}$	10^{13}	2.7×10^{5}	1.5×10^{5}	$> 10^{10}$
$10^{6.5}$	10^{14}	1.9×10^{6}	1.8×10^{8}	3.7×10^{9}

References

Alpar, M.A., Anderson, P.W., Pines, D., and Shaham, J. 1984a, *Astrophys. J.* **276**, 325.

Alpar, M.A., Anderson, P.W., Pines, D., and Shaham, J. 1984b, *Astrophys. J.* **278**, 791.

Alpar, M.A., Nandkumar, R., and Pines, D. 1984, preprint.

Applegate, J.H., Blandford, R.D., and Hernquist, L. 1984, in preparation.

Baym, G., Pethick, C.J., and Sutherland, P.G. 1971, *Astrophys. J.* **170**, 299.

Berestetskii, V.B., Lifshitz, E.M., and Pitaevskii, L.P. 1982, *Quantum Electrodynamics*, Pergamon Press, Oxford.

Blandford, R.D. and Hernquist, L. 1982, *J. Phys. C: Solid State Phys.* **15**, 6233.

Blandford, R.D., Applegate, J.H., and Hernquist, L. 1983, *Mon. Not. R. astr. Soc.* **204**, 1025.

Canuto, V. and Chiu, H.-Y. 1969, *Phys. Rev.* **188**, 2446.

Canuto, V. 1970, *Astrophys. J. Lett.* **160**, L153.

Canuto, V. and Chiuderi, C. 1970, *Phys. Rev. D* **1**, 2219.

Canuto, V., Lodenquai, J., and Ruderman, M.A. 1971, *Phys. Rev. D* **3**, 2303.

Canuto, V. and Ventura, J. 1977, *Fund. of Cosmic Phys.* **2**, 203.

Chen, H.-H., Ruderman, M.A., and Sutherland, P.G. 1974, *Astrophys. J.* **191**, 473.

Cox, J.P. and Giuli, R.T. 1968, *Principles of Stellar Structure* , Gordon and Breach, New York.

Epstein, R.I., Gudmundsson, E.I., and Pethick, C.J. 1983, *Mon. Not. R. astr. Soc.* **204**, 471.

Flowers, E. and Itoh, N. 1976, *Astrophys. J.* **206**, 218.

Flowers, E.G., Lee, J.-F., Ruderman, M.A., Sutherland, P.G., Hillebrandt, W., and Müller, E. 1977, *Astrophys. J.* **215**, 291.

Glen, G. and Sutherland, P.G. 1980, *Astrophys. J.* **239**, 671.

Gradshteyn, I.S. and Ryzhik, I.M. 1980, *Table of Integrals, Series, and Products*, Academic Press, New York.

Gudmundsson, E.I. 1981, licentiate thesis, University of Copenhagen.

Gudmundsson, E.I., Pethick, C.J., and Epstein, R.I. 1982, *Astrophys. J. Lett.* **259**, L19.

Gudmundsson, E.I., Pethick, C.J., and Epstein, R.I. 1983, *Astrophys. J.* **272**, 286.

Helfand, D.J. and Becker, R.H. 1984, *Nature* **307**, 215.

Hernquist, L. 1984, in press.

Hernquist, L. and Applegate, J. 1984, in press.

Itoh, N., Mitake, S., Iyetomi, H., and Ichimaru, S. 1983, *Astrophys. J.* **273**, 774.

Itoh, N., Kohyama, Y., Matsumoto, N., and Seki, M. 1984, preprint.

Kaminker, A.D. and Yakovlev, D.G. 1981, *Theor. and Math. Phys.* **49**, 1012.

Karzas, W.J. and Latter, R. 1961, *Astrophys. J. Suppl.* **6**, 167.

Lodenquai, J., Canuto, V., Ruderman, M., and Tsuruta, S. 1974, *Astrophys. J.* **190**, 141.

Manchester, R.N. 1981, in *Pulsars*, ed. Sieber, W. and Wielebinski, R., Reidel, Dordrecht, Holland.

Müller, E. 1984, *Astron. and Astrophys.* **130**, 415.

Nandkumar, R. and Pethick, C.J. 1984, preprint.

Nomoto, K. and Tsuruta, S. 1981, *Astrophys. J. Lett.* **250**, L19.

Pavlov, G.G. and Kaminker, A.D. 1975, *Sov. Astron. Lett.* **1**, 181.

Pavlov, G.G. and Panov, A.N. 1976, *Sov. Phys. JETP* **44**, 300.

Pavlov, G.G. and Yakovlev, D.G. 1977, *Astrophysics* **13**, 89.

Pollock, E. and Hansen, J. 1973, *Phys. Rev. A* **8**, 3110.

Raikh, M.E. and Yakovlev, D.G. 1982, *Ap. Sp. Sci.* **87**, 193.

Ruderman, M.A. 1974, in *Physics of Dense Matter* , ed. Hansen, C.J., Reidel, Dordrecht, Holland.

Silant'ev, N.A. and Yakovlev, D.G. 1980, *Ap. Sp. Sci.* **71**, 45.

Slattery, W.L., Doolen, G.D., and DeWitt, H.E. 1980, *Phys. Rev. A* **21**, 2087.

Tsuruta, S., Canuto, V., Lodenquai, J., and Ruderman, M. 1972, *Astrophys. J.* **176**, 739.

Tsuruta, S. 1974, in *Physics of Dense Matter* , ed. Hansen, C.J., Reidel, Dordrecht, Holland.

Tsuruta, S. 1975, *Ap. Sp. Sci.* **34**, 199.

Tsuruta, S. 1979, *Phys. Repts.* **56**, 237.

Urpin, V.A. and Yakovlev, D.G. 1980a, *Sov. Astron.* **24**, 126.

Urpin, V.A. and Yakovlev, D.G. 1980b, *Sov. Astron.* **24**, 425.

Usov, N.A., Grebenshchikov, Yu.B., and Ulinich, F.R. 1980, *Sov. Phys. JETP* **51** , 148.

Van Riper, K.A. and Lamb, D.Q. 1981, *Astrophys. J. Lett.* **244**, L13.

Ventura, J. 1973, *Phys. Rev. A* **8**, 3021.

Yakovlev, D.G. and Urpin, V.A. 1980, *Sov. Astron.* **24**, 303.

Yakovlev, D.G. and Urpin, V.A. 1981, *Sov. Astron. Lett.* **7**, 88.

Yakovlev, D.G. 1980a, Preprint No. 678, A.F. Ioffe Institute of Physics and Technology, Leningrad.

Yakovlev, D.G. 1980b, Preprint No. 679, A.F. Ioffe Institute of Physics and Technology, Leningrad.

Yakovlev, D.G. 1982, *Ast. Zh.* **59**, 683.

Yakovlev, D.G. 1984, *Ap. Sp. Sci.* **98**, 37.

Figure Captions

Figure 1.

The relation of $T_s / g_{s_{14}}^{1/4}$ to the core temperature for the magnetic field strengths $B = 0$ (solid line), $B = 10^{12}$ G (dotted line), $B = 10^{13}$ G (dashed line), and $B = 10^{14}$ G (dashed-dotted line).

Figure 2.

Temperature-density profiles for the surface temperature $T_s = 10^{5.5}$ and the field strengths as in Figure 1.

Figure 3.

The same as Figure 2 for the surface temperature $T_s = 10^6$.

Figure 4.

The same as Figure 2 for the surface temperature $T_s = 10^{6.5}$.

Figure 5.

The electron chemical potential, in units of mc^2, as a function of density for the surface temperature $T_s = 10^6$ and the field strengths as in Figure 1.

Figure 6.

The entropy per electron, in units of k, for the surface temperature

$T_s = 10^6$ and the field strengths as in Figure 1.

Figure 7.

Thermal conductivity as a function of density for the surface temperature $T_s = 10^{5.5}$ and the field strengths as in Figure 1.

Figure 8.

The same as Figure 7 for the surface temperature $T_s = 10^6$.

Figure 9.

The same as Figure 7 for the surface temperature $T_s = 10^{6.5}$.

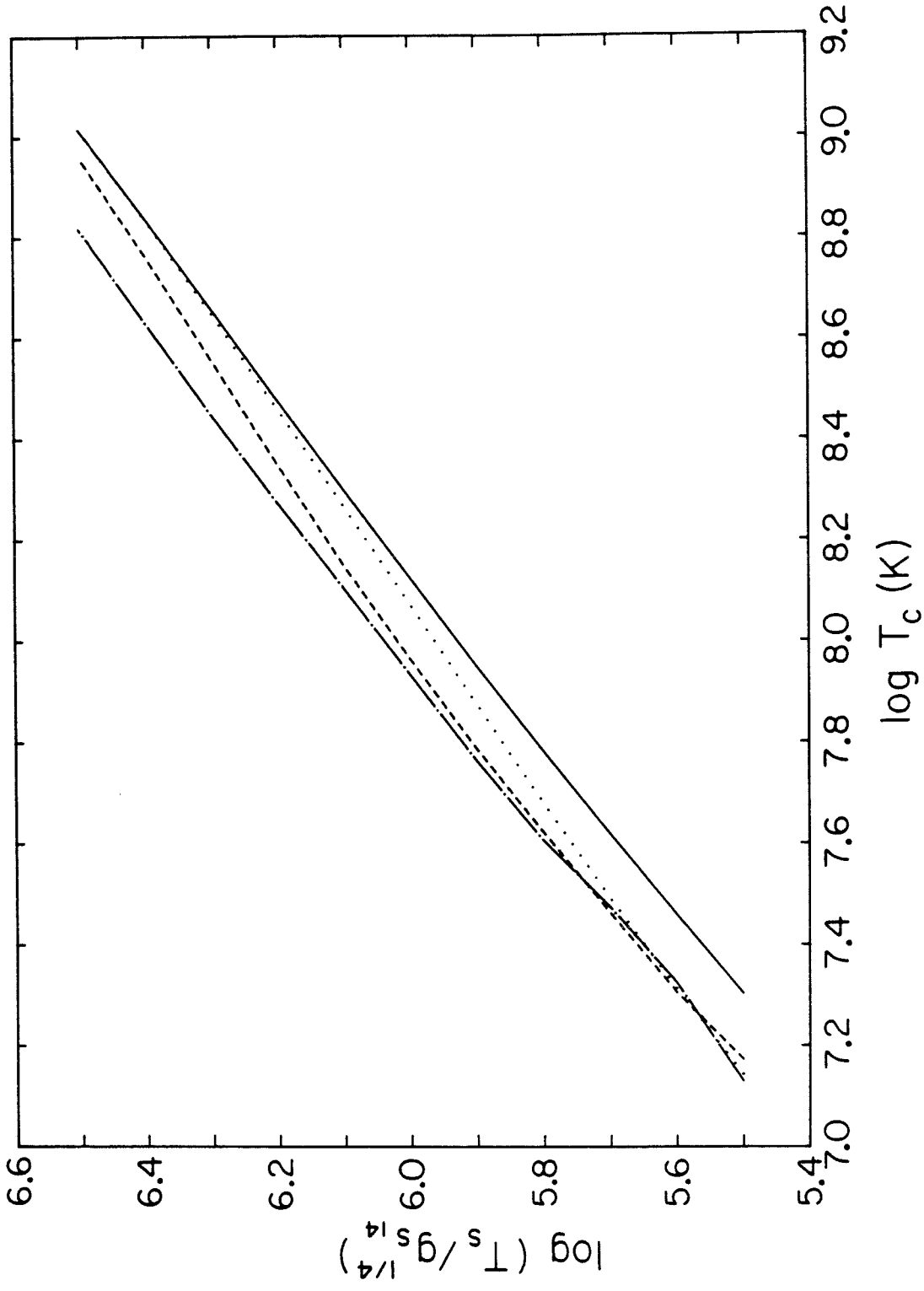
log T_c (K)
9.2
9.0
8.8
8.6
8.4
8.2
8.0
7.8
7.6
7.4
7.2
7.0
log ($T_s/g_{s14}^{1/4}$)
6.6
6.4
6.2
6.0
5.8
5.6
5.4

Figure 1

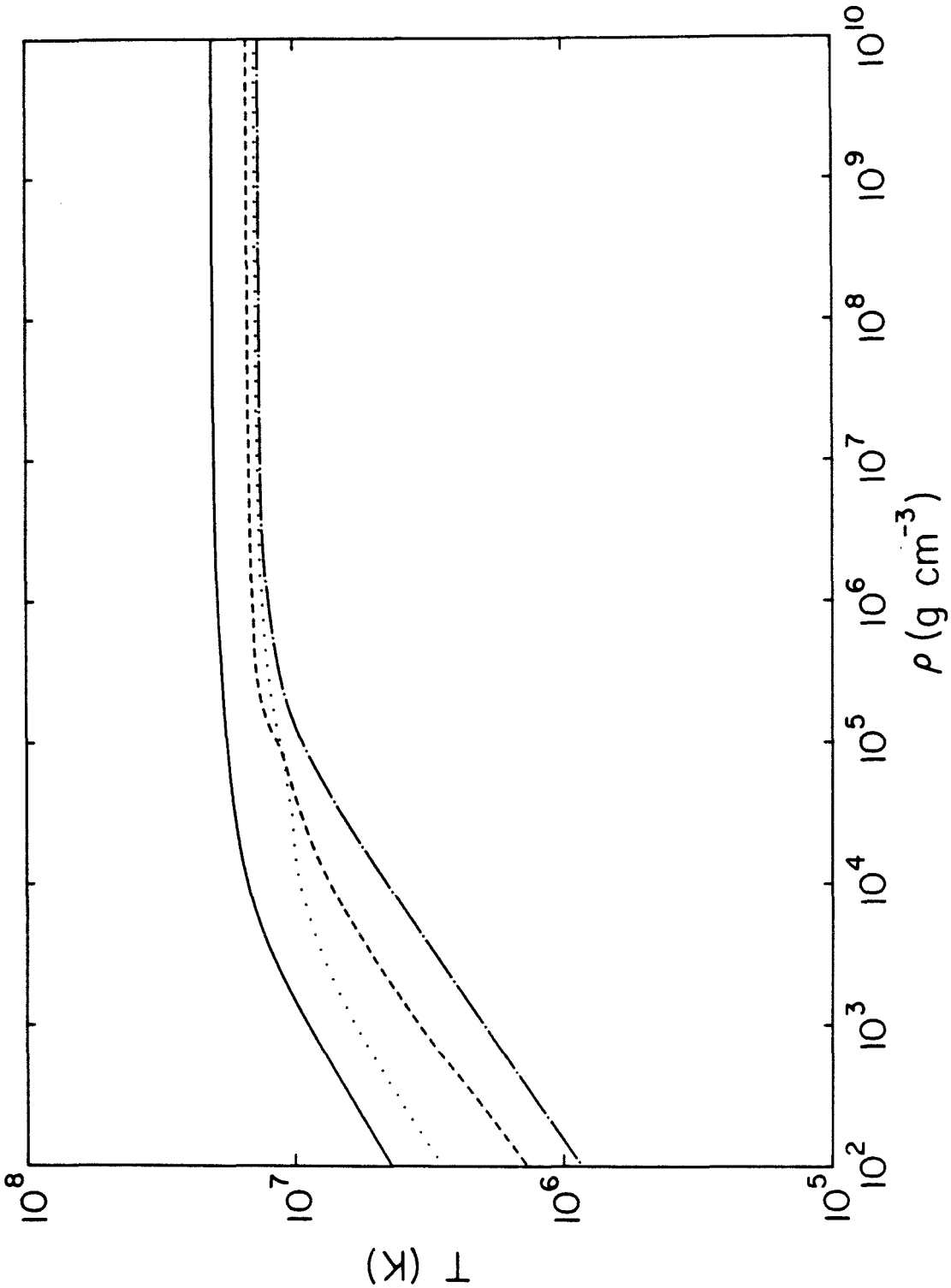

Figure 2

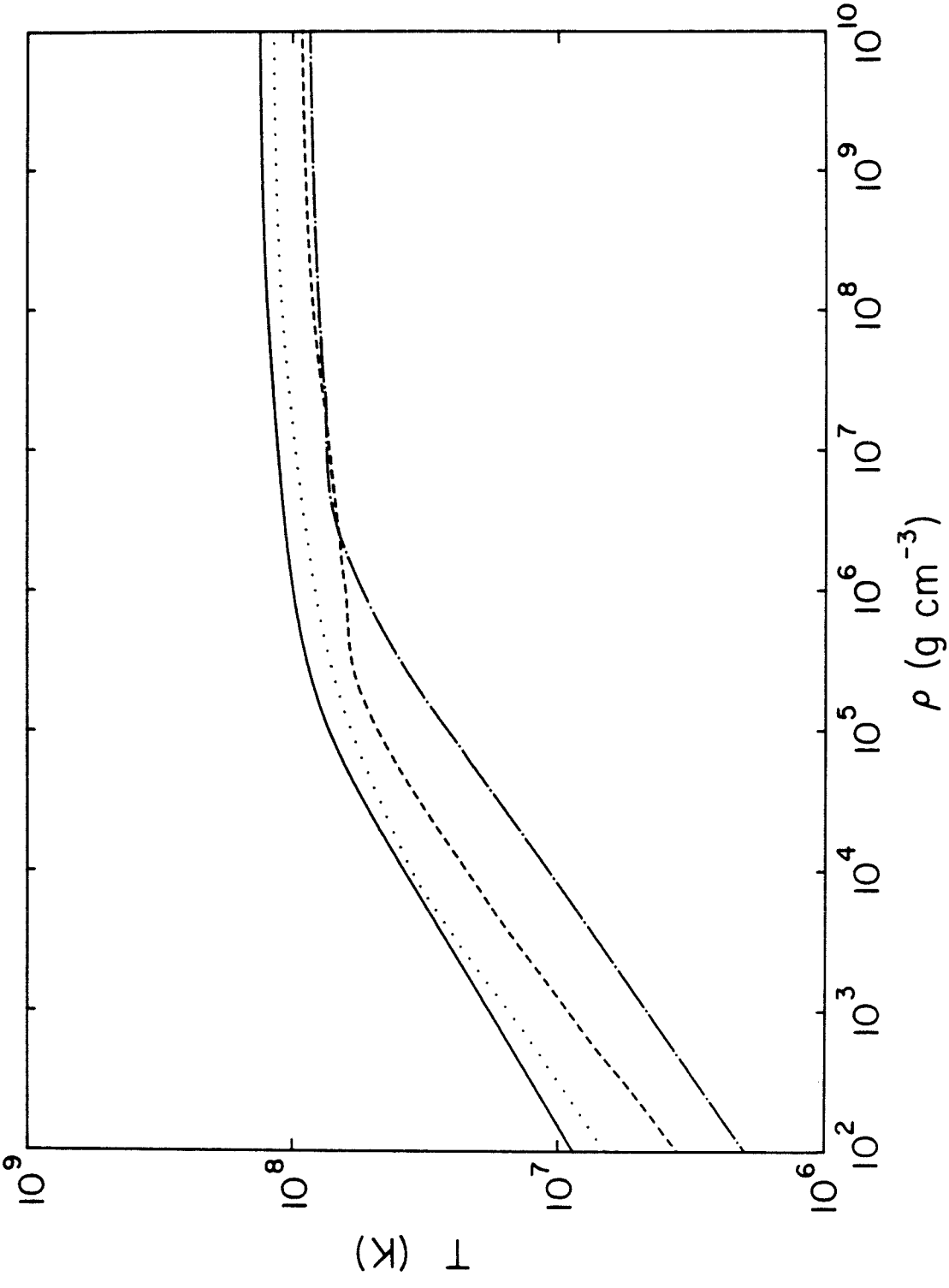

Figure 3

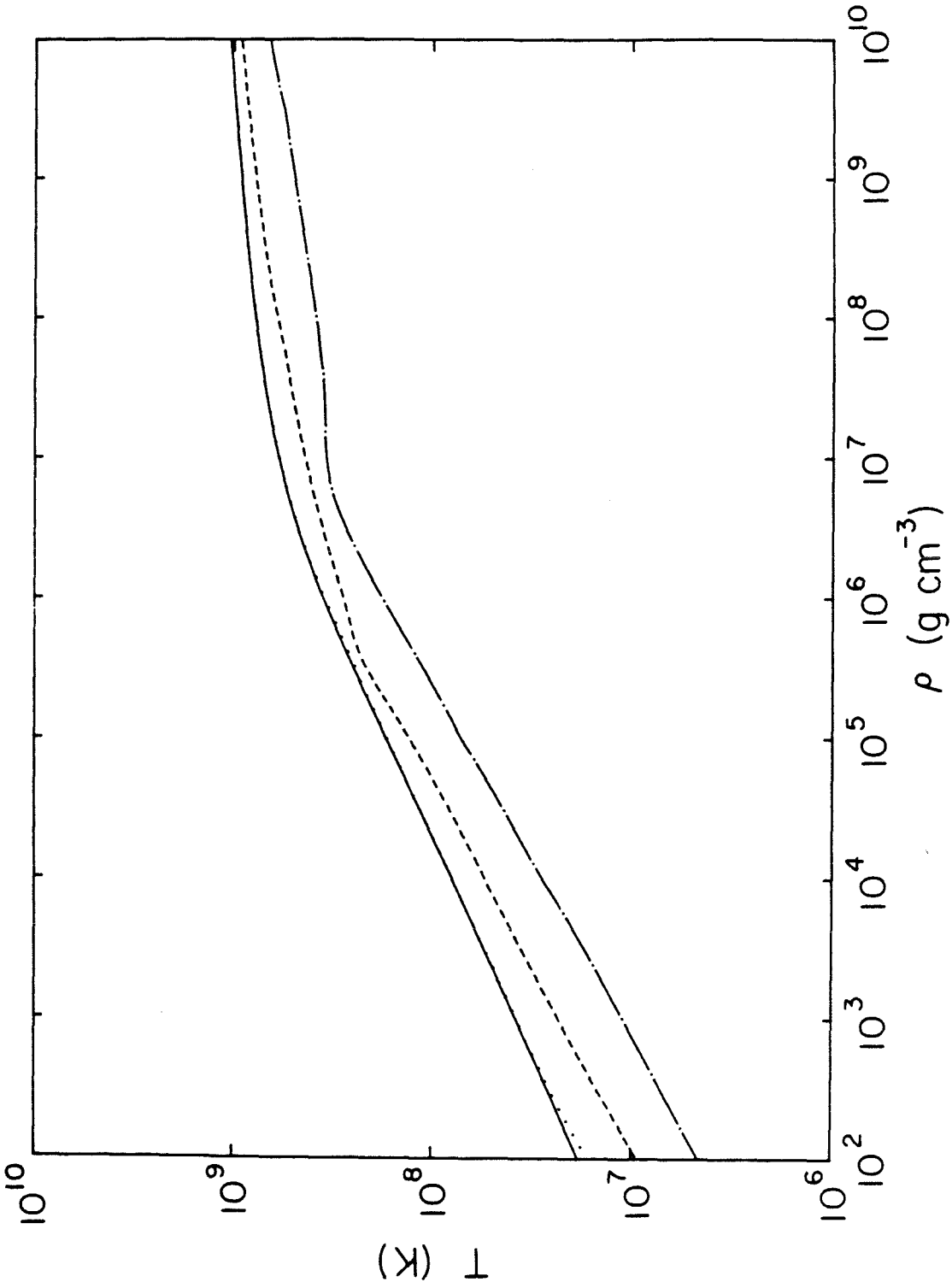
T (K)
10^{10}
10^{9}
10^{8}
10^{7}
10^{6}
10^{2}
10^{3}
10^{4}
10^{5}
10^{6}
10^{7}
10^{8}
10^{9}
10^{10}
ρ (g cm^{-3})

Figure 4

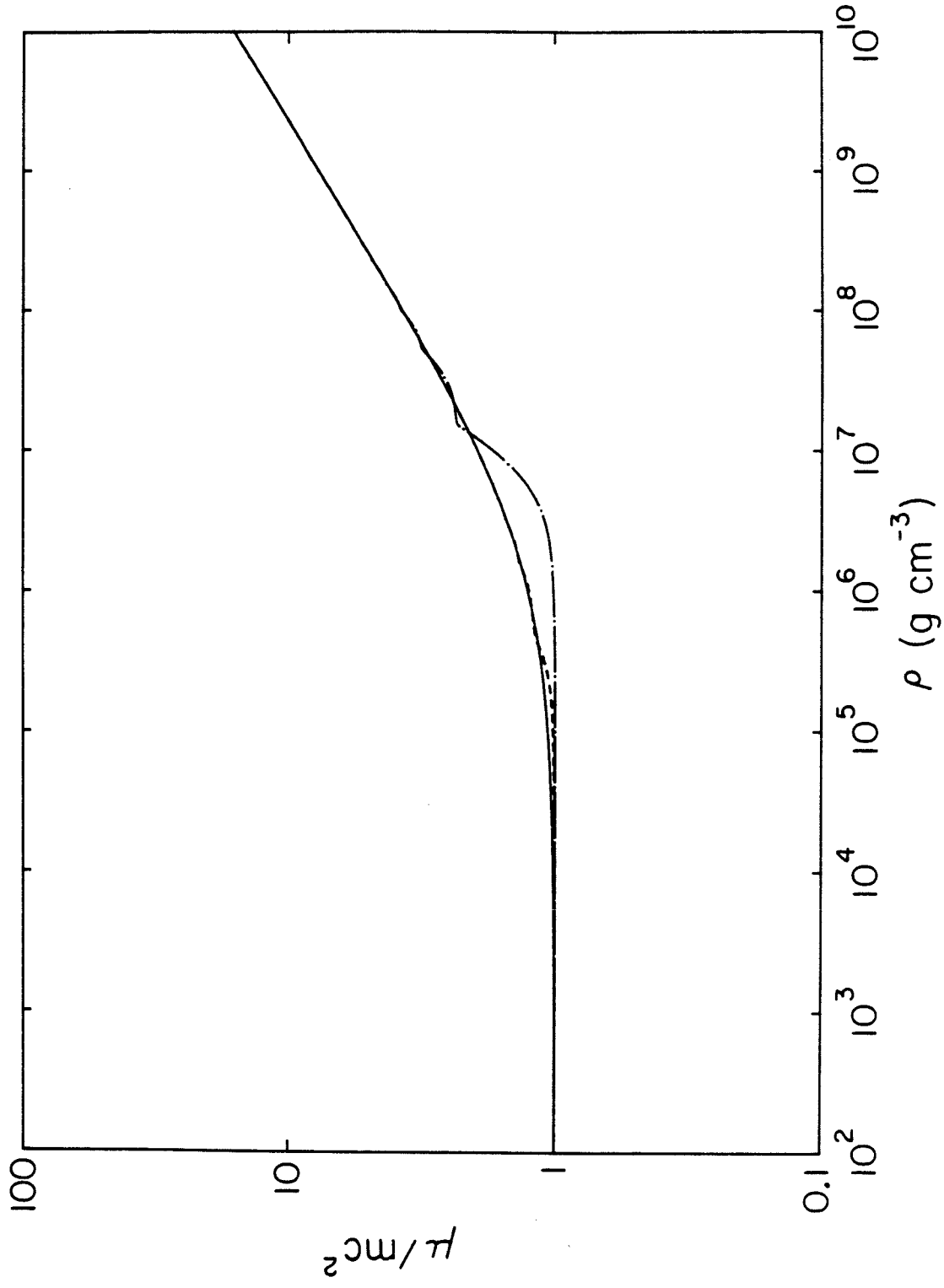

Figure 5

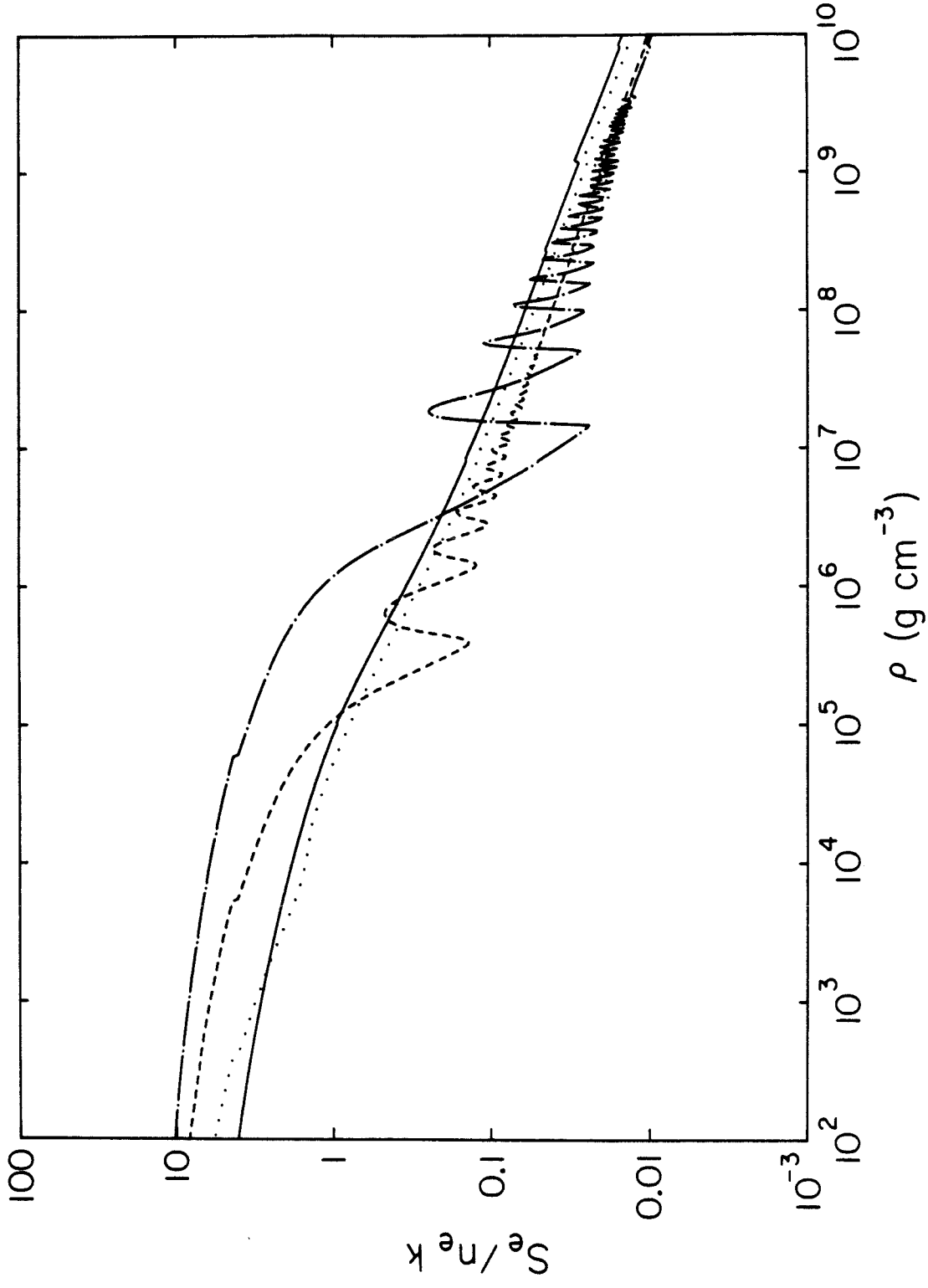
100
10
1
0.1
0.01
10^{-3}
$S_e/n_e k$
10^2
10^3
10^4
10^5
10^6
10^7
10^8
10^9
10^{10}
ρ (g cm^{-3})

Figure 6

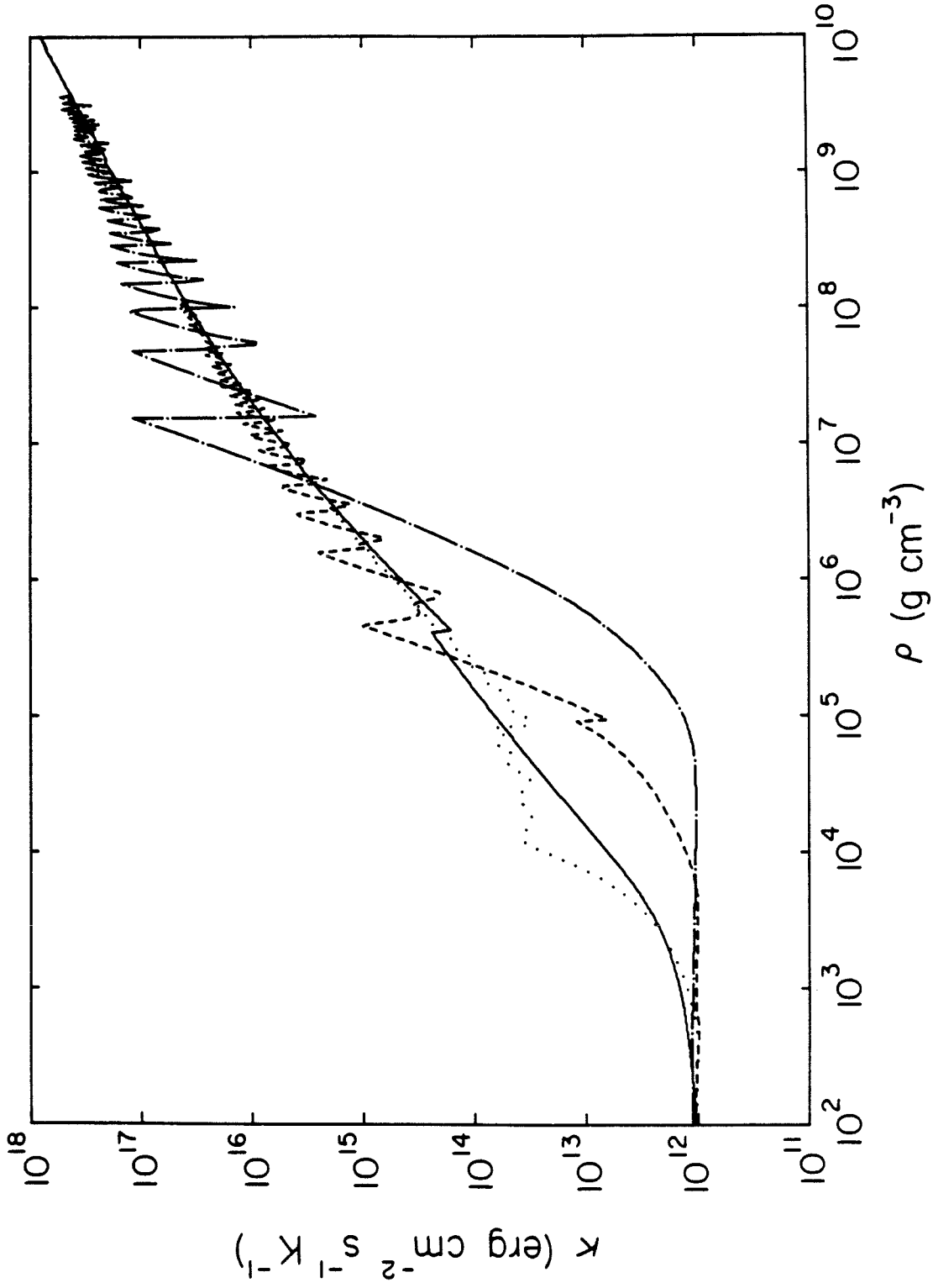
κ (erg cm⁻² s⁻¹ K⁻¹)
ρ (g cm⁻³)
10¹⁸
10¹⁷
10¹⁶
10¹⁵
10¹⁴
10¹³
10¹²
10¹¹
10²
10³
10⁴
10⁵
10⁶
10⁷
10⁸
10⁹
10¹⁰

Figure 7

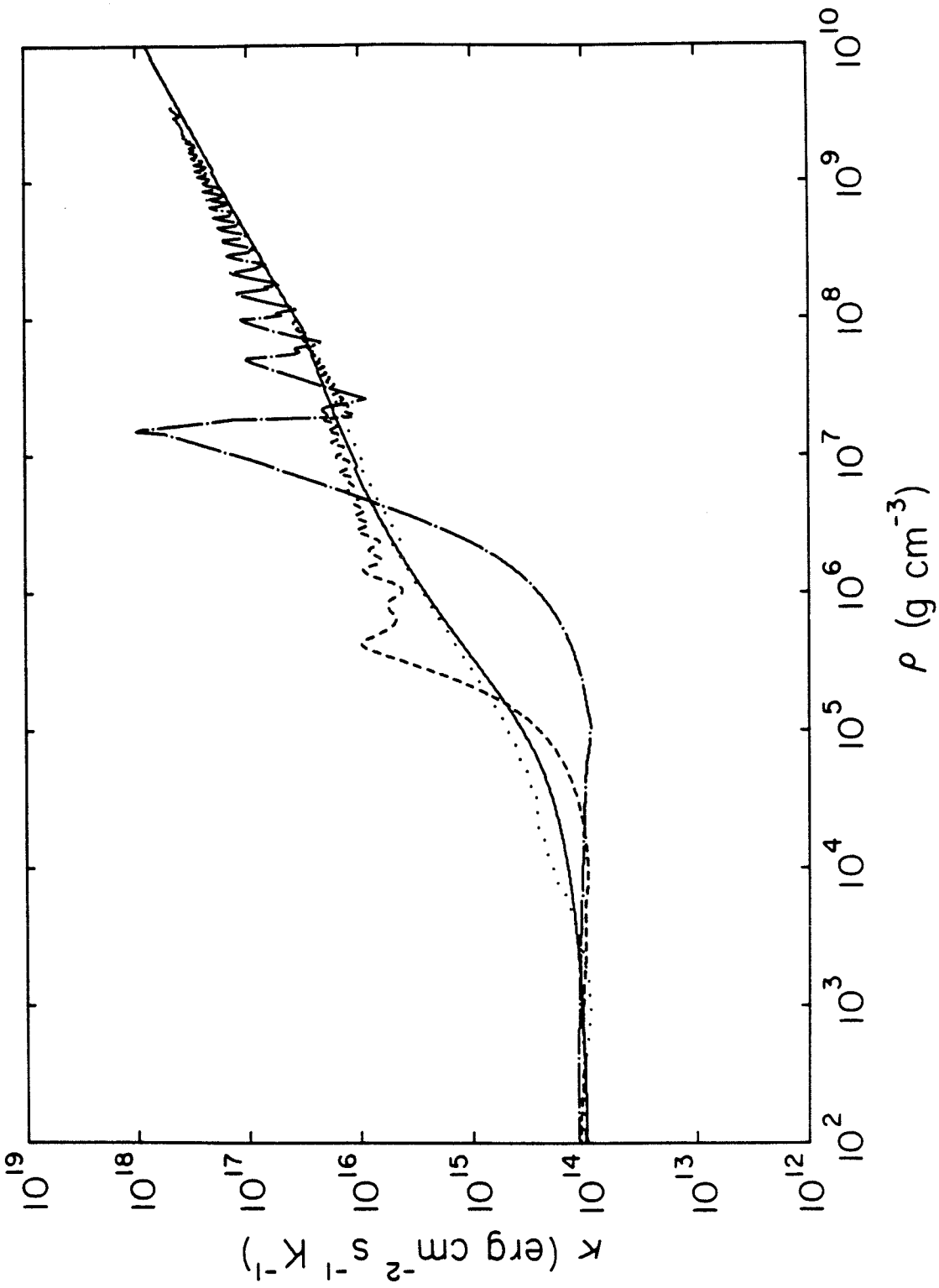
κ (erg cm⁻² s⁻¹ K⁻¹)
ρ (g cm⁻³)
10¹⁹
10¹⁸
10¹⁷
10¹⁶
10¹⁵
10¹⁴
10¹³
10¹²
10²
10³
10⁴
10⁵
10⁶
10⁷
10⁸
10⁹
10¹⁰

Figure 8

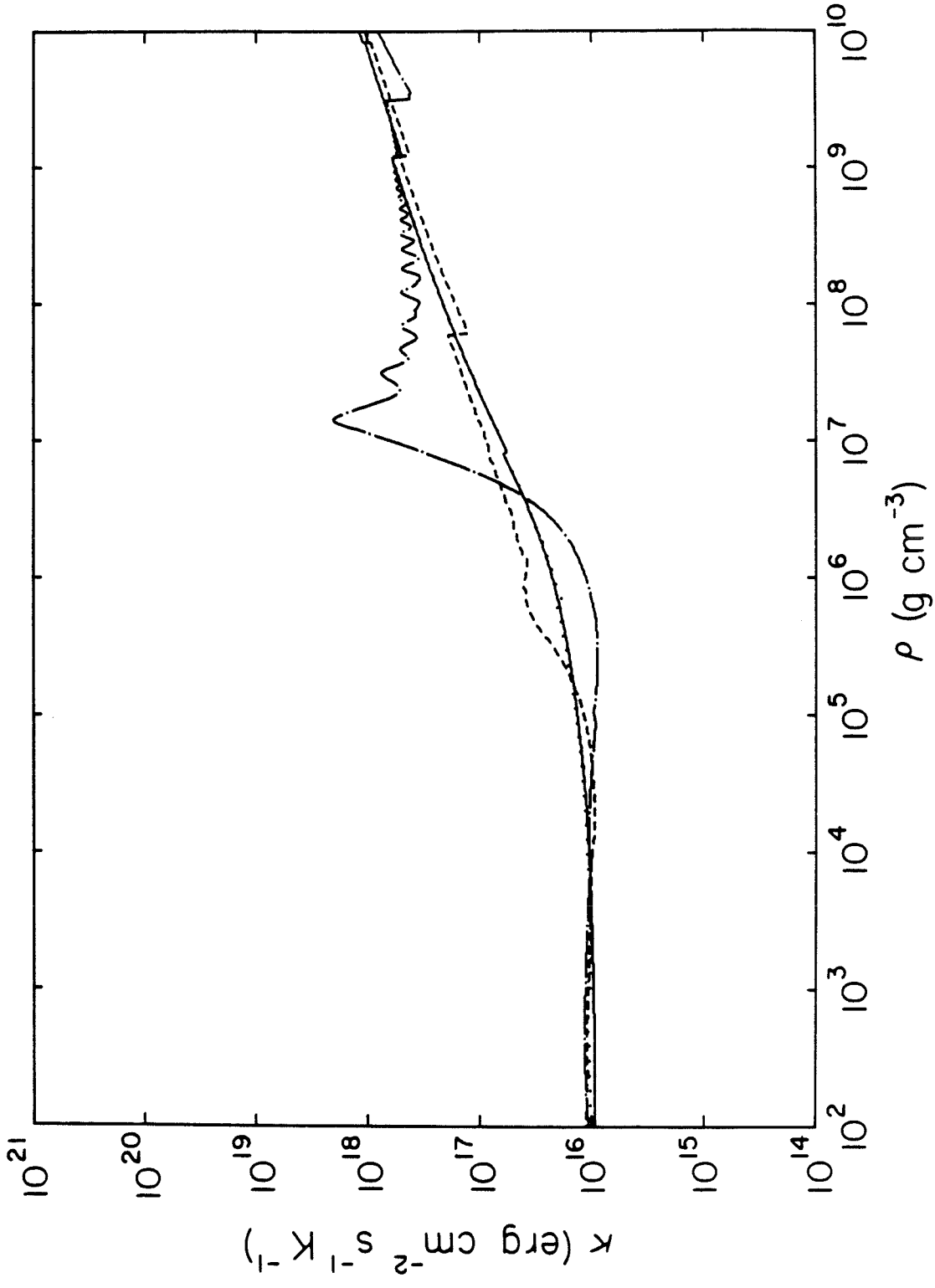
10^{21}
10^{20}
10^{19}
10^{18}
10^{17}
10^{16}
10^{15}
10^{14}
κ (erg cm^{-2} s^{-1} K^{-1})
10^{2}
10^{3}
10^{4}
10^{5}
10^{6}
10^{7}
10^{8}
10^{9}
10^{10}
ρ (g cm^{-3})

Figure 9